Lead and Mercury Inputs to Lakes in Kejimkujik National Park, Nova Scotia: Sources, Accumulation, and Remobilization

by

Michelle J'aime DesJardins
B.A., University of Victoria, 2000

A Thesis Submitted in Partial Fulfillment of the
Requirements for the Degree of

MASTERS OF SCIENCE

in the School of Earth and Ocean Sciences

We accept this thesis as conforming
to the required standard

[redacted]

Dr. K.H. Telmer, Supervisor (School of Earth and Ocean Sciences)

[redacted]

Dr. M.J. Whiticar, Departmental Member (School of Earth and Ocean Sciences)

[redacted]

Dr. E. Van der Flier-Keller, Departmental Member (School of Earth and Ocean Sciences)

[redacted]

Dr. J.D. Greenough, External Examiner (Department of Earth and Environmental Sciences, Okanagan University College)

Supervisor: Dr. Kevin H. Telmer

ABSTRACT

Sediment cores were collected from two lakes in Kejimkujik National Park, Nova Scotia to investigate natural and anthropogenic inputs of Hg and Pb to the lakes and the reliability of the lake sediments to record depositional history. The total mass of Hg accumulated in the sediments of Big Dam West Lake (BDW) and Big Dam East Lake (BDE) since inception after the Wisconsinan Glaciation 13,000 years ago is estimated to be 14.7 and 3.4 kg, respectively. Hg profiles indicate that the average flux of Hg to the lakes for the last 20 years has been 25.0 and 13.0 $\mu g/m^2/yr$ for BDW and BDE, respectively, which is 3 times higher than pre-industrial background sediments. Hg profiles show that the timing of recent historical anthropogenic activities have been preserved in the Hg profiles of both lakes. However, the magnitudes of the Hg increases are asynchronous when plotted as a function of time, but not when plotted as a function of depth, thereby suggesting that post-depositional diagenetic remobilization may partially be responsible for the upcore enrichments.

Unlike the Hg flux profiles, which show BDW having a greater flux of Hg throughout the cores, the Pb flux profiles show that the two lakes had similar fluxes of Pb at pre-1850 depths. Above these depths, BDE shows significantly larger Pb flux rates than BDW. In the top 3 cm, BDE's Pb flux of 5.3 $mg/m^2/yr$ is 1.9 times greater than BDW's Pb flux of 2.8 $mg/m^2/yr$. This difference is believed to be the result of upward remobilization, with more Pb being remobilized in BDE. The total mass of Pb accumulated since inception is estimated to be 5305 and 1502 kg in BDW and BDE, respectively.

Only the Pb increases in BDW coincide with historical increases in atmospheric Pb inputs associated with automobile emissions. Neither lake however records any significant decreases in the uppermost sediments as would be expected from the significant reductions in atmospheric Pb concentrations that have occurred since the phasing out of leaded gasoline in the 1970's. Furthermore, profiles of Pb isotope ratios

show fluctuations in the profiles that coincide with known historical events, but the anthropogenic component is always more radiogenic than expected, suggesting there is upward remobilization of Pb from deeper more radiogenic sediments in both lakes. This interpretation is further supported by concentration profiles from six cores which show that the Pb profiles align better when plotted as a function of depth rather than age. These results provide strong evidence that the Pb concentration profiles, at least in BDE, are more a function of depth, and thus diagenetic conditions, than of depositional history.

Porewater data provide further evidence to support the interpretation of Pb and Hg remobilization in the sediments of BDW and BDE. Upward decreasing concentrations of both Hg and Pb measured in porewaters suggest that diffusion of Hg and Pb will predominantly occur in an upward direction. Dissolved oxygen, pH and Eh profiles show the disappearance of DO by 4 cm depth accompanied by significant changes in pH and redox between 0 and 6-7 cm. BDE in particular shows rapid changes in pH and redox between 5 and 7cm depth, indicating that the decay of organic matter is much more rapid in BDE than BDW, which supports the data from the sediment profiles that indicate more Pb is remobilized in BDE than BDW.

Precipitation samples were collected over a one-year period to determine sources of anthropogenic heavy metal pollutants to the park using Pb isotope ratios. Pb isotope compositions indicate that anthropogenic pollution from populated and industrial regions of northeastern U.S. and southeastern Canada is being transported to Kejimkujik National Park. In general there was a dominantly Canadian source during the fall months of 2001 and a dominantly American source during the winter and spring months of 2002. The isotopic composition of the precipitation samples range from $^{206}Pb/^{207}Pb$ ratios of 1.165 to 1.20, indicating U.S. contributions ranging from 30-100% or Canadian contributions ranging from 0-70%. The annual average $^{206}Pb/^{207}Pb$ ratio is 1.181 and indicates that on an annual basis the U.S. contribution of Pb to Kejimkujik National Park is 62% (or 38% Canadian).

The average annual Pb isotope composition of the precipitation represents the value of the anthropogenic component that should be observed in the surface sediments. However the calculated $^{206}Pb/^{207}Pb$ anthropogenic component in all sediments cores is more radiogenic than would be expected, indicating that there is upward remobilization

of Pb from deeper more radiogenic sediments in both lakes. Knowing the true isotopic composition of anthropogenic Pb from precipitation and that of the background sediments, a calculation is presented to quantify the magnitude of remobilized background Pb in the topmost sediment layer. Only BDE provides the necessary conditions to allow such a calculation. The amount of remobilized background Pb in the topmost sediment sample from a BDE core is estimated to be approximately 25.1 μg/g, which is 51% of the total Pb in the labile fraction of that sample.

Examiners:

[redacted]

Dr. K.H. Telmer, Supervisor (School of Earth and Ocean Sciences)

[redacted]

Dr. M.J. Whiticar, Departmental Member (School of Earth and Ocean Sciences)

[redacted]

Dr. E. Van der Flier-Keller, Departmental Member (School of Earth and Ocean Sciences)

[redacted]

Dr. J.D. Greenough, External Examiner (Department of Earth and Environmental Sciences, Okanagan University College)

TABLE OF CONTENTS

LIST OF FIGURES

LIST OF TABLES

ACKNOWLEDGEMENTS

This work was supported by the Health Canada Toxic Substance Research Initiative (TSRI) as part of TSRI Project 124: "Multi-Disciplinary Study of Metal Cycling, Primarily Hg, in Aquatic and Terrestrial Environments". The research was a collaborative project between the Geological Survey of Canada, Environment Canada, University of Ottawa, University of Victoria, Nova Scotia Natural Resources, Canadian Wildlife Services, Dalhousie University, and Acadia University.

First and foremost, I would like to thank my supervisor Dr. Kevin Telmer, who was the one that initially sparked my interested in the field of environmental geochemistry. I consider it a great privilege to have had the opportunity to work with him on this project and I greatly appreciate all the support, encouragement, advice, and friendship he has given me. His invaluable words of wisdom have really built my scientific background, as well as given me insights about life. Thank you!

To my good friends and fellow students, Paul Ferguson and Roberta Press, I give a very special thanks for your invaluable assistance in the field. I greatly appreciate your efforts and truly enjoyed your company for those months. Both seasons were a real adventure with their own challenges and I will forever cherish the memories and your friendship. I would also like to acknowledge the efforts of a fellow graduate student, who has become one of my best friends during these years, Mike Sanborn. A special thank you for your many contributions to this project, both in the lab and in the field. In particular, your creative and innovative ideas in the development of sampling equipment and laboratory procedures were invaluable and greatly contributed to the success of this project.

I would like to acknowledge all of those who assisted us in our field work in the summers of 2000 and 2001. It took the efforts of many to make the sampling seasons a success, particularly in collecting the long cores in July of 2001, and we are grateful to them all. They are: Tom James and Tim Conway (GSC-Pacific Geoscience Centre) for teaching us the method of obtaining long cores and providing much of the equipment needed to do so; Terry Goodwin (N.S. Natural Resources) and Belinda for their assistance, strength, and patience in the field during the early developmental stage of perfecting the coring method; David Lean (U. of Ottawa), Andy Rencz (GSC Ottawa), Melissa Legrand, Tanya Peron, and Blaine Mailman (Kejimkujik National Park) for their assistance in obtaining the long cores; and Reg Theriault for his assistance with gravity coring in July 2000.

A very special thank you to Steve Beauchamp of the Atmospheric Science Division, Environment Canada, Dartmouth, N.S. for his invaluable assistance in many aspects of this project, including the use of his laboratory, collaboration in obtaining precipitation samples, and overall helpfulness throughout this project, particularly during field seasons. Thanks also to Colin Bell of Acadia University for his assistance in obtaining distilled de-ionized water and N_2 gas in July of 2000 and to Danielle Fortin for her advice on building and using dialysis porewater samplers.

With regards to sample analyses, I would like to give special thanks to Jianzhong Fan for his advice and assistance with sediment digestions and for all ICP-MS analyses. Thank you to everyone else that assisted in the preparation of samples for analyses: Roberta Press, Cheryl Peters, Paul Ferguson, Dianne Noseworthy, Tracye Keith and Kristy Hooker. I am particularly grateful to Jody Spence and Cheryl Peters for all their hard work in the analysis of mercury in sediments and porewaters. Thanks also to Jim Budahn of the ^{210}Pb Dating Laboratory at the USGS in Denver, Colorado for the ^{210}Pb and ^{137}Cs analyses of sediments and Janet Gabites of the UBC Geochronology Lab for Pb isotope analyses of precipitation samples.

I would like to specially thank all the friendly staff of Kejimkujik National Park, Nova Scotia. The following people in particular deserve special recognition: Bob Thexton and Cliff Drysdale for their cooperation and use of park facilities; Jonathan Sheppard and Sally O'Grady for their assistance with obtaining information about park history; and Blaine Mailman for his assistance with coring and retrieving porewater samplers and all his visits to check up on us at the Big Dam cabin.

I want to thank the unique group of people I've worked with here at the Geochemistry Lab, both past and present, for making the lab a fun and interesting place to work: Kevin Telmer, Mike Sanborn, Paul Ferguson, Laurie Gallagher, Roberta Press, Andrew Hamilton, Cheryl Peters, Dianne Noseworthy, Kristy Hooker, Tracye Keith, Richard Cox, Karolyn Jones, Brett Boniface, Amber Church, Lee Ferreira, and Jianzhong Fan. I enjoyed the company and friendship of all of you. To my two amigos, Mike and Paul, who always treated me like one of the guys, I give special thanks for all the good times, both in and out of the lab and for all the great things you introduced me to like soccer, ultimate, disc golf, skim boarding, and euchre. And thanks to Laurie and Karolyn for all the gab sessions. I enjoyed hearing your advice and opinions about....everything.

Thank you to my committee members, Micheal Whiticar, Eileen Van der Flier-Keller, and John Greenough for their helpful comments. Thank you also to all the staff, students, and professors from the School of Earth and Ocean Sciences for making my years here at the University of Victoria most enjoyable.

Finally, a heartfelt thanks to all my beloved family and friends to whom I will never have enough words of appreciation for all the love, support, and encouragement you have all given me. I cherish you all. To my mother, who made me the strong person that I am today, I thank you for all your words of love, encouragement, and wisdom that helped me get through this time. You are an inspiration. To my grandparents for all their love, support with Karly during field seasons, and for always providing a wonderful place to retreat. Most of all, I could not have completed this thesis without the constant love and support I received on a daily basis from Chris Gibson and my daughter Karly, to whom I am grateful.

1. INTRODUCTION

Kejimkujik National Park, Nova Scotia is noted for having the highest mercury concentrations in loon blood in North America (Burgess et al., 1998a). However, in comparison to other environments, the underlying reason for the high Hg levels in loons and the source of the Hg remains unknown. As such, Health Canada, Environment Canada, and the Geological Survey of Canada have chosen Kejimkujik Park to investigate the distribution and behaviour of metals in the environment.

Many aspects of human activities have led to environmental impacts such as increased heavy metal pollution. Some lines of evidence suggest that, today in the northern hemisphere, anthropogenic activities comprise > 90% of the worldwide emissions (Mart, 1983) and therefore have seriously affected the composition of the atmosphere and greatly affected the health of our environment. Evidence of such impacts is thought to be preserved in lake sediments.

Lead (Pb) and mercury (Hg), as well as other metals, often have upcore enrichment trends in lake sediments which have been interpreted to be the result of modern atmospheric pollution. However, the degree and variability in upcore enrichments illustrates problems with simple atmospheric deposition models, which predict less variable "inter-lake" enrichment. The profiles thus provide evidence for the increasingly accepted theory that the distribution of metal with depth in lake sediments reflects not only the depositional history, but also the post-depositional diagenetic processes caused by physiochemical and biochemical processes, such as porewater advection, molecular diffusion, microbial decomposition, and bioturbation.

Many heavy metals, particularly mercury, are dominantly associated with particulate matter in aquatic systems and are considered particle-reactive elements (Matty and Long, 1995). Processes that modify or alter particles in water bodies therefore influence particle-associated elements affecting bioavailability (Elder, 1988), altering residence times (Bacon and Rutgers van der Loeff, 1989), and determining the retention of particle-bound elements in the sedimentary record. One of the most important processes that can have this substantial impact on sediment particles is early diagenesis.

Early diagenesis is a set of reactions, occurring in the upper layers of sediments, that alters particle surfaces or changes metal speciation, and can thus remobilize metals that are bound to particle surfaces (Shaw et al., 1990). However, it has been suggested that mercury in sediments is not affected by diagenesis (Rossman, 1986), and therefore sediment profiles are commonly used as historic records of anthropogenic inputs.

Other studies (Gill and Fitzgerald, 1988; Gobeil and Cossa, 1993) have found evidence for the diagenetic remobilization of sediment-bound mercury during early diagenesis. This remobilization could have the consequence of increased metal content in the upper layers of sediment, producing metal concentration profiles that show high concentrations near the sediment surface and lower concentrations at depth, thus closely resembling the increases in heavy metal inputs due to anthropogenic activities.

While concentration measurements may provide useful information about the enrichments of Pb and Hg, they do not enable the discrimination between anthropogenic components and the geogenic background. Pb isotope investigations are a powerful tool for the reconstruction of heavy metal pollution of the environment by anthropogenic activities. Since virtually all of the Pb now present in the atmosphere originates from industrial sources, its isotopic composition is largely determined by that of the ores used to manufacture gasoline additives and other lead products. The isotopic composition of Pb and an understanding of where it is held in the lake sediment matrix, determined by sequential extraction, is very useful in assessing the original source of lead and its depositional and post-depositional history.

1.1 Thesis Objectives

As part of the Health Canada multi-disciplinary study on metal cycling, primarily Hg, in Kejimkujik Park (TSRI Project 124), this study has several objectives:

- In contribution to a mass balance model, this study will determine the flux of Hg and Pb to the lake sediments, as well as estimate the total Hg and Pb stored in the sediments.
- Quantitatively assess anthropogenic versus natural inputs of Hg and Pb to the lake sediments, as well as determine the source of anthropogenic inputs.

- Determine diagenetic conditions of sediments to investigate the processes affecting post-depositional distributions, thus determining whether lake sediments are good archives of anthropogenic activities.

Due to the wide range of objectives in this study, the Results and Discussion section is divided into three parts or chapters:

- ***Part I: Sedimentation, Flux, and Accumulation*** – This chapter presents and discusses sedimentation rates as determined by ^{210}Pb dating, Hg and Pb fluxes through time, and total Hg and Pb accumulations since lake inception.
- ***Part II: Pb Isotope Investigation of Sources and Diagenetic Remobilization*** – This chapter presents and discusses sources of Pb to the sediments as determined from Pb isotope measurements of precipitation and lake sediments. The Pb isotope results are also discussed in terms of diagenetic remobilization and then used to quantitatively determine the proportion of remobilized Pb in surface sediments.
- ***Part III: Supporting Evidence for Diagenetic Remobilization of Pb and Hg*** – This chapter will present porewater analyses that provide supporting evidence for the remobilization of Pb and Hg in these lake sediments.

An overview of mercury in the environment and of the use of lead isotopes for dating sediments and fingerprinting lead pollution is given in the following introductory chapters. However first a review of diagenetic processes in freshwater sediments is necessary to aid in the understanding of topics discussed in the other introductory chapters, as well as those in the Results and Discussion sections.

2. EARLY DIAGENESIS IN FRESHWATER SEDIMENTS

Diagenesis refers to processes that bring about change in a sediment or sedimentary rock subsequent to deposition in water (Berner, 1980). Early diagenesis refers to low temperature reactions occurring during burial to a few hundred metres. However such depths are rare in lacustrine environments, so early diagenesis is more on the order of tens of metres, with the most abrupt changes occurring within centimetres of the sediment-water interface.

Early diagenesis is the changes that occur in the composition and character of sediments due to physical, chemical, and biological processes which begin at the time of deposition. Examples of such diagenetic processes include bacterial decomposition of organic matter, compactive dewatering, bioturbation, diffusion, advection, and ion exchange. Changes arising from these diagenetic processes profoundly affect (1) the physical and chemical stability of organic and inorganic compounds; (2) the fate of pollutants resulting from anthropogenic activities; (3) the formation of humic substances which form metal complexes and act as metal transport agents; and (4) redox potentials, pH, precipitation of carbonates, and formation of sulphides (Barnes et al., 1990).

Although all of these processes are diagenetically important, this chapter will only examine the processes of redox reaction, organic matter decomposition, compaction, and diffusion. However, the process of organic matter decomposition will be emphasized, as this dominant process directly or indirectly affects most other diagenetic processes. For instance, the oxidation of organic matter not only produces energy for the microbial communities, but also results in the release of new compounds which significantly alter redox conditions, pH, and ionic composition of pore waters, the latter of which could result in molecular diffusion due to concentration gradients.

Before describing the diagenetic process of organic matter decomposition, an understanding of redox reaction is needed, as the two processes are closely related.

2.1 Redox Reactions

Many elements exist in nature in more than one valence state. Since the valence state of an element strongly affects its geochemical behaviour, the oxidation of a system is an important geochemical process. The valence state in which an element will be present in a system is determined by the availability of electrons. Oxidation-reduction (redox) reactions involve the transfer of electrons and the resultant change in valence state. Oxidation is the loss of electrons while reduction is the gain of electrons. A common example is the reduction of ferric iron to ferrous iron:

$$Fe^{3+} + e^- \Leftrightarrow Fe^{2+} \qquad [2.1]$$

Elements can be divided into electron acceptors and electron donors, the division of which is related to electronegativity. Electron acceptors are electronegative while electron donors are electropositive. Oxygen is the most common electron acceptor in redox reactions, hence the term 'oxidation'. A system with a low availabilty of electrons due to an excess of electron acceptors is said to be oxidized. Conversely, a reduced system is one with a high availability of electrons due to an excess of electron donors. Since oxygen is the most common electron acceptor, the abundance of oxygen usually, but not always, controls the oxidation state of a system (White, 1997).

To predict the equilibrium oxidation state of a system, the availability of electrons and the valence state of elements as a function of that availabilty needs to be determined (White, 1997). In low temperature geochemisty, this is done using electrochemical potential, or redox potential. Just as pH measures the concentration of H^+ in solution, redox potential measures the tendency of an environment to receive or supply electrons. Because O_2 is readily available as an electron acceptor in aerobic systems it is said to have a high redox potential. Heterotrophic organisms in aerobic systems utilize O_2 as a powerful acceptor of electrons to form H_2O. The electrons in this reaction are derived by the metabolism of reduced or electron-rich organic compounds and oxidized to CO_2.

The redox potential, or oxidation state, of a system is determined by the particular suite of chemical species that are present (Schlesinger, 1991). It is measured as the voltage, Eh, that must be applied to the system to stop the flow of electrons in a particular oxidation-reduction reaction. For example, in the reaction for the reduction of iron

mentioned above (Equation 2.1), the voltmeter measures the voltage, Eh, in millivolts necessary to prevent this reaction.

Most aerobic environments seldom show redox potentials less than +400 mV. In sediments, however, O_2 can be quickly depleted by aerobic respiration during organic matter degradation, such that strong gradients of redox potential may develop in sediments over depths as short as a few millimeters.

Many studies have determined that a particular sequence of reactions is expected as progressively lower redox potentials are achieved (see Table 2.1) (Schlesinger, 1991). As indicated in Table 2.1, once O_2 is depleted, denitrification begins when the redox potential falls to +421 mV, as anaerobic bacteria begin to use nitrate as an alternative electron acceptor in the oxidation of organic matter (Schlesinger, 1991). As redox potential continues to decrease with depth, the sequence of redox reactions continues provided that the necessary molecular species are present. Thus redox potential is important in early diagenesis as it controls the diagenetic reactions that can occur. Furthermore, many elements such as iron and manganese are immobile at the sediment-water interface, yet will dissolve into porewater, and hence become mobile, if conditions become reducing enough with depth (White, 1997).

Table 2.1 Thermodynamic sequence for reduction of inorganic substances at pH 7.0. (From Schlesinger, 1991).

Reaction	E_h
Disappearance of O_2	
$O^2 + 4H^+ + 4e \leftrightarrow 2H_2O$	0.816 V
Disappearance of NO_3^-	
$NO_3^- + 2H^+ + 2e \leftrightarrow NO_2^- + H_2O$	0.421 V
Formation of Mn^{2+}	
$MnO_2 + 4H^+ + 2e^- \leftrightarrow Mn^{2+} + 2\ H_2O$	0.396 V
Reduction of Fe^{3+} to Fe^{2+}	
$Fe(OH)_3 + 3H^+ + e^- \leftrightarrow Fe^{2+} + 3H_2O$	- 0.182 V
Formation of H_2S	
$SO_4^{2-} + 10H^+ + 8e^- \leftrightarrow H_2S + 4H_2O$	- 0.215 V
Formation of CH_4	
$CO_2 + 8H^+ + 8e^- \leftrightarrow CH_4 + 2H_2O$	- 0.244 V

2.2 *Diagenesis of Organic Matter*

2.2.1 Significance, Source, and Characterization of Organic Matter

Organic matter provides the energy source for almost all biochemical and geochemical reactions taking place in the sediments. Furthermore, degradation of organic matter is very important to other aquatic life as it facilitates the recirculation of essential nutrients to the lake systems. In the cycling of carbon, virtually all organic carbon produced by autotrophs is eventually oxidized by respiration, a process called remineralization.

Most of the organic carbon synthesized in aquatic systems never reaches the sediment. Sediment trap studies in Lake Michigan have shown that only 6% of the organic carbon photosynthetically formed in the surface waters reaches the sediment surface 100 m below (Eadie et al., 1984). Furthermore, nearly 85% of the carbon is oxidized before even leaving the thermocline. In shallow lakes however, organic matter has shorter sinking times and consequently less time to be oxidized in the water column. Therefore, the sediments of shallow lakes are usually richer in organic matter.

Of the organic matter deposited to the sediment surface, 30 – 99% is remineralized during early diagenesis (Henrichs, 1992), with a large fraction of the remineralization occurring near the sediment-water interface (McNichol et al., 1988).

Organic matter reaching the sediment surface is made up of a complex mixture of proteins, carbohydrates, lipids, and other hydrocarbons. Together these compounds are termed biopolymers. However, these original biopolymers are rapidly depolymerized to their monomers by microbial processes occurring during and after sedimentation (Barnes et al., 1990). When not utilized in the energy cycles of other microbes, these monomers (amino acids, sugars, and fatty acids) released by decomposition can randomly recombine through abiotic chemical processes to form the geopolymers (humic compounds or humus) found in sediments and sedimentary rocks (Barnes et al., 1990).

As decomposition continues, not only is there an overall decrease in total organic carbon with increasing sediment depth, but the composition of the organic matter also changes, as biopolymers are converted to humic substances. The percentage of humic substances increases from 60-70% in the upper sediments to over 90% in older sediments (Ishiwatari, 1985).

Humic substances are comprised of fulvic acids, humic acids, and humins, the molecular structures of which are poorly known. Since they form by random recombination, their structures are variable and have no consistent repeating units. The structures that they form depend on the monomers present and the diagenetic conditions at the time of formation.

As a result of their variable molecular structures, humic compounds also have no consistent molecular weight. However, it has been identified that humic compounds increase in molecular weight and decrease in solubility in progressing from fulvic acids through humic acids and humins to kerogen (Barnes et al., 1990). Chemical characterization of humic compounds is therefore simply defined on the basis of their solubility and molecular weight.

Humic and fulvic acids are distinguished by their solubility in bases and acids. Fulvic acids are soluble in both acids and bases. Humic acids are base soluble polymers which are soluble in acids with a pH of 2 or higher. At lower pH values, the humic acids are insoluble and will precipitate.

The nonsoluble fraction of organic matter is described by the term humin. Humins are partly hydrolyzable with hydrofluoric acid, that is, they can re-incorporate water and release monomers or lower weight polymers during demineralization (Barnes et al., 1990). Kerogens, in contrast, are high weight geopolymers that are not only insoluble in organic solvents, acids, and bases, but are also unstable to hydrolysis with HF. While some kerogens can arise directly from monomers without an intervening humic stage, particularly under anoxic conditions (Barnes et al., 1990), most form in late diagenesis during thermal maturation in the catagenic stage, and will therefore not be discussed further.

The diagenetically formed geochemical compounds grouped as humic substances, evidently continue to undergo limited diagenetic alteration in lake sediments. With increasing cross linkage and loss of functional groups (carboxyl and phenolic hydroxyl groups), the humic and fulvic acids lose their base solubility and form humins (Barnes et al., 1990). Rea et al. (1980) found the humin fraction of a 1 m sediment core of Lake Michigan to increase from 65% of the total humics at the surface to 85% of the total at the bottom. Some of this increase is thought to arise from conversion of fulvic and humic

acids to humin. However, an overall decrease in total sediment organic carbon downcore indicates that diagenetic loss of organic matter continues throughout the core and that a preferential degradation of fulvic and humic acids occurs. Overall, the decomposition rates of sedimentary organic matter during early diagenesis in lake sediments have been summarized as follows: amino acids >> amino sugars > carbohydrates > humic compounds > lipids (Kemp and Johnston, 1979).

The primary source of organic matter to bottom sediments is particulate detritus of plants within the lakes and terrestrial sources within the watershed catchment. The relative contributions of the two plant sources is strongly influenced by lake morphology, watershed topography, the relative abundance of lake and watershed plants, and the ratio of watershed area to lake area (Meyers and Ishiwatari, 1993).

Organic matter in lake sediments ranges from being predominantly algal in some lakes to land-derived in others. A budget of organic sources to Lake Michigan found that about 90% of organic carbon in waters of the lake originates from algal production, 5% is carried to the lake by rivers, and 5% is brought in with air-borne particulates and precipitation (Andren and Strand, 1981). However, these original source proportions are often not preserved in the sediment record due to selective degradation of more reactive (labile) biopolymers, such as proteins and carbohydrates, as they sink through the water column and upon deposition on the lake bottom.

In general, organic compounds from aquatic sources are more susceptible to microbial decomposition than materials from land sources. This is due to the much larger proportion of resistant lipids and lignins in vascular land plants, and to the fact that land-derived particles have already been weathered (degraded) by the time they arrive in lakes (i.e., they have already had the labile component removed). Organic matter in lake sediments consequently often has a large and relatively unreactive fraction of land-derived organic residues (Meyers and Ishiwatari, 1993), particularly in the humin fraction. This preferential degradation of algal components results in biases in the geopolymer record of organic matter sources retained in the sediments of most lakes (Goossens et al., 1989).

2.2.2 Microbial Decomposition of Organic Matter

Micro-organisms are the primary catalysts for many diagenetic processes. Larger organisms can also contribute to diagenetic changes in sediment composition, but their overall role in the turnover of chemical compounds is usually minor in comparison to micro-organisms, especially bacteria. This can be explained by the fact that bacteria, whose cell size is on the order of a few micrometers, expose a much greater surface area, per unit volume of protoplasm, to the interstitial waters than do larger organisms (Berner, 1980). This allows for much more rapid exchanges of dissolved substances across their outer cell membrane, thus allowing a more rapid metabolism.

The organic matter in sediments provides a large and continuous energy source for bacteria to maintain their metabolism through oxidation reactions. Organic matter decomposition through oxidation reactions starts immediately upon deposition on the sediment-water interface. Oxidation of organic matter is done by hydrolysis, which is the breakdown of larger organic compounds to form smaller ones with the elimination of a H_2O molecule.

In the oxic zone at the sediment water interface, aerobic bacteria utilize dissolved oxygen (O_2) in the breakdown of organic compounds. Upon depletion of dissolved O_2 due to burial or insufficient renewal of oxygenated bottom waters, anaerobic bacteria become the important decomposers. They utilize oxygen combined in inorganic compounds such as nitrate, iron oxides, and sulphate. Depending on the available oxidant (electron acceptor), six different zones or stages have been identified in the oxidative microbial breakdown of organic matter during burial (Claypool and Kaplan, 1974; Berner, 1980). These are:

(1) oxidation zone
(2) nitrate reduction zone
(3) manganese reduction zone
(4) iron reduction zone
(5) sulphate reduction zone
(6) carbonate reduction zone (methane production)

The lower boundary of zone (6) represents the natural boundary of early diagenesis, as bacterial activity ceases below this zone and thermocatalytic reactions begin.

The reason why such a succession of oxidative reactions occurs in sediments can be explained in terms of metabolic free energy yield: the greater the energy yield of a microbial process, the greater the likelihood it will dominate over other competing reactions (Claypool and Kaplan, 1974; Berner, 1980). Therefore, reactions will succeed in the order of their free energy yield, as each oxidizing agent is successively exhausted (Berner, 1980). Table 2.2 lists these bacterial reactions as well as their standard state free energy changes.

Table 2.2 Sequence of oxidative reactions in the bacterial decomposition of organic matter in sediments and their standard state free energy changes (From Berner, 1980).

Reaction	ΔG° (kJ mol^{-1} of CH_2O)
$CH_2O + O_2 \rightarrow CO_2 + H_2O$	-475
$5CH_2O + 4NO_3^- \rightarrow 2N_2 + 4HCO_3^- + CO_2 + 3H_2O$	-448
$CH_2O + 3CO_2 + H_2O + 2MnO_2 \rightarrow 2Mn^{2+} + 4HCO_3^-$	-349
$CH_2O + 7CO_2 + 4Fe(OH)_3 \rightarrow 4Fe^{2+} + 8HCO_3^- + 3H_2O$	-114
$2CH_2O + SO_4^{2-} \rightarrow H_2S + 2HCO_3^-$	-77
$2CH_2O \rightarrow CH_4 + CO_2$	-58

The reactions listed above in Table 2.2 are overall reactions. In reality, the metabolic reactions are much more complex with numerous microbacteria and simultaneous reactions involving enzymes or other natural catalysts. Very little is known about these intermediate reactions and molecules. In fact, biogeochemists are just starting to grasp an understanding of the complex biopolymers used as starting materials in organic decomposition and the resulting geopolymers.

The stepwise oxidation of organic matter results in an interdependence between various species within each community (zone), as well as between communities, as many species are dependent on the waste products of other species. For example, anaerobic bacteria depend on aerobic ones to consume all of the O_2 and produce anoxic conditions. On the other hand, reduced compounds produced by anaerobic communities in deeper

sediments diffuse upwards into the oxic zone where they are oxidized by various photosynthetic, chemosynthetic, and methylotrophic bacteria (White, 1997).

2.3 Advection and Sediment Compaction

Advection is the bulk flow of porewater or sediment relative to a particular reference frame, regardless of its cause. Advection in lake sediments is primarily due to burial and compaction. However, externally impressed flow (hydrologic flow), resulting from gradients in the effective pressure, can also be of significant importance in lacustrine sediments where aquifers come in contact with bottom sediments (Boudreau, 1997). This type of flow however is not common in muddy aquatic sediments because of their low permeabilities relative to sandy sediments.

The burial component of advection is defined by using the sediment-water interface as the reference point. As such, advection results in the solids and porewaters moving away from the interface as sediments are continuously deposited. With negligible compaction, the rate of porewater advection is the same as the rate of burial of sediments, as both solids and included porewater are buried at the same rate (Figure 2.1).

Compaction is the decrease in the volume of sediments from the expulsion of water due to compression arising from the deposition of overlying sediments. During early diagenesis, this results in the closer packing of sediment grains, with the consequent upward expulsion of pore water and decreased porosity. The expulsed porewaters move upward towards the sediment-water interface when viewed from the point of a sediment grain (Figure 2.2). However, with reference to the sediment-water interface, the porewaters still move downward but with a velocity less than that of the solid sediments (Figure 2.2).

If it is assumed that burial occurs without compaction, then the porosity within a given layer does not change during burial. Any variations in porosity with depth would be due to successive burial of layers with different initial porosities (Berner, 1980). When compaction is a significant factor, a concept of steady state compaction is often assumed to simplify calculations and models. Steady state compaction means that the porosity

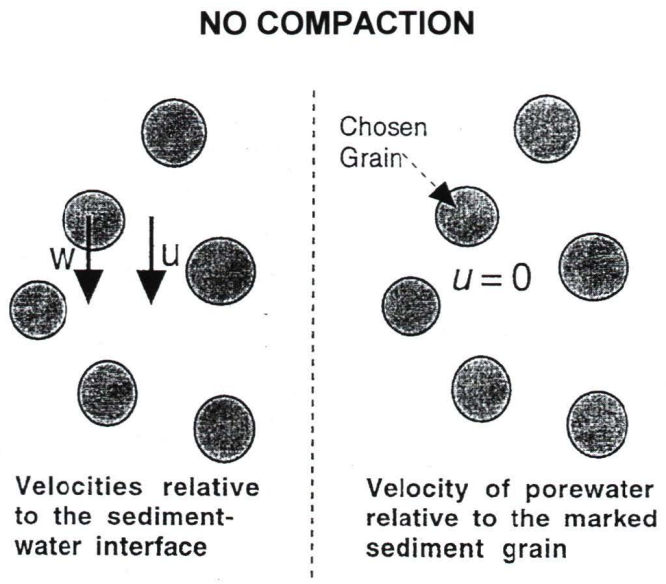

Figure 2.1 A magnified region of a hypothetical sediment with no compaction. (a) shows the velocity vectors of the porewater, u, and solid sediment, w, at a chosen depth relative to the sediment-water interface. (b) is the porewater velocity relative to a reference frame fixed to a chosen grain. The direction of the arrows indicates the direction of flow and their length the magnitude (From Boudreau, 1997).

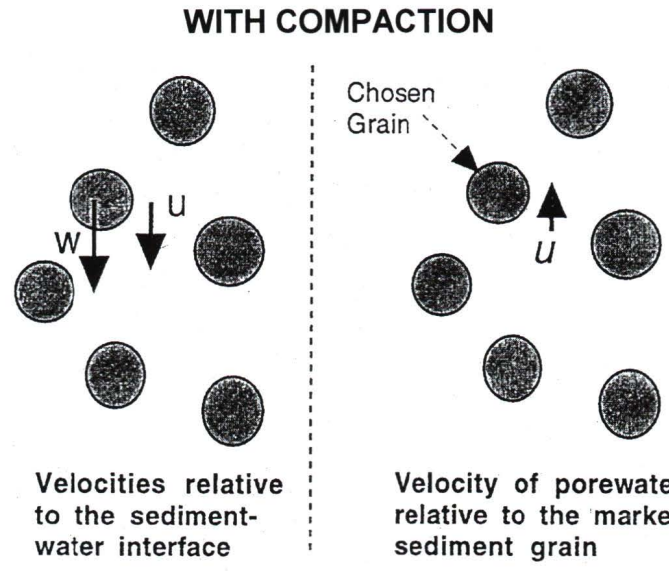

Figure 2.2 Same magnified region as Figure 2.1, but this time with compaction showing that (a) the porewater advection, u, is smaller than the solid sediment advection, w, when viewed from the sediment-water interface; and (b) that porewater advection relative to a sediment grain , u, is upward (From Boudreau, 1997).

changes only as a result of compaction and therefore the sedimentation rate is constant. Berner (1980) states that this would be appropriate for the common early-diagenetic situations of continuous deposition of fine-grained muds.

An important factor affecting compaction is porosity, which is primarily a function of grain size. Sand-sized particles are not as affected by compaction as clay-sized particle. With sand grains, there is simple geometric packing and a resistance to reorientation by slightly angular grains. Therefore sands undergo only minor compaction and, as a result, the change in porosity with depth is minimal.

Clay minerals, on the other hand, have the form of small platelets that form an open structure resembling a house of cards (Berner, 1980). This structure results in very high initial porosities. As such, these fine-grained sediments undergo continual compaction, even on a centimetre by centimetre basis (Berner, 1980). The weight of overlying sediments forces the electrostatically repelling particles together, thus causing a collapse in the house of card structure. However, adjustment of porosity to overlying compressive forces is not instantaneous, as water must be expelled. Rapidly depositing sediments therefore have less time to adjust and consequently have higher water contents (porosity).

2.4 Diffusion in Porewater

Diffusion of solutes is the process by which molecules and ions move from one point in a system to another as a result of random molecular motions. If there are more ions/molecules of a dissolved substance in one region of fluid, random molecular motions due to collisions between solutes and water molecules will eventually lead to homogenization (Boudreau, 1997). Diffusion therefore eliminates concentration gradients by moving solutes down gradient.

There are two dominant types of diffusion in sediment porewater: molecular and ionic diffusion. Molecular diffusion refers primarily to the movement of uncharged species, whereas ionic diffusion refers to the movement of charged species which interact electrostatically. One dimensional molecular/ionic diffusion in an aqueous solution in a porous medium takes place in accordance with Fick's first law:

$$F_D = -\varphi D'(\partial C/\partial x) \quad [2.2]$$

where F_D is the diffusion flux, φ is porosity, D' is the effective diffusion coefficient, C is the concentration of a component, and x is the direction of maximum concentration gradient. The negative sign indicates the flux is in a direction opposite to the concentration gradient.

The effective diffusivity, D', in the above equation is different than, but related to, the value of the molecular/ionic diffusion coefficient in free solution, D. The difference is due to changes in the diffusion coefficient of a solute due to an affect that arises in sediments from a phenomenon called tortuosity. Tortuosity results from the presence of solid particles, which hinder solutes from diffusing freely, as they do in the overlying water column. Instead, a solute must follow a longer tortuous path between and around sediment particles.

Although it is common and much simpler to consider the diffusion of a single species, natural porewaters are solutions of large numbers of different molecules and ions, with variable intrinsic mobilities, and therefore must be looked at as the collective movement of charged and neutral particles. However, neutral species are relatively unaffected by other species, in comparison with ionic species, and can therefore be assumed to migrate according to their tracer diffusion coefficients (Van Cappellen and Gaillard, 1996). In contrast, charged species create electrical potentials, due to their intrinsic differences in ionic mobilities, whose effect is to slow down the faster ions and speed up the slower ones (Van Cappellen and Gaillard, 1996). These electrical potentials have a significant effect on the rate of diffusion of ions in electrolyte solutions. To account for these effects, the electrostatic interactions between ions must be depicted using a complex multicomponent diffusion method.

In some environments, this multicomponent method may be of limited value because the coupling effects arising from electrostatic interactions are minor. This is true for ionic diffusion in most marine environments, where the presence of a large excess of background electrolyte (NaCl) cancels out the effects of small diffusion potentials (Van Cappellen and Gaillard, 1996). In freshwater sediments, cross-coupling effects are nearly always important because there is no background electrolyte, and because early diagenetic reactions cause major changes in the chemical composition of porewaters

(Van Cappellen and Gaillard, 1996). In particular, these effects are magnified at the sediment-water interface, where composition gradients in porewaters are largest. Unfortunately, the consequences of multicomponent diffusion for reactive transport in freshwater sediments have not yet been investigated in a systematic way.

3. MERCURY IN THE ENVIRONMENT AND LAKE SEDIMENTS AS HISTORICAL ARCHIVES

Due to potential impacts on human and ecosystem health, interest in mercury as an environmental contaminant has been high for the past four decades. This toxic heavy metal is of particular concern because of its ability to bioaccumulate and biomagnify in aquatic food chains. Elevated mercury levels are now commonly found in predatory fish in remote wilderness lakes far removed from industrial pollution sources (Driscoll et al., 1994a). As of 1998, five Canadian provinces and 39 American states had issued consumption advisories for freshwater sport fish because of mercury contamination (NESCAUM, 1998). Increased atmospheric mercury deposition from anthropogenic activities is generally accepted as a source contributing to the widespread contamination of mercury in terrestrial and aquatic ecosystems.

Lake sediments are commonly used by many researchers as natural recorders of changes in atmospheric mercury deposition through time. However despite intensive biogeochemical studies of mercury in freshwater lakes in Canada (Mierle, 1990; Lucotte et al., 1995), the United States (Driscoll et al., 1994a, 1998), and Scandinavia (Verta et al., 1994), our understanding of the mercury sources involved and processes controlling the chemical distribution, speciation, and fate of mercury in the global mercury cycle remains incomplete. With regards to lake sediments, the cause of depth concentration profiles and the degree to which downcore profiles represent a primary signal is still greatly debated. This section gives a general summary of mercury in the environment and the plausibility of lake sediments as archives of atmospheric mercury deposition.

3.1 Sources of Mercury in the Environment

Mercury is ubiquitous in the natural environment and exists in many chemical forms. However the numerous mercury species can be simplified to three general forms: elemental (Hg^0), ionic or inorganic [Hg(II)], and organic (MeHg). In the atmosphere, the main form of mercury is elemental mercury (Hg^0), while in water the predominant form is inorganic mercury, bound to various organic and inorganic ligands. In the food chain,

the most predominant form of mercury, and therefore most toxic, is methyl mercury (CH_3Hg^+) because of its ability to bioaccumulate and biomagnify.

Mercury undergoes transformations among its many chemical forms and the chemical form of mercury in turn affects its transport in and between air, land, and water, as well as its chemical and biological behaviour (Porcella, 1994). Such behaviour has resulted in the global distillation of mercury, also referred to as the grasshopper effect, in that it is volatile and when deposited can be re-volatilized only to be re-deposited again elsewhere (Beauchamp, 1998). This complexity in the chemical and physical behaviour of mercury is what makes the study of its biogeochemical cycle so difficult.

Quantifying the magnitude of mercury emissions from major sources and determining the relative importance of natural versus anthropogenic sources to the air, lakes, and biota is a topic of great interest and considerable debate in the scientific community. Mercury is present in the environment as a result of both natural and anthropogenic inputs, however the complex nature of mercury speciation has made it extremely difficult to differentiate between natural sources and loadings and those resulting from anthropogenic activities. Recent studies estimate the total mass of mercury in the atmosphere to be 5000 to 6000 metric tonnes (Fitzgerald, 1989), which is thought to be 3 times higher than preindustrial levels due to anthropogenic inputs (Mason et al., 1994; Fitzgerald et al., 1998).

3.1.1 Natural Sources

Mercury is naturally emitted from rocks, soil, water, and biota primarily as elemental mercury vapor and to a lesser extent as particulate and vaporous oxides, sulphides and halides of mercury, and methyl mercury vapors (Rutherford, 1998). The US EPA (1994) listed the following as primary sources of natural mercury emissions to the atmosphere, in order of probable importance: volatilization in aquatic environments; volatilization from vegetation; degassing of geological materials; expulsion of particulate matter and vapor during volcanic and geothermal activities; release from windblown dust; and wildfires. Together these natural sources are estimated to emit 2000 to 3000 tonnes of mercury to the atmosphere per year, accounting for approximately 40% of the total annual global emissions (US EPA, 1994). However, estimates of natural emissions are

uncertain, largely because a substantial portion of present-day terrestrial and aquatic inputs are from the re-emission of previously deposited anthropogenically-derived mercury (Porcella, 1994). Furthermore, estimates of mercury evasion from the land component of natural emissions are believed to be inaccurate because they have not been constrained by direct measurements and are instead determined by difference in global mass balance calculations (Porcella, 1994). Mason et al. (1994) also pointed out that many global mercury budgets ignore ocean recycling and may therefore underestimate the anthropogenic signal by about 25%. They estimate that only 20-30% of the current global emissions are from natural inputs.

3.1.2 Anthropogenic Sources – Past and Present

Over the last 500 years, an estimated 800,000 tonnes of mercury has been extracted from various mines around the world (Hylander and Meili, 2003). Initially, this mercury was primarily used for gold and silver extraction. Today it is utilized in a wide variety of industrial and agricultural applications. The primary sources of modern anthropogenic emissions to the atmosphere are industrial processes such as coal and oil combustion, waste incineration, base metal mining and smelting operations, and chlor-alkali plants (Lindqvist, 1994; Pirrone et al., 1998). Other significant anthropogenic sources include cement manufacturing, crematories, primary and secondary mercury production, agricultural chemicals, degassing of latex paints, fluorescence lamp breakage and disposal, and dental laboratories (Pirrone et al., 1998; Rutherford, 1998).

Figure 3.1 shows Pirrone et al.'s (1998) estimates of annual Hg emissions to the atmosphere from gold and silver mining and modern industrial sources for the 1800-1990 period. Historically, gold and silver mines were the dominant source of atmospheric mercury pollution (Nriagu, 1994), until about 1920 when fossil fuel combustion and waste incineration became the dominant sources.

Mercury has been used for centuries as a cheap and simple method for the extraction of silver and gold in the *patio* or mercury amalgamation process. The method was largely replaced by the cyanide concentration method by the late 1920's (Pirrone et al., 1998), but continues to be utilized in developing countries, particularly in the Amazon region of South America. The current loss of mercury associated with Hg

extraction techniques in the Brazilian Amazon is estimated to be 65-83% (1.3-1.7 kg/kg of gold recovered) (DeLacerda et al., 1991). These estimates are believed to be similar to pre-industrial and colonial losses (Nriagu, 1994, Pirrone et al., 1998).

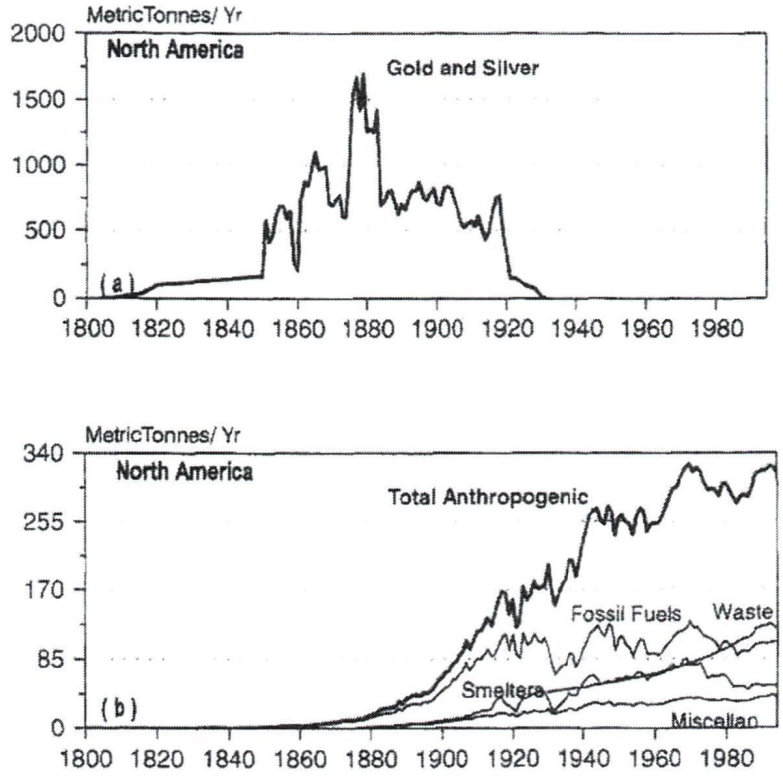

Figure 3.1 North American mercury emissions (t/yr) from (a) gold and silver mining, and (b) modern anthropogenic sources (From Pirrone et al., 1998).

The dramatic increase in gold and silver production in the mid-1800's, primarily in the Americas, resulted in significant increases in atmospheric mercury emissions between 1850-1900 (Nriagu, 1994)(See Figure 3.1a). Nriagu (1994) estimated average mercury emissions from gold and silver mining in the United Stated during the 1850-1900 period to be 780 tonnes/yr, which exceeds the estimates of current mercury emissions of 260-600 tonnes/yr in the United States from all industries. Central and South America averaged 525 tonnes/yr during the same period (Nriagu, 1994), while the current gold

rush in the Amazon is reported to release 90-120 tonnes/yr (DeLacerda et al., 1991). Pirrone et al. (1998) have estimated the cumulative amount of mercury added to the atmosphere from precious metals mining in North America during the 1800-1920 period shown in Figure 3.1a to be nearly 60,000 tonnes. The environmental implications of this historic source to the global and regional mercury cycle are only beginning to be realized. Nriagu (1994) pointed out that re-emission of only 0.2% of the mercury lost in the United States would amount to a substantial fraction of the mercury currently being released by anthropogenic sources in that country.

Fossil fuel combustion and waste incineration are presently the largest contributors of mercury to the global atmosphere. Nriagu and Pacyna (1988) estimated average worldwide mercury emissions from fossil fuel combustion to be 1500 tonnes/yr, with a range of 700-3800 tonnes/yr. The large variability in estimates of fossil fuel combustion is due to differences in the composition of fuels. Fuel can be quite clean or it may contain substantial inclusions of contaminants such as minerals that include mercury (Porcella, 1994). Estimates from waste incineration are also difficult because the number of incinerators is increasing, controls on emissions are rapidly changing, and the mercury content of the wastes being combusted is continuously changing (Porcella, 1994). Nriagu and Pacyna (1988) have estimated worldwide waste incineration to emit approximately 600 tonnes of mercury per year. However, in North America, waste incineration is thought to account for as much as 40% of current anthropogenic emissions (Pirrone et al. 1998) (See Figure 3.1b).

Due to anthropogenic activities, global atmospheric mercury levels are believed to have tripled since the industrial revolution (Mason et al., 1994; Fitzgerald et al., 1998), with estimates of an average annual increase between 0.6% (Fitzgerald, 1995) and 2% (Swain et al., 1992). Lindqvist et al. (1991) estimate anthropogenic mercury emissions to be 4500 tonnes/yr, approximately 60% of the total mercury influx to the atmosphere, but actual emissions could vary by a factor of two. More recently, Mason et al. (1994) estimate that as much as 70-80% of current emissions are of anthropogenic origin.

During the 1800-1990 period in North America, cumulative mercury emissions to the atmosphere from modern industrial sources are estimated to be 22,327 tonnes: 10,000 tonnes from fossil fuel combustion, 5077 tonnes from waste incineration, 4680 tonnes

from modern non-ferrous metals manufacturing, and 2570 tonnes from miscellaneous sources (Pirrone et al., 1998). Together with the estimated 60,000 tonnes released from precious metals mining during the 1800-1920 period, yields a cumulative estimate of 82,000 tonnes of mercury released to the atmosphere since 1800 in North America alone (Pirrone et al., 1998).

3.2 Mercury in the Atmosphere

The atmosphere plays an important role in the redistribution of mercury in the environment. Mercury in the atmosphere exists in all three phases (solid/particle, liquid, and gas), but occurs almost exclusively (~98%) as Hg^0 vapour (Mason et al., 1994). Natural sources primarily emit mercury to the atmosphere in elemental form (Hg^0), while anthropogenic sources emit both Hg^0 and Hg(II) in the gaseous and particulate phases (Pirrone et al., 1998). Mercury emitted to the atmosphere from both natural and anthropogenic sources enters the global mercury cycle if emitted as Hg^0, but is deposited locally or regionally if emitted as Hg(II). The Hg(II) from anthropogenic sources becomes associated with particles prior to or soon after emission and therefore has varying residence times that depend on particle size and wind speed (Porcella, 1994). The residence time of Hg(II) is estimated to be on the order of hours to days and is thus deposited on local (<100 km) and regional scales (100-2000 km) (Pirrone et al., 1998). In comparison, Hg^0 has an average residence time of one year (Fitzgerald, 1989). However, Hg(II) can contribute to the global atmosphere if associated with submicron particles, which can be transported long distances, or once deposited and reemitted as Hg^0 (Fitzgerald et al., 1994).

3.2.1 Atmospheric Deposition

The ultimate fate of atmospheric mercury is dry or wet deposition, the latter of which is believed to be the predominant form of removal (Lindqvist et al., 1991). Although the majority of mercury in the atmosphere is composed of Hg^0, atmospheric deposition occurs primarily in the oxidized forms [Hg(II) and MeHg] (Fitzgerald et al., 1991). Mercury can undergo various different chemical and physical transformations in the atmosphere including: oxidation by ozone, peroxide, sulphate, or other compounds;

photoreduction; adsorption and desorption from particulates; and removal by wet or dry deposition processes. Once converted to Hg(II) compounds, which are highly soluble, mercury is readily removed from the atmosphere by precipitation.

A number of estimates for mercury deposition (wet + dry) have been made in mid-latitude North America: 10-13 $\mu g/m^2/yr$ from rain data (Fitzgerald et al., 1994); 23 $\mu g/m^2/yr$ from an ombrotrophic peat bog (Benoit et al., 1994); and 12.5 $\mu g/m^2/yr$ from lake sediments. From a compilation of these and several other studies, Pirrone et al. (1998) estimate an average present day deposition of 16 $\mu g/m^2/yr$ for the mid-latitude regions of North America. Pre-industrial values have been estimated to be 3.7 $\mu g/m^2/yr$ (Swain et al., 1992).

3.3 Mercury in Terrestrial Environments

Terrestrial ecosystems are the main receptors of airborne contaminants and play an important role in the delivery of Hg and other heavy metals to lacustrine environments through the weathering and transportation of catchment soils. Several factors contribute to and influence mercury levels in soils including: parent rock material, wet and dry atmospheric exchanges (deposition and volatilization), uptake and degradation of organic matter, discharges of anthropogenic waste, and hydrologic and mass movement processes (Schuster, 1991). Mercury in soils can exist in the following forms (from Schuster, 1991):

- Dissolved (soluble inorganic and organic complexes, MeHg)
- Non-specifically adsorbed (e.g. electrostatic forces)
- Specifically adsorbed (e.g. covalent bonding)
- Chelated (i.e. involving multiple bonds with functional groups)
- Precipitated (e.g. HgS, $HgCO_3$, etc)

Most of the atmospherically deposited mercury is immobilized by organic material in the shallow soil horizons. Lorey and Driscoll (1999) reported a watershed retention of atmospheric Hg of 78% for the Adirondack study lakes. Other studies have

estimated mercury retention rates as high as 94% (Kamman and Engstrom, 2002; Scherbatskoy et al., 1998). Even though only a small percentage of the mercury in soil (<0.1% of catchment total: Aastrup et al., (1991)) is transported in runoff from soil to surface waters, this terrestrial input can make up 25 to 75% of the mercury reaching lakes (Johansson et al., 1991). A variety of factors controlling Hg delivery through watersheds have been identified, including DOC, pH, and alkalinity (Driscoll et al., 1994a,b,1998), wetland area (Driscoll et al., 1994b), land use (Hurley et al., 2000), and watershed size (Mieli, 1995; Lorey and Driscoll, 1999).

3.4 Mercury in Aquatic Environments

Mercury cycling in lakes is complicated and many gaps still remain in our understanding of mercury speciation in aquatic systems and the mechanisms of its reactions. However, knowledge of the basic reactions that govern the behaviour of mercury in the environment have enabled the formulation of mercury cycling models (Hudson et al., 1994; Bjornberg et al., 1988). Figure 3.2 is a depiction of the simplified steady-state lacustrine mercury cycling model of Hudson et al. (1994). The figure illustrates the essential components – Hg^0, Hg(II), and CH_3Hg; reactions – reduction, methylation, and demethylation; and transport processes – deposition, gas exchange, and scavenging by particles (Hudson et al., 1994).

Total mercury concentrations in remote lakes typically range from 0.5 - 4 ng/L (Watras et al., 1994). Major sources of mercury to lakes are atmospheric deposition and surface and ground water inputs. The relative importance of these sources is variable and largely dependant on watershed to lake area ratios. The form of mercury released into aquatic systems and the geochemical conditions of that system (pH, Eh, DOC, SO_4, Cl^-, etc.) control its reactivity and transformation rates (Stumm and Morgan, 1996; Hudson et al., 1994). Mercury inputs are primarily in the form of Hg(II), both reactive and unreactive (inert). Reactive Hg(II) species, which includes dissolved inorganic Hg complexes (e.g., $HgCl_4^{2-}$, $Hg(OH)_2$), labile organic complexes, and labile particulate Hg species, provide the reactant for Hg^0 formation and monomethylmercury production in

natural waters (Mason et al., 1994, Fitzgerald et al., 1994). There is some indication that reduction and methylation processes compete for the available Hg inputs, with reduction of reactive Hg occurring principally in oxic surface waters and methylation often confined to deeper low oxygen regions (Mason et al., 1994; Watras et al., 1994). Methylation may be affected by redox conditions and sulphur cycling via sulphate reduction (Watras et al., 1994). Demethylation is the principal source of Hg^0 in low oxygen waters (Mason et al., 1994).

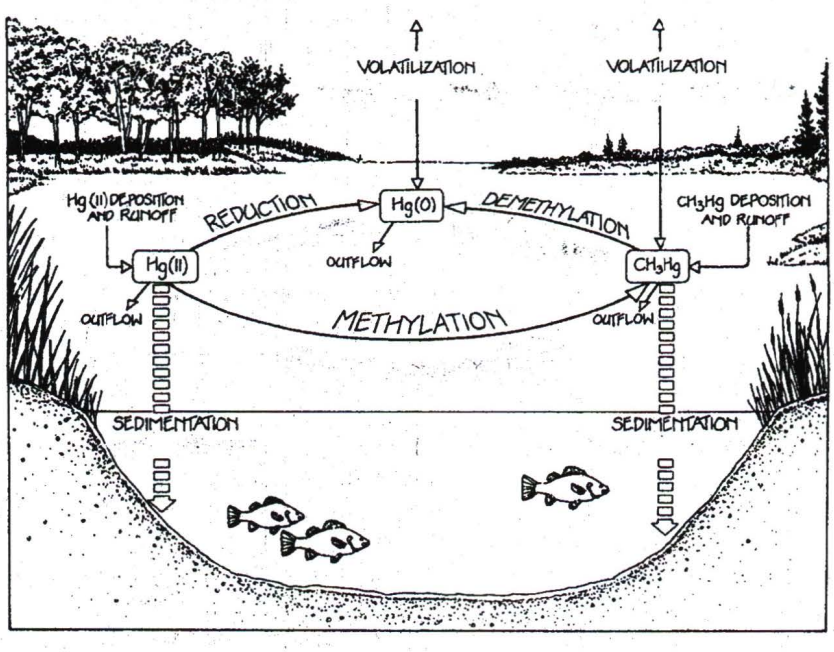

Figure 3.2 Schematic depiction of the lacustrine mercury cycle in the steady-state MCM (From Hudson et al., 1994).

There are three main routes of mercury loss from a lake: (i) outflows, (ii) evasion to the atmosphere, and (iii) sedimentation (US EPA, 1997). Dissolved elemental mercury (Hg^0) has a low solubility in water (Stumm and Morgan, 1996) and therefore most of the reduced mercury (Hg^0) produced in the water column, and perhaps in porewaters, is lost to the atmosphere through evasion. Measurements from seepage lakes from the Mercury in Temperate Lakes project (MTL) found that Hg evasion ranged from 5 to 50% of the total deposition (Watras et al., 1994). Hg(II) and MeHg losses primarily occur by outflow

and sedimentation. Both Hg(II) and MeHg have a strong tendency to adsorb to particulates, thus suspended matter plays an important role in the transport of mercury. Mercury accumulated in sediments is still available to biotic and abiotic processes that can convert Hg(II) to MeHg or Hg^0 (Ramlal et al., 1985; Hudson et al., 1994). Therefore, although sediments are considered important Hg sinks, they are also an important source of Hg to the overlying water column (O'Driscoll, in review; Ramlal et al., 1985).

3.4.1 Methylmercury and Bioaccumulation in Aquatic Biota

Methylmercury (MeHg or CH_3Hg) is the main form of mercury that bioaccumulates in aquatic biota. Dissolved mercury compounds are primarily uptaken by primary producers (i.e. phytoplankton), although higher trophic levels may also be able to process Hg directly from water. As secondary producers (i.e. zooplankton) consume primary producers, both inorganic Hg and MeHg are bioconcentrated, but the process is much less efficient for inorganic Hg (Mason et al., 1995). The inefficiency continues up the food chain resulting in increased MeHg to inorganic Hg ratios in higher organisms (Lasorsa and Allen-Gil, 1995). Watras et al. (1994) found that the bioconcentration factor for MeHg in remote Wisconsin seepage lakes increased threefold for each trophic level, leading to a biomagnification factor in fish of about $10^{6.5}$ relative to water concentrations. Such high degrees of biomagification have lead to contaminated fish stocks in even very remote northern lakes (Lindqvist et al., 1991).

Typically, methylmercury makes up a very small percentage of total mercury inputs to lakes. MeHg inputs to Wisconsin seepage lakes have been estimated to be about 1% of total Hg (Watras et al., 1994), however drainage lakes and lakes with adjacent wetlands have larger MeHg inputs (Driscoll et al., 1994a), likely due to mercury's strong affinity to humic substances and DOC (Petterson et al., 1995; O'Driscoll and Evans, 2000). Lake sediments also contain low concentrations of MeHg: <0.1 to 3% (Gilmour and Henry, 1991; Watras et al., 1994). These findings together with high biotic MeHg concentrations indicate that in-situ production of MeHg is a major source of MeHg to lakes and biota and that transport of MeHg to the food chain is rapid (Watras et al., 1994).

3.5 Mercury in Lake Sediments

Sediments are the largest reservoir of mercury in lacustrine ecosystems. Sedimentary concentration profiles of Hg (and other trace metals) from natural lakes around the world exhibit exponential-like increases in the surface (modern) sediments relative to deeper background sediments. Because the increases appear to coincide with the history of anthropogenic pollution and because Hg (and other metals) have been shown to form stable complexes with organic ligands and oxides (Davis, 1984; Tessier et al., 1996), lake sediments have been used by many researchers for many years as recorders of paleo-deposition (Swain et al., 1992: Lucotte et al., 1995; Fitzgerald et al., 1998; Lorey and Driscoll, 1999; Lamborg et al., 2002). As such, upcore enrichments in Hg concentrations profiles have been attributed to increased global inputs from anthropogenic activities. Similarly, decreases in some surface sediments are interpreted to be the result of recent regional or local emission reductions (Vile et al., 2000). While increased anthropogenic emissions likely have contributed to increased deposition, the cause of depth concentration profiles and the degree that downcore trends represent a primary signal is still hotly debated. Lakes are dynamic biogeochemical reactors and several authors argue that vertical concentration profiles can be influenced by sediment composition and post-depositional diagenetic reactions (Matty and Long, 1995; Rasmussen et al., 1998; Gobiel et al., 1999; El Bilali et al., 2002). The following two sections will examine both sides of this debate whether lakes sediments are reliable archives of atmospheric Hg deposition.

3.5.1 Lake Sediments as Historical Archives

In a recent critical review of atmospheric Hg contamination in remote areas, Fitzgerald et al. (1998) presented arguments for the utility of lake sediments to preserve the Hg accumulation signal. This section will review the main arguments and studies discussed in that article.

Fitzgerald et al. (1998) explain that lake sediment records from around the world show a pattern of recent Hg enrichments that are both spatially and temporally coherent and not easily explained by either diagenetic processes or local geological factors. As previously discussed, global anthropogenic Hg emissions have been increasing for the last 100-150 years. Numerous well-dated sediment cores from the midwestern United

States show increases in Hg concentrations (or fluxes) starting in the mid-1800's (Swain et al., 1992; Engstrom and Swain, 1997). More remote locations such as northern Canada (Lucotte et al., 1995) and Scandinavia (Verta et al., 1989) show the Hg rise occurring somewhat later but the chronologies are consistent within each geographical region. As such, it is thought to be highly improbable that synchronous inter-lake and intra-lake Hg increases could be generated in sediment profiles of varying thickness by post-depositional diagenetic processes (Fitzgerald et al., 1998).

Further supporting the argument that lake sediment profiles represent a primary signal is that the magnitude of Hg increases relative to background sediments is similar across large geographic areas (Fitzgerald et al., 1998). Studies of remote lakes in North America, Europe, and New Zealand report a similar range of enrichments (2-5 times; Lindqvist et al., 1991), with modern Hg concentrations (or fluxes) being an average of 3 times higher than background levels (Swain et al., 1992; Lucotte et al., 1995, Fitzgerald et al., 1998; Lamborg et al., 2002; Yang et al., 2002). These enrichments also show spatial trends with higher enrichments occurring closer to industrialized areas (Johansson et al., 1991). Thus, even though the Hg loading among lakes is variable, the similarity in timing and magnitude of Hg increases since industrialization, together with spatial trends that are in concordance with direct atmospheric measurements, strongly suggests that long-range transport of anthropogenic Hg is the cause of upcore enrichments in sediments of remote lakes (Fitzgerald et al., 1998).

To test the fidelity of lake sediment core records to known Hg contamination histories, Lockhart et al. (2000) compared the sediment records of three Canadian lakes to their independently known Hg input histories: Clay Lake, ON with a known history of Hg discharges from a chlor-alkali plant; Giauque Lake, NWT where Hg was used at a gold mine for a known period; and Stuart Lake, BC, which is located 5 km downstream of Pinchi Lake where a Hg mine operated for two distinct periods. The histories of Hg deposition derived from sediment cores from each lake agreed well with the known histories of inputs. The lake producing the most convincing evidence that diagenetic processes are not a major influence on Hg accumulation patterns in lake sediments is the Clay Lake site, which has also been cored two other times over the last 30 years. Clay Lake received inputs from a chlor-alkali plant that discharged Hg from 1962 until 1970

(Armstrong and Hamilton, 1973). In 1971 a core was taken from the lake that showed a Hg peak at the surface of the sediments (Armstrong and Hamilton, 1973). Another core was taken in 1978 that showed the Hg peak several centimetres deeper (Rudd et al., 1983). Then when Lockhart et al. (2000) cored the lake in 1995, they found the Hg peak a few centimetres deeper than observed in 1978, presenting compelling evidence that the sediments have preserved a faithful record of Hg inputs to the lake over the last 50 years. However, while these three study lakes are commonly used to argue the case that lake sediments cores are reliable records of historical Hg inputs, Lockhart et al. (2000) themselves point out that their case histories cannot establish the credibility of sediment cores in general.

3.5.2 Evidence for Diagenetic Remobilization in Sediments

As previously discussed, microbial decomposition of organic matter in sediments consumes free oxygen and oxygen donors, forming a classical redox profile from oxic conditions near the surface to highly reducing (low Eh) at depth. In freshwater sediments, free oxygen is often consumed within the first 2 to 5 centimetres (Stumm and Morgan, 1996). After NO_3^- and Mn-oxides have been stripped of their oxygen and at around the same conditions that reduce Fe-oxyhydroxides, the oxidized mercury ion (Hg^{2+}) can be reduced to form aqueous elemental mercury $Hg^0(aq)$, also called dissolved gaseous mercury (DGM). If sulphur is present, the microbial reduction of sulphate (SO_4^{2+}) can cause Hg to precipitate as HgS, which is relatively insoluble and biologically unavailable to organisms. In this case, all, or a portion of available Hg may be permanently sequestered into the sediments. Hg is also known to co-precipitate with Fe- and Mn-oxyhydroxides. Typically, this occurs in the uppermost sediments in the presence of molecular oxygen. And so in some settings, lake sediments can contain both a shallow and deep biogeochemical sink for Hg. In such environments, Hg may be sequestered almost immediately after its reduction, with very little, if any vertical movement within the sediment column, thus not significantly altering the primary depositional record. Another possibility is that the reduced Hg may be mobilized and diffuse or advect to the depths at which these traps occur, possibly causing significant alterations to the

concentration profile such as greater surface enrichments or false peaks that are only indirectly related to atmospheric inputs.

However, the occurrence of these Hg traps is dependent primarily on the concentrations of SO_4^{2+}, and Fe(aq), and the type and flux of organic matter delivered to the sediments, which ultimately control the Eh and pH. And so, in some settings, the formation of sedimentary Hg sinks may not occur and so aqueous and desorbed Hg that is released through organic matter decay may diffuse upwards to the sediment water interface (SWI) and back into the water column.

This diagenetic release and mobilization of Hg by diagenetic processes is the main argument against using metal enrichments (including Hg and Pb) in surface sediments as historical records of atmospheric pollution (Matty and Long, 1995; Rasmussen et al., 1998; El Bilali et al., 2002). The basis of this argument comes from detailed partitioning studies of trace metal distribution in sediment phases that show, despite a wide range of organic matter and clay contents, Hg (as well as other heavy metals including Pb) in lake sediments is primarily associated with humic and fulvic acids and to a lesser extent with amorphous Fe and Mn oxides in surface sediments (Matty and Long, 1995; Rasmussen et al., 1998; El Bilali et al., 2002). In deeper sediment, Hg is mainly associated with insoluble organics and sulphides and crystalline Fe and Mn oxides (El Bilali et al., 2002; Matty and Long, 1995). The association of Hg and Pb with humic material and Fe and Mn oxides in surface sediments can, as discussed, result in recycling via release to porewaters as a consequence of organic matter decay and/or oxide dissolution, followed by upward migration and subsequent sorption by humic material or coprecipitation with oxides at the surface (El Bilali et al., 2002). Matty and Long (1995) provide further support for this view with porewater profiles from sediments of the Great Lakes, which show Hg concentration gradients that suggest upward diffusion of Hg may be occurring. Other studies have also found evidence for the diagenetic remobilization of Hg including Eganhouse et al. (1978), Strunk (1991), Krabbenhoft and Babiarz (1992), and Gobeil and Cossa (1993). However detailed porewater Hg profiles which could confirm the diagenetic release of mercury are often lacking from most sediment studies.

While Fitzgerald et al. (1998) acknowledge that metal enrichments in the study lakes of Matty and Long (1995) and Rasmussen et al. (1998) may have been affected by diagenetic processes, they argue that this is not the case in general. They argue that if this were generally true, we should find (1) approximately the same kind of profiles for Fe, Mn, and Hg, (2) a probable correlation of Hg with Fe and Mn in surface sediments when comparing several lakes, and (3) no clear geographical pattern for Hg (Fitzgerald et al., 1998). They then point out that none of these points are valid in several studies conducted by Verta and co-workers in Finland (Verta et al., 1989, 1994). Furthermore, deep porewater release is dismissed as being unimportant arguing that porewater Hg concentrations of several hundred nanograms per litre would be necessary to create a diffusion gradient (Hurley et al., 1994) and no such levels have been reported by researchers (Fitzgerald et al., 1998).

In summary, there are strong arguments supporting the reliability of lake sediments to preserve historical inputs of anthropogenic mercury, however there is also a growing body of evidence that diagenetic processes may contribute to surface enrichments. As such, studies attempting to utilize lake sediments for the measurement of historical atmospheric deposition, should carefully examine the diagenetic conditions of the sediments to evaluate the possible influence of post-depositional diagenetic processes on concentration profiles.

4. LEAD ISOTOPES IN ENVIRONMENTAL STUDIES

The earth's atmosphere has been contaminated in varying degrees by Pb due to anthropogenic activities since about 4500 yr bp, when technologies for smelting lead sulphide ores and cupellation of silver from Pb were developed in Southwestern Asia (Patterson, 1971). Shirahata et al. (1980) have estimated that today anthropogenic Pb pollution accounts for 96 to >99% of total atmospheric Pb deposition. Deposition of such large quantities of this toxic heavy metal into the environment has become a major ecological and health concern. As such, studies of the magnitude, timing, and transport of Pb pollution have become exceedingly important in the last few decades.

Anthropogenic Pb is derived from lead sulfide ore deposits and is released to the environment primarily by the combustion of gasoline and as a by-product of industrial activities (Chow and Johnstone, 1965; Chow et al., 1973; Shirahata et al., 1980; Sturges and Barrie, 1987). The isotopic composition of anthropogenic Pb emitted to the atmosphere is largely controlled by the isotopic value of the ore bodies used for the production of petrol (alkyl)-Pb. Each natural lead deposit has a characteristic isotopic composition, and this unique property can be used to trace Pb pollutants in the environment.

Pb isotopic values can be measured directly from the atmosphere as well as preserved in natural archives such as lake and marine sediments, snow and ice, coral reefs, lichen, and peat bogs. From the concentration of radiogenic Pb data, it is difficult to evaluate the relative importance of the different anthropogenic components, and to discriminate the non-geogenic components from the geogenic background (Kober et al., 1999). Pb isotope distributions and the fingerprint method for Pb in the environmental archives help to quantify the anthropogenic component for a given site, and to identify the heavy metal sources and the pathways of contaminating elements.

In the case of lake and marine sediments, continuous pollution records over time can be derived which display onset and variations of Pb contamination of the studied sites. Concentrations of Pb in the environment, however, have significantly declined since the late 1970's after the use of alkyl-leaded gasoline was banned subsequent to the

adoption of clean air legislations by Canada and the USA. Evidence of these changes are often preserved in lake sediments and therefore an accurate chronology tool is required for determining the history of such changes in lakes and their watersheds. Traditionally chronology has been based on qualitative methods, such as stratigraphy and palynology, applicable to clay and biogenic sediments that are laminated (Krishnaswamy et al., 1971). However, radiogenic dating using ^{210}Pb has become more common for dating sediments deposited in the last 100-150 years (Turner and Delorme, 1996).

Unlike the radiogenic Pb isotopes used to fingerprint the sources of Pb pollution, the ^{210}Pb isotope is radioactive and can therefore be used as a geochronology tool to determine sedimentation rates and thus date pollution events. Initial geochronology work using the decay of naturally occurring ^{210}Pb was done by Goldberg (1963) on permanent snowfields of Greenland. Rates of accumulation of snow were found to be in agreement with those determined from stratigraphic markers. Later, Krishnaswamy et al. (1971) began using ^{210}Pb chronology to determine rates of sedimentation in lakes. Assuming a constant rate of ^{210}Pb deposition with time, results were also in agreement with those determined by independent techniques. The successful utilizations of the ^{210}Pb method in sedimentation processes have since prompted the wide use of it in both lacustrine and marine environments.

This chapter is an overview of the ^{210}Pb dating method and the use of Pb isotope ratios in fingerprinting sources of Pb pollution. However, an explanation of isotopes and radioactive decay will be given first to aid in the understanding of these radiogenic isotope methods.

4.1 Radiogenic Isotopes

4.1.1 Nuclides and Radioactive Decay

In isotope geology, the fundamental building blocks of the atom are neutrons, protons, and electrons (Dickins, 1995). Atoms, or nuclides, are typically described by the composition of their nuclei. Nuclei are made up of various numbers of neutron (N) and protons (Z). However, not all possible combinations of protons and neutrons result in

stable nuclei. A chart of known nuclides with Z plotted against N is given in Figure 4.1. The 264 presently known stable nuclides define a central path of stability or an energy valley in Figure 4.1 (Dickins, 1995). The nuclides on either side of this path are unstable and tend to undergo increasingly rapid decays as distance from the path increases. The shape of the path in Figure 4.1 also shows that the greatest stability for low atomic mass nuclides is when N≈Z. For heavier nuclides, the field of stability moves in the direction of N>Z (White, 1997).

The process of radioactive decay is the movement of unstable nuclides into or towards the energy valley by the emission particles and energy. The type of particle emitted (α, β, or γ) depends on the position of the radionuclide relative to the energy valley.

Nuclear decay of unstable nuclides occurs at a rate that follows the law of radioactive decay. The decay rate is proportional to the number of atoms present at any time and independent of the past history of the nucleus and external forces such as pressure, temperature, etc. (White, 1997). Although it cannot be predicted when a given nucleus will decay, it is possible to predict the probability a nucleus will decay in a given time interval. This is known as the rate constant, λ, and has units of time^{-1}. The rate of decay therefore of N nuclides is:

$$dN/dt = -\lambda N \qquad [4.1]$$

By integrating this equation from t=0 to t, given that at time t=0 the number of atoms present is N_o , the following equation can be obtained:

$$N = N_o e^{-\lambda t} \qquad [4.2]$$

However, a more common and useful way of referring to this decay rate is the 'half-life', $t_{1/2}$, which is defined as the time required for one half of the parent atoms to decay. By substituting $N = N_o/2$ and $t = t_{1/2}$ into equation [4.2] and rearranging, we obtain:

$$t_{1/2} = \ln 2 / \lambda \qquad [4.3]$$

The number of daughter, or radiogenic, nuclides produced by radioactive decay is just the difference between the initial number of parents (N_o) and the number remaining (N) after time t:

$$D = N_o - N \qquad [4.4]$$

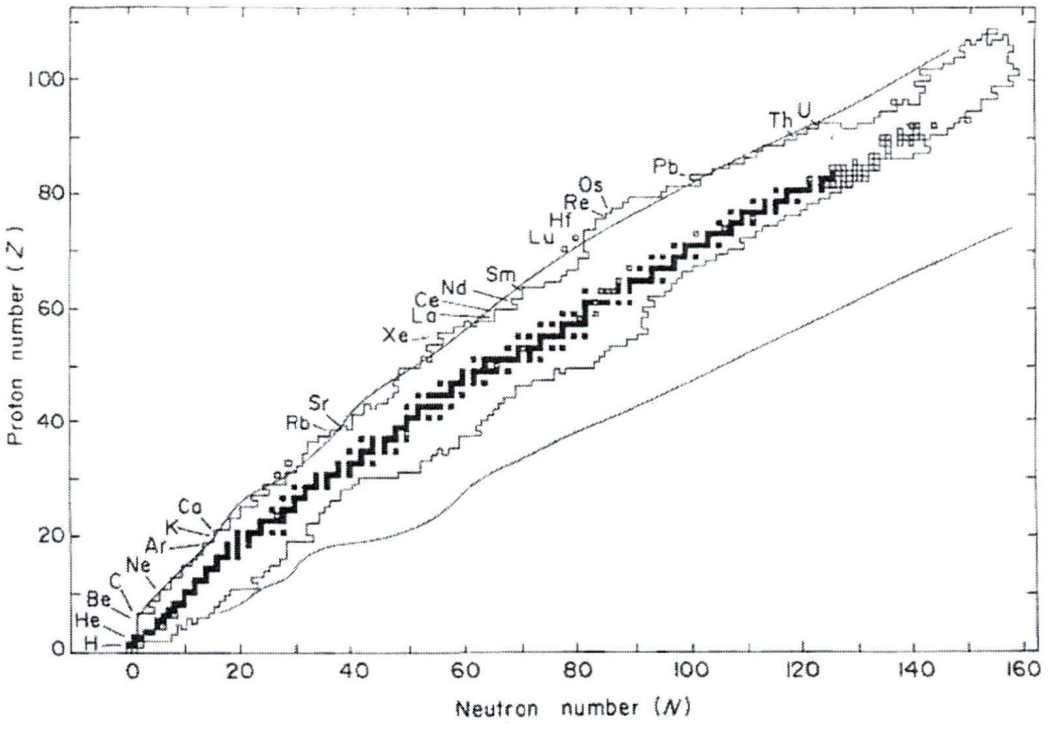

Figure 4.1 Chart of the nuclides in coordinates of proton number (Z) against neutron number (N). (■) = stable nuclides; (□) = unstable nuclides; (◘) naturally occurring long-lived unstable nuclides; (□) = naturally occurring short-lived unstable nuclides. Smooth envelope = theoretical nuclide stability limits (From Dickins, 1995).

Rearranging equation [4.2] to isolate N_0 and substituting into equation [4.4] provides the following equation:

$$D = N e^{-\lambda t} - N = N (e^{-\lambda t} - 1) \qquad [4.5]$$

Since there will generally be some atoms of the daughter nuclide around to begin with (D_o), a more general expression is:

$$D = D_o + N (e^{-\lambda t} - 1) \qquad [4.6]$$

This equation is the fundamental basis of geochronological dating tools (Dickins, 1995).

4.1.2 Secular Equilibrium and Disequilibrium

In the uranium series decay chains, the daughter products (except the final stable Pb nuclides) are themselves radioactive. The abundance of such daughter products is given by the difference between its production rate from the parent and its own decay rate:

$$dN_D / dt = \lambda_P N_P - \lambda_D N_D \qquad [4.7]$$

where N_P and λ_P are the abundances and decay constant of the parent, and N_D and λ_D are that of the daughter.

When dealing with intermediate daughters of the U-series, it is more common to work with activities, measured in the number of decays per unit time, rather than with atomic abundances. This is because the abundances of these isotopes are generally detected by their decay. Activities are related to atomic abundances by the same basic equation of radioactive decay given in equation [4.1] where dN/dt is the activity, commonly expessed in units of disintegrations per minute (dpm).

Eventually, if the system is not perturbed (remains closed), a state of radioactive or secular equilibrium will be achieved. In such a state, the activities of the daughter and parent radionuclides are equal. The equilibrium state is the steady state where the abundance of the daughter does not change. As such, the left side of equation [4.7] becomes zero, and thus by substituting the dN/dt terms for the λN terms, the following expression is obtained:

$$dN_D / dt = dN_P / dt \qquad [4.8]$$

When a system in secular equilibrium is disturbed, thereby resulting in fractionation, it will ultimately return to the equilibrium state. The rate at which it does so is determined by the decay constants of the parent and daughter radionuclides. If it is known how far out of equilibrium the system was when it was distrubed, the amount of time that has past since it was disturbed can be determined by measuring the present rate of decay of the parent and daughter. This situation of secular disequilibrium can be ultilized as a chronological dating tool in two different ways, called daughter deficiency and daughter excess dating methods.

In the daughter deficiency method, fractionation processes during the geological formation of a deposit, such as erosion or sedimentation, cause it to take up a radioactive parent without any of its daughter. The age of the deposit can then be determined by

measuring the growth of the daughter as the system returns to secular equilibrium (Figure 4.2).

In the daughter excess method, fractionation processes have resulted in deposits with amounts of the daughter beyond a level that can be sustained by the abundance of the parent nuclide. Over time, this excess or "unsupported" daughter (radioactive itself) decays back into secular equilibrium (Figure 4.2). The age of such deposits can then be determined if the original amount of fractionation is known. It is this daughter excess method that is used in the ^{210}Pb dating method.

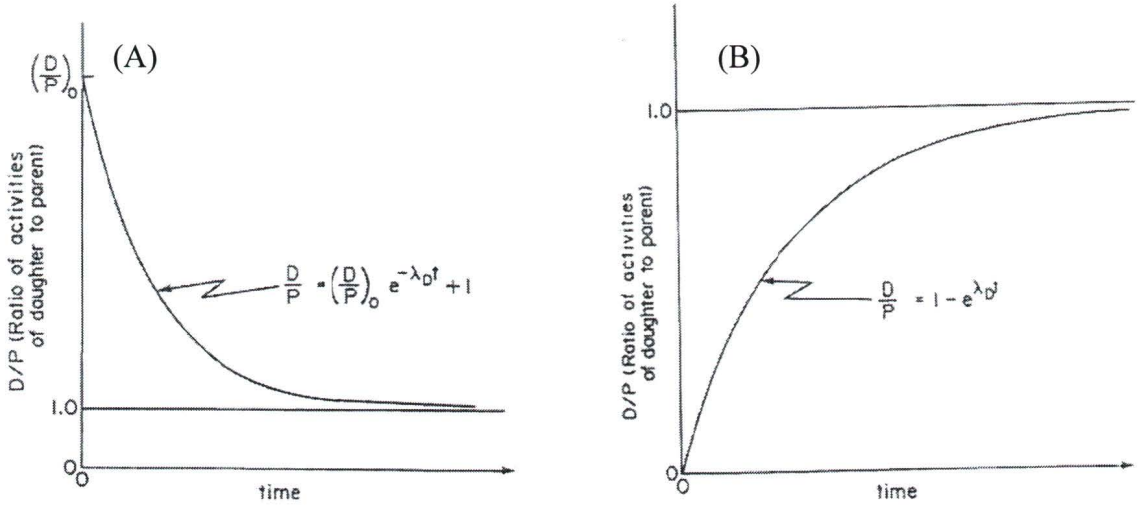

Figure 4.2 Types of disequilibrium in the ^{238}U decay series. (A) Decay of a partially unsupported daughter, some parent initial present (daughter excess). (B) Ingrowth of a deficient daughter, no daughter originally present (daughter deficiency) (From Blackwell and Schwarcz, 1995).

4.2 Pb-210 Dating of Lake Sediments

Lake sediments provide an important record of the past. In any serious attempt to reconstruct past conditions, whether the focus is sediment accumulation or erosion, acidification, or industrial pollution, such sediment-based histories require a reliable chronology. In some environments, seasonal variations in sediment type lead to laminated deposits, which can be directly dated by counting of the varved layers.

Unfortunately, many environments do not have such favourable conditions, and so recent studies utilizing sediments generally rely on short-lived and naturally dispersed radionuclide chronologies. ^{210}Pb, a member of the ^{238}U natural radioactive series (Figure 4.3), with a half-life of only 22.3 years, is an ideal geochronological tool for such geological processes with time periods on the order of 100-150 years (Oldfield and Appleby, 1984). A series of favourable nuclear and chemical properties of the ^{238}U series have combined to allow ^{210}Pb to become the parent isotope in nuclear decay schemes of the major sedimentary cycle (Koide et al., 1972).

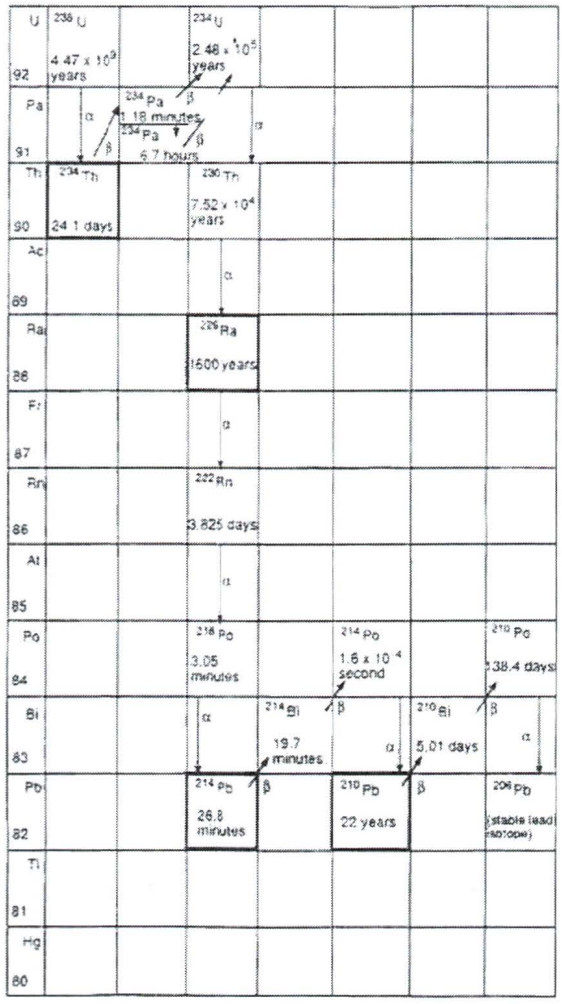

Figure 4.3 Simplified diagram of ^{238}U decay series (From Zielinski and Budahn, 1998).

4.2.1 Pb-210 Geochemical Cycle

^{210}Pb geochronoloy utilizes the daughter excess dating method descibed in the previous section. The disequilibrium between ^{210}Pb and its distant relative, Radium-226, is caused by the physiochemical activity of the intermediate gaseous progenitor, Radon-222. Formed by the α-decay of ^{226}Ra, ^{222}Rn escapes to the atmosphere from the land surface either by recoil on the ejection of the α-particle, or by diffusion (Appleby and Oldfield, 1992). With a half-life of only 3.82 days (Koide et al., 1972), ^{222}Rn rapidly decays through a sequence of four short-lived radionuclides to ^{210}Pb (see sequence in Figure 4.3).

In the atmosphere, ^{210}Pb atoms become readily attached to airborne particulate material and are removed by precipitation and dry deposition after a mean residence time of 9.6 days, which is about the average time between rainfalls (Koide et al., 1972). Binford et al. (1993) estimate that 90% of all ^{210}Pb fallout is delivered by wet deposition, with the remainder by dry deposition. Therefore fallout rate is correlated with precipitation. Global average fallout rates for ^{210}Pb are about 0.5 picocuries/cm^2·year (pCi/cm^2·yr), but vary according to latitude, longitude and elevation (Binford et al., 1993). Locally, the ^{210}Pb fallout flux will also vary significantly on short time scales, but in most cases, can be considered reasonably constant when measured over periods of years.

After the precipitation of ^{210}Pb onto land and water surfaces, the highly reactive Pb is rapidly adsorbed to sediment particles and in the case of streams and lakes, it is incorporated into the depositing sediment layers. Because ^{210}Pb in lake waters has a residence time on the order of months (Benoit and Hemond, 1987) to about a year or two (Dickins, 1995) before adsorption on to the sediments, it can be used to date recent sedimentation. A major exception to this however has been pointed out by Binford et al. (1993) for the case of drainage lakes. In drainage lakes, the residence time of the water can be shorter than that of ^{210}Pb in the water column and so significant amounts of unsupported ^{210}Pb will be lost from the system.

Unsupported ^{210}Pb may also be derived from ^{222}Rn entering a lake in groundwater or stream water (Benoit and Hemond, 1987). In addition, but generally in small amounts, it may be contributed from the drainage basin via erosion of soil material into the lake

(Binford et al., 1993). In general however, ^{210}Pb falling directly onto the catchment is for the most part trapped in the surface soils and only a small portion escapes into lakes. This is due to the long residence time of ^{210}Pb in the catchment (estimated to be up to ~2700 years) relative to its short half-life (Appleby and Oldfield, 1992). Regardless of the source of unsupported ^{210}Pb, the rate it is incorporated into the sediments is generally about equal to the local atmospheric fallout rate (Davis et al., 1984; Benoit and Hemond, 1987).

The flux of ^{210}Pb into lakes produces a concentration of unsupported ^{210}Pb whose activity in the sediments is higher than that of its *in situ* detrital grandparent, ^{226}Ra. The excess ^{210}Pb decays in accordance with the radioactive decay law (see section 4.1.1). Dates of the sediment deposition are calculated by determining the decrease in ^{210}Pb activity at each level in the sediment column, which is a function of time.

^{210}Pb radiochronology, based on the geochemical cycle described here, is dependent on the assumption of negligible post-depositional mobility of ^{210}Pb. Once incorporated into the sediment however, ^{210}Pb moves with the particulate fraction during resuspension and redeposition processes and may be focused into the deeper part of lakes (Binford et al., 1993). Benoit and Hemond (1991) found that some ^{210}Pb is remobilized under reducing conditions and may diffuse in the sediment column before being quickly reincorported by iron and manganese precipitates when oxygen is reintroduced into the bottom waters. Such findings can significantly affect dating models based on this assumption.

4.2.2 Methodology

Unsupported ^{210}Pb activity is determined by subtracting the contribution of ^{210}Pb activity supported by ^{226}Ra from the total ^{210}Pb activity. Assuming secular equilibrium between supported Pb and Ra, the activity of supported ^{210}Pb is just equal to that of radium, and the following equation can be used (Dickins, 1995):

$$^{210}Pb_{excess} = {}^{210}Pb_{total} - {}^{226}Ra \qquad [4.9]$$

Validity that the secular equilibrium exists can be seen from the bottom sections of most cores, where excess ^{210}Pb has completely decayed away. However, Brenner et al.

(1994) have documented deposits from lakes in central Florida that display disequilibrium between ^{226}Ra and unsupported ^{210}Pb. They attribute such occurrences to the erosion and mining of Ra-rich phosphate deposits.

The activities of ^{210}Pb have traditionally been mostly determined by α- or β-spectrometry. Beta-spectrometry is done by counting the β-particles emitted as ^{210}Pb decays to Bi-210 or, more commonly, by the decay of Bi-210 (half-life of 5 days), which emits more energetic β-particles than ^{210}Pb (Koide et al., 1972). Alpha-spectrometry, on the other hand, counts the α-particles emitted by the granddaughter Po-210.

Alpha-spectrometry is also used to measure the activity of ^{226}Ra (and thus supported ^{210}Pb) as it decays to ^{222}Rn. However, this is also often determined just by taking the asymptotic value of total ^{210}Pb from the bottom of cores, where secular equilibrium is reached.

Both the α- and β-spectrometry methods require extensive chemical preparation. As such, more authors have recently begun using γ-ray spectrometry to measure the decay of ^{210}Pb. This method, although slightly less precise, is non-destructive and provides simultaneous determinations of the relative abundances of ^{238}U, ^{226}Ra and ^{210}Pb in sediment samples (Zielinski and Budahn, 1998).

Once the abundances of unsupported ^{210}Pb have been determined, the ages of the sediment deposits and thus sediment accumulation rates can be determined. There are two ^{210}Pb models used to calculate sedimentation rates called the Constant Initial Concentration (CIC) model and the Constant Rate of Supply (CRS) model.

The CIC model of Robbins and Edington (1975) assumes a constant intial concentration (activity) of unsupported ^{210}Pb in the surface sediments during deposition that is independent of any changes in the sedimentation rate. Thus, changes in the flux of sediments from the water column result in proportional changes in the amount of unsupported ^{210}Pb removed by the falling sediments. For this model, the dating equation becomes:

$$C_t = C_o e^{-\lambda t} \qquad [4.10]$$

where C_t is the unsupported ^{210}Pb activity at some depth interval at age t years, C_o is the initial specific activity of unsupported ^{210}Pb at the sediment-water interface, and λ is the ^{210}Pb decay constant (0.03114 yr^{-1}) (Allen et al., 1993).

Binford et al. (1993) explain that for ^{210}Pb activity in the sediment surface to be constant, the flux of ^{210}Pb atoms from all atmospheric and terrestrial sources to the water column must be greater than or equal to the flux to the sediment in order to maintain a reservoir of ^{210}Pb atoms in the water column large enough so that the removal by sedimentation does not exhaust it.

According to the assumption of the CIC model, a plot of ln excess ^{210}Pb activity against depth would be expected to show a monotonic decline of unsupported ^{210}Pb in sediments (Blais et al., 1995). Thus, the sedimentation rate can more easily be determined by the slope of such a plot using the following equation (Turner and Delorme, 1996):

$$\text{slope} = \lambda / S_o \qquad [4.11]$$

where S_o is the sedimetation rate in centimetres per year. Since the decay constant λ is known, S_o can be calculated.

The CRS model of Appleby and Oldfield (1978) assumes a constant rate of supply of unsupported ^{210}Pb to the sediment surface that is independent of any changes in sedimentation rate. The concentration of unsupported ^{210}Pb in the sediments varies inversely with bulk sediment accumulation rates. This model does not assume that increases in sedimentation rates sweep more ^{210}Pb from the water column, but rather that it dilutes the unsupported ^{210}Pb sedimenting. Conversely, decreases in sedimentation rates would result in an increase in the concentration of ^{210}Pb. For this CRS model, the dating equation becomes:

$$A_t = A_o e^{-\lambda t} \qquad [4.13]$$

where A_t is the cumulative unsupported ^{210}Pb activity below the depth representing time t, and A_o is the total integrated unsupported ^{210}Pb activity in the core (Binford et al., 1993).

Under the assumptions of the CRS model, the input flux of ^{210}Pb atoms to the lake must be less than the maximum possible flux to the sediments, given some infinite sedimentation rate, or else the ^{210}Pb flux would change with changing bulk sedimentation (Binford et al., 1993). Thus the reservoir of ^{210}Pb atoms in the water column must be nearly zero such that every atom that enters the lake is scavenged and deposited to the bottom (Binford et al., 1993).

Logarithmic plots of ^{210}Pb versus depth, as mentioned in the CIC model, are often non-monotonic for the CRS model, thereby indicating variable sedimentaion rates. Oldfield and Appleby (1984) point out that if these changes in sedimentation rates are short term, such as slope slumping or droughts, they will give rise to concentration minima and maxima, respectively, in a ^{210}Pb profile.

Both of the ^{210}Pb models assume a constant flux of unsupported ^{210}Pb to the sediment-water interface and both assume no stratigraphic alterations after deposition, although terms for mixing and other diagenetic processes can be incorporated into the calculations (Oldfield and Appleby, 1984; Benoit and Hemond, 1991).

The two alternative dating models often give very different predictions of the age of sediment sections, as shown in Figure 4.4. The CRS model predicts lower sedimentation rates (thus older ages) than the CIC model (McCall et al. 1984). This contrast often increases with depth as shown in Figure 4.4 due to the increasing difficulty of determining unsupported ^{210}Pb at greater depths. These differences in age determination have resulted in many studies attempting to determine which ^{210}Pb dating model is better.

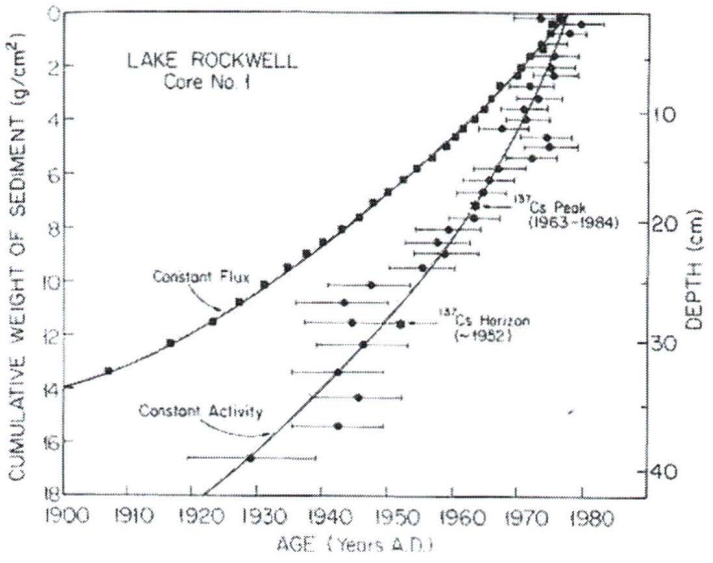

Figure 4.4 The relationship between sediment depth (in g/cm^2) and model age for the CIC model (constant flux) and the CRS model (constant activity) in a Lake Rockwell core. The stars indicate the position of the ^{137}Cs peak (1963) and horizon (1952). The constant activity model is preferred here (From McCall et al., 1984).

Turner and Delorme (1996) studied the ^{210}Pb activity from 22 lake sediment cores from the Canadian prairies to compare the sediment accumulation rates using the two models. As with most studies, other dating techniques are used to calibrate the methodology. Their results found that for half of the cores examined, the bulk sedimentation rate was constant, and thus both the CRS and CIC models were valid. For the other half of the cores, variability was observed in the CRS mass accumulation trends. Where such variability was moderate to high, they found the CRS model to be more satisfactory.

Binford et al. (1993) analysed ^{210}Pb activity in 51 sediment cores from 32 lakes in four PIRLA (Paleoecological Investigations of Recent Lake Acidification) project regions in the U.S.A. Their results support the hyposthesis that the CRS model dates are reliable in most cases. Many other authors have also concluded that the CRS model dates have consistently better agreement than CIC model dates when compared against markers of known history (Appleby et al., 1979; Oldfield and Appleby, 1984; Allen et al., 1993; Blais et al., 1995).

However, a study by McCall et al. (1984) studied sediment cores from three reservoirs in northern Ohio. These reservoirs possess well-established changes in sedimentation rates, due to increased population density, thereby providing a means to test the alternate models for ^{210}Pb dating. The CIC model was found to be preferred in this model because of supporting data from ^{137}Cs dating. It should be noted however, that more recently it has been found that ^{137}Cs is highly mobile in some sediments (Blais et al., 1995).

There appears to generally be an increasing preference for the CRS model as more and more assessments of the model are made. This is likely due to the more robust nature of the CRS model. For example, in the case of sediment mixing, the mixed zone can be as much as 15% of the depth of the unsupported ^{210}Pb profile before CRS model dates lower in the sediment core become unreliable (Binford et al., 1993). In contrast, CIC dates are significantly affected by mixing, and the model must employ explicit mixing functions (Binford et al., 1993; Benoit and Hemond, 1991). Mixing terms can of course be used with both models to produce more accurate dates.

Although the CRS model is more widely accepted, the CIC model is still a valid one, particlularly in lacustrine environments with constant sediment accumulation rates, as demonstrated by Turner and Delorme (1996). The question of which model is better requires a thorough evaluation of the characteristics of the lake and their catchments. The best approach it seems is to calculate both models and compare the results to those obtained by other chronostratigraphy methods. Whenever possible, ^{210}Pb dates are verified by counting the laminations in varved sediment cores. When annual sediment deposits are not distinguishable, a discrete stratigraphic marker of known history must be used. The most common such methods used with the ^{210}Pb dating method are ^{137}Cs and pollen stratigraphy.

4.3 Pb Isotope Ratios: Fingerprints of Anthropogenic Pollution

4.3.1 The Isotopic Composition of Atmospheric Pb

Pb isotope investigations are a powerful tool for the reconstruction of the heavy metal pollution of the environment by anthropogenic activities. Since virtually all of the Pb now present in the atmosphere originates from industrial sources, its isotopic composition is largely determined by that of the ores used to manufacture gasoline additives.

Atmospheric Pb is concentrated mostly in submicrometer aerosols that can be transported long distances and deposited over large areas of the earth (Simonetti et al., 2000a,b,c). Because the atmospheric residence time of Pb aerosols is about the same as that of water (1-2 weeks), the isotopic composition of atmospheric Pb in the mixed troposphere changes rapidly in response to changes in production from different ore deposits having different isotopic compositions (Shirahata et al., 1980). While Pb concentration measurements may provide useful information about the enrichments of Pb, they do not enable the determination of the Pb source. To resolve this ambiguity, one must look at Pb isotope ratios rather than absolute concentrations. Isotopic ratios will give information about the Pb source regardless of the variabilities in concentration.

Pb has four stable isotopes: ^{204}Pb, ^{206}Pb, ^{207}Pb, and ^{208}Pb. The last three are radiogenic isotopes produced by the radioactive decay of ^{238}U, ^{235}U, and ^{232}Th,

respectively. ^{204}Pb is a non-radiogenic stable Pb isotope and therefore often used as a reference isotope. However it is mostly used by geochemists due to the mathematical simplification of using a non-radiogenic isotope (Monna et al., 1997). Most environmental scientists tend to use $^{206}Pb/^{207}Pb$ and $^{208}Pb/^{206}Pb$ because of their better analytical precision and so this study will only discuss these radiogenic isotope ratios.

Most ore leads have $^{206}Pb/^{207}Pb$ ratios that are significantly less than the natural geogenic leads of soils and soil related components. This is because Pb is separated from its radioactive parent radionuclides (U and Th) during the formation of ore bodies, which thereby stops the accumulation of ^{206}Pb, ^{207}Pb, and ^{208}Pb. However, the accumulation of ^{206}Pb, ^{207}Pb, and ^{208}Pb from ^{238}U, ^{235}U, and ^{232}Th decay, respectively, continues in crustal rocks from which soils are derived. In general, therefore, $^{206}Pb/^{207}Pb$ ratios in anthropogenic leads are shifted to characteristically less radiogenic range values (~1.19-1.25) (Shirahata et al., 1980). The range of values is caused by the varying ages of the different ore deposits.

Prior to 1967, the $^{206}Pb/^{207}Pb$ ratio of atmospheric Pb in the U.S. was about 1.15 (Chow and Johnstone, 1965; Shirahata et al., 1980; Sturges and Barrie, 1987). After this period, the characteristic isotopic difference between industrial and natural Pb was drastically altered by the increased production of Pb smelted from enormous deposits of Mississippi Valley ores. These ore deposits are more radiogenic than most and therefore have uncharacteristically high $^{206}Pb/^{207}Pb$ ratios of ~1.28-1.33 (Shirahata et al., 1980). Industrial Pb in the U.S. now has isotopic compositions that are more radiogenic and similar to those of natural soils. These changes in isotopic composition of industrial Pb in the atmosphere were measured in air, snow, and sediment samples at various places and times in California. In that region, the atmospheric ratio had increased to ~1.23 by 1977 (Shirahata et al., 1980).

In Canada, Pb additives have been produced exclusively by the Canadian divisions of Dupont and Ethyl corporations, who obtained ores from New Brunswick and British Columbia, respectively. The average $^{206}Pb/^{207}Pb$ ratio of these ore bodies is ~1.15 (Sturges and Barrie, 1987). Less than 1% of additive Pb ore and leaded gasoline used in Canada was imported (Sturges and Barrie, 1987). Thus the isotopic ratios from Pb emission in Canada can be distinguished from that of U.S. emissions. However,

significant reductions in the concentrations of anthropogenic Pb in the atmosphere have been seen in both countries since the use of leaded gasoline was banned in the 1980's.

4.3.2 Studies of the Pb Isotope Record

Pioneering studies of the Pb record by Goldberg and associates (Chow et al., 1973) and the later studies of Ng and Patterson (1979) of marine sediments in basins off the coast of Los Angeles found records of increasing concentrations of Pb for recent times. These sediments also showed changes in the isotopic composition of those excess amounts of Pb which paralleled chronological changes in the isotopic composition of atmospheric Pb. The annual layers in these sediments were confidently dated radiometrically with ^{210}Pb and confirmed by appropriate chronological occurrence of nuclear fission debris (Shirahata et al., 1980). This work along with numerous other studies using sediments has contributed to the general acceptance of using sediments as archives of atmospheric Pb deposition. This section will look at some Pb isotope studies in North America.

Shirahata et al. (1980) studied sediment cores obtained from a remote subalpine pond in the Thompson Canyon area of the U.S. to determine the Pb concentrations and isotopic compositions of atmospheric deposition in a vastly remote and non-domesticated region of North America. In order to assign dates to the depositional intervals of the sediment samples, they established sedimentation rates using ^{210}Pb chronology and found that the sedimentation to the pond has been constant and that no systematic disturbance of the sediment has occurred.

The major features of Shirahata et al.'s (1980) data are that the Pb concentrations decrease precipitously from high values at the surface to relatively small values in layers 130 years old, with a corresponding increase in the ^{206}Pb/^{207}Pb ratio from lower industrial-like values near the surface to larger natural values at depth. The changes in isotopic composition through the modern sediments are shown in Figure 4.5. These changes are not directly related to changes in Pb concentration, since the Pb-206/Pb-207 ratios apply to all of the Pb in great or small amounts, collected from each sample of sediment or air at the given dates. The change of ^{206}Pb/^{207}Pb in gasoline which occurred after 1967 is faithfully recorded at dated levels in these sediments and the isotopic

composition of atmospheric Pb correlates with known ratios from the combustion of Pb ores from the Mississippi Valley ore deposits in Missouri.

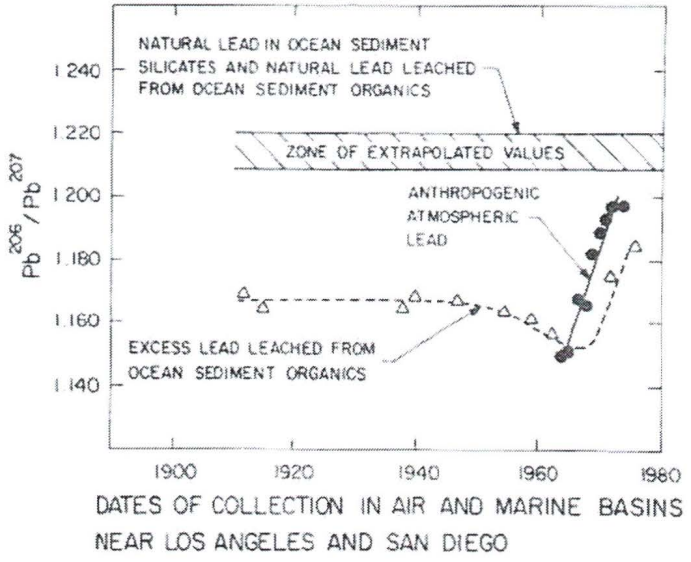

Figure 4.5 $^{206}Pb/^{207}Pb$ ratios in excess Pb leached from pond sediment humus, natural Pb in pond sediment silicates, natural Pb leached from pond sediment humus, and atmospheric deposited Pb in Thompson Canyon correlated with dates of collection in Thompson Canyon (From Shirahata et al., 1980).

Measurements of Pb concentrations and stable Pb isotopic compositions in sediment cores from Lake Erie were done by Ritson et al. (1994) in order to document temporal and spatial variations in Pb sources to the lake. The isotopic compositions of the sediments revealed two sources of natural Pb (fluvial and shoreline bluff erosion) and three sources of anthropogenic Pb (coal combustion, gasoline additives and municipal waste water discharge) to the lake. The ^{210}Pb analyses of cores from three different basins within the lake showed pronounced differences in sedimentation rates and disturbances between the sites. The changes in anthropogenic Pb concentrations for the different basins plotted as a function of time are shown in Figure 4.6. The figure shows that the atmospheric Pb profiles of the two basins are not the same, and that only the East Basin has a profile similar to the recorded atmospheric source function.

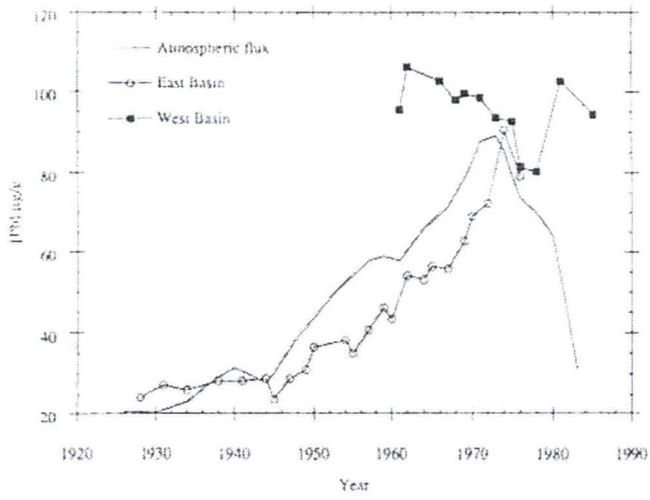

Figure 4.6 Changes in anthropogenic lead concentration for the West (WB) and East (EB) Basins. The atmospheric source function is on a relative scale. The profile of the East Basin is similar to the atmospheric source function while the West Basin is different (Ritson et al., 1994).

Other studies of the Pb isotopic compositions of aerosols (Sturges and Barrie, 1987) and surface waters (Flegal et al., 1989) of Lake Erie indicate that the anthropogenic inputs of industrial Pb aerosols from U.S. and Canada were the predominant sources of Pb to the region. However, Ritson et al. (1994) found that the isotopic compositions in the West Basin were dissimilar to these surface water values and instead indicated that municipal effluent is the dominant source of Pb in this urbanized region of the lake. The more rural eastern areas of Lake Erie however were found to be dominated by atmospheric deposition. The isotopic ratios on these eastern deposits were also found to be dissimilar to the previous findings of surface water ratios and consistent with those of U.S. atmospheric Pb ($^{206}Pb/^{207}Pb = 1.211$) rather that Canadian.

Some recent work by Simonetti et al. (2000a,b) investigated the Pb isotopic composition of snowpack from Quebec to determine the sources and deposition budgets of atmospheric heavy metals in northeastern North America. The Pb isotope ratios for most of the 1998 samples plot on a single "mixing line" between the isotopic compositions for the Canadian and U.S. anthropogenic end-members (Figure 4.7). However, snow samples from the North Shore region that plotted on the mixing line in

1998, plot outside of the line for the 1997 samples (Figure 4.7). This suggests that during the 1997 winter, the snowpack from this region recorded the input of an additional anthropogenic end-member. Simonetti et al. (2000a) suggest that this additional source is Eurasian pollution transported over the high Arctic.

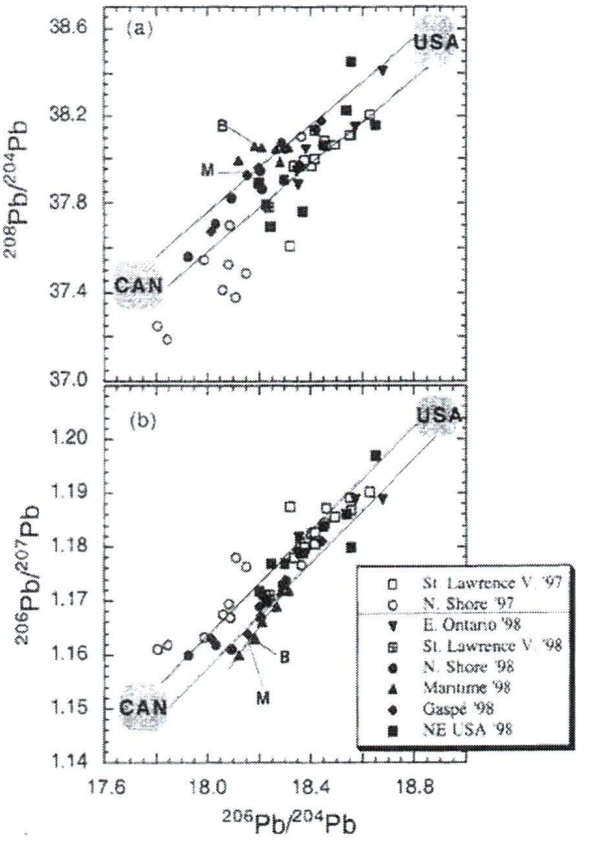

Figure 4.7 (a) $^{208}Pb/^{206}Pb$ and (b) $^{206}Pb/^{207}Pb$ vs. $^{206}Pb/^{204}Pb$ showing the data for the 1997 and 1998 snow samples. The fields (shaded grey) define the U.S. and Canada anthropogenic end-members. (From Simonetti et al., 2000b)

5. STUDY AREA: KEJIMKUJIK NATIONAL PARK, N.S.

5.1 Geographical Area

Kejimkujik National Park is located in south-central Nova Scotia (44° 20' N, 65° 15'W), approximately 200 km southwest of Halifax and approximately 50 km from both the Atlantic Ocean and the Bay of Fundy (Figure 5.1). Park boundaries straddle the counties of Annapolis, Queens, and Digby, with the nearest town of Caledonia located 18 km to the east. This relatively remote park hosts over 50 interconnected shallow lakes and ponds with numerous wetlands and covers a 381 km^2 area representative of surface-water-rich terrains of the Atlantic Coastal Uplands section of the Acadian Forest Region. Within this area, natural processes have resulted in some lakes having high dissolved organic carbon (DOC) levels, and therefore dark tea-coloured waters, while neighbouring lakes have clear waters. To study the different processes that may be occurring within each lake system, this research will focus on two neighbouring end-member lakes located near the northern park boundary; Big Dam West (BDW) – a brown-water lake, and Big Dam East (BDE) – a clear water lake.

5.2 Physiochemical Characteristics

Kejimkujik National Park is relatively flat and typifies the glacially-modified, rolling drumlin topography of southwestern Nova Scotia. Regional soils are thin, nutrient-poor, and often characterized by poor drainage conditions, resulting in many wet and boggy soils (Clair et al., 1996). Vegetation in lake catchments is mainly composed of White and Black Spruce (*Picea glauca, Picea mariana*) and poor fens dominated by Sphagnum mosses (Basquill et al., 2001). The bedrock consists of Lower Paleozoic metasedimentary rocks of the Meguma Group which have been intruded by Devonian to Carboniferous Granitoids (Stea and O'Reilly, 1982). The two lakes that are the focus of this study each lie above a different formation of the Meguma Group. Big Dam West Lake is underlain by the Goldenville Formation, which is characterized by greywacke, quartzite, gneiss, and slates, while Big Dam East Lake is underlain by the younger

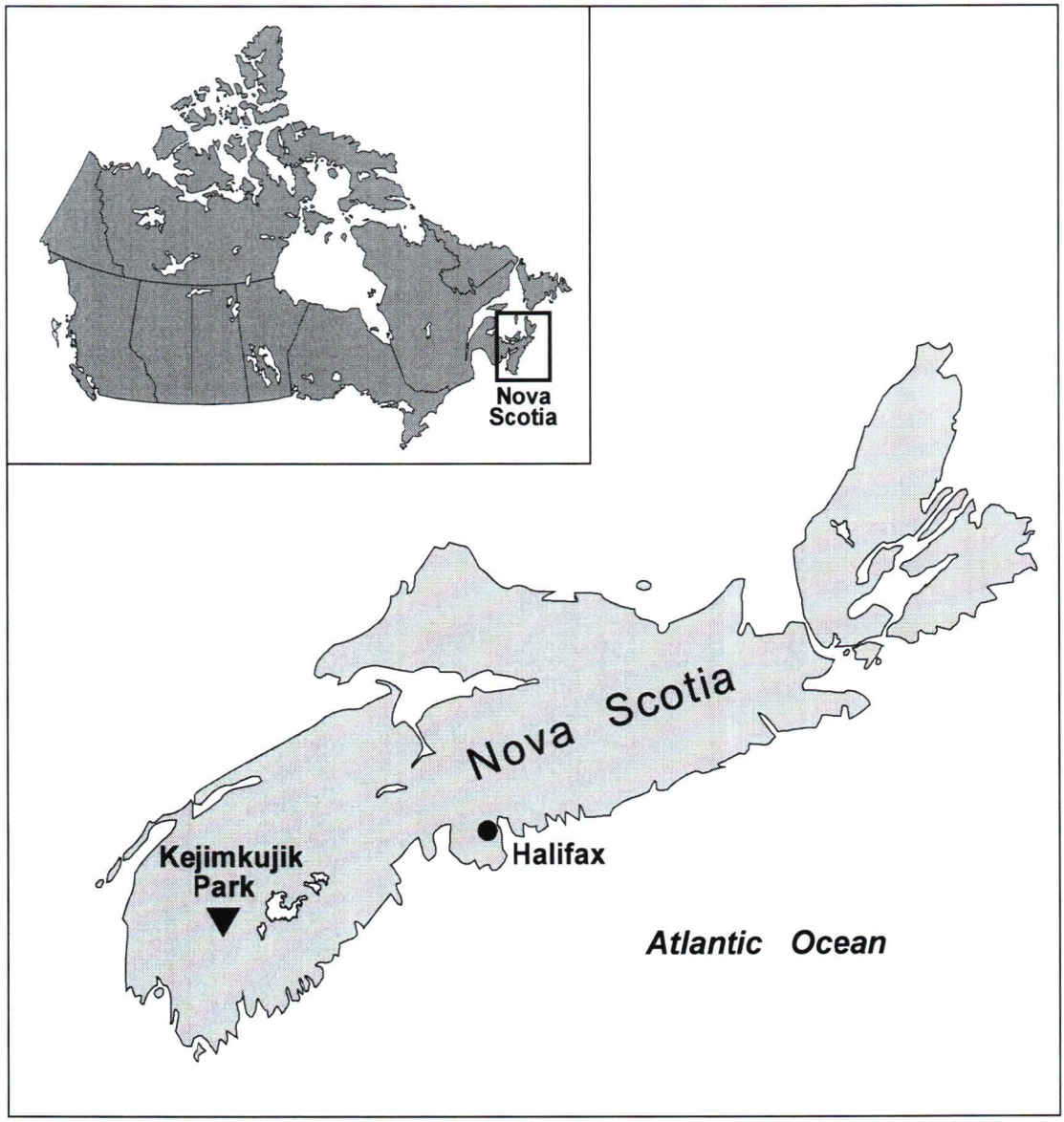

Figure 5.1 Study Area, Kejimkujik National Park, NS, Canada.

Halifax Formation, characterized by slates, schists, and quartzites (Gimbarzevsky, 1975). Ubiquitous post-glacial deposits are derived from local granitic materials and are therefore predominantly comprised of granitic, gneissic, and quartzitic minerals which weather slowly and release little nutrients (Kerekes et al., 1989). Weathering of such hard rocks is slow and yields little in terms of dissolved cations. Due to the physical conditions listed here, lakes in Kejimkujik Park are all oligotrophic, weakly-buffered, and acidic to varying degrees with pH ranging between 6.0 and 4.2 (Freedman et al. 1989). Lakes are characterized by high dissolved organic carbon (DOC) concentrations, low pH, and lake catchments contain a relatively high percentage of wetlands (Freedman et al., 1989). Big Dam West, the larger of the two lakes in this study, is a typical brown-water lake with relatively high [DOC] of 10.5 mg/L, and a pH of 5.0. In contrast, Big Dam East is very clear, with relatively low [DOC] of 3.7 mg/L and a higher pH of 5.9 (Freedman et al., 1989). Both lakes have poor productivity and receive low nutrient inputs (oligotrophic) (Freedman et al., 1989). The physical and chemical characteristics of the two lakes are presented in Table 5.1.

Table 5.1 Physical and chemical characteristics of study lakes

	Surface Area (km^2)	Mean Depth (m)	Max. Depth (m)	Watershed Area (km^2)	pH	DOC (mg/L)	Water Residence Time
Big Dam West	1.19	3.3	7.2	40	5.0	10.5	28 days
Big Dam East	0.53	3.0	4.1	2	5.9	3.7	228 days

5.3 Hydrology

Big Dam West Lake and Big Dam East Lake are both relatively small at 1.2 km^2 and 0.5 km^2 and have watersheds of 40 and 2 km^2, respectively. They are shallow with mean depths of 3.3 and 3.0 m, respectively (Ferguson, 2002), and are seasonally-stratified (diamictic). The two lakes are separated, but still hydrologically connected, by a small land bridge with a narrow boggy stream. The obstruction has enabled the two lakes to

develop their distinctly different water chemistries in what would otherwise be a singular lake. The bathymetry of these lakes is shown in Figure 5.2.

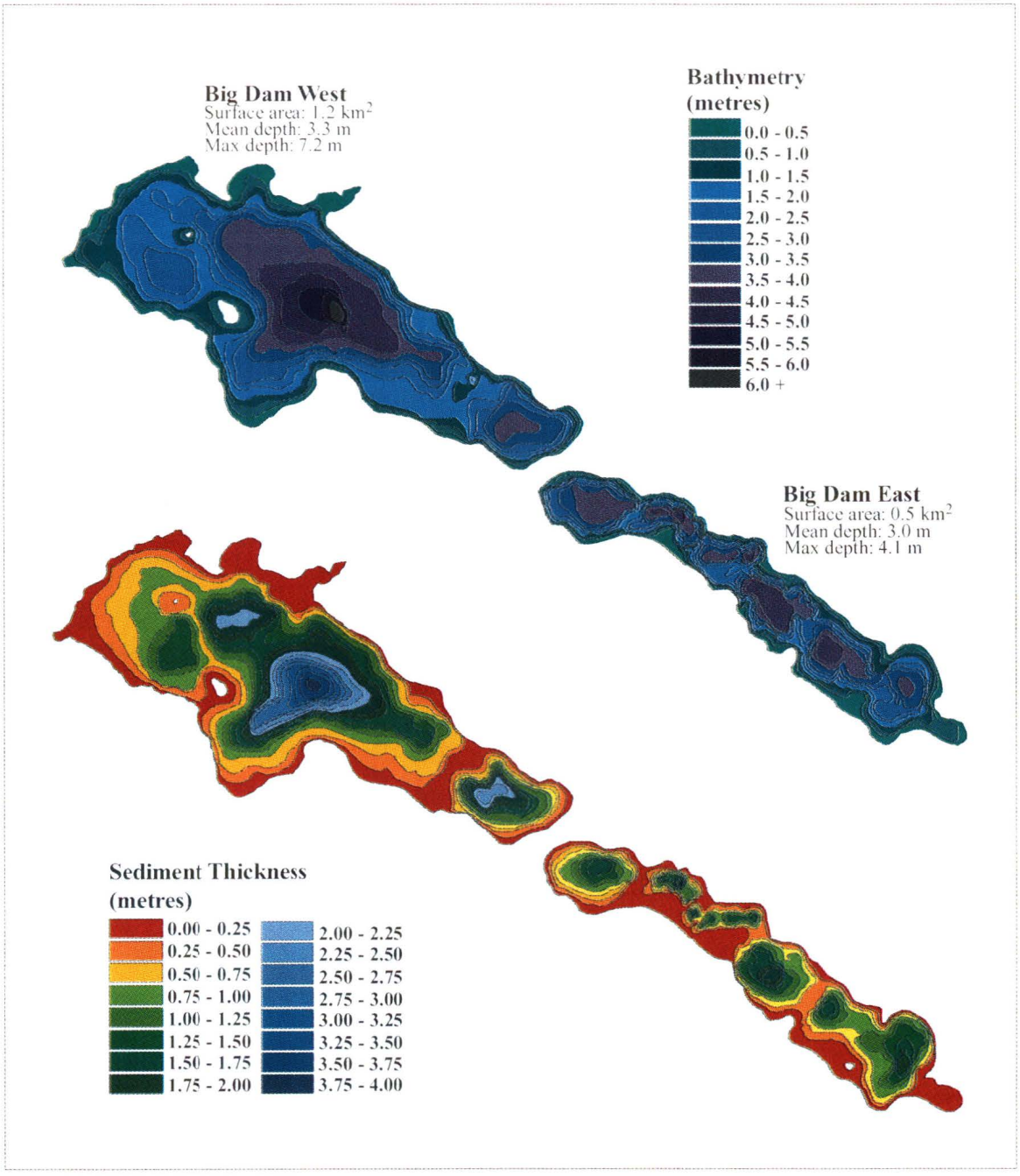

Figure 5.2 Bathymetry and Isopach maps for Big Dam Lakes, Kejimkujik National Park, NS (From Ferguson, 2002).

Big Dam East Lake is a clear headwater lake with no inflow streams. Hydrologic inputs from the terrestrial watershed are predominantly from near-shore subsurface seepages of groundwater flowing over the surface bedrock (Kerekes et al., 1989). With only one small outlflow stream that drains into the eastern end of BDW, the water renewal time of BDE is 1.6 times per year (Kerekes and Schwinghamer, 1973).

Big Dam West Lake is a highly coloured lake with 3 inflow streams, 1 outflow stream, and a water renewal rate of 13.1 times per year (Kerekes and Schwinghamer, 1973). The main inlet, Little River, drains the large wetland, Thomas Meadow Brook, on the northern side of the lake. The presence of this wetland within the catchment is largely responsible for the high DOC and low pH levels of the lake water, which in turn have been correlated with higher methyl mercury concentrations in the lake water column (Driscoll et al., 1998).

5.4 Sediment Composition and Distribution

The lake sediments of BDW and BDE are classified as organic gyttja. On average the sediments of BDW contain 2-3% more organic carbon than BDE, with the uppermost 50 cm containing 10-15% in BDW and 6-10% in BDE (Ferguson, 2002). A study of stable carbon isotopes and C:N ratios of these two lakes indicated that the sources of organic matter in the two lakes is significantly different with a larger proportion of autochthonous (lacustrine production) carbon in BDE and greater terrestrial inputs to BDW (Telmer et al., in review). The nature of the organic carbon in the sediments may play a significant role in the magnitude of Hg and Pb remobilization associated with microbial decay during early diagenesis.

The isopach and bathymetry maps of BDW and BDE (Figure 5.2) show that bathymetry is a relatively good predictor of gyttja thickness in these lakes, but there are exceptions and the relationship is not straightforward. Generally, sediment distribution is very heterogeneous with each lake having several distinct sedimentary basins and plateaus. Most of the sediments occupy a relatively small portion of the overall lake basin area (See Figure 5.2). For example, in BDW almost half of the lake basin contains

only 1 m or less of gyttja, and there are large areas, particularly in BDE, that are essentially barren of significant sediment accumulation.

5.5 Climatology

The mean daily temperature in Kejimkujik Park is 6.5°C annually, and 15°C during the growing season of May-September (Kerekes et al., 1989). Annual precipitation averages ca. 1400 mm/yr (18% snow), with a tendency for a lower mean precipitation during May-September, however the seasonal variations are not large (Kerekes et al., 1989). Wind direction is generally from the northwest to southwest quadrants, which is coincident with the direction weather patterns most frequently travel (Kerekes et al., 1989; Beauchamp et al., 1998). That being the case, Kejimkujik Park lies downwind of major industrial and populated regions in the northeast United States, the Great lakes basin, and the Windsor-Quebec corridor region of Canada, which are also areas that would have the most anthropogenic influence with respect to Hg and Pb emissions. A recent analysis of seasonal trajectory climatologies associated with elevated total gaseous mercury (TGM) concentrations at Kejimkujik Park for the years 1995-1997 (Beauchamp et al., 1998) indicated that elevated TGM concentrations were most commonly associated with transport from these regions, however there were seasonal differences in trajectory patterns as well as differences within a season between the 2 years. In general, winds are predominantly from the southwest quadrant in the summer, while for the rest of the year winds are predominantly from the northwest (Kerekes et al., 1989).

5.6 History

Kejimkujik National Park was established to preserve an area of ecological and cultural heritage unique to southwestern Atlantic Canada. The Kejimkujik region has been used for centuries by native Mi'kmaq peoples primarily as a route to cross between Nova Scotia's two coasts, but also as a hunting and foraging ground. However, with the coming of Europeans, the native population was greatly diminished. Having depleted their coastal forests, Europeans moved to interior regions of the province for wood. The

first house in nearby Caledonia was built in 1817, followed by a sharp rise in European settlement throughout the region during the middle of the nineteenth century (Basquill et al., 2001). Vast expanses of forest were cleared for lumber and farming. Logging and land clearing activities often sparked fires too large for existing technology to extinguish, and so the frequency of anthropogenic fires rose to greater levels than ever before (Basquill et al., 2001). A historical quote describes the Kejimkujik area circa 1906 as "little more than waste and desolation" (Albert Bigelow Paine in Basquill et al., 2001). Also during this period, several gold mines were established, including three within the present day park boundaries. In the beginning of the twentieth century, the park area became a popular location for outdoor recreation and is today a major regional tourist destination for wilderness and outdoor activities.

While the general history of the Kejimkujik area is well established, there is little in the way of specific information about anthropogenic activities within the watersheds of BDW and BDE. Due to difficult access to the Big Dam Lakes, particularly BDE, logging activities in these watersheds appear to have been significantly less than some of the other areas of the park. There are only two documented periods of logging and/or extensive forest fires in these watersheds; the 1880's and 1945-1956 (Basquill et al., 2001). Exactly when logging began in these watersheds is not known, however Basquill et al. (2001) document a large forest fire associated with logging activities in 1885 in the Big Dam West and neighbouring Frozen Ocean Lake watersheds that extended as far as 10 km west of the lakes. Several small understory and overstory fires were also indicated in the BDE watershed, but there does not appear to have been any logging in the watershed at this time. Major logging within both watersheds occurred between 1945 and 1956, but it may have been more selective.

Gold mining in the park area and nearby counties began in the mid 1880's and ended in 1939, however no known mining activities took place in either of the Big Dam watersheds (Cumming, 1979). The three gold mines that are within the present day park boundaries are all near the eastern park boundary and make up the extreme western part of the West Caledonia Gold District (Sheppard, pers. comm.). The West Caledonia Gold District was not a major gold mining district and the part of it within the park was minor. Over its years, the West Caledonia Gold District only produced 1,675 ounces of gold

compared to the other viable Queens County mines that produced 10,000 ounces (Whiteburn), 20,000 ounces (Molega), and 42, 000 ounces (Brookfield) (Cumming, 1979). The deepest shaft within the park was sunk only to 13 metres, where as the Brookfield mine went down to 700 metres (Cumming, 1979). No stamp mills were used and it is believed that the ore was processed offsite at the other mills in the county. In regards to mercury, some information from oral history suggests that the quartz that was removed was mortared and smelted in pans with mercury and in the 1930's a "mineralin' rod" was used, which was a crotched stick containing a mercury vessel that was said to dip down to the ground where gold lay underneath (Sheppard, pers. comm.).

6. METHODS AND ANALYSES

This chapter is purposely extensive to provide detailed information on both sampling equipment and analytical procedures for others interested in employing similar methods.

6.1 Lake Sediments

6.1.1 Short Cores

Geochemical investigations of pollution history and metal dynamics in lake sediments require the acquisition of representative sediment samples. To obtain high-resolution cores and sub-sample them in precise increments, a custom coring and extrusion system was built. Detailed figures of the equipment that should enable replicas to be made are given in Appendix A. The coring system is an open-barrelled Kajak-Brinkhurst (KB) type gravity corer modified to have an auto suction seal and a percussion knocker to extend penetration. The open-barrel design has been reviewed to be the best suited for quantitative sampling of soft-bottom sediments (Blomqvist, 1991). Its design allows unimpeded water flow through the corer and coring tube during descent, thus reducing the formation of a hydraulic shock wave at the orifice of the core tube which can cause the resuspension or loss of surficial sediments (Blomqvist, 1991). The use of a percussion knocker further reduces the chances of perturbing the surficial sediments because the core tube can be lowered into the sediment very slowly, and then, once the surficial sediments are isolated and protected from currents within the core tube, the knocker is used to slowly drive the core tube a sufficient depth – usually 50 cm in this case. The corer was fitted with 1-metre long polycarbonate tubes with an internal diameter of 7.62 cm, an outer diameter or 8.26 cm, and a wall thickness of 0.32 cm. The lower ends of the tubes are sharply tapered on the outside to ease penetration of sediments and minimize smearing. Furthermore, tapering on the outside of the coring tubes, as opposed to the inside, effectively ensures a sampling area similar to the cross-sectional area inside of the tubes (Blomqvist, 1991).

Sediment cores were obtained and subsampled in the months of July of 1999 and 2000. Coring was done over the side of an 8-foot zodiac boat anchored from three sides to prevent drifting. The corer was lowered at a controlled speed so as to prevent oblique impact and minimize disturbance of surficial sediments and core shortening (compression). Once the corer had penetrated the sediments, the corer was then hammered deeper into the sediments using a 20-lbs percussion knocker. The coring system is lowered using two ropes – one to operate the knocker, one to lower and raise the corer and to keep it in an upright position while knocking. Repetitive knocks are made simply by jigging the rope attached to the knocker. Once sufficient penetration is reached, the corer is pulled to near the water surface and a plastic puck with O-rings is inserted in the bottom (tapered) end of the core tube before the core breaks the water surface. This puck secures the sediments in the core tube and also is part of the extrusion system. Using this coring system, retrieved cores had a clear supernatant fluid and an undisturbed sediment-water interface (SWI). Any cores that appeared to have had the SWI disturbed were discarded.

All cores were extruded and sectioned immediately in the field using the Sanborn Extruder shown in Appendix A. A bushing is pushed into the core tube adjacent to the existing core plug in the bottom of the core. These are fitted onto an aluminium extruding rod. The rod has holes drilled in it at 0.25 cm increments and an "increment pin" is inserted into these holes to control the amount of sediment extruded. The rod pushes against the first puck to make it act as a piston to push the sediments upwards and the bushing acts as a guide and stabiliser. A plexiglass extruding platform is fitted onto the top of the coring tube. Once mounted, the supernatant water above the sediments is siphoned off until only 5 cm of water remain. The sediments are then extruded through the top of the core tube and onto the platform in precise increments by pushing the core tube down over the extruding rod until the bushing strikes the increment pin. The size of the increment is controlled simply by moving the pin down any number of holes, with the minimum being 0.25 cm. Notably, there is no chance for the size of the increments to drift with this system – 100 increments always equals 25 centimetres.

The increments of sediment that are extruded onto the extruding platform are pulled across the extruding platform with a plastic plaster knife or spatula and into clean and sterile 18 or 24 oz WhirlPak bags. Excess air is squeezed out of the bag and then sealed. Typically most cores were sectioned according to the following sequence: every 0.5 cm for first 10 cm, every 1-cm from 10-30 cm, every 2 cm from 30-50 cm, and every 4 cm for depths greater than 50 cm, however deviations from this sequence did occur. After each increment is collected, the extruding platform and the plastic plaster knife were carefully cleaned with ultrapure deionized Milli-Q water (MQ water) and Kimwipes to prevent cross contamination between samples.

All bagged subsamples from a single core were placed together in a large Ziplock bag. While in the field and during transportation, all core samples were stored in a cooler and kept cold with ice and Ice-Paks. Upon arrival at the Aqueous Geochemistry Laboratory at the University of Victoria, the samples were relocated to a refrigerator and stored there until preparation for analysis.

6.1.2 Long Cores

Long core sub-samples analyzed in this study are a sub-set of samples from long cores collected in July 2001 using a modified percussion coring system typically used in shallow marine environments (Reasoner, 1993). A detailed description of the coring equipment is given by Ferguson (2002). Essentially, this system works by pounding Poly-Vinyl tubes into the sediment with a sledgehammer and then winching the core out. This is done from a stable platform constructed on top of two zodiac inflatable boats. A series of tubes are pushed into the sediment by attaching one to the other until they pass through the entire thickness of gyttja. For the geophysical determination of sediment distribution by Ferguson (2002), a total of three cores were taken from Big Dam West, two from the deepest part of the lake and one from a secondary basin in the eastern portion of the lake. A single core was collected from Big Dam East, located in the deepest basin of the lake. However, for this study, only sub-samples from two of these cores (one from each lake) were analyzed. The two cores analyzed were from the same basin as the short cores and porewater samples.

Cores were cut on-site into 150-cm sections and transported upright to cold-storage at the Bedford Institute of Oceanography (BIO), Dartmouth, Nova Scotia, within 48 hours. After the physical property measurements were taken for the geophysical study (Ferguson, 2002), cores were split length-wise and sub-samples were taken approximately every 10-cm for chemical analysis, of which a sub-set of 6 samples from both the LC-BDW01-05 and LC-BDE01-01 core were analyzed for Hg, Pb, and Pb isotopes for this study.

6.1.3 Bulk Density and Water Content

The determination of bulk density on sediment cores is essential information for per unit thickness or per depositional period (time) determinations of the total mass of Hg, Pb, or any other component of the sediment. Three BDW short cores and two BDE short cores were used to determine the down core changes in water content and thus bulk density (Appendix B). The main difficulty in determining bulk density for the sediment water interface is determining the volume of the collected sample. There are always losses during extrusion so the volume cannot be estimated from the geometry of the core tube and the thickness of the extruded increment. Each sediment sample is transferred into pre-rinsed and pre-weighed 15 mL polypropylene Falcon graduated centrifuge tubes. For sediment sections greater than 2 cm, the samples are transferred to 50 mL centrifuge tubes. The filled tubes were reweighed to determine the wet sediment weight by subtraction and then centrifuged at 1500 rpm for 15 minutes. Centrifuging causes the solid sediment portion of the samples to settle to the bottom of the tubes which then allows determination of the total volume of the sample by observing the bottom of the meniscus.

To determine dry sediment weight, bulk density, and water content, the sediment samples were freeze-dried. For freeze drying, the samples were first frozen, either with dry ice or in a freezer over night, and then placed in 2 L freeze-drying canisters and attached to the freeze-dryer for 3-5 days, depending on the amount of sediment in the tubes. Once dried, the tubes were weighed again to determine the dry sediment weight by subtraction. These measurements, together with those for wet weight and estimated

volume, were then used to calculate water content and bulk density for each sample. Since each sample was transferred to more that one centrifuge tube, the calculations for each sample were made using a weighted average of all the corresponding tubes.

6.1.4 Radiometric Dating

Dating of the sediment deposits and determination of the sedimentation rates were based on ^{210}Pb and ^{137}Cs methods, measured by γ-ray spectrometry at the USGS Geochronology Laboratory in Denver, Colorado. ^{210}Pb and ^{137}Cs activity measurements were done with a high-purity Germanium well-type semiconductor of 16 mm diameter (Budahn, pers. comm.). To maximize detection sensitivity and precision, large samples are needed, and so four cores from roughly the same location in each lake were combined. Fifteen freeze-dried samples from each lake were selected for γ-ray spectrometry. The use of multiple cores for ^{210}Pb dating results in average sedimentation rates representative of their respective basins.

Activity measurements of ^{210}Pb and ^{137}Cs were done on sediment samples obtained in July 2000. Excess ^{210}Pb ($^{210}Pb_{ex}$) measurements were obtained by subtracting the amount of supported ^{210}Pb activity, determined from ^{214}Pb and ^{214}Bi measurements assumed to be in secular equilibrium with ^{238}U, from direct measurements of total ^{210}Pb activity. Activity data is given in Appendix C.

Dates and sedimentation rates were determined using the CIC model of Robbins and Edgington (1975) as described by Turner and Delorme (1996). From the slope of ln $^{210}Pb_{ex}$ vs uncompacted depth plots, the age and sedimentation rates were determined. The uncompacted depths were calculated, assuming steady state compaction, using experimentally determined porosity values from several other cores taken from the same locations in each lake as the cores used for ^{210}Pb analyses. Sedimentation rates were also calculated using the CRS model of Appleby and Oldfield (1978), but only results obtained using the CIC method were in good agreement with a stratigraphic marker of known age, and therefore only the CIC model results are given in this study. The counting errors for total ^{210}Pb activity, supported ^{210}Pb activity (i.e. ^{214}Pb and ^{214}Bi), and ^{137}Cs activity are 0.3 dpm/g, 0.15 dpm/g, and 0.025 dpm/g, respectively.

6.1.5 Elemental and Lead Isotope Analysis

Dried sediment samples selected for trace metal and Pb isotope analysis were ground to a homogenous powder in a class 100 cleanroom using an agate mortar and pestle. Three high-resolution short cores and one low-resolution long core from each lake were digested for elemental and Pb isotope analyses. All cores, except one short core from each lake, were digested by a two-step sequential digestion method. The remaining two cores were digested by a one-step total digestion method. However, several samples used for sequential digestions were also digested by the total digestion method in order to compare the summed results (concentrations and isotope ratios) from the sequential method to values determined by the total digestion. Summed values were within 5% of those from the total digests.

The sequential digestion is a two-part procedure in which a dilute acid is used to extract the labile components from the mineralogical components, thus for Pb, extracting the anthropogenic component. It has previously been demonstrated that a dilute acid leaching can be used to separate the anthropogenic Pb from the mineralogical component (Ng and Patterson, 1982; Shirahata et al., 1980). Furthermore, Graney et al. (1995) determined that the strength and type of acid used to leach the anthropogenic Pb has little effect on the concentration and isotopic ratios of the leached fraction and that this fraction is distinctly different than the isotopic composition of the residual fraction digested with HF acid. Monna et al. (1999) however pointed out that this does not mean that only anthropogenic Pb is removed by the dilute acid, nor that the residue is totally free of all anthropogenic Pb, but simply that the dilute acid preferentially extracts anthropogenic Pb from contaminated sediments.

The first step of the sequential digestion is a partial digest in which 0.2 g of dried and homogenized sediment was weighed into a pre-rinsed 12 mL polypropylene tube and then 3 mL of 10% HCl and 3 mL of 10% HNO_3 (both environmental grade) were added. The tube was then covered with Parafilm and, along with several other tubes, placed in a beaker and put in an ultrasonic bath for 1 hour. After this time, the tube was shaken vigorously by hand for one minute and then centrifuged at 3500 rpm for 15 minutes. The

aqueous phase was then pipetted from the tube, using a pre-rinsed glass 5 ¾" disposable pasteur pipette, into a pre-rinsed and preweighed 125 mL HDPE Nalgene bottle. Approximately 5 mL of MQ water was then added to the tube with the remaining sediment residue and then shaken vigorously for one minute, centrifuged as before, and aqueous phase again pipetted from the tube and put into the bottle. This step was repeated one more time and then the aqueous phase in the HDPE was diluted with MQ water to a final weight of 60 g.

For the second step of the sequential digest, the remaining sediment residue in the tube was dissolved using a concentrated HF- HNO_3 digest. Prior to the arrival of the microwave digestion oven, sediment residues from the KJ99-BDW1 and KJ99-BDE3 core samples were digested on a hot plate for this portion of the digest. For this method, the remaining sediment in the tube from the partial digest was transferred to a clean Teflon jar. The tube was then flushed with 5 mL of environmental grade concentrated HNO_3 and added to the jar. Then 2 mL of environmental grade concentrated HF was added to the jar. The jar was capped and heated on a hot plate at 100-150°C for 3-5 days until complete dissolution. The cap was then removed and rinsed with MQ water into the jar. The digested sample was then evaporated until dry on the hot plate. Once dry, 2 mL of environmental grade 8N HNO_3 was added and evaporated again. This step was repeated one more time and then 2.5 mL of environmental grade 8N HNO_3 was added to the jar, recapped, and put back on the hot plate until all of the residue dissolved. The cover was then rinsed into the jar with MQ water and the contents of the jar were transferred to a pre-rinsed 125 mL HDPE Nalgene bottle. The Teflon jar was rinsed a few times with MQ water, added to the bottle, and then the digestate was diluted with MQ water to a final weight of 100 g.

Sediment residues from the KJ00-BDW5 and KJ00-BDE5 samples were treated the same chemically as those digested on the hot plate, however, they were digested with the assistance of a microwave digestion oven and only the evaporations were done on the hot plate. The two heating steps described above, (1) after the addition of the HF and HNO_3 acids and (2) the final dissolution with 8N HNO_3, were carried out in a Questron QLAB 6000 Microwave Digestion Oven. For each of the heating steps, the residues and acids were put into closed Very High Pressure (VHP) Teflon digestion vessels and run

under a pressure control program for 25 minutes with the following settings: 600 W power, 200°C temperature limit, and 200 psi pressure limit.

The procedure for the total digestion of sediments was the same as the second half of the sequential extraction procedure just described. 0.2 g of the dry, homogenized sediment samples were put into VHP Teflon digestion vessels and then chemically treated as described above for the HF- HNO_3 digest using the assistance of the microwave digestion oven.

The digested samples from both the total and sequential digestions were analyzed for Pb isotope ratios and a suite of 30 trace element concentrations by quadrapole inductively coupled plasma mass spectrometry (ICP-MS) at the University of Victoria. However, only the Pb concentration and isotope ratio data will be presented in this study. The ICP-MS used was a high sensitivity VG PGII S+ with a Gilson Minipuls 3 autosampler. Analysis of trace element concentrations was performed using a method described by Longerich et al. (1987) and calibrated to a multi-element standard solution made from single element standard reference solutions from Absolute Standards, Inc. The detection limit (LOD) of Pb is 5 ng/g. Procedural blanks were less than 5%. Analyses of procedural duplicates determined that reproducibility was better than ±5%.

Lead isotope ratios were measured using methods described by Begley and Sharp (1994; 1997) and calibrated to the National Institute of Standards and Technology Standard Reference Material 981 (NIST SRM 981) Common Lead. Mass bias corrections were performed to Pb isotope determinations using the Tl internal standard correction method described by Ketterer et al. (1991). For this correction method, each sample is spiked with 0.5 mg/L of Tl stock solution (Absolute Standards, Inc) prior to ICP-MS measurement and then instrumental and sample-induced sources of bias are corrected for using the value of the ^{205}Tl:^{203}Tl measured in the sample during simultaneous measurement of ^{202}Hg, ^{204}Pb, ^{206}Pb, ^{207}Pb, and ^{208}Pb. ^{204}Hg was determined from ^{202}Hg in order to make corrections for isobaric interference between ^{204}Hg and ^{204}Pb. Precision and accuracy were determined by repeat analysis of NIST SRM 981 Pb to be better than ±1%. The Pb isotope and concentration data are given in Appendix D.

Four of the sequentially digested samples were also analyzed for Pb isotopes by Thermal Ionization Mass Spectrometry (TIMS) at the Geochronology Laboratory at the

University of British Columbia in order to compare the analytical precision of the ICP-MS results. Generally, there was good agreement between the TIMS and ICP-MS values with ICP-MS values within ±5% of TIMS.

6.1.6 Mercury Analysis

Mercury was measured by Cold Vapour Atomic Flourescence Spectrometry (CV-AFS). One high-resolution short core and one low-resolution long core was analyzed for each lake. Sediment samples were digested using aqua-regia, a mixture of 3 parts HCl and 1 part HNO_3, and in this case an additional oxidant of 0.01% $K_2Cr_2O_7$ was added to ensure that all Hg is converted into and remains in the non-volatile oxidized state (Hg^{2+}). Because aqua regia is used, the results are considered to be something the analytical community calls "partial totals" which means all the Hg in all phases except silicate minerals. Hg in rocks is typically found in sulphide, organic, oxide, and carbonate minerals and/or is adsorbed to clay minerals and other particles. Hg concentrations in silicate minerals are typically very minor. Since the aqua-regia residual is typically composed entirely of silicate minerals, the "partial totals" determined here can be regarded as "totals" for Hg, but this is not always true for other elements. It is worth noting as well that, in terms of Hg released to the environment, either naturally or by humans, that Hg would be sequestered into lake sediments exclusively in the non-silicate phases. And so aqua-regia digestion is a robust and appropriate method for the digestion of lake sediments for the determination of Hg.

The procedure is as follows: 5 mL of aqua-regia was slowly added to 0.1 g of dry, homogenized sample in a pre-weighed 50 mL polypropylene Falcon centrifuge tube. The tubes are then loosely capped and left to stand for at least 5 hours or overnight until the reaction dies down. The caps are tightened and the tubes are quickly shaken vigorously for about one minute to ensure acid is in contact with all sample material. The caps are again loosened to release pressure from agitation and the tubes are placed in a hot water bath for 5 hours at 80°C and then left overnight to cool. Once cooled, the digest is diluted to ~50 mL with a mixture of 0.01% $K_2Cr_2O_7$ in MQ water, re-capped, and then re-weighed to determine the precise volume. Finally, the diluted digests are shaken again

for approximately one minute and then centrifuged for 10 minutes at 3500 rpm in order to separate the digested solution from any undigested mineralogical residue. Mercury concentration was determined by CV-AFS using a PS Analytical Millenium Merlin/Galahad Mercury Analyzer. Calibration standards were made from $HgCl_2$ and diluted in 5% Aqua-Regia with 0.01% $K_2Cr_2O_7$. Precision and accuracy were determined by repeat analysis of CANMET standards LKSD3, LKSD4, TILL3 and TILL4 and the NRCan Dog Fish Liver Tissue standard (DOLT). Precision was always better than +/-5% based on replicate analyses and accuracy better than +/-10% based on the SRMs. Precision accounts for instrumental drift, and daily variations in operating conditions. Procedural blanks were run, and contained no detectable Hg. The limit of detection (LOD) for the method was determined to be 0.05 ng/g dry weight for the samples. Instrumental LOD for Hg is ~5 pg Hg and so ultimately LOD depends only on sample size and reagent purity. All Hg results are given in Appendix E.

6.1.7 Accumulation

The total mass of Pb and Hg in the lake sediments was determined using sediment mass and distribution together with elemental composition and bulk density measurements. Using high-resolution seismic reflection profiles together with sediment coring, Ferguson (2002) quantitatively determined the sediment distribution within the Big Dam Lakes of Kejimkujik Park, including total mass and thickness of sediments. The seismic reflection profiles enabled a 3-dimensional picture of sediment morphology, and thus allowed accurate estimates of sediment volume. The sediment distribution within the Big Dam Lakes is illustrated in Figure 5.2.

Ferguson (2002) divided sediment thickness into "classes", each representing a 5-cm vertical section. Each class was assigned a specific bulk density value determined from physical property measurements. Then, in combination with class area information from the isopach maps, the sediment volume and mass of each class was estimated, the sum of which produced estimates for the entire lake.

To calculate Pb and Hg accumulation for this study, the sediment volume and mass of each class from Ferguson (2002) were combined with elemental data determined

by chemical digestion of sediments and ICP-MS and CV-AFS analyses. However, since the focus of this study is primarily the uppermost portions of the sediments, some changes were necessary to improve the calculations of sediment mass in these portions. In calculating sediment mass from class volume and dry bulk density (DBD), the DBD values in the top metre of the cores from Ferguson (2002) were replaced by DBD values determined from the short cores used in this study (Appendix F). This was done because the DBD values for these portions of the long cores from Ferguson (2002) are believed to be unreliable. The coring method used to obtain the long cores can be very destructive to the upper portions of the core and results in the mixing of the top centimetres with the overlying waters. The upper portions are further disturbed during transportation and when the cores are laid horizontally during physical property measurements using the whole core multi-sensor track system. The very low DBD values in the uppermost sediments from the long cores from both lakes in Ferguson (2002) are evidence that these sediments were well mixed with the overlying waters, thus giving low or watery DBD values (see Appendix F).

Short core sub-sampling was done at intervals ranging from 0.25 cm to 2 cm. In order to apply the DBD data, as well as Hg and Pb, the 5-cm thick classes had to be divided into smaller classes, 0.5 cm classes in the top 10 cm and 1 cm classes below 10 cm, until reaching the length of the short cores. Below this depth, the classes were left at their original 5-cm thickness.

Pb and Hg concentrations for both short and long core samples were applied to the classes that contained their corresponding depths. Where multiple samples existed within a class, the average concentration of those samples was used. For depths where there were no samples analyzed, an average of the closest samples analyzed above and below that depth was used. Data used to calculate whole lake accumulations of Pb and Hg are given in Appendix G and H.

6.2 Porewaters

6.2.1 Sampling and Analyses

Lake sediment porewater was sampled by in-situ dialysis using diffusion-type porewater samplers, commonly called "peepers", similar to those described by Carignan et al. (1994). This method of interstitial water sampling was first introduced by Hesslein (1976) and has since become widely used for studies of the distribution and mobility of chemical species in sediments and their associated porewaters (Carignan et al., 1985; Comans et al., 1989; Davis and Galloway, 1993). In terms of obtaining reliable results for porewater chemistry, peepers have several advantages over the more common method of centrifugation and filtration: they require less equipment, are less time-consuming, and their inherent simplicity allows maximal replication and minimizes the chances of sample contamination (Carignan, 1984; Carignan et al., 1985). The main disadvantages of peepers are: (i) aliasing the depths of results from peepers with depths from sediment cores is not always straight forward and so misalignment is possible; (ii) it is possible that the sediment and porewater chemistry where a peeper is emplaced is different from that of a core taken several meters away. However both of these can be minimized by careful work.

The peepers used in this study were constructed out of 1-cm thick sheets of acrylic (Lucite) having dimensions of either 50 × 8 cm (single peeper) or 50 × 19 cm (double peeper). A detailed figure of the equipment that should enable replicas to be made is given in Appendix A. Sampling chambers were machined in vertical rows at one cm intervals, centre to centre, each having horizontal dimensions of 60 × 6 × 10 mm and sampling a volume of about 3.6 mL. Single peepers contained one vertical row of 38 sampling chambers, while double peepers contained two such vertical rows spaced 4.5 cm apart. A 3 mm thick acrylic (Plexiglas) plate, with dimensions and apertures matching those of the main peeper body, secures a Pall Gelman HT-Tuffryn 200 (0.2 μm pore size) membrane sheet over the sampling chambers. The membrane and faceplate were fastened to the main body with Nylon screws spaced 5 cm apart.

Peepers were cleaned with biodegradable Sparkleen (Fisher Scientific) to remove any machining lubricants and shavings, soaked in a 10% HNO_3 bath for 24 hours, and

then rinsed and soaked in MQ water for another 24 hours. Before emplacement in sediments, peepers need to be de-gassed to remove any free oxygen because its presence will alter the chemistry of "reduced" porewaters. This is done by assembling the peepers, submerging them in an enclosed tank of DI and bubbling with ultra-pure N_2 gas. The peepers were assembled by filling the sampling compartments with DI water and overlaying them with a strip of filter membrane before reattaching the faceplate, taking care to ensure that no air pockets were present in any of the sampling compartments. All peepers were placed into one large polypropylene Rubbermaid container filled with DI water and degassed for 24-48 hours by bubbling with ultra high purity N_2 gas (Praxair), as this method and duration has been indicated to be sufficient for the removal of dissolved oxygen from the samplers (Carignan, 1984). However, Carignan et al. (1994) (1994) have indicated that substantial amounts of O_2 are lost by the plastic, thus reacting with reduced constituents in the porewaters, and suggest that acrylic diffusion samplers should be degassed with N_2 for 30 days, particularly for anoxic sediments of oligotrophic lakes. Peepers in this study were observed to have a small band of orange iron oxide staining at or near the sediment-water interface and the porewater samples gradually changed from having an orange tint at the sediment-water interface to being clear at depth. It was also noted that samples above the sediment-water interface were all the colour of the lake water and there was a sharp change to orange tinted water at or near the sediment-water interface. These changes in porewater colour, as opposed to all samples being orange-tinted (Carignan et al., 1994), indicates that any oxygen being released from the acrylic itself is not significant enough to change the composition of the surrounding porewaters and therefore results of this study are believed to be a good reflection of nature rather than an artifact of incomplete de-oxygenation of the samplers.

Separate peepers for the determination of Hg, Pb, cations such as Fe and Mn, and pH and redox potential were emplaced into the sediments. A peeper was also used as a procedural blank, undergoing all steps except insertion into sediments. Peepers were inserted by a SCUBA diver to a depth that would leave several of the top sampling cells protruding above the sediment-water interface to equilibrate with the lake bottom waters. The top of each peeper was attached to an adjacent weight, which was tied to a marker buoy floating at the lake surface. Adjacent weights were placed approximately one metre

from the peepers. Small buoys were chosen to minimize tugging on the equipment from wind and waves. Any pulling that did occur would be absorbed by the weights and prevent movement of the emplaced peepers. The peepers were left to equilibrate for a period of 17 days in July 2000 and 21 days in July 2001, as this has been demonstrated to be an adequate period of time to attain equilibrium with ambient porewaters (Carignan, 1984).

Extraction of porewater samples was done on site in the boat immediately after removing the peepers from the sediment in order to minimize exposure to oxygen. To further minimize exposure, the peepers were covered with clean polyethylene bags while sampling. Porewaters were extracted from the sampling chambers by directly puncturing the filter membrane with the tip of a sterile luer slip tip 10 mL all polyethylene/ polypropylene syringe (no black plunger) and injecting the samples into pre-rinsed 8 mL HDPE Nalgene bottles. Samples for Pb or cation analysis were acidified with 40 μL of trace metal grade HNO_3 and samples for Hg analysis were acidified with 40 μL of BrCl made according to U.S. EPA method 1631 (1999). The samples were stored in the cooler with ice and gelpaks for two days while being transported to the University of Victoria where they were stored in a refrigerator at 4°C until analyzed. Hg was analyzed by CV-AFS as described above and Pb and other cations were measured by micro-nebulization ICP-MS in the University of Victoria Aqueous Geochemistry Lab. The Hg and Pb porewater concentrations are given in Appendix I, as well as Mn concentrations.

For Hg analyses, analytical error is estimated at +/- 0.8 pg/g or 20% of a 4 pg/g standard. LOD for samples of volume 4mL is 0.8 pg/g. Error is relatively high for these samples because the total mass of Hg available to collect on the gold trap is small due to sample size (<4 mL) and so LOD is relatively high.

For Pb and Mn, the LOD is less than 0.01 ng/g and 0.1 ng/g, repsectively. Analytical error for Pb and Mn is +/- 5% based on repeat analyses of NRC Certified Reference material SLRS-4.

6.2.2 Dissolved Oxygen, Redox, and pH

Dissolved oxygen (DO), redox potential, and pH in interstitial waters are important characteristics for the determination of diagenetic conditions in lake sediments. Measurements of these properties were taken by two different in-situ methods: (1) probing the sediments of a specially designed core tube, and (2) probing the porewater samples obtained with peepers. Data was recorded using a PC-based Duo-18 2-channel data acquisition system, which is a multi-functional meter and real-time chart recorder operated under Microsoft Windows on a laptop PC computer. With this system, two different probes can be connected to the Duo-18 to collect data at the same time. The pH microprobe used for this study was an Orion micro-combination pH electrode with 16 gauge bevel needle tip, the DO microprobe was a WPI oxygen electrode probe oxel-1 with ISO_2 dissolved oxygen meter, and the redox probe was a Cole Parmer platinum combination ORP electrode.

Four sediment cores, two from each lake, were taken specifically for the measurement of pH and DO. These cores were obtained using a modified KB gravity corer as described in the previous section. However, the 1-m long polycarbonate tubes used for these cores were pre-drilled with two vertical rows of 3 mm wide holes spaced 1-cm apart, centre to centre. The two vertical rows were 1.5 cm apart and the holes in the second row were offset by 0.5 cm from those in the first row, thus enabling the sediments to be probed at 0.5 cm intervals. Prior to sample collection, the core tubes were sealed with two layers of tightly wrapped Parafilm secured with a tightly wrapped layer of electrical tape. Once collected, the sediment cores were brought to shore where the electrodes were poked through the Parafilm and into the sediments sequentially from top to bottom. Data was acquired at each depth for a period of 20 seconds. This allowed rapid and uncontaminated "in-situ" measurements of both pH and DO to be made every 0.5 cm through the depth profile. A micro-probe that would fit into the core tube holes could not be found or made and so redox (and pH) measurements were made on additional peepers emplaced in the lake sediments solely for this purpose. Measurements were taken in the boat immediately after each peeper was retrieved from the sediments.

All pH, redox and DO measurements are given in Appendix I.

6.3 Precipitation

Sampling and analysis of wet deposition samples such as rain or snow is the closest indirect method of determining atmospheric composition, next to directly measuring atmospheric aerosols with high- or low-volume air samplers. Rain and snow are known to be effective scavengers of aerosols present in the atmosphere (Jones and Stein, 1990) and therefore variations in the chemical composition of precipitation events should largely be a reflection of the chemical differences within the air masses they are derived from.

Wet precipitation samples were collected at the Canadian Air and Precipitation Monitoring Network (CAPMon) site in Kejimkujik Park, which is only 5 km from the Big Dam Lakes. Collection was carried out using a CAPMon wet precipitation sampler equipped with a funnel trap system with an automated lid. The automated sampling is controlled by a thermal sensor that removes the lid from the collector upon detection of precipitation (rain or snow) and returns the lid back into position over the sampling funnel within minutes after the cessation of the precipitation event. Dust cannot enter any part of the system when the cover is over the funnel. Consequently, there is no dry deposition component in these samples.

Precipitation samples are integrated samples collected over 1 week intervals for a period of 1-calendar year (July 2000 to June 2001). Samples are collected in pre-cleaned and pre-acidified 500 mL HDPE bottles. Samples are acidified with 1 mL of trace metal grade HNO_3. Upon retrieval, each sample was sealed in a Ziploc storage bag and couriered to the University of Victoria Aqueous Geochemisty Lab. Field blanks representing sampling periods with no precipitation events were filled with DI immediately upon retrieval and acidified. ICP-MS analyses of field blanks and unused pre-cleaned sampling bottles indicated that both had negligible levels of Pb (<1%).

Eighteen precipitation samples (at least one per month) were analyzed for Pb isotope ratios by TIMS at the Geochronology Laboratory at the University of British Columbia. Results are given in Appendix J and have been normalized using a fractionation factor of 0.15% based on multiple analyses of NBS 981 standard lead, and the values in Thirlwall (2000).

7. RESULTS AND DISCUSSION Part I: Sedimentation, Flux, and Accumulation

7.1 Sedimentation Rates

7.1.1 Pb-210 dating and Sedimentation

The $^{210}Pb_{ex}$ activity profiles for both the BDW and BDE cores show decreasing activity with depth until reaching background levels (Figure 7.1a). The occurrence of maximum activities at the sediment-water interface in both lakes indicates that bioturbation and sediment mixing are not significantly altering these sediment profiles. Furthermore, no macrobenthos have been found in any of the cores collected over two field seasons. Freshwater clams have been seen in the sediments of BDE while SCUBA diving but were very scarce with a concentration of <1 clam per 10 m^2. Both cores show small deviations from the overall decreasing trends. The BDE core shows an increase in $^{210}Pb_{ex}$ activity at 7 cm depth, while the BDW core shows such an increase at 8 and 9 cm depth. These deviations correspond with fluctuations in the sediment density profiles and therefore do not appear to be the result of counting errors associated with measurement of small amounts of ^{210}Pb in older sediments at greater depths. Instead, the $^{210}Pb_{ex}$ deviations appear to be the result of changes in sedimentation rates.

Figure 7.1b-c are semilog plots of $^{210}Pb_{ex}$ activity vs the uncompacted mid-depths. As would be expected for BDE, a nearly closed basin system with no inflow streams, the logarithmic plot shows a relatively monotonic decline of unsupported ^{210}Pb in the sediments with only small deviations. In contrast, the logarithmic plot for BDW, an open basin system with several input streams and a more extensive history of logging within the watershed, shows much more variability than that of BDE. The CRS model is commonly found to be a more reliable method for lakes with variable sediment accumulation rates, such as BDW (Figure 7.1b), however for this study, only sedimentation rates determined by the CIC model produce results that are in good

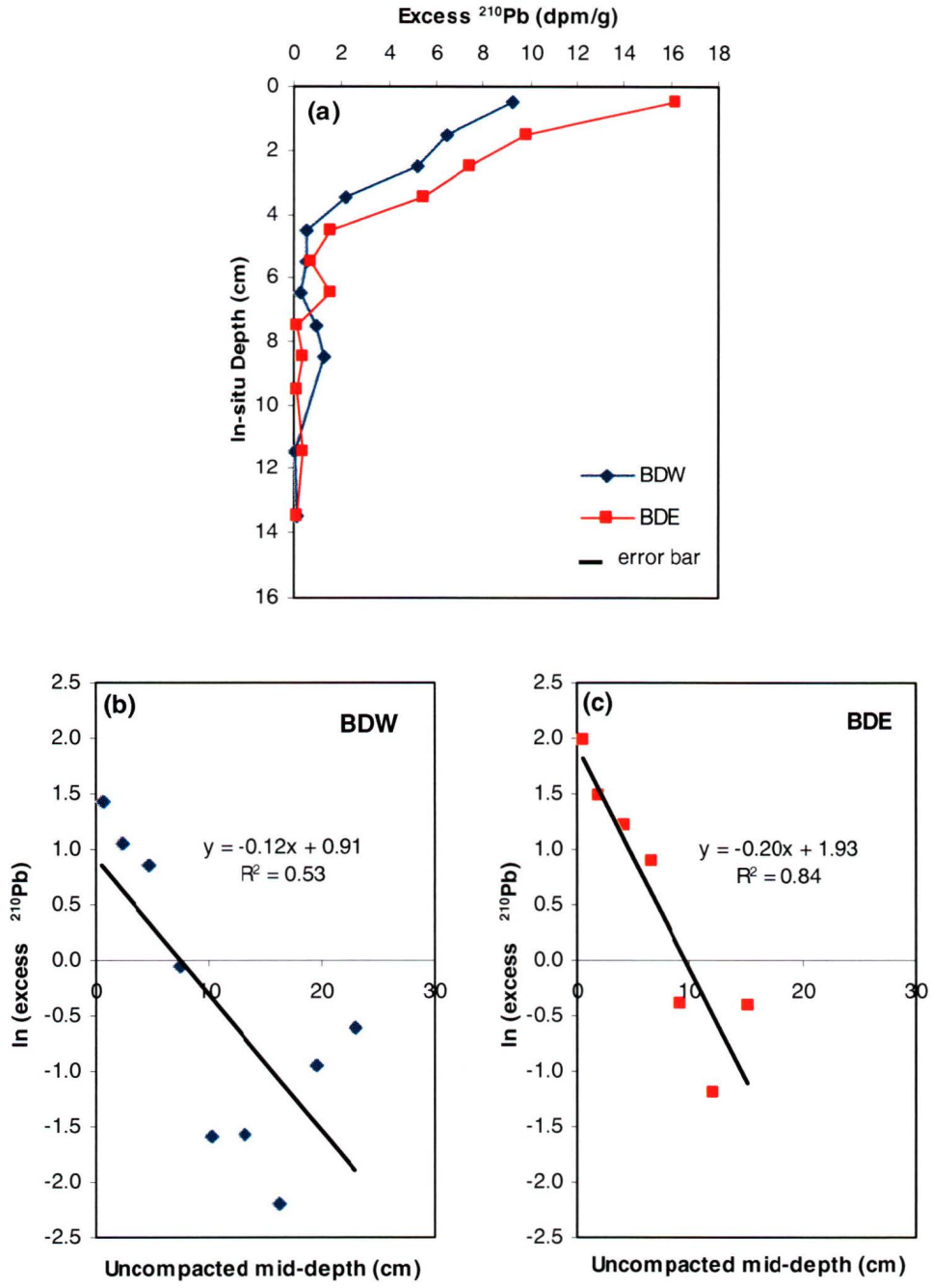

Figure 7.1 (a) In-situ distribution of unsupported ^{210}Pb in sediments of BDW and BDE; (b) and (c) plots of ln($^{210}Pb_{ex}$) as a function of uncompated mid-depth for BDW and BDE, respectively. Sedimentation rates are derived from the slope of the lines given in figures.

agreement with a stratigraphic marker of known age in both lakes. A number of studies have shown good agreement between the two dating models, particularly in systems with little variation in sedimentation rates. Thus it is not surprising that the CIC method would produce reliable results for BDE, however the results are unexpected for BDW. This result might be explained by a short water residence time that could produce a system that approximates the CIC assumption (Binford et al., 1993) of an inexhaustible reservoir of ^{210}Pb in the water column. Binford et al. (1993) hypothesized that ^{210}Pb atoms input to the lake, and possibly those that have been resuspended, may be transported out of a drainage lake before they have a chance to sediment, thereby producing a potential loss rate that is less than the supply. Indeed, a study of three other lakes in Kejimkujik Park (one clear headwater lake and two high DOC drainage lakes) showed that only a small fraction (<10%) of the seston and associated trace metals are retained in the sediments with the rest being exported out of the lakes (Nriagu and Wong, 1989). Therefore, with a water residence time of only 28 days, this seems a likely possibility for BDW as well. Supporting this interpretation is the fact that Pb concentration profiles show relatively constant concentrations at depth regardless of changes in sedimentation. Further supporting this interpretation is the difference between BDE and BDW ^{210}Pb concentrations with BDW having roughly half the initial ^{210}Pb, as would be expected for a system with a short residence time. The CIC model was therefore used.

Sedimentation rates based on the CIC model were determined from the slopes of the logarithmic plots in Figure 7.1 using equation 4.11. While 15 samples were analyzed for each lake, only of the first 9 and 7 cm of sediment in BDW and BDE, respectively, were used to determine sedimentation rates. The majority of samples below these depths produced $^{210}Pb_{ex}$ activity measurements that were below the counting errors, and thus unreliable. BDW has a linear sedimentation rate of 2.55 ± 0.36 mm/yr, which is 1.7 times greater than BDE's sedimentation rate of 1.54 ± 0.23 mm/yr. These sedimentation rates represent average rates before compaction and include any sediment focussing. The fact that the sedimentation rate in BDW is 1.7 times greater than in BDE agrees well with the sediment distribution map, which shows BDW basins having almost twice as much sediment as any BDE basins per unit area (Figure 5.2). The ages and mass sedimentation

rates derived for both lakes are listed in Table 7.1. All other cores used in this study were tuned to these cores by chemo-stratigraphic correlation to Pb isotope horizons.

Table 7.1 Ages and mass sedimentation rates determined from ^{210}Pb dating.

	Sample	In-situ depth (cm)	Uncompacted depth (cm)	Dry weight (g)	Cumulative dry weight (g/cm^2)	Excess Pb-210 (pCi/g)	Age at in-situ depth (yrs)	Mass sed. rate ($g/m^2/yr$)
BIG DAM WEST	BDW-1	1.0	1.0	6.52	0.04	4.14	4	90.9
	BDW-2	2.0	3.4	20.36	0.15	2.87	13	118.3
	BDW-3	3.0	6.0	27.21	0.30	2.35	24	145.8
	BDW-4	4.0	8.8	29.36	0.46	0.95	35	146.1
	BDW-5	5.0	11.7	32.36	0.63	0.21	46	156.8
	BDW-6	6.0	14.7	34.09	0.82	0.21	58	160.5
	BDW-7	7.0	17.8	36.71	1.02	0.11	70	165.1
	BDW-8	8.0	21.0	36.28	1.22	0.39	83	154.3
	BDW-9	9.0	24.8	36.56	1.42	0.54	98	134.1
	BDW-10	10.0	28.1	38.69	1.63		110	165.3
	BDW-12	12.0	34.9	39.64	2.07		137	162.8
	BDW-14	14.0	41.7	37.37	2.48		164	143.1
	BDW-16	16.0	48.5	36.87	2.88		190	135.2
	BDW-18	18.0	55.3	39.54	3.32		217	139.0
	BDW-20	20.0	62.0	38.56	3.74		244	130.2
						Average Mass Sed Rate =		**143.5**
BIG DAM EAST	BDE-1	1.0	1.0	9.75	0.05	7.25	6	82.3
	BDE-2	2.0	2.9	25.68	0.19	4.40	19	113.5
	BDE-3	3.0	5.2	28.94	0.35	3.35	34	106.9
	BDE-4	4.0	7.7	30.96	0.52	2.43	50	103.8
	BDE-5	5.0	10.6	32.26	0.70	0.68	69	94.2
	BDE-6	6.0	13.6	35.22	0.89	0.30	88	100.5
	BDE-7	7.0	16.5	34.57	1.08	0.66	107	97.8
	BDE-8	8.0	19.5	35.68	1.28		126	102.6
	BDE-9	9.0	22.5	33.57	1.46		146	92.6
	BDE-10	10.0	25.7	33.39	1.64		167	89.7
	BDE-12	12.0	31.7	33.67	2.01		206	94.2
	BDE-14	14.0	37.7	32.82	2.37		245	92.9
	BDE-16	16.0	44.3	33.57	2.74		288	84.9
	BDE-18	18.0	50.9	34.25	3.12		330	88.5
	BDE-20	20.0	57.3	32.25	3.47		372	85.0
						Average Mass Sed Rate =		**98.4**

Changes in sedimentation for each lake are examined using mass sedimentation rates determined by applying the ^{210}Pb ages for each sample to the corresponding dry weights in g/cm^2. A plot showing the mass sedimentation rates relative to uncompacted depth and age is given in Figure 7.2. The figure shows that BDW has had two periods of

increased sedimentation over the last 150 years, with an average mass sedimentation rate over this period of time of 143.0 ± 20 g/m^2/yr. Both increases in sedimentation coincide with known logging activities in the BDW watershed (Basquill et al., 2001). BDE, having a nearly closed basin system and a small watershed area, shows significantly less variability in sedimentation over the last 150 years, with an average mass sedimentation rate of 98.0 ± 1.5 g/m^2/yr. Only a small increase in sedimentation can be seen coinciding with the period of local logging activities, as logging in the BDE watershed was significantly less than in BDW's and may have been selective logging (Basquill et al., 2001). BDE also shows an overall increase in sedimentation throughout the entire top 20 cm, however the greatest increase in sedimentation in BDE has occurred in the last 50 years. This increase may be due to recreational activities within the watershed over this period of time, which have resulted in the development of a parking lot, picnic area, hiking trails, a canoe dock, and campsites in close proximity (inside 100 m) of the lake. However the majority of these activities are on the opposite end of the lake from where the sediment cores for this study were obtained. Another explanation is that the long-term trend for BDE represents organic decay.

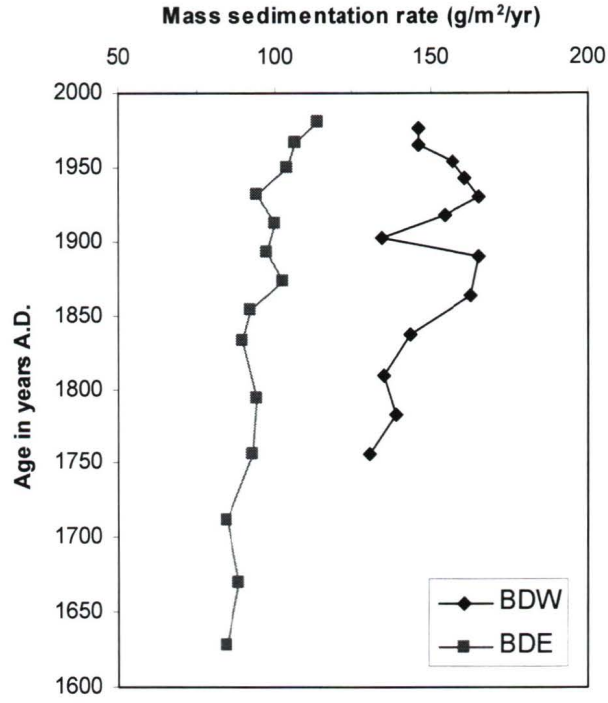

Figure 7.2 Changes in mass sedimentation rates through time.

7.1.2 Verification of ^{210}Pb Results

In an attempt to check the reliability of the ^{210}Pb dating results, measurements of ^{137}Cs activity were made for each ^{210}Pb sample in order to examine the ^{137}Cs profile. Figure 7.3 shows the ^{137}Cs profiles in sediments of BDW and BDE. Both lakes show maximum surface concentrations rather than subsurface maxima that correspond to peak production in the 1960's. Under ideal conditions in which the sediments are undisturbed and the ^{137}Cs is immobile, the activity profile of this radionuclide should reflect fallout history from nuclear weapons testing. Fallout from the atmosphere began around 1952 and reached a peak in 1963 (Robbins and Edgington, 1975). Several authors have documented deviations from the ^{137}Cs production record, such as multiple peaks or maximum surface concentrations and have attributed such results to sediment mixing or post-depositional remobilization (Davis et al., 1984; Blais et al., 1995; Benoit and Rozan, 2001). Blais et al. (1995) noted that discrepancies between ^{210}Pb and ^{137}Cs were common and that these discrepancies were most severe in soft water lakes due to an inability of sediments with low mineral content to immobilize ^{137}Cs. This is likely the case for these dilute oligotrophic lakes and so the ^{137}Cs profiles are the result of diagenetic remobilization of ^{137}Cs. Although Cs is an alkali metal with very different chemical behaviour than Pb, its remobilization towards the surface raises questions about the preservation of the Pb profiles. If Pb were remobilized, this would increase the ^{210}Pb activity of the surface sediments while also decreasing the activities at depth, giving the appearance of a more rapid decay with depth, which would then produce older age dates and under estimate the sedimentation rates. However, ^{14}C dating of long cores suggests that the sedimentation rates are not underestimated (Telmer et al., in review).

Depth profiles of Hg concentrations in lake sediments of BDW and BDE, together with local logging and mining history, were used as an alternate means to check the validity of the ^{210}Pb dating results. Historical records indicate that European settlement commenced in the vicinity of Kejimkujik park circa 1850, with logging and mining beginning shortly there after (Basquill et al., 2001). Assuming that the Hg peaks (Figure 7.4) seen at 12 and 9 cm depth in BDW and BDE, respectively, are primarily the result of logging (and perhaps gold mining in the Kejimkujik area), a calculation using the corresponding uncompacted depths of the rise in Hg associated with these peaks yields

linear sedimentation rates of 2.6 and 1.7 mm/yr for BDW and BDE, respectively. These results are consistent with those produced by the ^{210}Pb dating method.

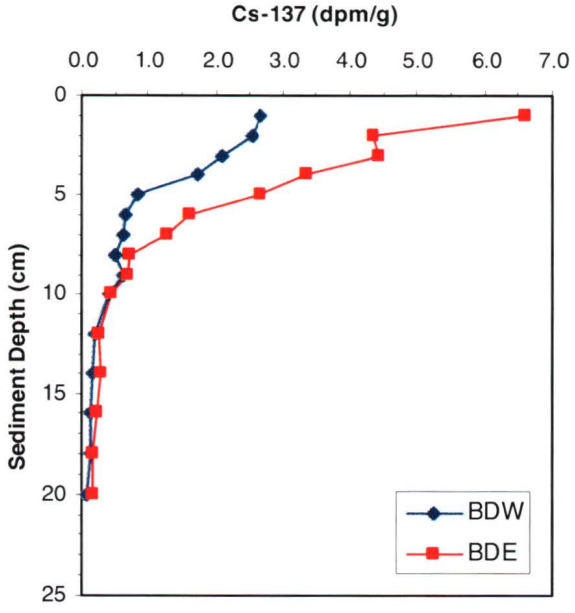

Figure 7.3 Profiles of ^{137}Cs activity showing maximum surface concentrations rather than subsurface maxima. Counting errors are within the size of the data points.

An independent study of accumulation rates in lakes of Kejikmujik Park provides further support that the ^{210}Pb dating results obtained here are reasonable. Nriagu and Wong (1989), using ^{210}Pb geochronology, determined the mass sedimentation rate of Kejimkujik Lake, another high DOC lake within Kejimkujik Park, to be approximately 33 g/m^2/yr and together with surficial Pb concentrations, estimated current Pb accumulation rates to be 2.6 mg/m^2/yr. While the mass sedimentation rate of BDW determined here is over four times greater than that in Kejimkujik Lake, the concentration of Pb in the surficial sediments of BDW are approximately 4 times lower, thus producing Pb flux rates that are in excellent agreement with those for Kejimkujik Lake.

The fact that the ^{210}Pb dating has produced results that are consistent with other work suggests that remobilization of ^{210}Pb is not significant. This is not to say that remobilization of common Pb from deeper horizons is not occurring but that Pb may not be being remobilized until such depths where very little ^{210}Pb exists and thus upward remobilization of a small fraction of what little ^{210}Pb there is at depth is insignificant relative to the amount of ^{210}Pb in the surface sediments.

7.2 Mercury in Lake Sediments

7.2.1 Mercury Concentrations

High-resolution depth profiles of Hg in these sediments (Figure 7.4a-b) exhibit typical upcore enrichments, with sharp increases beginning at depths of about 8 cm in BDW and at 6-7 cm in BDE. According to the ^{210}Pb dating results, sediments at these depths are approximately 100 years of age, indicating rapid increases in Hg inputs beginning around AD 1900. For BDW, Hg concentrations increase from 62 ng/g at 40 cm depth to a maximum of 178 ng/g at the sediment water interface. BDE increases from 36 ng/g at 40 cm to a sub-surface maximum (1.25 cm) of 121 ng/g. Relative to the average pre-industrial background concentrations, which were taken as an average of the bottom 10 centimetres of each core, the surface sediments (0-2 cm) in BDW are enriched 2.8 times versus 3.1 for BDE. A smaller Hg peak possibly due to local anthropogenic activities appears in the concentration profiles of both lakes at depths between 1850 and 1900 AD. These peaks are attributed to logging and possibly gold mining but are discussed after the next section.

The mercury concentrations measured in the sediments of BDW and BDE are within the range of concentrations found in other natural lakes throughout the world. The concentrations in the surface sediments of BDW and BDE are towards the lower end of concentrations measured in lakes of northern Quebec (60-480 ng/g; Lucotte et al., 1995), north-eastern Ontario to south-western Quebec (3-267 ng/g; Tremblay et al., 1995), Vermont and New Hampshire (220-660 ng/g; Kamman and Engstrom, 2002), Sweden (50-500 ng/g; Björklund et al., 1984) and Scotland (150-250 ng/g; Yang et al., 2002). They however fall in the high end of the range of concentrations reported for Norwegian and Russian Arctic lakes (20-160 ng/g; Rognerud et al., 1998), southern and eastern Greenland lakes (20-60 ng/g; Riget et al., 1997) and headwater lakes of Newfoundland (3-156 ng/g; French et al., 1999). While Hg measurements here generally fall in the lower end of concentrations measured in many other lakes, in terms of surface enrichments they are often in the upper range, suggesting greater anthropogenic pollution. However this may partially be explained by differences in the age of sediments chosen to represent background (pre-industrial) concentrations between different studies. Globally,

background Hg concentrations (deeper sediments) are as varied as concentrations in surficial sediments, with concentration ranges of 60-220 ng/g in Vermont and New Hampshire lakes (Kamman and Engstrom, 2002), 30-80 ng/g in a Scotland lake (Yang et al., 2002) and <10-25 ng/g in remote lakes of northern Quebec (Lucotte et al., 1995).

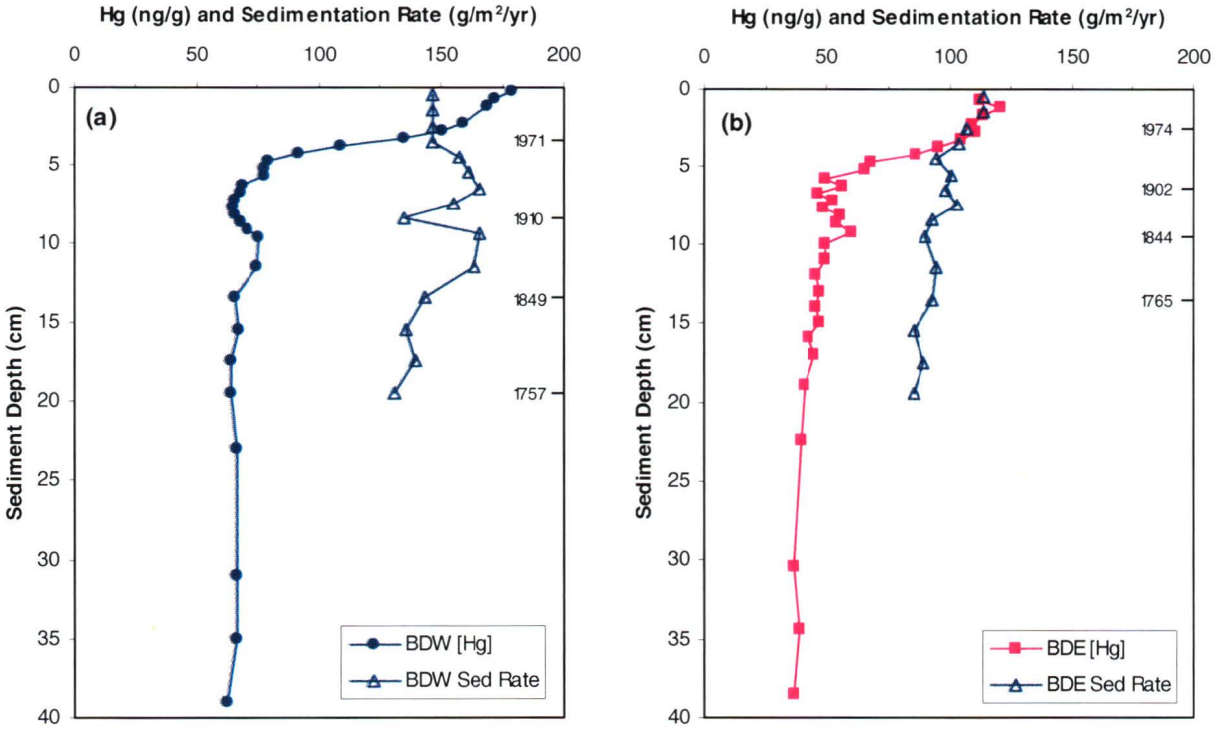

Figure 7.4 Mercury concentrations and sedimentation rates in sediments of (a) BDW and (b) BDE. Analytical uncertainties for Hg are within the size of the symbol.

7.2.2 Mercury Flux and Flux Ratios

As shown by Engstrom and Wright (1983), concentration profiles of Hg, as well as other trace metals, can be significantly influenced by changes in sedimentation. They showed that concentrations of many elements increase during periods of low sedimentation and become diluted during periods of high sedimentation. It is therefore more appropriate to evaluate potential shifts in anthropogenic inputs through time and to make inter-lake comparisons by comparing flux rates rather than concentrations. The flux rate, $F(t)$, at any depth is calculated as follows:

$$F(t) = C(t) \times R(t) \qquad [7.1]$$

where $C(t)$ is the concentration at a particular depth/age and $R(t)$ is the sedimentation rate at that depth/age in $g/m^2/yr$. By using the sedimentation rate at each age rather than an average rate for the entire core, concentration profiles are normalized to sedimentation rates and the downcore trends can be significantly modified. Interestingly, Hg concentrations in these two lakes appear to have different relationships with changing sedimentation rates (Figure 7.4a-b). In BDW, Hg concentrations increase with increasing sedimentation rates, except in the uppermost surficial sediments (<5 cm) where Hg increases regardless of how sedimentation changes. BDE however shows an inverse relation to sedimentation rate, again with the exception of the top 5 cm. This is not the result of differences in sedimentation rates (i.e. misalignment between the different cores) as examination of the $^{206}Pb/^{207}Pb$ profiles for these cores showed good alignment. Instead, the different relationships to sedimentation rates seen in these two lakes can be explained by the different water residence times, watershed composition, and size. BDE has a very small watershed with no inflow streams and a long water residence time – 228 days versus 28 days for BDW (Kerekes and Schwinghamer, 1973). With these characteristics, a large proportion of Hg in BDE is from direct deposition to the lake surface, thus increases in sediment input to the lake would be expected to dilute the relatively limited supply of Hg in the lake, producing the inverse relationship to sedimentation rate. In contrast, BDW has short water residence time, which, as discussed in relation to ^{210}Pb, produces a system where Hg flux to the sediment-water interface is proportional to sedimentation rate. However, this does not explain why the Hg concentrations increase with increased sedimentation. With BDW's larger watershed to lake area ratio (20 versus 4 for BDE), the majority of Hg to BDW sediments is transported to the lake in particulate form via the watershed rather than direct deposition to the lake surface. Therefore increased Hg concentrations occurring simultaneously during periods of high sedimentation suggests that different soil horizons with higher Hg levels are being eroded during these periods (i.e. the source changes along with the hydrography or land use).

The Hg fluxes, as well as the corresponding age and flux ratio for each depth, for the last 250 years for both lakes are listed in Table 7.2. Flux rates for the uppermost

samples, where there are no sedimentation data due to unreliable measurements, are calculated using the same sedimentation rate as that of the sample at the next closest depth, thereby assuming that sedimentation rates have not changed in the last 20 years. Figure 7.5a illustrates the changes in Hg flux to the two lakes as a function of time. It is useful to compare these Hg fluxes to history. Engstrom and Swain (1997) state that global Hg production increased from the 1910's to the 1970's and then decreased by the 1990's. However, global mercury burdens have not declined with recent decreases in production (Martinez-Cortizas et al., 1999). The increases in Hg inputs to these lake sediments parallel that of global production until the 1970s but do not show a subsequent steady signal or significant decrease post 1970. The lack of a recent decrease has been commonly reported except in lakes where there have been local decreases in emissions (Pirrone et al., 1998; Engstrom and Swain, 1997). Assuming diagenetic remobilization is not a significant factor, the lack of a recent decrease in Hg flux in these sediments suggests that the majority of Hg deposited to Kejimkujik Park is from the global Hg pool rather than regional sources, otherwise the sediments would show decreases in Hg flux associated with reductions in North American emissions as have been found in sediments from the Great Lakes (Pirrone et al., 1998). The BDE profile does show a possible small decrease in the top 1 cm, but as mentioned above, due to unreliable measurements at this depth, it is not certain whether this decrease is real.

In terms of a rate of change, the annual increase in Hg flux to these sediments since the beginning of the 20th century has been 0.2 $\mu g/m^2/yr$ in BDW and 0.01 $\mu g/m^2/yr$ in BDE. This works out to an average annual rate of increase of 1.9 %/yr and 1.8 %/yr, respectively, which is in excellent agreement with the 2% average annual increase estimated by Swain et al. (1992) and in good agreement with the 1.5%/yr estimated for the Northern Hemisphere by Slemr and Langer (1992). The average Hg fluxes for the last 20 years of 25.0 and 13.0 $\mu g/m^2/yr$ together with their respective lake areas indicate that 29.7 and 6.9 g of Hg are deposited each year to the lake sediments of BDW and BDE, respectively.

Figure 7.5a shows that the flux of Hg to BDW sediments is greater than that to BDE sediments, and has been for at least the 250 years shown in the figure. On average,

Table 7.2 Mercury fluxes for BDW and BDE. Values in bold are those used to determine the average pre-industrial flux. The flux ratio is the flux listed in the table divided the pre-industrial average. Sedimentation rates in italics are assumed due to unreliable data at these depths.

In-situ	Big Dam West Lake					Big Dam East Lake				
Mid-Depth (cm)	BDW Age (yrs A.D.)	Sed Rate ($g/m^2/yr$)	Hg (ng/g)	Hg Flux ($ug/m^2/yr$)	Hg Flux Ratio	BDE Age (yrs A.D.)	Sed Rate ($g/m^2/yr$)	Hg (ng/g)	Hg Flux ($ug/m^2/yr$)	Hg Flux Ratio
0.5	1998	*145.8*	174.64	25.46	3.00	1997	*113.5*	111.64	12.67	3.03
1.5	1991	*145.8*	168.12	24.51	2.88	1987	113.5	116.81	13.26	3.17
2.5	1982	145.8	153.97	22.45	2.64	1974	106.9	109.93	11.75	2.81
3.5	1971	146.1	121.37	17.73	2.09	1958	103.8	99.66	10.35	2.47
4.5	1960	156.8	84.75	13.29	1.56	1941	94.2	76.43	7.20	1.72
5.5	1948	160.5	76.94	12.35	1.45	1922	100.5	57.06	5.74	1.37
6.5	1936	165.1	67.74	11.18	1.32	1902	97.8	51.00	4.99	1.19
7.5	1924	154.3	64.37	9.93	1.17	1883	102.6	49.84	5.12	1.22
8.5	1910	134.1	66.09	8.87	1.04	1864	92.6	54.40	5.04	1.21
9.5	1896	165.3	72.27	11.95	1.41	1844	89.7	59.59	5.34	1.28
11.5	1876	162.8	73.99	12.05	1.42	1804	94.2	48.74	4.59	1.10
13.5	1849	143.1	64.75	9.27	1.09	1765	92.9	46.93	**4.36**	1.04
15.5	1819	135.2	66.32	8.96	1.05	1723	84.9	46.97	**3.99**	0.95
17.5	1789	139.0	63.00	**8.76**	1.03					
19.5	1757	130.2	63.32	**8.24**	0.97					
Pre-Industrial Average				8.50					4.18	

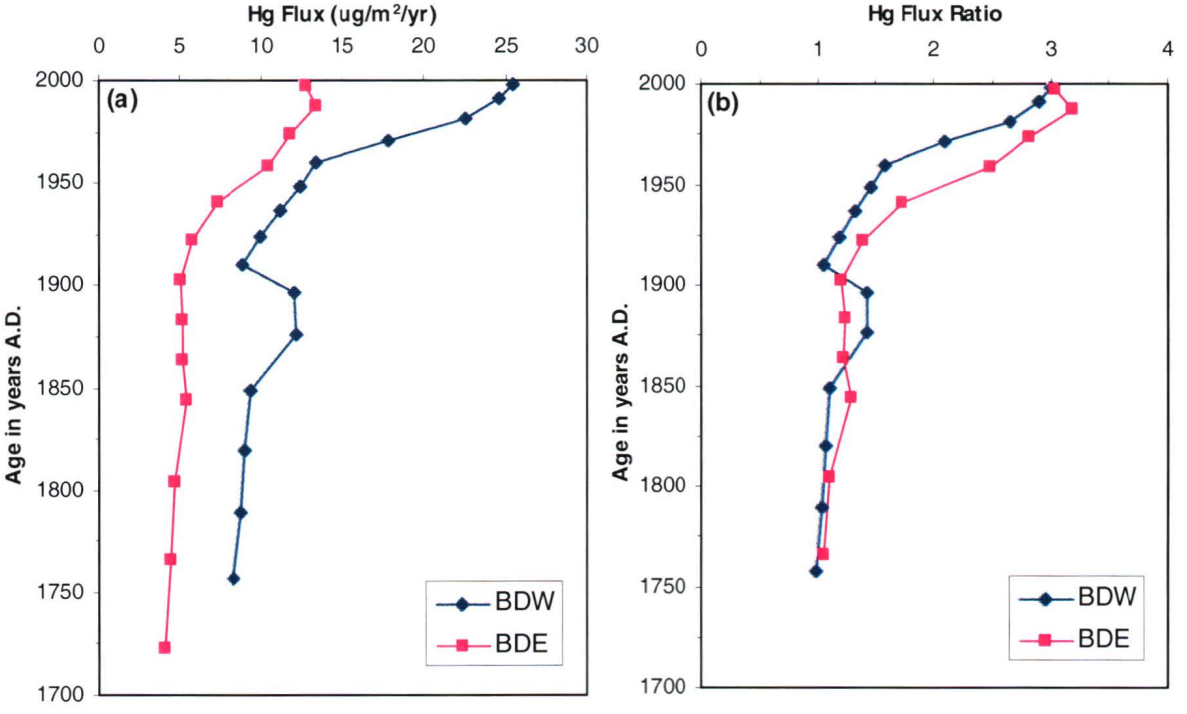

Figure 7.5 Profiles of (a) Hg fluxes and (b) Hg flux ratios through time for data presented in Table 7.2. Flux ratios are the ratio of Hg accumulation at various times relative to the average pre-industrial value.

the Hg flux to BDW sediments is 1.9 times greater than the flux to BDE sediments, with a range of 1.3 to 2.4. Since these two lakes are only a few metres apart from each other, local variations in atmospheric deposition cannot be used to explain the difference. Therefore, the larger flux of Hg to BDW sediments is most likely due to a greater watershed input, since the watershed to lake area of BDW is 5 times greater than BDE. However, differences in geochemical characteristics between the lakes, such as lake water DOC, alkalinity and pH levels (Driscoll et al., 1998) and organic carbon content of the sediments (El Bilali et al., 2002), are likely also significant contributing factors that may aid in a greater amount of the Hg being deposited and preserved in the sediments of BDW.

To compare the changes in Hg inputs through time of one lake system to another, the flux ratio is used. The flux ratio is the ratio of Hg flux at a particular depth in the sediment column relative to that at another depth and assumes that changes in the magnitude of Hg flux between the two depths are the result of changes in inputs rather than processes. The use of flux ratios to assess changes in inputs to a system also assumes that post-depositional diagenetic processes have not significantly altered the Hg concentration profiles. The flux ratios given for each depth listed in Table 7.2 and presented in Figure 7.5b are determined as the flux at each depth and age relative to preindustrial levels, which are taken as the average flux between 1750 to 1800 AD. The flux ratio data indicates that the present flux of Hg to both lakes has increased by a factor of 3.0 relative to preindustrial levels. The Hg fluxes and flux ratios measured here are within the range of those reported for recent lake sediments from Northern Quebec (Lucotte et al., 1995), Vermont and New Hampshire (Kamman and Engstrom, 2002), Scotland (Yang et al., 2002), and Finland, Sweden, and Western Canada (as compiled by Landers et al., 1998).

The ratio of post- to pre-industrial Hg flux data in Figure 7.5b also indicates that since the increased Hg flux around 1900 AD, BDE has shown larger Hg flux increases throughout most of this time period, despite the fact that the actual flux of Hg has been greater for BDW. These larger flux ratios seen in BDE may be the result of one or more of the following reasons: (a) due to BDW's greater watershed to lake area ratio and the presence of a wetland, the latter of which have been shown to be important sinks of

atmospherically derived metals (Shotyk et al., 1998), there is a greater delay in the delivery of atmospherically deposited Hg from the watershed to the lake sediments, which then delays the magnitude of increased atmospheric Hg inputs as recorded in the sediments (Mieli, 1995); (b) the Hg profiles in the uppermost sediments vary with depth rather than age (depositional history) and therefore may be controlled by diagenetic processes; (c) Error in the sedimentation rates determined for one or both lakes. According to the arguments in the section on ^{210}Pb, the latter is unlikely. The second point is a possibility as a number of recent studies have shown that trace metal enrichments in surface sediments may be to some extent attributed to redistribution caused by recycling mechanisms associated with the decay of organic matter and oxide dissolution in the anoxic zone (El Bilali et al., 2002; Gobiel et al., 1999). Indeed porewater analyses in this study (discussed in a subsequent chapter) indicate that Hg is being remobilized in these sediments but the degree to which this may have affected these Hg profiles is unclear. However, the fact that the smaller Hg fluctuations associated with historical logging and mining events have been preserved suggests that remobilization may not be significantly altering these profiles, at least in the shallow depths studied here. The fact that the ratio of present day to pre-industrial Hg fluxes is 3, similar to estimates of the increase in the global atmospheric Hg burden, and that the average annual rate of increase in Hg flux to these sediments is similar to the annual rate of increase in the global atmospheric Hg burden, further suggests that at these shallow depths the Hg flux profiles may be a reliable representation of depositional history. This is not to say that there is no remobilization, just that at these depths it may not be significantly altering the profiles.

If the separation between flux ratios of BDW and BDE seen during the anthropogenic Hg rise (Figure 7.5b) is assumed to be a primary signal, then the lower flux increases in BDW during the rise can only be explained by a watershed delay. If this assumption is valid, the flux ratio profiles indicate a 20-year delay before the magnitude of increased Hg inputs in BDE are seen in the sediments of BDW. Thus even if atmospheric Hg levels were reduced to pre-industrial levels in the next year or two, it could be at least 20 years before we see the BDW watershed ecosystem return to pre-industrial conditions.

7.2.3 A Secondary Mercury Peak – Local Mining or Logging

As mentioned previously, a second smaller Hg peak occurs in the Hg concentration profiles of both lakes at 10.5 and 9 cm, with rises beginning at depths of 13.5 and 10 cm for BDW and BDE, respectively (Figure 7.4a-b). This fluctuation occurs between the years of 1850 to 1910, with the peak dated at 1883. This fluctuation can also be seen in the Hg flux profiles (Figure 7.5), although not as clearly in BDE.

The rise of this peak corresponds with European settlement and logging in the Kejimkujik area in 1850 (Basquill et al., 2001). Gold mining in the park area and nearby counties did not begin until the mid 1880's, however no known mining activities took place in either of the Big Dam watersheds (Cumming, 1979; Sheppard, pers. comm.). Extensive logging and numerous associated forest fires occurred in and around the Big Dam watersheds at this time, primarily in the BDW watershed. Basquill et al. (2001) document a large forest fire in 1885 in the Big Dam West and neighbouring Frozen Ocean Lake watersheds that extended as far as 10 km west of the lakes. Several small understory and overstory fires were also indicated in the BDE watershed at this time. The timing of this Hg peak between 1850 and 1910 is likely first the result of increased sediment inputs due to the clearing of vegetation from logging and forest fires and secondly due to increased atmospheric deposition of Hg from the forest fires, local mining activities, and coal burning. However the timing of this fluctuation also coincides with the North American mining signal predicted by the analyses of Nriagu (1994) and Hudson et al. (1995) for gold and silver mining during the 1850-1900 period. While local Hg deposition and watershed disturbances would be significantly stronger contributing factors here, all events could have contributed to the formation of this peak.

Unlike BDW, there is no documentation of logging in the BDE watershed until the mid-1940's (Basquill et al., 2001) and in fact BDE shows lower sedimentation rates throughout this 1850-1910 period, and yet BDE still shows an increase in Hg flux of 22% during this time period compared to BDW's 42% increase (Table 7.2, Figure 7.5a). This increase in BDE must therefore be due to increased atmospheric deposition, be it from logging activities in the neighbouring watersheds, local coal and forest fire burning, or local or North American mining activities. The larger increase in Hg flux in BDW during

this period compared to that in BDE shows the significant influence of having anthropogenic activities occur within the watershed.

A peak associated with the North American mining signal has not been resolved in other studies, including a study which included three cores from Kejimkujik Park (Lamborg et al., 2002), one of which was also taken from Big Dam East Lake. The fact that the smaller Hg peak observed in this study was not previously seen in a core taken from one of the same lakes studied here is likely due to sampling resolution. Therefore, even though the significance of North American mining inputs to these lakes is unclear due to the impact of local anthropogenic activities during the same period, it is possible that such a peak associated with the North American mining signal may be found in future studies of remote lakes.

7.3 Lead in Lake Sediments

7.3.1 Lead Concentrations from Sequential Digestions

The two-step sequential leaching of Pb from the sediments shows that the upcore enrichments of Pb typically found in lake sediments exist in the labile and weakly bound phases (leached Pb) digested by the weak HCl- HNO_3 digest. Figure 7.6 shows the concentration profiles of leached and residual Pb, as well as the summed totals of the two. The profiles of labile Pb from both lakes show relatively constant concentrations at depth followed by rapid increases starting at 10 cm depth. Both lakes have subsurface peaks at approximately 3 cm depth with slightly lower and fluctuating concentrations to the sediment water interface. The appearance of little change in concentrations in the top 3 cm is not an artefact of bioturbation or sediment mixing as other elements, including Hg and ^{210}Pb, do not display such a trend.

While the shapes of the Pb profiles for both lakes appear very similar, there are some interesting differences that are summarized in Table 7.3. Firstly, in the surface sediments, the total concentrations of Pb in BDE are 2.1 times greater than in BDW. Secondly, at depth, the total concentrations are nearly the same for both lakes, however, the proportion of Pb in the residual and labile phases are significantly different, with

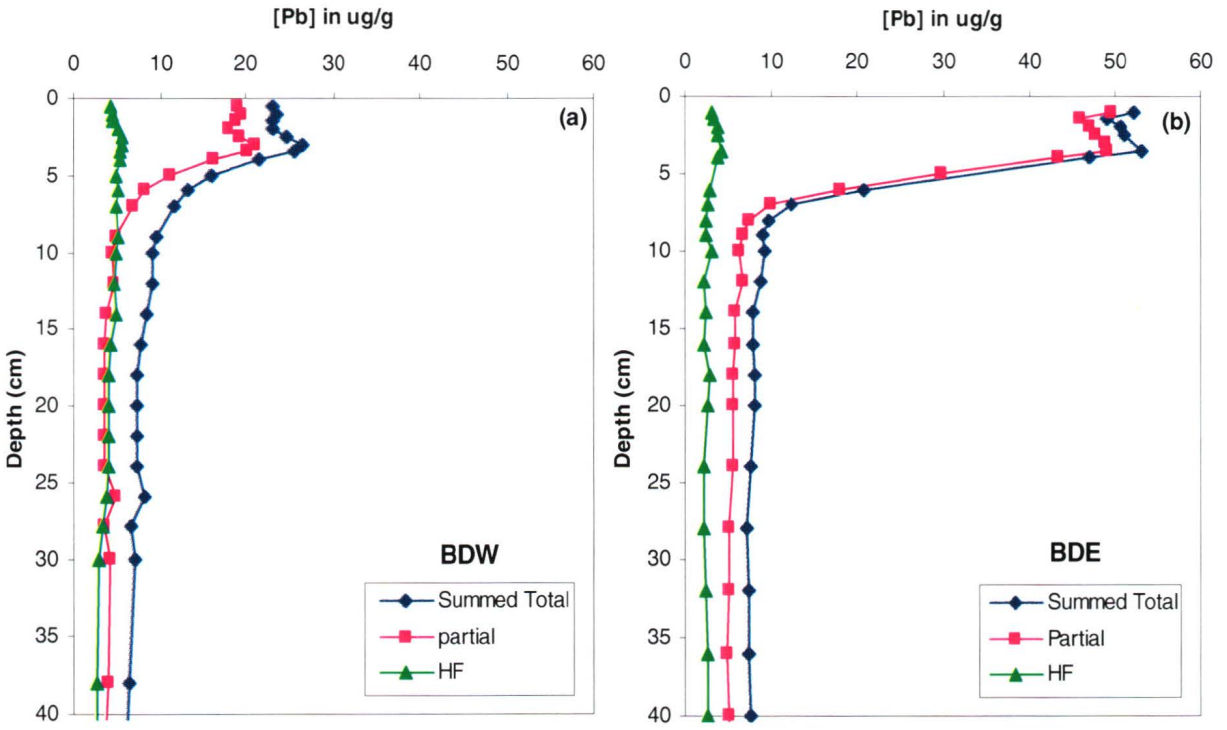

Figure 7.6 Lead concentrations for the labile phase (partial digest), residual phase (HF digestion), and the summed totals of the two digests for (a) BDW and (b) BDE.

Table 7.3 Summary of sequential digestion results in µg/g showing the differences in the distribution of Pb at the surface and at depth for BDW and BDE. A comparison of enrichment factors calculated using total Pb concentrations versus labile concentrations is also given.

	BDW	BDE	BDW:BDE
Average at Depth			
(20-25 cm)			
Residual Pb	3.84 (53%)	2.24 (29%)	1.71
Labile Pb	3.35 (47%)	5.44 (71%)	0.62
Total Pb	7.19	7.68	0.94
Average Surface			
(0-3.5 cm)			
Residual Pb	4.82 (20%)	3.43 (7%)	1.41
Labile Pb	19.24 (80%)	47.65 (93%)	0.40
Total Pb	24.05	51.08	0.47
Enrichment Factor			
Labile Pb	5.7	8.8	
Total Pb	3.3	6.7	

BDE having 24% more of its' Pb in the labile phases. Since anthropogenic Pb exists in the labile phases, attempting to assess increases in anthropogenic inputs using total Pb concentrations instead of labile Pb would underestimate the magnitude of the increased inputs. From the labile Pb data, concentrations of Pb in the surface sediments (0-3.5cm) are enriched by a factor of 5.7 in BDW and by a factor of 8.8 in BDE.

The Pb in the residue fraction is nearly constant throughout the length of the cores. Small fluctuations may correspond to changes in sedimentation rates or may come from the labile phase. Both residual Pb profiles show maximum concentrations in the surface sediments that coincide with maximum concentrations in the leached Pb profiles. This could be due to incomplete digestion with the weak acid. Monna et al. (1999) found that up to 5% of labile Pb may remain in the residue after a dilute HNO_3 digest. By comparison to residual Pb at depth, we estimate the maximum contribution of labile Pb to the residue fraction is 2.6%. It would be less if changing sedimentation were also a contributing factor.

The fact that BDE has a greater proportion of its Pb in the labile phase than BDW is logical since BDE has a smaller watershed, and so almost certainly receives relatively less inorganic particulate load. It is surprising, however, that the concentration of labile Pb in the surface sediments of BDE is 2.5 times greater than in BDW and only 1.6 times greater in the pre-industrial sediments. The simplest explanation for this is that Pb is remobilized in BDE. If the depth profiles were primary, an increase in atmospheric Pb deposition should lead to a greater increase in Pb in BDW due to its larger watershed and watershed:lake area ratio. Even in the impossible case that all Pb inputs were from the atmosphere directly to only the lake surface, BDE would only have a Pb concentration 1/1.5 higher than BDW owing to its lower sedimentation rate of 1/1.5 (or 0.67).

7.3.2 Lead Flux and Flux Ratios

Flux and flux ratio profiles of Pb from the labile phases are given in Figure 7.7 and listed in Table 7.4. Unlike the Hg flux profiles, which show BDW having a greater flux of Hg throughout the cores, the Pb flux profiles show that the two lakes had similar fluxes of Pb at depths prior to anthropogenic increases. However above these depths, BDE shows

Table 7.4 Labile Pb fluxes for BDW and BDE. Values in bold are those used to determine the average pre-industrial flux. The flux ratio is the flux listed in the table divided the pre-industrial average. Sedimentation rates in italics are assumed due to unreliable data at these depths.

In-situ	Big Dam West Lake					Big Dam East Lake				
Mid-Depth (cm)	BDW Age (yrs A.D.)	Sed Rate ($g/m^2/yr$)	Labile Pb (ug/g)	Pb Flux ($mg/m^2/yr$)	Pb Flux Ratio	BDE Age (yrs A.D.)	Sed Rate ($g/m^2/yr$)	Labile Pb (ug/g)	Pb Flux ($mg/m^2/yr$)	Pb Flux Ratio
0.5	1998	*145.8*	19.10	2.79	6.19	1997	*113.52*	49.29	5.60	9.99
1.5	1991	*145.8*	18.22	2.66	5.90	1987	113.52	45.77	5.20	9.28
2.5	1982	145.8	19.98	2.91	6.47	1974	106.86	47.17	5.04	9.00
3.5	1971	146.1	18.04	2.64	5.86	1958	103.80	48.76	5.06	9.04
4.5	1960	156.8	10.95	1.72	3.82	1941	94.18	46.03	4.33	7.74
5.5	1948	160.5	8.09	1.30	2.89	1922	100.53	36.46	3.67	6.55
6.5	1936	165.1	6.72	1.11	2.47	1902	97.83	23.81	2.33	4.16
7.5	1924	154.3	*5.68*	0.88	1.95	1883	102.64	17.90	1.84	3.28
8.5	1910	134.1	4.65	0.62	1.39	1864	92.62	9.78	0.91	1.62
9.5	1896	165.3	4.21	0.70	1.55	1844	89.70	8.49	0.76	1.36
11.5	1876	162.8	4.49	0.73	1.63	1804	94.24	6.60	0.62	1.11
13.5	1849	143.1	3.61	0.52	1.15	1765	92.94	6.06	**0.56**	1.01
15.5	1819	135.2	3.45	0.47	1.03	1723	84.90	6.50	**0.55**	0.99
17.5	1789	139.0	3.45	**0.48**	1.06					
19.5	1757	130.2	3.30	**0.43**	0.96					
Pre-Industrial Average				0.45					0.56	

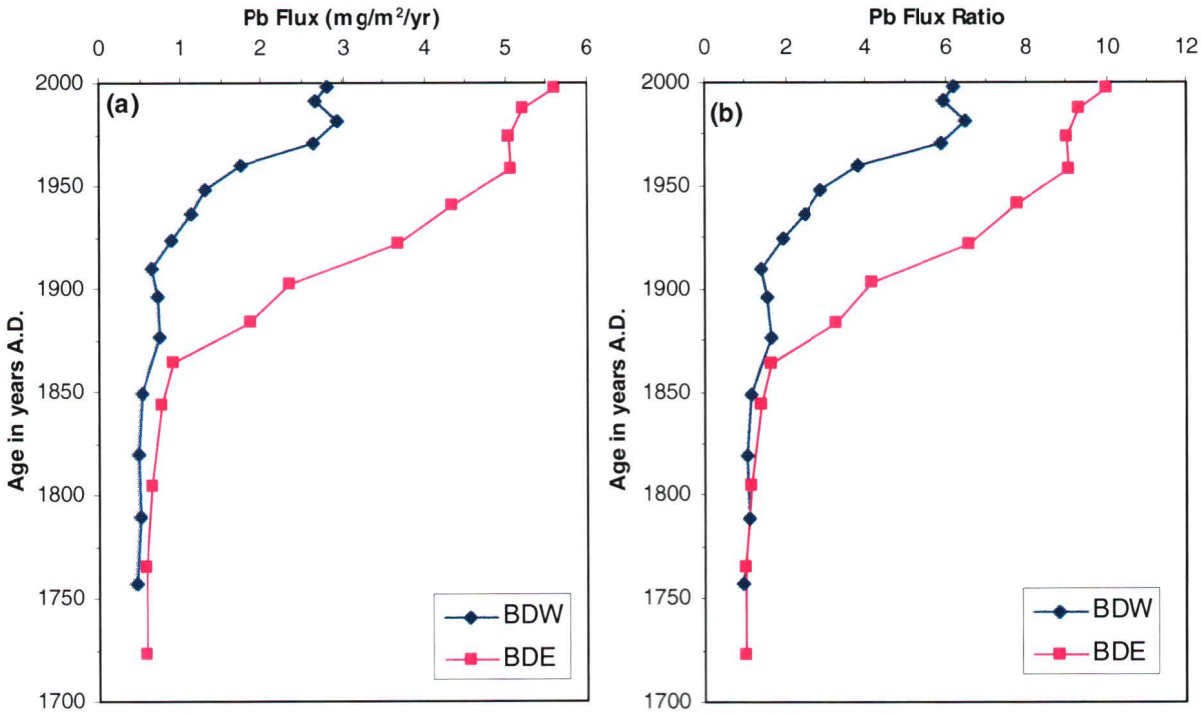

Figure 7.7 Profiles of (a) Pb fluxes and (b) Pb flux ratios through time for data presented in Table 7.4. Flux ratios are the ratio of Hg accumulation at various times relative to the average pre-industrial value.

significantly larger Pb flux rates than BDW. In the surface sediments (top 3 cm), BDE's Pb flux is 1.9 times greater than BDW. This is further evidence that Pb is remobilized in BDE sediments. Notably, it does not mean that Pb is not remobilized in BDW.

The Pb flux values measured in these lakes are much lower than those determined for a Scottish mountain lake considered to have been significantly contaminated since industrialization (Yang et al., 2002), however the ratios of pre- to post-industrial flux are far greater than that of the Scottish lake (1.5) even though these lakes are relatively more remote. BDW flux ratios are similar to those of Lake Constance, Central Europe (Kober et al., 1999) but the flux values are as much as two orders of magnitude lower. Unlike Hg studies, few have discussed Pb pollution in terms of flux and so it is difficult to make comparisons with literature.

Ignoring remobilization for the moment, Pb inputs to BDE increase beginning around 1860. Pb in BDW increases only a little at this time and does not show the same rapid increase until about 1920. Historically, atmospheric Pb concentrations are estimated to have increased about 10-fold above natural levels at the beginning of the industrial revolution 250 years ago, however sharp increases in global atmospheric Pb concentrations occurred around 1930 due to emissions from automobile exhausts (Shirahata et al., 1980; Graney et al., 1995). Atmospheric Pb concentrations continued to grow rapidly reaching maximum emissions in the early 1970's, and decreasing thereafter (Graney et al., 1995). With its small watershed to lake area ratio of 4, compared to BDW's 20, BDE should better reflect direct atmospheric deposition but the Pb flux and flux ratios (Figure 7.7) show that BDW better fits historical inputs. And neither shows the expected decrease after 1970 due to removal of Pb gasoline as found in other studies (Graney et al., 1995; Kober et al., 1999). The lack of significant or any decreases in other studies has been attributed to watershed delay (Yang et al., 2002), recent local inputs from sources other than gasoline Pb, and diagenetic remobilization.

As mentioned in the ^{210}Pb section, the average Pb flux of 2.7 mg/m^2/yr over the last ten years in BDW is in excellent agreement with the Pb flux of 2.6 mg/m^2/yr that Nriagu and Wong (1989) determined for Kejimkujik Lake, a lake similar to BDW. However, in the same study, Nriagu and Wong (1989) determined the Pb flux to sediments of Mountain Lake, a clear water lake similar to BDE, to be 1.0 mg/m^2/yr. This is

significantly less than the average flux measured to BDE (5.4 $mg/m^2/yr$). BDE may see more recreational use than either BDW or Mountain Lake (this is uncertain), but motors are forbidden in the park and in all three systems. Kejimkujik Lake, for example, is the most recreationally used lake in the park and its Pb flux is equal to that of the more remote BDW lake. This, along with the other evidence re-inforces the idea that Pb profiles are being diagenetically altered by remobilization – with clear lakes more so than dark water lakes.

7.4 Whole Lake Accumulations

7.4.1 Sediment Accumulation since Lake Inception

Initial dry bulk density (DBD) values for long cores reported by Ferguson (2002) were low because the sampling method alters the uppermost portions of the long cores. These were replaced with DBD from short cores that are well constrained. The corrected estimates of the total mass of sediments accumulated since lake inception are $4.13x10^5$ Mg for BDW and $1.11x10^5$ Mg for BDE. The data is in Appendix F.

7.4.2 Lead and Mercury Accumulations

Applying the concentrations of Hg and Pb to the sediment accumulations allows the determination of the mass accumulated since inception ~13,000 years BP. 14.7 and 3.4 kg of Hg and 5305 and 1502 kg of Pb accumulated in BDW and BDE, respectively (see Apendix G and H).

It has been suggested by Rada et al. (1993) that bioavailable trace metals are those in the top 5 cm of sediments. This ignores remobilization but nevertheless the amount of Hg and Pb in the top 5 cm is calculated for comparison and as a crude estimate of what is instantaneously available to organisms today. The total mass of Hg in the top 5 cm of BDW and BDE is 1144 and 389 g respectively (see Apendix G and H), and the total mass of labile Pb in the top 5 cm is 148 and 165 kg, respectively.

8. RESULTS AND DISCUSSION Part II: Pb Isotope Investigation of Sources and Diagenetic Remobilization

This chapter will examine the Pb isotopic compositions of precipitation and lake sediments to identify the heavy metal sources to these lakes and to assess the reliability of these sediments to record historical inputs.

Kejimkujik Park is located downwind of populated and industrial North American emission sources that may contribute Hg and Pb to the atmosphere. Due to the chemical properties and behaviour of Hg and its long residence time in the atmosphere (~1 year), it is difficult to directly fingerprint and quantify different anthropogenic and natural sources of Hg. Conversely, Pb has a relatively short atmospheric residence time of ~10 days that does not allow sufficient time for global homogenization. Anthropogenic Pb is predominantly derived from ore deposits, each of which have characteristic Pb isotope ratios that relate to their age and initial U and Th content of the source rock. The Pb released to the environment from anthropogenic activities, such as combustion of alkyl-leaded gasoline and mining and smelting operations, reflects the isotopic composition of the ore(s) used in its production (Chow and Earl, 1972), thereby making it possible to differentiate between different emission sources and between anthropogenic and natural components in a variety of sampling mediums. The average atmospheric Pb isotope compositions in terms of $^{206}Pb/^{207}Pb$ have been determined to be ~1.15 for Canadian (Sturges and Barrie, 1987; Carignan and Gariépy, 1995) and ~1.20 for U.S. (Véron et al., 1992; Rosman et al. 1994) anthropogenic sources.

8.1 Isotopic Composition of Precipitation: Sources of Anthropogenic Pollution

The Pb isotope ratios for weekly precipitation samples collected at the CAPMon meteorological station in Kejimkujik National Park are listed in Appendix J. The values given have not been corrected for field blanks or natural background contributions. Field blanks were analyzed and determined to be negligible. And according to Rosman et al.

(1998), due to the overwhelming global emission of industrial Pb, the natural component can usually be neglected, unless sampling in pristine remote environments such as Arctic ice sheets.

Figure 8.1 illustrates the temporal variation in the $^{206}Pb/^{207}Pb$ ratios of precipitation for the one-year period that the samples were collected. The figure shows that the $^{206}Pb/^{207}Pb$ ratios vary within a range of ~1.165 to ~1.20, however a significant seasonal variation is evident with the least radiogenic values recorded in summer and fall.

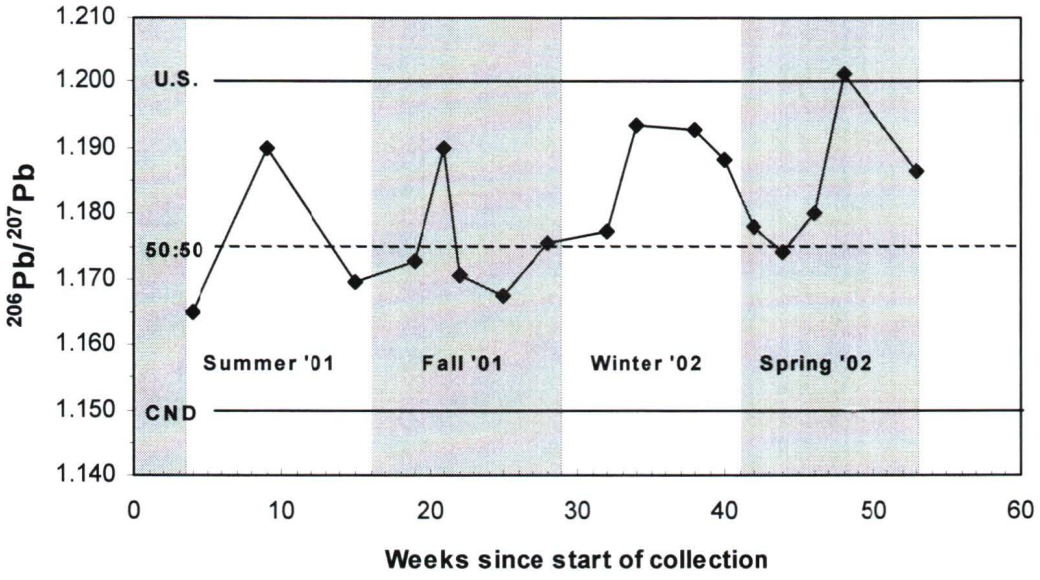

Figure 8.1 Temporal variation in $^{206}Pb/^{207}Pb$ for precipitation samples. Values representing U.S. (Véron et al., 1992; Rosman et al., 1994) and Canadian (Carignan and Gariépy, 1995) anthropogenic emissions are given as a reference. Analytical uncertainties are within the size of the symbol.

Table 8.1 presents the Pb isotope ratios from precipitation as monthly values and lists the monthly precipitation totals (mm). For months with only one weekly sample analyzed, that sample is taken to be representative of that month. Weighted averages are used for months with multiple samples. Conventional Pb-Pb diagrams of the monthly Pb isotope data are given in Figure 8.2. These plots show that the precipitation samples plot in a linear array between the estimated Pb isotope compositions of the Canadian and U.S. anthropogenic end-members. As indicated by the temporal variations of $^{206}Pb/^{207}Pb$

Table 8.1 Monthly precipitation totals and Pb istope compositions. Values in italics are the weighted average of multiple samples in that month. Annual weighted average Pb istope ratios are also given.

Date (month-yr)	Monthly precip (mm)	206Pb/ 204Pb	207Pb/ 204Pb	208Pb/ 204Pb	208Pb/ 206Pb	206Pb/ 207Pb
July-01	45.3	18.194	15.619	37.998	2.089	1.165
August-01	28.5	18.652	15.675	38.358	2.057	1.190
September-01	117.3	18.352	15.693	38.320	2.088	1.169
October-01	94.2	*18.448*	*15.638*	*38.179*	*2.070*	*1.180*
November-01	66.9	*18.300*	*15.660*	*38.130*	*2.084*	*1.169*
December-01	90.6	*18.389*	*15.644*	*38.215*	*2.078*	*1.175*
January-02	134	*18.534*	*15.638*	*38.283*	*2.066*	*1.185*
February-02	106.8	18.713	15.691	38.522	2.059	1.193
March-02	275.8	*18.463*	*15.642*	*38.243*	*2.071*	*1.180*
April-02	134.7	*18.392*	*15.637*	*38.205*	*2.077*	*1.176*
May-02	85.7	18.793	15.646	38.572	2.052	1.201
June-02	74.1	18.591	15.670	38.398	2.065	1.186
Annual Weighted Average		18.483	15.653	38.287	2.072	1.181

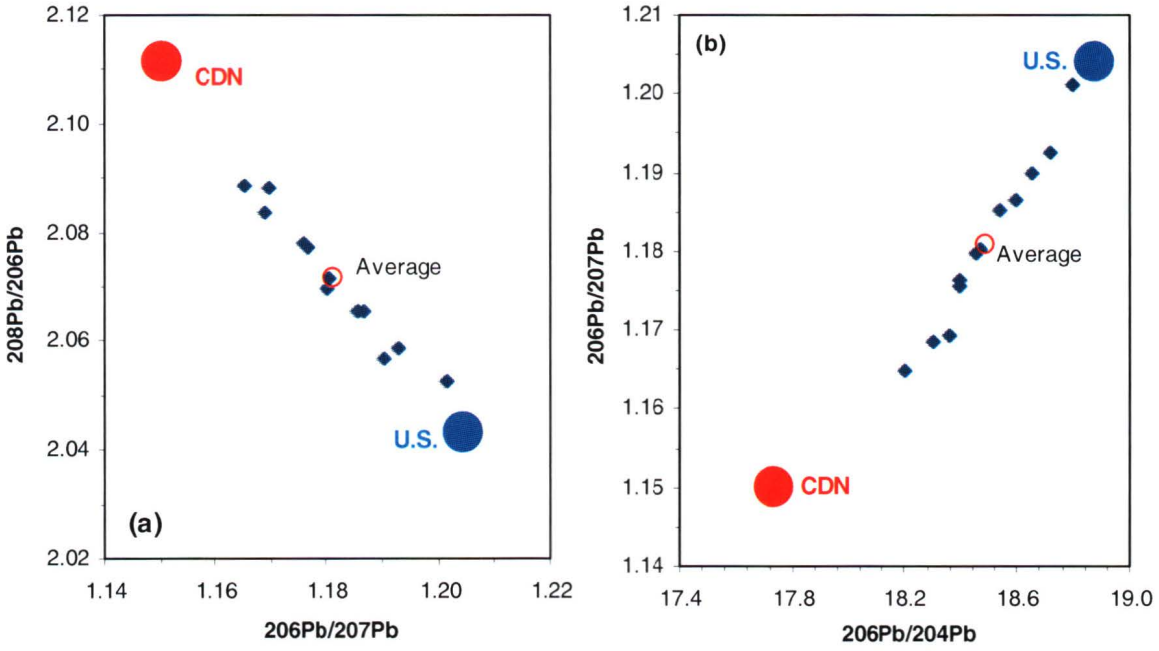

Figure 8.2 Pb isotope data for monthly precipitation values: (a) $^{208}Pb/^{206}Pb$ versus $^{206}Pb/^{207}Pb$ and (b) $^{206}Pb/^{207}Pb$ versus $^{206}Pb/^{204}Pb$. The field defined for U.S. anthropogenic emissions taken from Véron et al. (1992), Rosman et al. (1994), and that for Canadian anthropogenic emissions taken from Carignan and Gariépy (1995). Analytical uncertainties are within the size of the symbol.

ratios in Figure 8.1, these Pb-Pb diagrams illustrate that the majority of anthropogenic Pb pollution to Kejimkujik Park is dominantly from American sources.

Overall, the Pb isotope precipitation data show that anthropogenic pollution from populated and industrial regions of northeastern U.S. and southeastern Canada is being transported to relatively remote regions of Nova Scotia. In general there was a dominantly Canadian source during the fall months of 2001 and a dominantly American source during the winter and spring months of 2002 (Figure 8.1). With only three data points during the summer season, largely due to a lack of precipitation, the dominant sources cannot be confidently determined for this period. Analyses of seasonal trajectory climatologies associated with elevated total gaseous mercury concentrations at Kejimkujik Park for the years 1995-1997 (Beauchamp et al., 1998) indicated that, in general, winter trajectories originated from the southwest to northwest quadrants (which includes the Great lakes region) and spring trajectories originated from the north. However, deviations from these trends were not uncommon. The $^{206}Pb/^{207}Pb$ values measured here for the 2002 winter months are in excellent agreement with the general trends observed in winter 1995-1997. The spring 2002 values do indicate a more northern, less radiogenic signal than the winter months, but still show a dominantly American signal that might indicate more of a western trajectory from the Great Lakes area for spring 2002 compared to that of 1995-1997. The range of American contributions recorded in these samples was 30 to 100% versus 0 to 70% for Canadian contributions. In terms of an annual average that would be expected to represent the anthropogenic component of Pb measured in lake sediments of Kejimkujik Park, the average $^{206}Pb/^{207}Pb$ ratio for the period of July 2001 to June 2002 was determined as a weighted average using monthly precipitation totals to be 1.181. This value indicates that on an annual basis, approximately 62% of the Pb pollution is American.

8.2 Pb Isotope Composition of Lake Sediments

8.2.1 Natural Background Sediments

The primary sources of natural Pb to the lake sediments of BDW and BDE are from physical and chemical erosion of bedrock and overlying glacial till within the watershed. Secondary sources include locally derived wind blown dust and dry and wet deposition of long-range atmospherically transported natural particulates. Since the Industrial Revolution, these secondary sources can be considered negligible relative to anthropogenic inputs (Rosman et al., 1998). The bedrocks of BDW and BDE watersheds are both comprised of Cambro-Ordovician metasedimentary rocks of the Meguma Series (Gimbarzevsky, 1975) overlain by an almost continuous cover of thin glacial tills derived from local granitoid intrusives of Devono-Carboniferous age (South Mountain Batholith) (Stea and O'Reilly, 1982). The age and rock type of these two watersheds is therefore about the same.

The isotopic composition of Pb in old (early Holocene) sediments of BDW and BDE was determined from long cores to establish pre-industrial conditions. The isotopic ratios of sequential digestions of the long cores are listed in Appendix D. The data are plotted on a Pb-Pb diagram (Figure 8.3) using $^{206}Pb/^{207}Pb$ and $^{208}Pb/^{206}Pb$ ratios, as ICP-MS analyses are most precise for these ratios. The average Canadian and U.S. atmospheric Pb isotope compositions are also plotted to assist in evaluating the sources of Pb.

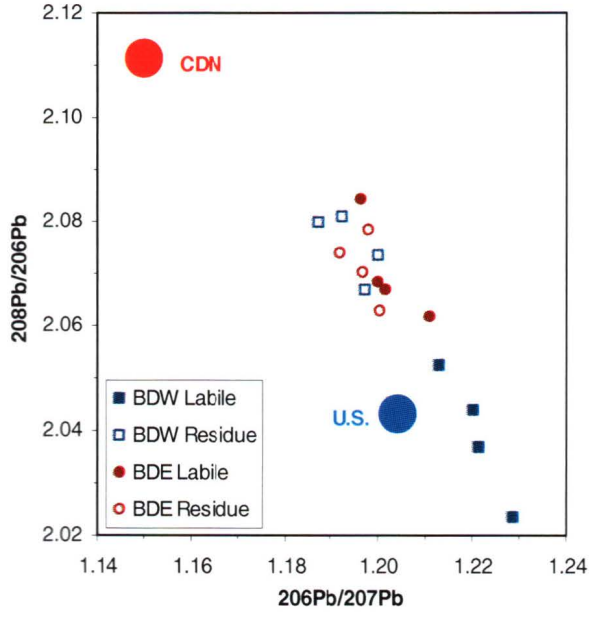

Figure 8.3 $^{208}Pb/^{206}Pb$ versus $^{206}Pb/^{207}Pb$ plot showing the isotopic composition of Pb from the sequential digestion of long cores, which are taken to represent background. Fields representing Canadian and U.S. anthropogenic emissions are plotted inorder to assess differences in sources. Analytical uncertainties are within the size of the symbol.

The average $^{206}Pb/^{207}Pb$ ratios for the mineral fraction of BDW and BDE are 1.194 and 1.196 respectively. These values are within analytical uncertainty of one another and therefore indicates the same rock type and age is entering both lakes. Using Pb-Pb geochronology (Faure, 1986), the age of the source material for the mineral fraction of the lake sediments is approximately 300 million years (L. Carboniferous). This agrees well with the reported age range of granitoid rocks such as the South Mountain Batholith (Stea and O'Reilly, 1982) that are the source of tills in the watersheds. This clearly illustrates that physical weathering of local till is the source of the mineral fraction in lake sediments of BDW and BDE.

The average $^{206}Pb/^{207}Pb$ ratio of labile Pb from long cores is 1.220 and 1.202 for BDW and BDE respectively, both of which are more radiogenic than the Pb in their respective mineral fractions. However, for BDE, this difference between the mineral and labile fractions is within analytical uncertainly and therefore not significant. Only the labile fractions of BDW are significantly more radiogenic than its mineral fractions (Figure 8.3). Graney et al. (1995) explain that "the rates and type of erosion experienced by different rock types affects the isotopic composition of the Pb incorporated into lake sediments". Furthermore, they explain that partial rock dissolution could release radiogenic Pb preferentially from metamict U and Th rich minerals resulting in preferential incorporation of Pb into lake sediments with isotope ratios more radiogenic than those of the rock formation (Graney et al., 1995). The differences in the Pb isotope compositions of the labile fractions could be explained by this phenomenon or by the slightly different bedrock units that underly each lake basin and watershed tills. Chemical weathering of till in the watersheds could differ because of the large wetland in BDW. Alternatively, although the bedrocks of both watersheds belong to the Meguma Series, BDW is located on the Goldenville Formation characterized by greywacke, quartzite, gneiss, and slates, while BDE is located on the Halifax Formation characterized by slates, schists and quartzites (Gimbarzevsky, 1975). The contact between the two Formations runs almost exactly along the separation between the two lakes. Perhaps bedrock in BDW is more susceptible to chemical weathering than the bedrock in BDE,

thereby having a greater influence on the isotopic composition of the labile fraction in its watershed.

8.2.2 Sequential Digestion of Short Core Sediments

Figure 8.4 shows the $^{206}Pb/^{207}Pb$ profiles for the labile and mineral fractions of cores BDW5 and BDE5, and the weighted totals of the two. The Pb isotope profiles of the labile and mineral fractions are similar until depths of about 9 cm (~1900) and 6 cm (~1880) for BDW and BDE respectively. These trends coincide with the beginning of anthropogenic activities in these watersheds as documented by Basquill et al. (2001). Also important is that the $^{206}Pb/^{207}Pb$ of the totals essentially mimics the labile profiles. This allows us to compare the sequentially leached cores to cores that were only analyzed in bulk (BDW6 and BDE6).

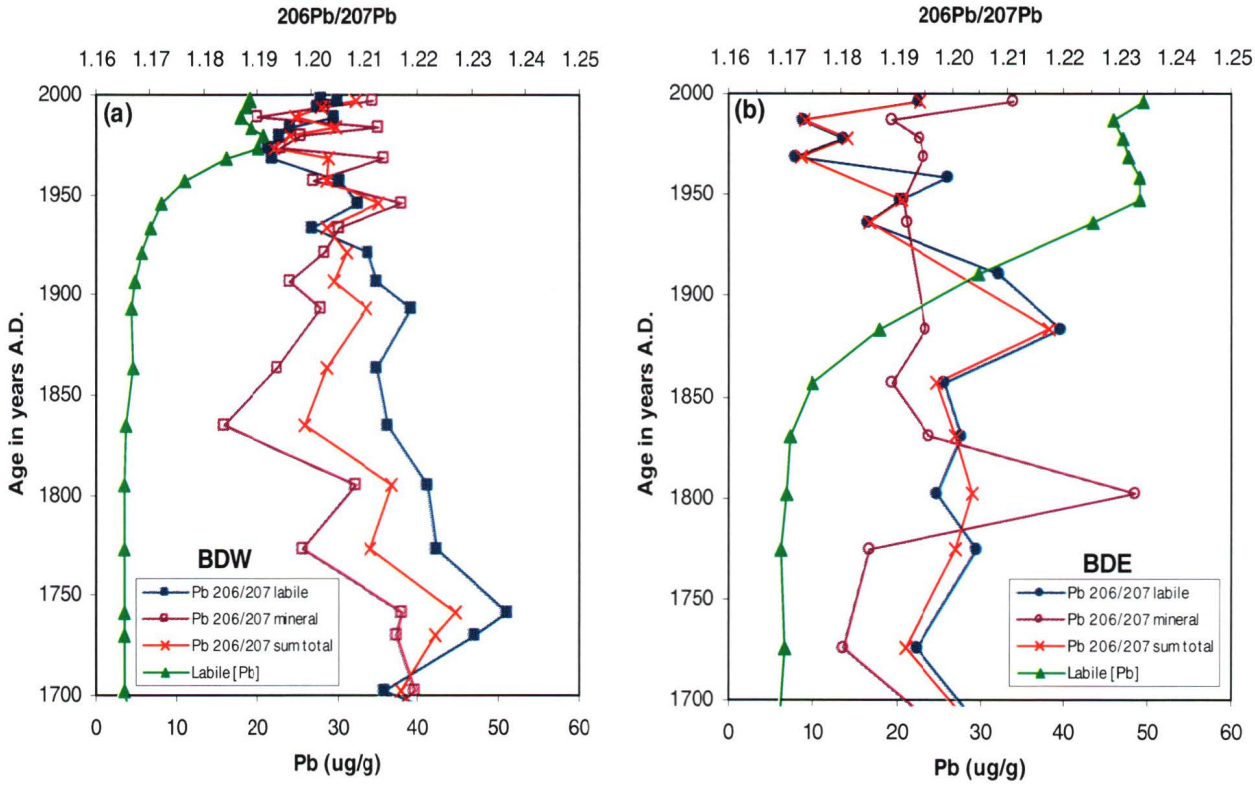

Figure 8.4 $^{206}Pb/^{207}Pb$ profiles as a function of age for the labile and mineral fractions of cores BDW5 and BDE5, and the weighted totals of the two. The Pb concentration profile for the labile fraction is also given inorder to compare the timing of changes between the different profiles. Analytical uncertainties for Pb are within the size of the symbol.

8.2.3 Reliability of Lake Sediments as Historical Archives

In general, temporal changes in sources of Pb emitted to the atmosphere are believed to be reflected in the isotopic profiles of lake sediments. In addition, concentration profiles are often assumed to be a reflection of the magnitude of historical inputs and numerous studies solely rely on concentration profiles in lake sediments to assess the magnitude of anthropogenic pollution to an area. This section will show that lake sediments can isotopically record the *timing* of changes in atmospheric and watershed Pb inputs, while also having concentration profiles significantly impacted by diagenetic alteration.

Historically, atmospheric Pb concentrations began to increase significantly after the Industrial Revolution. These increases were relatively gradual until the advent of automobiles and alkyl-leaded gasoline, which quickly became the dominant source of Pb to the atmosphere and resulted in sharp increases in global atmospheric Pb concentrations around 1930 (Shirahata et al., 1980; Graney et al., 1995). Global atmospheric Pb concentrations continued to grow rapidly reaching maximum emissions in the early 1970's, and decreasing thereafter (Graney et al., 1995; Nriagu, 1994). This was accompanied by changes in the isotope composition of Pb. In North America, this initially resulted in shifts toward less radiogenic values, as U.S. and Canada had characteristically used sources with low $^{206}Pb/^{207}Pb$ ratios of about 1.15 (Chow and Johnstone, 1965; Shirahata et al., 1980; Sturges and Barrie, 1987). After 1967, the isotopic ratio of industrial Pb in the U.S. was drastically altered due to increased production of Mississippi Valley-type ore deposits that have high radiogenic values, with $^{206}Pb/^{207}Pb$ ratios of ~1.28-1.33 (Shirahata et al., 1980). Atmospheric concentrations then dropped from the phasing out of leaded gasoline by the Clean Air Act in the 1970's (Graney et al., 1995). The history of Pb use in North America where atmospheric compositions were increasingly less radiogenic between the 1920's and 1960's, followed by more radiogenic compositions has been documented in sediment cores from the Great Lakes (Ritson et al., 1994; Graney et al., 1995)

In this study, watershed disturbances such as the large scale logging and forest fires that occurred in or in close proximity to BDW and BDE would result in fluctuations in Pb inputs and therefore a varying mix of local and atmospheric isotope signatures. This is true because partial (incongruent) rock dissolution and development of soil

concentrates Pb with more radiogenic compositions (Graney et al., 1995), and therefore logging and forest fires would release the more radiogenic top soils into lakes.

Figure 8.5 plots the $^{206}Pb/^{207}Pb$ profiles as a function of age for four cores (BDW1, BDW5, BDE5 – labile; BDW6 – total). All cores have similar isotopic trends even though the absolute values of the isotope ratios vary from core to core. In accordance with regional and global historical inputs, the overall trend is towards less radiogenic values starting between 1920 and 1930 and peaking between 1970 and 1985. All cores become more radiogenic during the extensive logging and numerous forest fires that occurred between 1860 and 1900. The cores also become more radiogenic during a second documented wave of logging from 1945-1954 (Basquill et al., 2001). The similarity of the trends shows that the sediments of BDW and BDE have preserved the *timing* of changes in Pb inputs, but not necessarily the original isotopic composition, as indicated by the range of isotopic values from one core to another.

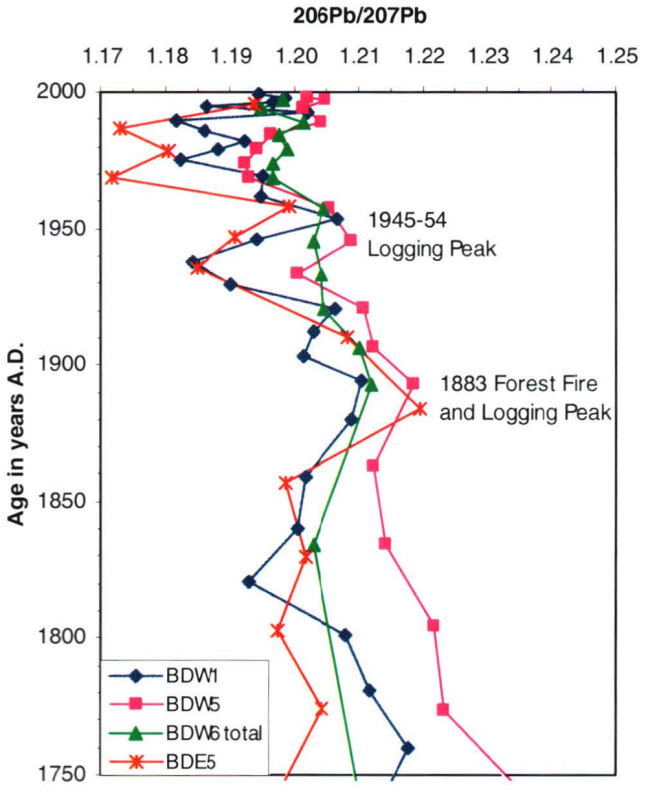

Figure 8.5 $^{206}Pb/^{207}Pb$ profiles as a function of age for four sediment cores. Three profiles are from the labile fraction of each core (BDW1, BDW5, BDE5) and one is from a total digest (BDW6). All cores show fluctuations in the profile that coincide with known anthropogenic events. Analytical uncertainties for Pb are within the size of the symbol.

Figure 8.6a and b are plots of the Pb concentration profiles of the four cores shown in Figure 8.5 as well as two other cores (BDE3 – labile; BDE6 – total) that also have similar isotopic trends. The isotope and concentration profiles for these cores suggest that diagenetic remobilization has occurred. Fluctuations in the Pb isotope profiles associated with known events (Figure 8.5) show that all cores are well aligned in terms of age. Pb concentration profiles versus age (Figure 8.6a) for BDE are not well aligned and don't appear to be a function of age. The BDE profiles show three different surface concentrations, different ages for peak concentrations, and different ages for the rapid increases in concentrations. Figure 8.6b is a plot of the same six cores plotted against sediment depth rather than age. When plotted as a function of depth the profiles align better, as would be expected if chemical conditions rather than depositional history were the dominant control on the profiles.

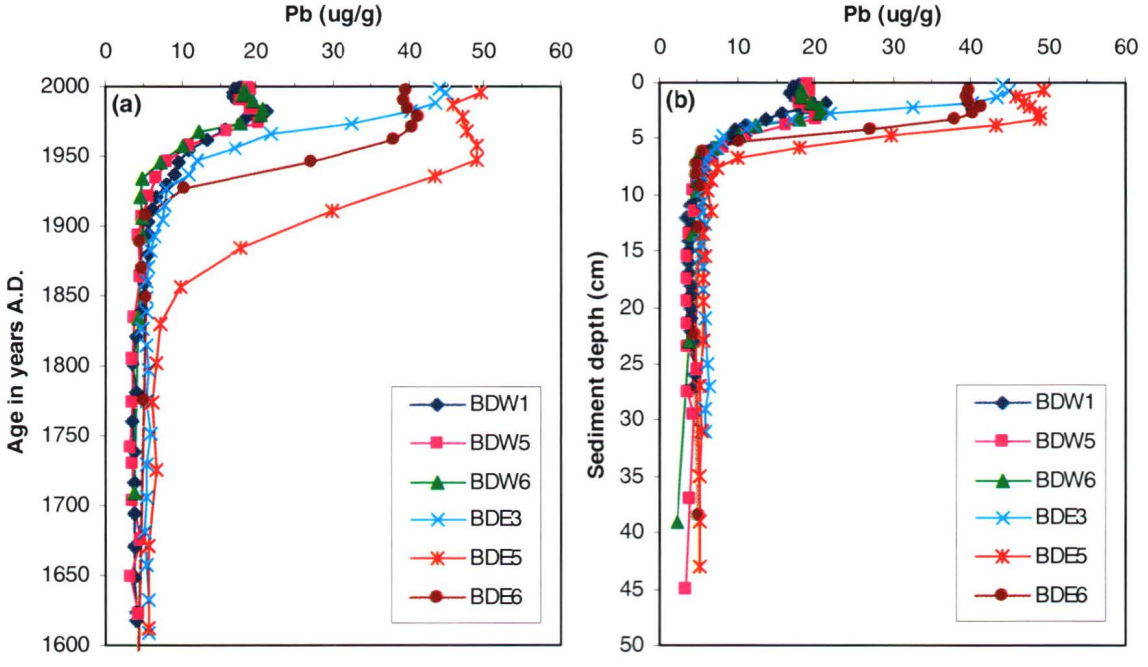

Figure 8.6 Pb concentration profiles as a function of (a) age and (b) depth for the four cores shown in Figure 8.5 as well as two others (BDE3, BDE6) that also have similar isotopic trends. Analytical uncertainties for Pb are within the size of the symbol.

Diagenesis may also be influencing Pb profiles in BDW, but to a lesser degree than BDE. Evidence of remobilization in both lakes is given in Figure 8.7, which plots $^{206}Pb/^{207}Pb$ versus the inverse of Pb concentrations. Such plots are typically used to determine if observed isotopes can be explained by binary mixing between two end-members, which would be defined by a linear array. The data plotted in Figure 8.7 are from the sediment-water interface down to depths just above the pre-industrial background (post-1850). Background sediments were not included because, as expected, they confuse the plot. Interestingly, Figure 8.7 shows two distinct populations: (1) a group of data points that form a linear array typical of binary mixing; and (2) a group of data points that form a vertical line showing a range of isotope ratios without significant changes in concentrations. The points that form the binary mixing line are from the sharp rise in the concentration profiles. The points forming the vertical line are from surficial sediments with depths less than 4 cm. The existence of these two populations is difficult to explain as a primary loading. Binary mixing and depositional history cannot explain the samples above 4 cm depth. Pb is being added to this depth maintaining surface concentrations even though atmospheric concentrations of anthropogenic Pb have been greatly reduced since the early 1970's. Remobilization of Pb from deeper anoxic sediments to the oxic surface layers can explain the profiles effectively. Porewater results presented in the following chapter show that oxygen is depleted by about 3.5 cm depth followed by rapid changes in redox potential and pH. These chemical shifts are coincident with the depth separating the two Pb populations in Figure 8.7 and therefore suggest they are a significant factor controlling the distribution of Pb in depth profiles.

Upward movement of background Pb with more radiogenic compositions than anthropogenic Pb would result in a shift towards more radiogenic values. If remobilization is not considered, the so-called anthropogenic component would be calculated to come from more radiogenic sources. In the case of Kejimkujik Park and other North American localities, such shifts to more radiogenic values would result in overestimates of the U.S. contribution. Indeed the calculated isotopic ratios of anthropogenic Pb from BDE sediments are more radiogenic than would be expected from precipitation data and known historical values.

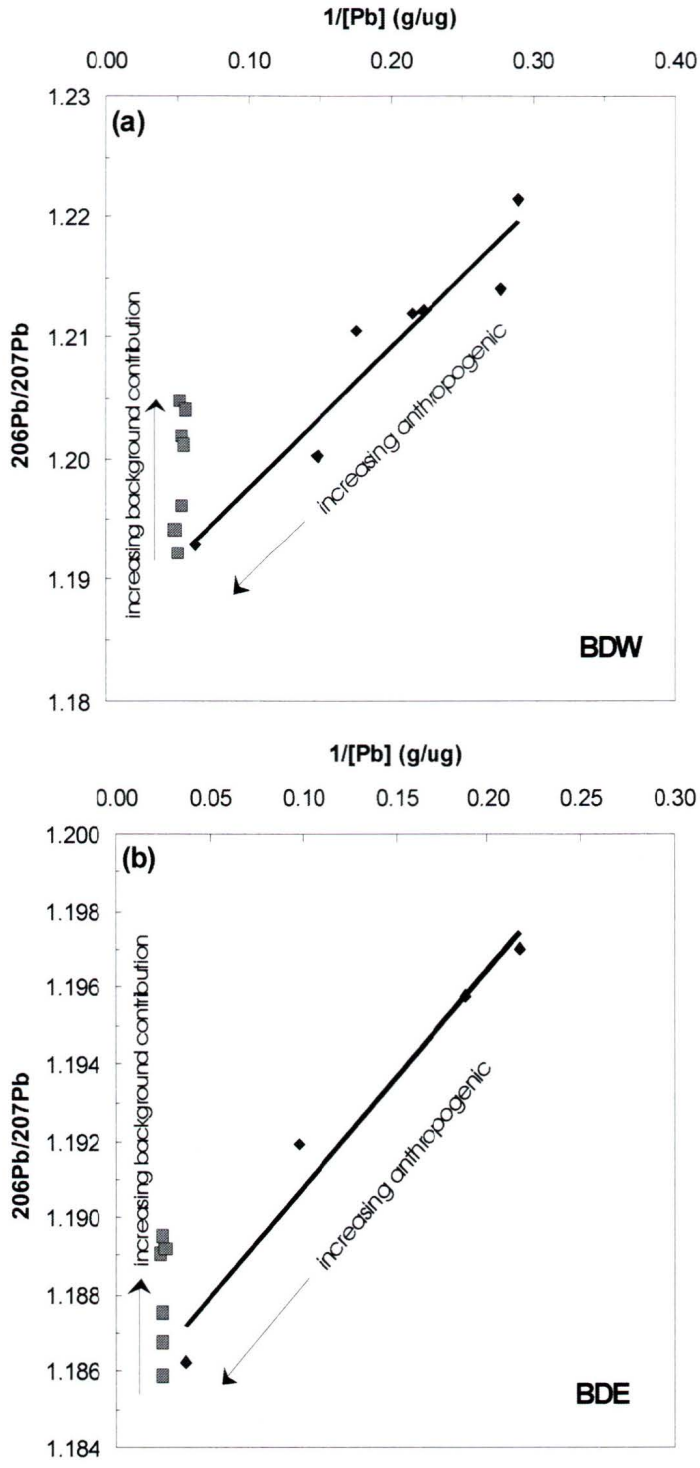

Figure 8.7 $^{206}Pb/^{207}Pb$ versus 1/Pb concentrations in post-1850 sediments of (a) BDW and (b) BDE. Both figures show two distinct populations, with the square data points from depths $\leq$ 3.5 cm and diamond points from depths > 3.5 cm. Only data points from >3.5 cm depth (diamonds) form a linear array typical of binary mixing. The pathways for increased anthropogenic inputs are shown. Contrary to expected, sediments from $\leq$ 3.5 cm (squares) form a vertical array rather than a return to lower concentrations and less anthropogenic ratios – the expected behaviour for decreasing anthropogenic inputs. This suggests background Pb contributions from diagenetic remobilization.

The anthropogenic component can be calculated by subtracting the Pb concentration and isotopic composition of the background labile fraction from post-1850 sediments. This method requires the condition of constant sedimentation rates and is calculated using a standard equation for a binary mixing system (Stumm and Morgan, 1996) as has been done by Graney et al. (1995). The equation is:

$$^{206}Pb/^{207}Pb \text{ Anthropogenic component} = \quad [8.1]$$
$$[(^{206}Pb/^{207}Pb \text{ TL})(\text{ppm Pb TL}) - (^{206}Pb/^{207}Pb \text{ BC})(\text{ppm Pb BC})]/(\text{ppm Pb TL} - \text{ppm Pb BC})$$

where TL = total labile and BC = background. The $^{206}Pb/^{207}Pb$ ratio is given here as an example, but the equation can be used to calculate any isotope ratios. The values for anthropogenic Pb determined for BDE5 sediments are given in Table 8.2 and the $^{206}Pb/^{207}Pb$ profile is shown in Figure 8.8. Values are not given for BDW because the ^{210}Pb dating results have shown that the sedimentation rates in this lake are too variable and so the assumption is not valid (Figure 7.2). A profile estimating the expected $^{206}Pb/^{207}Pb$ composition of anthropogenic Pb inputs, based on present (precipitation results) and historical Pb compositions, is also shown in Figure 8.8.

Table 8.2 Anthropogenic Pb isotope compositions and concentrations for BDE5 sediments.

Sample	Mid-depth (cm)	Age (yrs A.D.)	Labile Pb (ug/g)	Anthro. Pb (ug/g)	Anthro. $^{206}Pb/^{207}Pb$	Anthro. $^{208}Pb/^{206}Pb$
BDE5-02	0.75	1995	49.29	43.85	1.193	2.058
BDE5-03	1.25	1987	45.77	40.33	1.169	2.098
BDE5-04	1.75	1978	46.86	41.42	1.178	2.069
BDE5-05	2.25	1968	47.47	42.03	1.168	2.088
BDE5-06	2.75	1958	48.76	43.32	1.199	2.032
BDE5-07	3.25	1947	48.85	43.41	1.189	2.049
BDE5-08	3.75	1936	43.20	37.76	1.182	2.061
BDE5-10	4.75	1910	29.72	24.28	1.210	2.027
BDE5-12	5.75	1883	17.90	12.46	1.227	2.052
BDE5-14	6.75	1856	9.78	4.34	1.194	2.068

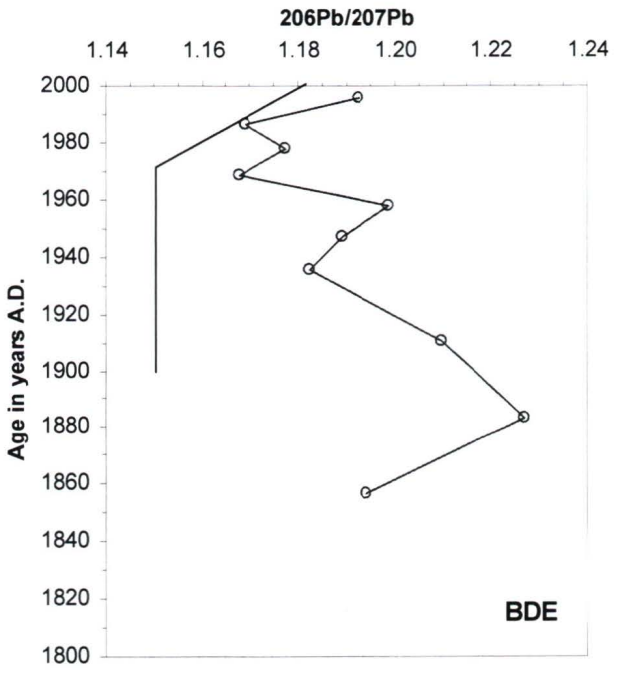

Figure 8.8 Anthropogenic $^{206}Pb/^{207}Pb$ profile for BDE5 sediments. A profile of the expected $^{206}Pb/^{207}Pb$ composition of anthropogenic Pb inputs based on present (precipitation results) and historical Pb compositions is also given for comparison.

Figure 8.8 shows that the anthropogenic Pb is always more radiogenic than expected. For pre-1940 sediments, coal burning is likely a significant factor other than remobilization that might explain the more radiogenic values at these depths. The expected $^{206}Pb/^{207}Pb$ profile shown here only considers gasoline and ore smelting, yet coal burning contributed as much Pb as ore smelting prior to the 1930's before gasoline became the dominant source (Graney et al., 1995). However, the anthropogenic Pb in sediments deposited after 1940 was dominantly from gasoline emissions, ore smelting, and other industrial sources and should therefore record the isotopic composition of these sources, assuming no remobilization or significant changes in sedimentation rates. The fact that the calculated anthropogenic Pb is consistently more radiogenic than expected in these sediment layers indicates that changes in anthropogenic Pb inputs and composition is not enough to explain the magnitude of the more radiogenic values. Therefore, as indicated by the data presented in Figure 8.6 and 8.7, upward remobilization of more radiogenic Pb from deeper sediments is necessary to explain the magnitude of the shift to more radiogenic values in the upper sediments.

8.3 Quantifying the Proportion of Remobilized Pb in Surface Sediments

The average Pb isotope composition of anthropogenic Pb deposited to Kejimkujik Park over a one-year period from July 2001 to June 2002 was determined from precipitation data and given in Table 8.1. In a small relatively closed lake system such as that of BDE, these values should be reflected in the topmost lake sediments as the anthropogenic component determined by equation 8.1. However this is not the case as the calculated anthropogenic Pb from the sediments is more radiogenic than the precipitation (Table 8.1). This is because equation 8.1 assumes that all of the Pb above background concentrations is anthropogenic Pb when in fact it is a mixture of anthropogenic Pb and Pb remobilized from deeper anoxic layers. Since only 2-3 cm of the anthropogenic Pb rise in BDE is located below the oxic/anoxic boundary at 3.5-4 cm depth, it can be assumed that the majority of remobilized Pb is background Pb from the remaining 200 cm of gyttja (Ferguson, 2002) and therefore has an average Pb isotope composition equal to that of the long cores. Knowing the average background Pb isotope composition and concentration as well as the average present day composition of anthropogenic Pb to the lake, it is proposed here that the equation for a binary mixing system can be used to calculate the proportions of remobilized background Pb and anthropogenic Pb necessary to give the isotopic values previously determined by equation 8.1, and herein referred to as "apparent anthropogenic component".

Calculation of the concentration of remobilized Pb in the surface sediment layer requires several assumptions:

(1) The average composition of anthropogenic Pb determined from precipitation is a representative average for the period of time represented by the topmost sediment sample, which in the case of BDE5 is ~6 years.

(2) The majority of remobilized Pb is from background sediments and therefore its Pb isotope composition is approximately equal to the average composition of the labile fraction of background sediments (i.e. the majority of the anthropogenic Pb rise should lie above the oxic/anoxic boundary).

(3) No other watershed or basinal processes have significantly altered the composition of atmospherically deposited Pb.

BDE meets these conditions.

The following two equations are used to obtain an equation that describes the binary mixing between anthropogenic Pb and remobilized background Pb in the surface layer of BDE sediments:

$$[Pb]OAC = [Pb]AAC - [Pb]RB \quad [8.2]$$

and

$$(^{206}Pb/^{207}Pb\ AAC)([Pb]AAC) = (^{206}Pb/^{207}Pb\ OAC)([Pb]OAC) + (^{206}Pb/^{207}Pb\ RB)([Pb]RB) \quad [8.3]$$

where AAC is the apparent anthropogenic component as determined by equation 8.1, OAC is the observed anthropogenic component as determined from precipitation samples, and RB is the remobilized background component. By substituting equation [8.2] into equation [8.3] and rearranging to isolate [Pb]RB, we obtain:

$$[Pb]RB = [(^{206}Pb/^{207}Pb\ AAC)([Pb]AAC) - (^{206}Pb/^{207}Pb\ OAC)([Pb]AAC)] / [(^{206}Pb/^{207}Pb\ OAC) - (^{206}Pb/^{207}Pb\ RB)] \quad [8.4]$$

This equation gives the concentration of remobilized background Pb in the surface sediments and can then be subtracted from the concentration of the apparent anthropogenic component to obtain the true concentration of anthropogenic Pb. The calculation should only be used to quantify the proportion of remobilized Pb in the topmost sediments for which the precipitation is representative. The proportion of remobilized Pb in lower sediments cannot be determined without corresponding historical measurements of the local isotopic composition of atmospheric Pb. Although the historic isotopic composition of North American anthropogenic Pb sources have been well documented, the composition from one area to another can be highly variable due to the different proportions of the contributing regions, as well as differences in local sources. For instance, in more remote locations, Pb from wood and coal burning from nearby small towns may make up a larger proportion to the anthropogenic signal. As such, use

of large-scale atmospheric Pb compositions, both recent and past, is an unreliable estimate of the true isotopic composition of the anthropogenic Pb input to any particular lake and will result in unreliable estimates of the proportion of remobilized Pb in a sample.

It should be noted that it is not necessary to first calculate the apparent anthropogenic component using equation 8.1 in order to determine the concentration of remobilized Pb in the surface sediments. The total labile fraction can be used in equation 8.4 instead of the apparent anthropogenic component. In doing so, the resulting concentration will instead be a sum of recently deposited natural background Pb and the remobilized background Pb from deeper sediments. The concentration of remobilized background Pb can then be determined by subtracting the average background concentrations from the deeper sediments. However, it is perhaps better that the apparent anthropogenic component be determined first as a way to verify that it is a value between the true anthropogenic and natural background end members. If it is not, then the system is more complex than simple binary mixing between these two end members and may indicate that one or more of the assumptions above is not valid in that particular location.

Table 8.3 lists the variables used in the calculation of remobilized background Pb in BDE5 sediments. Using the above method, the concentration of remobilized background Pb in the top 1 cm of the BDE5 core is estimated to be 25.1 μg/g, which is 51% of the total Pb in the labile fraction of that sample. This value represents a maximum estimate for the amount of remobilized Pb in that sample. If in fact anthropogenic Pb is contributing significant amounts of remobilized Pb, than the remobilized component will be less radiogenic than the average background value used here and thus a smaller proportion of remobilized Pb is necessary to explain the apparent anthropogenic component. An investigation of the Pb isotope composition of porewaters would help constrain the composition of the Pb being remobilized.

The estimated concentration of 25.1 μg/g of remobilized background Pb in the surface layer of BDE5 is a first approximation based on precipitation. The confidence in this estimate could be even higher with data from Pb isotope analyses of air filters. Air filter samples were obtained for the same year-long sampling period as that of the precipitation samples presented here but analysis is incomplete at this time.

Table 8.3 Data used in the calculation of remobilized background Pb in surface sediments of the BDE5 core. Abbreviations given correspond to the variables in Equations 8.1-8.4.

	$^{206}Pb/^{207}Pb$	[Pb] in μg/g
Data used in Eqn. 8.1		
Labile Pb (TL)	1.193	49.29
Background Pb (BC)	1.202	5.44
Data used in equation 8.4		
Apparent Anthr. Pb (AAC)	1.193	43.85
Observed Anthr. Pb (OAC)	1.181	
Remobilized Background Pb (RB)	1.202	

It should be stressed that no one core is representative of an entire lake. Differential sedimentation rates and processes such as sediment focussing can cause significant differences in the thickness of sediments and the concentration of Pb and other trace metals within them. These and other factors such as water depth may cause significant differences in the chemical composition and properties of sediments and porewaters, thus producing different diagenetic conditions and different degrees of remobilization within a basin.

9. RESULTS AND DISCUSSION Part III: Supporting Evidence for Diagenetic Remobilization of Pb and Hg

Investigations on the partitioning of Hg and Pb in lake sediments have indicated that most of the Hg and Pb is associated with organic components of the sediment ($Hg^{2+} > Pb^{2+}$; El Bilali et al., 2002), with lesser, but significant, amounts associated with iron and manganese oxides (El Bilali et al., 2002; Strunk et al., 1991; Eganhouse et al., 1978). It seems logical then that the decomposition of organic matter and the redox reactions utilizing iron and manganese oxides, together with upward porewater advection due to compression and diffusion, would remobilize and redistribute Hg and Pb in the sediment column. However, detailed profiles of Hg and Pb in porewaters, which could confirm their diagenetic release, are lacking from most such studies (Matty and Long, 1995). The previous chapter showed isotopic evidence that Pb is being remobilized in the sediments of BDW and BDE, and this chapter will present porewater analyses that provide supporting evidence for the remobilization of Pb and Hg in these lake sediments. Then Hg flux ratios will be re-examined to show that evidence of Hg remobilization does potentially exist in the sediment profiles.

9.1 Porewater Chemistry – Dissolved Oxygen, Redox and pH

The transformation of Hg and Pb to aqueous phases is dependant on the ambient Eh, pH, temperature, concentration of Hg and Pb, concentration of ligands such as SO_4^{2-}, and the presence of other cations and various solid phases such as sulphides and oxyhyroxides. To document the redox behaviour and fate of Hg and Pb in BDW and BDE, in-situ measurements of DO, pH and Eh were made on porewaters and are given in Appendix I, along with Hg, Pb, and Mn concentrations which will be discussed in the next section. The results for DO, pH and Eh are shown in Figure 9.1. The dissolved oxygen measurements show that the levels of DO at the sediment water interface are already very low and then disappear completely around 3.5-4 cm. Furthermore, Eh values of about 650 mV and 430 mV were measured at the sediment-water interface in BDW and BDE

respectively. The data indicate that a significant amount of oxygen is consumed in the bottom waters of BDW and BDE in the summer. This is not surprising since the lakes are known to become thermally stratified in the summer months – a strong thermocline was observed during diving to emplace the peepers in BDW, less so in BDE.

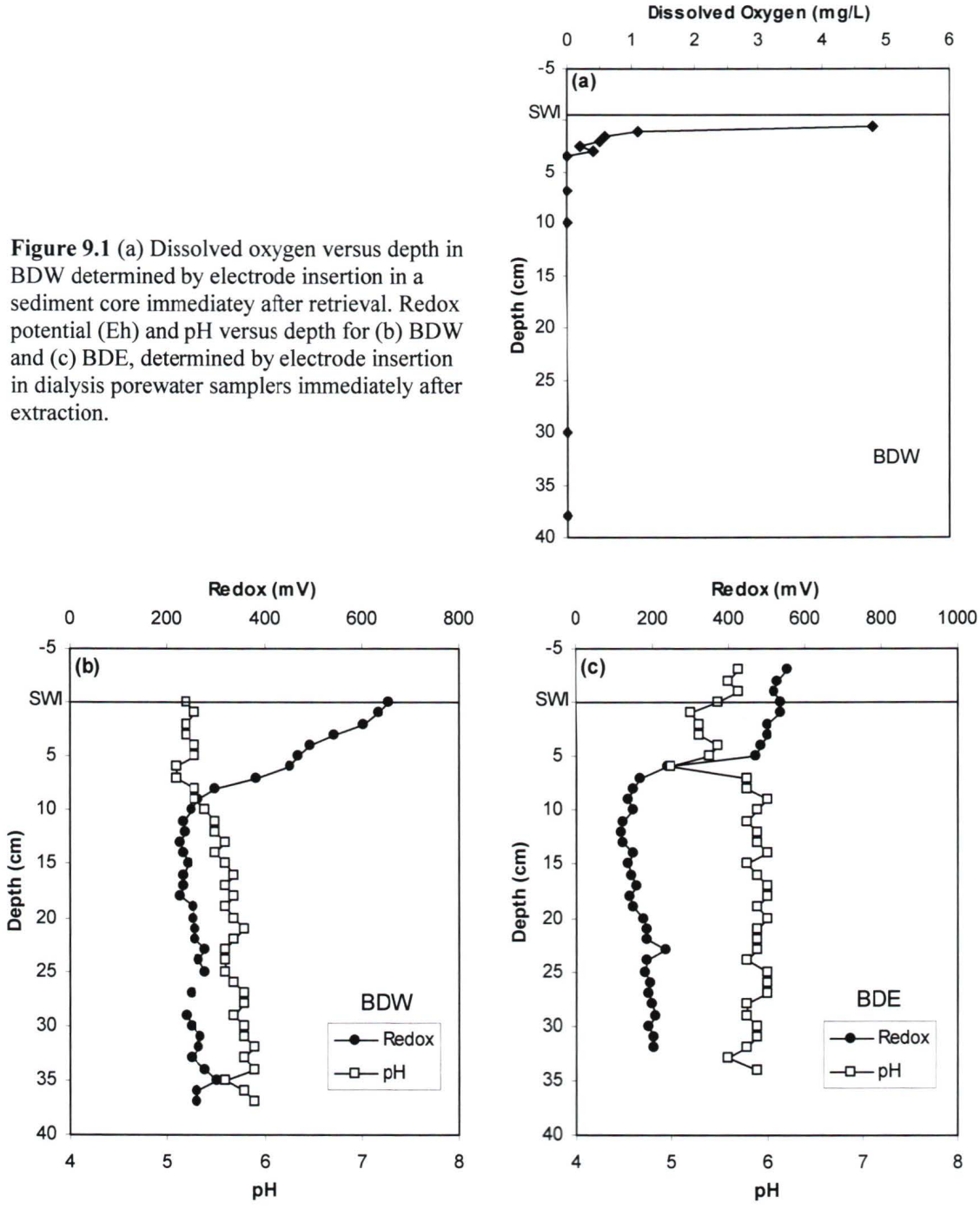

Figure 9.1 (a) Dissolved oxygen versus depth in BDW determined by electrode insertion in a sediment core immediatey after retrieval. Redox potential (Eh) and pH versus depth for (b) BDW and (c) BDE, determined by electrode insertion in dialysis porewater samplers immediately after extraction.

The pH profiles in Figure 9.1b-c show that in BDW the pH at the sediment water interface is around 5.3 and then steadily increases to around 6.0 at a depth of about 37 cm, however a zone with a slightly higher rate of increase can be seen just below 5 cm depth. This gradual increase in pH is expected for the progressive anaerobic decay of organic matter by the thermodynamic sequence of reduction reactions listed in Table 2.1. The pH depth profile for BDE shows more abrupt changes than BDW. Between the sediment-water interface and 5.0 cm depth, the pH in BDE sediments decreases from 5.5 to 5.0 and then rapidly increases and remains at 6.0. This suggests some aerobic decay of organic matter in the top 5 cm, which would release carbonic acid and lower the pH levels. Below this depth, anaerobic decay of organic matter is similar to that in BDW.

The Eh profile supports this interpretation. In BDW, Eh steadily decreases from 650 to 200 mV between 0 and 10 cm depth and then stabilizes with only slight increases with greater depths. In BDE, the Eh only decreases slightly from 580 to 480 in the top 5 cm, then rapidly decreases to around 170 mV by 10 cm depth, and increases only slightly with depth thereafter. The sharp decrease in Eh in BDE is coincident with the sharp increase in pH and, according to Table 2.1, marks the boundary between aerobic and anaerobic decay of organic matter. The sharpness of the shift in Eh and the fact that the Eh reaches lower values in BDE suggests that the rate of organic matter decay is higher in BDE than in BDW. This is likely due to differences in the types of organic matter in each lake, with BDE having larger proportions of autochthonous (lacustrine produced) carbon, which would be more labile and more rapidly decayed resulting in overall less organic matter burial than BDW. This is documented by profiles of organic carbon, C:N ratios, and carbon isotopes for these two lakes presented by Telmer et al. (in review).

Overall, the porewater data in Figure 9.1 show that significant changes in DO, pH and Eh are occurring in the top 6 cm of BDW and BDE, particularly between 3.5 to 5 cm depth. These are the depths to which the Pb data presented in this study have been shown to be a function of depth rather than age (Figure 8.6 and 8.7). A similar relationship for Hg in the surficial sediments is discussed at the end of this chapter. It is unlikely that this is just a coincidence. It is more likely that the diagenetic conditions that control DO, Eh, and pH also play a role in controlling Pb and Hg.

9.2 Mercury and Lead in Porewaters – Evidence of Upward Remobilization

The results for Hg, Pb, and Mn concentrations in porewaters are shown in Figure 9.2. The primary trend for both Hg and Pb is an increase in concentration with depth. Porewater concentrations of Hg increase from 2 pg/g near the surface to 7 pg/g at a depth of 30 cm. Pb concentrations increase from 0.5 ng/g to 3 ng/g over the same depth interval. Concentration profiles of Mn in the porewaters also showed continually increasing concentrations with increased depth indicating that the increased concentrations of Hg and Pb in the porewaters are strongly correlated with the decay of organic matter at these depths. Both organic matter and oxyhydroxides are known to adsorb many cations in waters including Hg and Pb (El Bilali et al., 2002) and so the continuous reduction of oxides and the decay of organic matter provides a source of dissolved Hg and Pb to porewaters at various depths. This supports the interpretation that Pb is remobilized.

The upwards decreasing gradients of dissolved Hg and Pb in porewaters means that these elements diffuse towards the sediment-water interface. For Hg, this interpretation is supported by the results of O'Driscoll (2003), which show elevated dissolved gaseous mercury (DGM) concentrations in the lake waters of BDW immediately above the sediment-water interface, which implies that the sediments of these lakes are sources of Hg to the lake waters.

The relatively low dissolved Hg gradient compared to the Pb gradient suggests that either: (a) dissolution of Hg in porewaters from solid phases is slow, perhaps because Hg has a higher affinity for organic matter (El Bilali et al, 2002); or (b) dissolved gaseous mercury (DGM) diffuses more rapidly than Pb because it is expected that a non-charged species such as Hg^0 will not retard as strongly as a charged one - Pb^{2+} (Stumm and Morgan, 1996). High Hg diffusion rates result in low gradients on short time scales. Either case helps explain why Hg profiles in solid phases preserve more of the fluctuations associated with known local anthropogenic activities than the Pb profiles, which show relatively smooth concentration profiles regardless of changes in inputs and sedimentation rates.

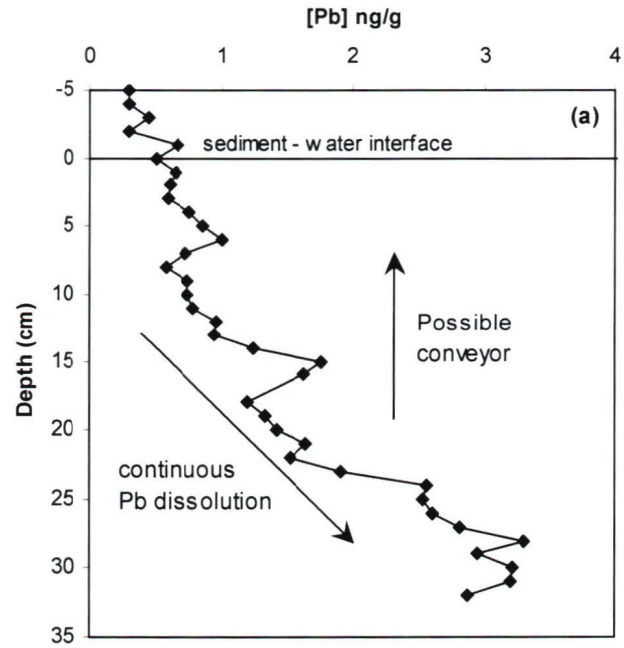

Figure 9.2 Concentrations of (a) Pb, (b) Hg, and (c) Mn in porewaters versus depth measured in-situ dialysis porewater samplers. Precision of Pb and Mn data is within the size of the symbol. Precision for Hg is indicated by an error bar on plot.

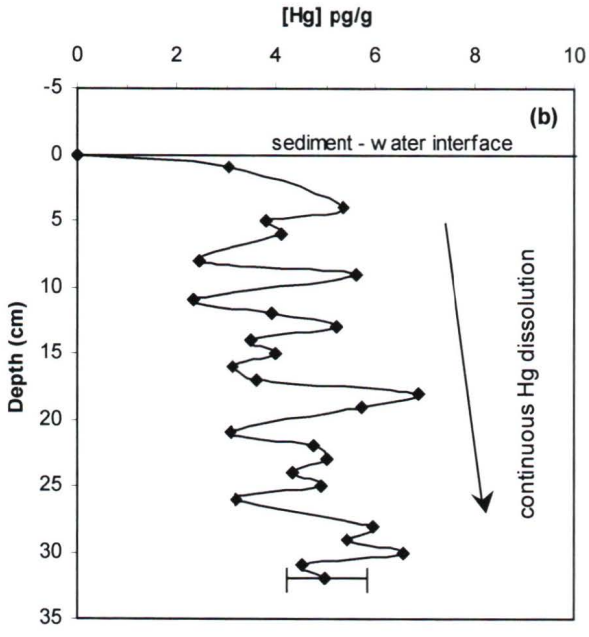

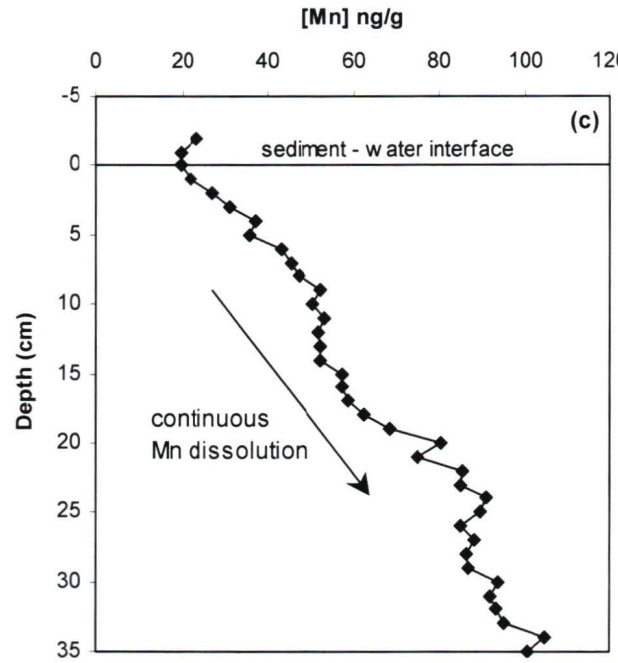

9.3 Mercury Flux as Evidence of Remobilization

The Pb isotope results showed that the Pb concentration profiles for BDE were more a function of sediment depth rather than age, thus indicating that the shape of the profile is more a function of diagenetic conditions than historical deposition. Unfortunately, a similar Hg isotope investigation is not possible, but a comparison between Hg profiles plotted against time and those plotted against depth can provide some clues. Figure 9.3a presents the same age profiles of pre- to post-industrial Hg flux ratios as given in Figure 7.5. As previously discussed, the post-1900 increases in Hg inputs are not synchronous and if remobilization is not considered, this can be explained by delayed Hg inputs from the BDW watershed. However, upward remobilization of Hg is an equally plausible explanation. Figure 9.3b is a plot of the Hg flux ratios as a function of depth rather than age. A comparison of the profiles in Figure 9.3 shows that the upper portions (~6-7 cm) of the profiles for these two lakes show simultaneous changes only when plotted against depth. Simultaneous increases would not be expected to occur at the same depths in two different lakes with two different sedimentation rates and chemical characteristics. The fact that they do occur at similar depths in both lakes (Figure 9.3b) strongly suggests that the distribution of Hg in the surface sediments may be influenced by similar diagenetic conditions. This is supported by the redox data which also shows rapid changes in Eh occurring at similar depths in both lakes (Figure 9.1) and these depths coincide with the Hg increases.

While this comparison of Hg age and depth profiles suggests the influence of remobilized Hg in the upper sediments, it is by no means a smoking gun for this highly debated topic. As discussed in section 7.2.3, the fact that the smaller Hg fluctuations believed to be associated with known local anthropogenic activities appear to have been preserved in these sediments and the fact that both lakes indicate present day flux ratios of 3, suggests that remobilization may not be significantly altering the profiles at the shallow depths studied here. Furthermore, the timing of the smaller fluctuations overlaps with the beginning of global anthropogenic Hg increases, making it difficult to determine if the beginning of these rapid increases in Hg occur simultaneously in the age or depth profiles. If the timing of the global anthropogenic Hg rise occurred simultaneously in the

age profiles of these two lakes, then the fact that BDE shows greater increases in Hg inputs than BDW throughout most of the anthropogenic Hg rise could be explained by greater watershed delay in the BDW watershed.

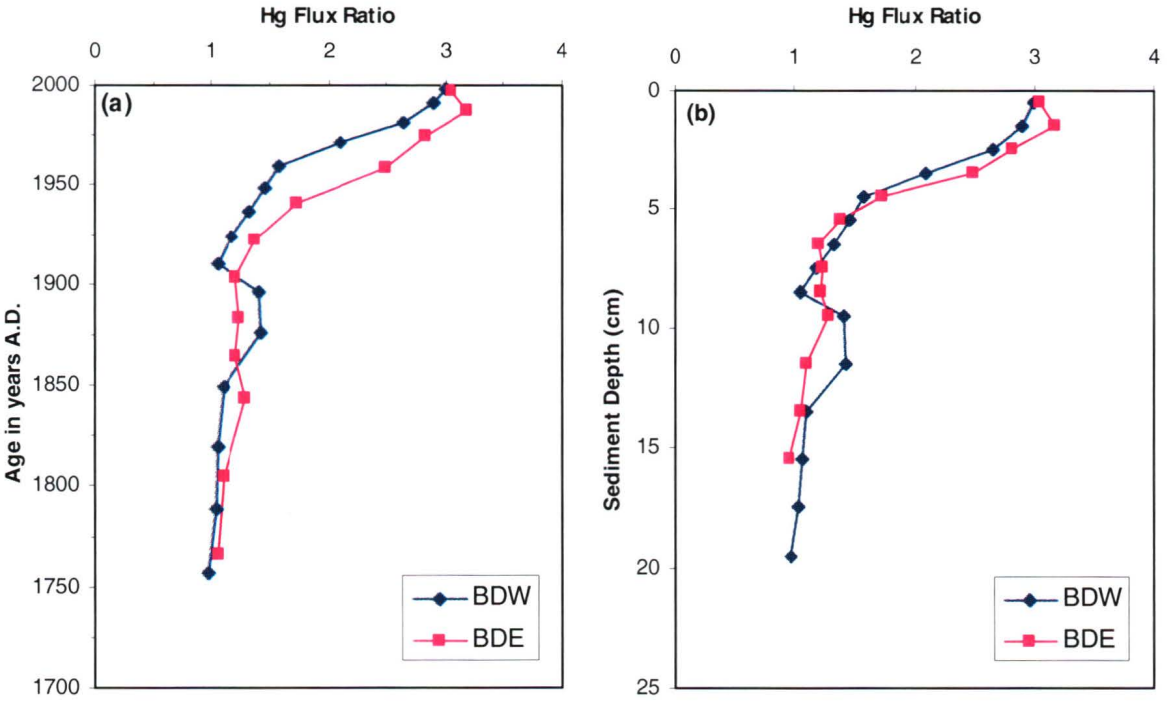

Figure 9.3 Profiles of Hg flux ratios as (a) a function of time and (b) a function of depth. Flux ratios are the ratio of Hg accumulation at various times relative to the average pre-industrial value.

10. CONCLUSIONS

The Hg and Pb concentrations and fluxes measured from ^{210}Pb dated sediment cores of BDW and BDE are within the range of values found in other natural lakes around the world. However the flux ratios in these lakes, particularly for Pb in BDE, are higher than would be expected for relatively remote lakes. For the last 20 years, average Hg fluxes to BDW and BDE are 25.0 and 13.0 $\mu g/m^2/yr$, or 29.7 and 6.9 g per year, respectively. Relative to background sediments, the Hg flux ratios for these two lakes indicate that Hg inputs to both lakes have increased by a factor of 3 since the industrial revolution 150 years ago. The total mass of Hg accumulated in the sediments since inception after the Wisconsinan Glaciation 13,000 years ago is estimated to be 14.7 and 3.4 kg in BDW and BDE, respectively. Hg profiles show that the timing of recent historical anthropogenic activities have been preserved in the Hg profiles of both lakes. However, the magnitudes of the Hg increases are asynchronous when plotted as a function of time, but not when plotted as a function of depth, thereby suggesting that post-depositional diagenetic remobilization may partially be responsible for the upcore enrichments.

Unlike the Hg flux profiles, which show BDW having a greater flux of Hg throughout the cores, the Pb flux profiles show that the two lakes had similar fluxes of Pb at pre-1850 depths. Above these depths, BDE shows significantly larger Pb flux rates than BDW. In the top 3 cm, BDE's Pb flux of 5.3 $mg/m^2/yr$ is 1.9 times greater than BDW's Pb flux of 2.8 $mg/m^2/yr$. This difference is believed to be the result of upward remobilization, with more Pb being remobilized in BDE. The total mass of Pb accumulated since inception is estimated to be 5305 and 1502 kg in BDW and BDE, respectively.

Only the Pb increases in BDW coincide with historical increases in atmospheric Pb inputs associated with automobile emissions. Neither lake however records any significant decreases in the uppermost sediments as would be expected from the significant reductions in atmospheric Pb concentrations that have occurred since the phasing out of leaded gasoline in the 1970's. This lack of agreement between historical Pb inputs, together with the unusually high Pb fluxes in the surface sediments of BDE,

suggests that diagenetic remobilization of Pb is occurring in these sediments, with greater remobilization in BDE than BDW. This interpretation is strongly supported by a Pb isotope investigation of $^{206}Pb/^{207}Pb$ sediment profiles. Known historical events causing shifts in the $^{206}Pb/^{207}Pb$ profiles of the six cores show that all cores are well aligned in terms of age. However the concentration profiles of the same six cores plotted against age show that not all of the peak concentrations and rapid increases in Pb concentration occur at the same ages. Only the BDW cores show good agreement between peak concentrations and timing of rapid increases. The three BDE cores show three different peak concentrations, different depths for the Pb peaks, and different timing in rapid Pb increases. When Pb concentrations are plotted against sediment depth, there is much better agreement between the three BDE cores and between the BDE and BDW cores. These results provide strong evidence that the Pb concentration profiles, at least in BDE, are more a function of depth, and thus diagenetic conditions, than of depositional history. The fact that the calculated $^{206}Pb/^{207}Pb$ anthropogenic component in all cores is more radiogenic than would be expected, indicates that there is upward remobilization of Pb from deeper more radiogenic sediments in both lakes.

Anthropogenic inputs of Pb determined from precipitation samples taken over a one-year period indicate that anthropogenic pollution from populated and industrial regions of northeastern U.S. and southeatern Canada is being transported to Kejimkujik National Park. In general there was a dominantly Canadian source during the fall months of 2001 and a dominantly American source during the winter and spring months of 2002. The isotopic composition of the precipitation samples range from $^{206}Pb/^{207}Pb$ ratios of 1.165 to 1.20, indicating U.S. contributions ranging from 30-100% or Canadian contributions ranging from 0-70%. The annual average $^{206}Pb/^{207}Pb$ ratio is 1.181 and indicates that on an annual basis the U.S. contribution of Pb to Kejimkujik National Park is 62% (or 38% Canadian).

The average annual Pb isotope composition of the precipitation represents the value of the anthropogenic component that should be observed in the surface sediments. Knowing this value and the isotopic composition of the background sediments, enables the concentration of remobilized background Pb in the topmost sediment layer to be

calculated. Only BDE provides the necessary conditions to allow such a calculation. The amount of remobilized background Pb in the topmost sediment sample from a BDE core is estimated to be approximately 25.1 μg/g, which is 51% of the total Pb in the labile fraction of that sample.

Porewater data provide further evidence to support the interpretation of Pb and Hg remobilization in the sediments of BDW and BDE. Dissolved oxygen, pH and Eh profiles show the disappearance of DO by 4 cm depth accompanied by significant changes in pH and redox between 0 and 6-7 cm. BDE in particular shows rapid changes in pH and redox between 5 and 7cm depth, indicating that the decay of organic matter is much more rapid in BDE than BDW, which supports the data from the sediment profiles that indicate more Pb is remobilized in BDE than BDW. Both Hg and Pb are known to be associated with organic matter and Fe- and Mn-oxyhydroxides, therefore the decomposition of organic matter and dissolution of Mn at these depths provides a potential source of dissolved Hg and Pb to porewaters, which should move upward in the sediment column due to sediment compaction and concentration gradients.

Upward decreasing concentrations of both Hg and Pb measured in porewaters suggest that diffusion of Hg and Pb will predominantly occur in an upward direction, however the diffusion rate could not be calculated because of several unknowns such as sediment geometry, porosity, physical properties, and retardation factor. However, the flux ratio profiles, together with the fact that the sediment-water interface of these lakes has been determined to be a constant source of DGM (O'Driscoll, in review), indicate that Hg diffusion may be faster than Pb diffusion such that much of the diffusing Hg quickly passes through the oxic sediment layers into overlying waters while most of the Pb is re-oxidized or re-adsorbed to organic matter or oxyhydroxides in the surface sediments. Furthermore, high rates of Hg diffusion, together with a higher proportion of Hg being remobilized in BDE than BDW due to association with more reactive (labile) carbon species, would help explain why, despite having a sedimentation rate nearly half that of BDW, sediments in BDE, contrary to dilution models, are less concentrated in Hg.

In summary, multiple lines of evidence given in this study make it difficult to conclude that the depth profiles of Hg and Pb in lake sediments of BDW and BDE quantitatively record atmospheric inputs through time. Both elements show evidence of some degree of diagenetic remobilization, with the Pb, particularly in BDE, showing significantly more remobilization than Hg. It may just be however that more Hg is transported to the water column while most of the remobilized Pb is re-oxygenated or re-adsorbed in the oxic layer of surface sediments. In either case, the Pb profile in sediments is significantly more affected by diagenetic remobilization than Hg, and cannot be considered reliable recorders of atmospheric inputs, at least in BDE. The Hg concentration and flux data indicate that the timing of recent historical anthropogenic activities in or near these watersheds have been preserved in the Hg profiles of both lakes, but the absolute values of the concentrations can not be considered to be solely the result of changes in Hg inputs, as a portion of the upcore enrichments of Hg may to be the result of post-depositional remobilization from deeper sediments.

Interestingly, most studies of historical anthropogenic trace metal pollution would choose to core the sediments BDE over BDW because it has characteristics that are typically expected to better preserve depositional history, such as a higher proportion of direct deposition due to a lower watershed to lake area ratio, no inflow streams, low DOC levels, and no adjacent wetlands. However, as this study has shown, these watershed characteristics of BDE have instead created conditions allowing much more diagenetic remobilization than BDW, and in fact, against intuition, the sediments of BDW appear to be more reliable at recording changes in Pb and Hg inputs.

REFERENCES

Aastrup, M., Johnson, J., Bringmark, E., Bringmark, L., and Iverfeldt, Å. (1991) Occurrence and transport of mercury within a small catchment. *Water, Air and Soil Pollution* **56**: 155.

Allen, J.R.L., Rae, J.E., Longsworth, G., Hasler, S.E., and Ivanovich, M. (1993) A comparison of the ^{210}Pb dating technique with three other independent dating methods in an oxic estuarine salt-marsh sequence. *Estuaries* **16:** 670-677.

Andren, A.W., and Strand, J.W. (1981) Atmospheric deposition of particulate organic matter and polyaromatic hydrocarbons in Lake Michigan. In *Atmospheric Pollutants in Natural Waters*. Eisenreich, S.J. (ed.), Ann Arbor Science, Ann Arbor, pp.459-479.

Appleby, P.G., and Oldfield, F. (1978) The calculation of ^{210}Pb dates assuming a constant rate of supply of unsupported ^{210}Pb to the sediment. *Catena* **5:** 1-8.

Appleby, P.G., and Oldfield, F. (1992) Application of lead-210 to sedimentation studies. *In* Uranium-series disequilibrium: Applications to earth, marine, and environmental sciences. Second edition. M. Ivanovich and R.S. Harmon (eds.), Clarendon Press, Oxford: 730-782.

Appleby, P.G., Oldfield, F., Thompson, R., and Huttunen, P. (1979) ^{210}Pb dating of annually laminated lake sediments from Finland. *Nature* **280:** 53-57.

Armstrong, F.A.J. and Hamilton, A.L. (1973) Pathways of mercury in a polluted northwestern Ontario lake. *In*: Trace metals and metal-organic interactions in natural waters. Singer, P.C. (editor) Ann Arbor, MI: Ann Arbor Science, 131-156.

Bacon, M. P. and Rutgers van der Loeff, M. M. (1989) Removal of thorium-234 by scavenging in the bottom nepheloid layer of the ocean. *Earth and Planetary Science Letters* **92:** 157-164

Basquill, S.P., Woodley, S.J., and Pardy, A.B. (2001) The History and Ecology of Fire in Kejimkujik National Park. Parks Canada – Technical Reports in Ecosystem Science. Report 029.

Barnes, M.A., Barnes, W.C., and Bustin, R.M. (1990) Chemistry and diagenesis of organic matter in sediments and fossil fuels. *In:* Diagenesis. McIlreath, I.A. and Morrow, D.W. (eds.), pp. 189-204. Geological Association of America.

Beauchamp, S. (1998) Mercury in the Atmosphere. *In* Mercury in Atlantic Canada. Environment Canada Technical Report. Burgess, N., Beauchamp, S., Brun, G., Clair, T., Roberts, C., Rutherford, L., Tordon, R., and Vaida, O., (eds.), Environment Canada - Atlantic Region, Sackville, N.B.

Beauchamp, S., Tordon, R., Schroeder, J., Witte, J., and EMAN (1998) Mercury in the Atmosphere – Total Gaseous Mercury. *In* Mercury in Atlantic Canada. Environment Canada Technical Report. Burgess, N., Beauchamp, S., Brun, G., Clair, T., Roberts, C., Rutherford, L., Tordon, R., and Vaida, O., (eds.) Environment Canada - Atlantic Region, Sackville, N.B.

Begley, I.S. and Sharp, B.L. (1994) Occurrence and Reduction of Noise in Inductively-Coupled Plasma-Mass Spectrometry for Enhanced Precision in Isotope Ratio Measurement. *Journal of Analytical Atomic Spectrometry* **9(3)**: 171-176.

Begley, I.S. and Sharp, B.L. (1997) Characterisation and correction of instrumental bias in inductively coupled plasma quadrupole mass spectrometry for accurate measurement of lead isotope ratios. *Journal of Analytical Atomic Spectrometry* **12(4)**: 395-402.

Benoit, G., and Hemond, H.F. (1987) A biogeochemical mass balance of ^{210}Pb and ^{210}Po in an oligotrophic lake with seasonally anoxic hypolimnion. *Geochimica et Cosmochimica Acta* **51:** 1445-1456.

Benoit, G., and Hemond, H.F. (1988) Improved methods for the measurement of ^{210}Po, ^{210}Pb, and ^{226}Ra. *Limnology and Oceanography* **33(6, part 2):** 1618-1622.

Benoit, G., and Hemond, H.F. (1991) Evidence for diffusive redistribution of ^{210}Pb in lake sediments. *Geochimica et Cosmochimica Acta* **55:** 1963-1975.

Benoit, G., and Rozan, T.F. (2001) ^{210}Pb and ^{137}Cs dating methods in lakes: A retrospective study. *Journal of Paleolimnology,*25(4): 455-465.

Benoit, J., Fitzgerald, W.F., and Damman, A.W.H. (1994) Historical atmospheric mercury deposition in the mid-continental United States as recorded in an ombrotrophic peat bog. *In* Mercury Pollution: Integration and Synthesis. C.J. Watras and J.W. Huckabee (eds.). Lewis Publishers, Boca Raton, Fl. p 187-202.

Berner, R.A. (1980) Early Diagenesis: A Theoretical Approach. Princeton University Press, New Jersey.

Binford, M.W., Kahl, J.S., and Norton, S.A. (1993) Interpretation of ^{210}Pb profiles and verification of the CRS dating model in PIRLA project lake sediment cores. *Journal of Paleolimnology* **9:** 275-296.

Björklund, I., Borg, H., and Johansson, K. (1984) Mercury in swedish lakes - its regional distribution and causes. *Ambio* **13(2):** 118-121.

Bjornberg, A., Hakanson, L., and Lundbergh, K. (1988) A theory on the mechanisms regulating the bioavailability of mercury in natural waters. *Environmental Pollution* **49**: 53.

Blackwell, B., and Schwarcz, H.P. (1995) The uranium series disequilibrium dating methods. *In* Dating Methods for Quaternary Deposits. Rutter, N.W. and Catto, N.R. (eds.), Geological Association of Canada: 167-208.

Blais, J.M., Kalff, J., Cornett, R.J., and Evans, R.D. (1995) Evaluation of the ^{210}Pb dating in lake sediments using stable Pb, Ambrosia pollen, and ^{137}Cs. *Journal of Paleolimnology* **13:** 169-178.

Blomqvist, S., (1991) Quantitative Sampling of Soft-Bottom Sediments - Problems and Solutions. *Marine Ecology-Progress Series* **72(3)**: 295-304.

Boudreau, B.P. (1997) Diagenetic Models and their Implementation. Springer-Verlag, Germany.

Brenner, M., Peplow, A.J., and Schelske, C.L. (1994) Disequilibrium between ^{226}Ra and supported ^{210}Pb in a sediment core from a shallow Florida lake. *Limnology and Oceanograghy* **39:** 1222-1227.

Budhahn, J.R. (2000) Personal communication. Research Chemist. ^{210}Pb Dating Lab. U.S. Geological Survey, Denver Fedral Center, Denver, Colorado, 50225-0046, U.S.A.

Burgess, N., Evers, D., Kaplan, J., Duggan, M., and Kerekes, J. (1998a) Mercury levels in common loons breeding in the Maritimes and their prey. *In* Mercury in Atlantic Canada. Environment Canada Technical Report. Burgess, N., Beauchamp, S., Brun, G., Clair, T., Roberts, C., Rutherford, L., Tordon, R., and Vaida, O., (eds) Environment Canada - Atlantic Region, Sackville, N.B., pp.96-100.

Burgess, N (1998b) Introduction. *In* Mercury in Atlantic Canada. Environment Canada Technical Report. Burgess, N., Beauchamp, S., Brun, G., Clair, T., Roberts, C., Rutherford, L., Tordon, R., and Vaida, O., (eds) Environment Canada - Atlantic Region, Sackville, N.B.

Carignan, R. (1984) Interstitial Water Sampling by Dialysis - Methodological Notes. *Limnology and Oceanography* **29(3)**: 667-670.

Carignan, J. and Gariépy, C. (1995) Isotopic composition of epiphytic lichens as a tracer of the sources of atmospheric lead emissions in southern Québec, Canada. *Geochimica et Cosmochimica Acta* **59**: 4427-4433.

Carignan, R., and Nriagu, J.O. (1985) Trace metal deposition and mobility in the sediments of two lakes near Sudbury, Ontario. *Geochimica et Cosmochimica Acta* **49**: 1753-1764.

Carignan, R., Rapin, F. and Tessier, A., (1985) Sediment Porewater Sampling for Metal Analysis - a Comparison of Techniques. *Geochimica et Cosmochimica Acta* **49(11)**: 2493-2497.

Carignan, R., St pierre, S. and Gachter, R., (1994) Use of Diffusion Samplers in Oligotrophic Lake-Sediments - Effects of Free Oxygen in Sampler Material. *Limnology and Oceanography* **39(2)**: 468-474.

Chow, T.J. and Earl, J.L. (1972) Lead Isotopes in North American Coals. *Science* **176**: 510-511.

Chow, T.J., Bruland, K.W., Bertine, K.K., Soutar, A.A., Koide, M., and Goldberg, E.D. (1973) Records in Southern California coastal sediments. *Science* **181:** 551-552.

Chow, T.J. and Johnstone, M.S. (1965) Lead isotopes in gasoline and aerosols of Los Angeles Basin, California. *Science* **147:** 502-503.

Clair, T.A., Kramer, J.R., Sayer, B.G., and Eaton, D. (1996) Seasonal variation in the composition of aquatic organic matter in some Nova Scotian brownwaters: a nuclear magnetic resonance approach. *Hydrobiol.* **317:** 1141-150.

Claypool, G.E. and Kaplan, I.R. (1974) The origin and distribution of methane in marine sediments. *In*: Natural Gases in Marine Sediments. Marine Science, **3:** 99-140.

Comans, R.N.J., Middelburg, J.J., Zonderhuis, J., Woittiez, J.R.W., Delange, G.J., Das, H.A., and Vanderweijden, C.H. (1989) Mobilization of Radiocesium in Pore Water of Lake-Sediments. *Nature* **339(6223)**: 367-369.

Cumming, L.M. (1979) Bedrock Geology of Kejimkujik National Park - Manuscript Report for Parks Canada. Regional and Economic Geology Division, Geological Survey of Canada, Ottawa.

Davis, J.A. (1984) Complexation of trace metals by adsorbed natural organic matter. *Geochimica et Cosmochimica Acta* **46**: 2381-2393.

Davis, A. and Galloway, J.N., (1993) Distribution of Pb between Sediments and Pore Water in Woods Lake, Adirondack-State-Park, New-York, USA. *Applied Geochemistry* **8(1)**: 51.

Davis, R.B., Hess, C.T., Norton, S.A., Hanson, D.W., Hoagland, K.D., and Anderson, D.S. (1984) ^{137}Cs and ^{210}Pb dating of sediments from soft-water lakes in New England (U.S.A.) and Scandinavia, a failure of ^{137}Cs dating. *Chemical Geology* **44:** 151-186.

DeLacerda, L.D., Salomons, W., Pfeiffer, W.C., Bastos, W.R. (1991) Mercury distribution in sediment profiles from lakes of the high Pantanal, Mato-Grosso state, Brazil. *Biogeochemistry* **14(2)**: 91-97.

Dickins, A.P. (1995) Radiogenic Isotope Geology. Cambridge University Press. United Kingdom.

Driscoll, C.T., Yan, C., Schofield, C.L., Munson, R. and Hosapple, J. (1994a) The mercury cycle and fish in the Adirondack lakes. *Environmental Science and Technology* **17**: 136A-143A.

Driscoll, C.T., Blette, V., Yan, C., Schofield, C.L., Munson, R. and Hosapple, J. (1994b) The role of dissolved organic carbon in the chemistry and bioavailability of mercury in remote Adirondack Lakes. *Water, Air and Soil Pollution* **80**: 499-508.

Driscoll, C.T., Holsapple, J., Schofield, C.L., and Munson, R. (1998) The chemistry and transport of mercury in a small wetland in the Adirondack Region of New York, USA. *Biogeochemistry* **40**: 137-146.

Eadie, B.J., Chambers, R.L., Gardner, W.S., and Bell, G.E. (1984) Sediment trap studies in Lake Michigan: Resuspension and chemical fluxes in the southern basin. *Journal of Great Lakes Research* **10:** 307-321.

Eganhouse, R. P., Young, D. R., and Johnson, J. N. (1978) Geochemistry of mercury in Palos Verdes sediments. *Environmental Science and Technology* **12:** 1151-1157.

El Bilali, L., Rasmussen, P.E., Hall, G.E.M., and Fortin, D. (2002) Role of sediment composition in trace metal distribution in lake sediments. *Applied Geochemistry* **17**: 1171-1181.

Elder, J. F. (1988) Metal biogeochemistry in surface systems – A review of principles and concepts. U.S. Geological Survey Circulation, 1013.

Engstrom, D.R. and Swain, E.B. (1997) Recent declines in atmospheric mercury deposition in the upper mid-west. *Environmental Science and Technology* **31(4)**: 960-968

Engstrom, D.R. and Wright, H.E. (1983) Chemical stratification of lake sediments as records of environmental change. *In*: Lake Sediments and Environmental History. Haworth, E.Y., Lund, J.W. (Eds.), University of Minnesota Press, Minneapolis, MN.

Faure, G. (1986) Principles of Isotope Geology. Second Edition. John Wiley and Sons, Inc., New York, NY, p.291.

Ferguson, P.R. (2002) Quantifying the magnitude and rate of carbon accumulation in Eastern Canadian lake sediments trhough the Holocene. B.Sc. Honours thesis, University of Victoria, Victoria, BC. pp. 44.

Fitzgerald, W.F. (1989) Atmospheric and oceanic cycling of mercury. *In*: Chemical Oceanography, Academic Press, New York, Chap. 57.

Fitzgerald W.F. (1995) Is mercury increasing in the environment? The need for an atmospheric mercury network (AMNET). *Water, Air, and Soil Pollution* **80**: 245-254.

Fitzgerald, W.F., Engstrom, D.R., Mason., R.P., and Nater, E.A. (1998) Critical Review: The case for atmospheric mercury contamination in remote areas. *Environmental Science and Technology* **32(1)**:1-7.

Fitzgerald, W.F., Mason, R.P., and Vandal, G.M. (1991) Atmospheric cycling and air-water exchange of mercury over mid-continental lacustrine regions. *Water, Air and Soil Pollution* **56**: 745-768.

Fitzgerald, W.F., Mason, R.P., Vandal, G.M., and Dulac, F. (1994) Air-water cycling of mercury in lakes. *In* Mercury Pollution: Integration and Synthesis. C.J. Watras and J.W. Huckabee (eds.). Lewis Publishers, Boca Raton, Fl. p 203-220.

Flegal, A.R., Nriagu, J.O., Niemeyer, S., and Coales, K.H. (1989) Isotopic tracers of lead contamination in the Great Lakes. *Nature* **339:** 455-458.

Freedman. B., Kerekes, J., and Howell, G. (1989) Patterns of water chemistry among twenty-seven oligotrophic lakes in Kejimkujik National Part, Nova Scotia. *Water, Air, and Soil Pollution* **46:** 119-130.

French, K.J., Scruton, D.A., Anderson, M.R. and Schneider, D.C. (1999) Influence of physical and chemical characteristics on mercury in aquatic sediments. *Water, Air, and Soil Pollution* **110:** 347-362.

Gill, G. A. and Fitzgerald, W. F. (1988) Vertical mercury distributions in the oceans. *Geochimica et Cosmochimica Acta* **52:** 1719-1728.

Gilmour, C.C. and Henry, E.A. (1991) Mercury methylation in aquatic systems affected by acid deposition. *Environmental Pollution* **71**: 131.

Gimbarzensky, P. (1975) Biophysical survey of Kejimkujik National Park. Information Report FMR-X-81. Forest Management Institute. Petawawa, Ontario.

Gobiel, C., and Cossa, D. (1993) Mercury in sediments and sediment pore water in the Laurentian Trough sediments. *Canadian Journal of Fisheries and Aquatic Sciences* **50:** 1794-1800.

Gobiel, C., Macdonald, R.W., and Smith, J.N. (1999) Mercury profiles in sediments of the Arctic Ocean basins. *Environmental Science and Technology* **33**: 4194-4198.

Goldberg, E.D. (1963) Geochronology with lead-210. *In*: Radioactive Dating. Vienna: International Atomic Energy Agency. pp.121-131.

Goossens, H. Duren, R.R., de Leeuw, J.W., and Schenck, P.A. (1989) Lipids and their mode of occurance in bacteria and sediments – II. Lidips in the sediment of a stratified, freshwater lake. *Organic Geochemistry* **14:** 27-41.

Graney, J.R., Halliday, A.N., Keeler, G.J., Nriagu, J.O., Robbins, J.A., and Norton, S.A. (1995) Isotopic record of lead pollution in lake sediments from the northeastern United States. *Geochimica et Cosmochimica Acta* **59(9)**: 1715-1728.

Henrichs, S.M. (1992) Early diagenesis of organic-matter in marine-sediments - progress and perplexity. *Marine Chemistry* **39(1-3)**: 119-149.

Hesslein, R.H. (1976) An in situ sampler for close interval pore water studies. *Limnology and Oceanography* **22**: 913-915.

Hudson, R.J.M., Gherini, S.A, Fitzgerald, W.F., and Porcella, D.B. (1995) Anthropogenic influences on the global mercury cycle: A model-based analysis. *Water Air and Soil Pollution* **80**: 265-272.

Hudson, R.J.M., Gherini, S.A., Watras, C.J., and Porcella, D.B. (1994) Modeling the biogeochemical cycle of mercury in lakes: The Mercury Cycling Model (MCM) and its application to the MTL study lakes. *In* Mercury Pollution: Integration and Synthesis. C.J. Watras and J.W. Huckabee (eds.), Lewis Publishers, Boca Raton, Fl. p 473-523.

Hurley, J.P., Barbiaz, C.L., Cleckner, L.B., Rolfhus, K., Shafer, M.M., and Back, R.C. (2000) Partitioning of mercury and methylmercury in Lake Superior tributaries. *In*: Proceedings of the 43rd Conference on Great Lakes and St. Lawrence River Research, 2000 Annual Symposium. International Association of Great Lakes Research. 2205 Commonwealth Blvd., Ann Arbor, MI.

Hylander, L.D. and Meili, M. (2003) 500 years of mercury production: Global inventory by region and associated emissions until 2000. *The Science of the Total Environment* **304 (1):** 13-29.

Ishiwatari, R. (1985) Geochemistry of humic substances in lake sediments. *In*: Humic Substances in Soils, Sediment, and Water: Geochemistry, Isolation, and Characterization. McKnight, D.M. (ed.), Wiley, NewYork, pp. 147-180.

Johansson, K., Astrup, M., Andersson, A., Bringmark, L., and Iverfeldt, A. (1991) Mercury in Swedish forest soils and waters – assessment of critical load. *Water, Air, and Soil Pollution* **56**: 267-281.

Jones, H.G. and Stein, J. (1990) Hydrochemistry of snow and snowmelt in catchment hydrology. *In:* Process Studies in Hillslope Hydrology. M.G. Anderson and Burt, T.P. (eds.), John Wiley and Sons, pp.255-297.

Kamman, N.C., and Engstrom, D.R. (2002) Historical and present fluxes of mercury to Vermont and New Hampshire lakes inferred from 210Pb dated sediment cores. *Atmospheric Environment* **36**: 1599-1609.

Kemp, A.L., and Johnston, L.M. (1979). Diagenesis of organic matter in the lake sediments of Lakes Ontario, Erie, and Huron. *Journal of Great Lakes Research* **5:** 1-10.

Kerekes J. and Schwinghamer P. (1973) Kejimkujik National Park, N.S. Aquatic Resources Inventory Part 2: Lake Drainage and Morphometry. Canadian Wildlife Service, Eastern Region, Parks Canada, 72 p.

Kerekes, J., Freedman, B., Beauchamp, S., and Tordon, R. (1989) Physical and chemical characteristics of three acidic, oligotrophic lakes and their watershed in Kejimkujik National Park, Nova Scotia. *Water, Air and Soil Pollution* **46**: 99-117.

Ketterer, M.E., Peters, M.J. and Tisdale, P.J. (1991) Verification of a Correction Procedure for Measurement of Lead Isotope Ratios by Inductively Coupled Plasma Mass-Spectrometry. *Journal of Analytical Atomic Spectrometry* **6(6)**: 439-443.

Kober, B., Wessels, M., Bollhöfer, A., and Mangini, A. (1999) Pb isotopes in sediments of Lake Constance, Central Europe constrain the heavy metal pathways and the pollution history of the catchment, the lake and the regional atmosphere. *Geochimica et Cosmochimica Acta* **63(9)**: 1293-1303.

Koide, M., Bruland, K.W., and Goldberg, E.D. (1973) Th-228/Th-232 and Pb-210 geochronologies in marine and lake sediments. *Geochimica et Cosmochimica Acta* **37:** 1171-1187.

Koide, M., Soutar, A., and Goldberg, E.D. (1972) Marine geochronology with ^{210}Pb. *Earth and Planetary Science Letters* **14:** 442-446.

Krabbenhoft, D. P. and Babiarz, C. L. (1992) The role of groundwater transport in aquatic mercury cycling. *Water Resources Research* **28**: 3119-3128.

Krishnaswamy, S., Lal, D., Martin, J.M. and Meybeck, M. (1971) Geochronology of lake sediments. *Earth and Planetary Science Letters* **11:** 407-414.

Lamborg, C.H., Fitzgerald, W.F., Damman, A.W.H., Benoit, J.M., Balcom, P.H., and Engstrom, D.R. (2002) Modern and historic atmospheric mercury fluxes in both hemispheres: Global and regional mercury cycling implications. *Global Biogeochemical Cycles* **16(4)**: 1104.

Landers, D.H., Gubala, C., Verta, M., Lucotte, M., Johansson, K., Vlasova, T., and Lockhart, W.L. (1998) Using lake sediment mercury flux ratios to evaluate the regional and continental dimensions of mercury deposition in arctic and boreal ecosystems. *Atmospheric Environment* **32 (5)**: 919-928.

Lasorsa,B. and Allen-Gill,S. (1995) The methylmercury to total mercury ratio in selected marine, freshwater, and terrestrial organisms. *Water, Air and Soil Pollution* **80**: 905-914.

Lindqvist, O., Johansson, K., Åstrup, M., Andersson, A., Bringmark, L., Hovsenius, G., Iverfeldt, Å., Mieli, M., and Timm, B. (1991) Mercury in the Swedish environment. Recent research on causes, consequences and corrective methods. *Water, Air, and Soil Pollution* **55**:i-261.

Lindqvist, O. (1994) Atmospheric cycling of mercury: An overview. *In* Mercury Pollution: Integration and Synthesis. C.J. Watras and J.W. Huckabee (eds.), Lewis Publishers, Boca Raton, Fl. pp.181-186.

Lockhart, W.L., Macdonald, R.W., Outridge, P.M., Wilkinson, P., DeLaronde, J.B., and Rudd, J.W.M. (2000) Tests of the fidelity of lake sediment core records of mercury deposition to known histories of mercury contamination. *The Science of the Total Environment* **260**: 171-180.

Longerich, H.P., Fryer, B.J. and Strong, D.F. (1987) Determination of Lead Isotope Ratios by Inductively Coupled Plasma-Mass Spectrometry (ICP-MS). *Spectrochimica Acta Part B-Atomic Spectroscopy* **42(1-2)**: 39-48.

Lorey, P. and Driscoll, C. (1999) Historical trends of mercury deposition in Adirondack Lakes. *Environmental Science and Technology* **33**: 163-173.

Lucotte, M., Mucci, A., Hillaire-Marcel, P., Pichet, P., and Grondin, A. (1995) Anthropogenic mercury enrichment in remote lakes of northern Quebec (Canada). *Water Air and Soil Pollution* **80 (1-4)**: 467-476.

Mart, L. (1983) Seasonal variations of Cd, Pb, Cu, and Ni levels in snow from eastern Arctic Ocean. *Telus* **35B:** 131-141.

Martinez-Cortizas, A., Pontevedra-Pombal, X., Garcia, E., Nóvoa-Munoz, J.C., and Shotyk, W. (1999) Mercury in a Spanish Peat Bog: Archive of Climate Change and Atmospheric Metal Deposition. *Science* **284:** 939-943.

Mason, R.P., Fitzgerald, W.F., and Morel, F.M.M. (1994) The biogeochemical cycling of elemental mercury: Anthropogenic influences. *Geochimica et Cosmochimica Acta* **58(15)**: 3191-3198.

Mason, R.P., Reinfelder, J.R., and Morel, F.M.M. (1995) Bioaccumulation of mercury and methylmercury. *Water, Air and Soil Pollution* **80**: 915-921.

Matty, J. M. and Long, D. T. (1995) Early diagenesis of mercury in the Laurentian Great Lakes. *Journal of Great Lakes Research* **21**: 574-586.

McCall, P.L., Robbins, J.A., and Matisoff, G. (1984) ^{137}Cs and ^{210}Pb transport and geochronology in urbanized reservoirs with rapidly increasing sedimentation rates. *Chemical Geology* **44:** 33-66.

McNichol, A.P. Lee, C., and Druffel, E.M. (1988) Carbon cycling in coastal sediments: 1. A quantitative estimate of the remineralization of organic carbon in the sediments of Bazzards Bay, MA. *Geochimica et Cosmochimica Acta* **52**: 1531-1543.

Meyers, P.A. and Ishiwatari, R. (1993) Lacustrine organic geochemsitry – An overview of indicators of organic matter sources and diagenesis in lake sediments. *Organic Geochemistry* **20:** 867-900.

Mieli, M. (1995) Preindustrial atmospheric deposition of mercury: uncertain rates from lake sediment and peat cores. *Water Air and Soil Pollution* **80**: 637-640.

Mierle, G. (1990) Aqueous inputs of mercury to Precambrian Shield lakes in Ontario. *Environ. Toxicol. Chem.* **9**: 843-851.

Monna, F., Dominik, J., Loizeau, J.L., Pardos, M. and Arpagaus, P. (1999) Origin and evolution of Pb in sediments of Lake Geneva (Switzerland-France). Establishing a stable Pb record. *Environmental Science & Technology* **33(17)**: 2850-2857.

Monna, F., Lancelot, J., Croudace, I.W., Cundy, A.B., and Lewis, J.T. (1997) Pb isotopic composition of airborne particulate material from France and the Southern United Kingdom: Implications for Pb pollution sources in urban areas. *Environmental Science and Technology* **31:** 2277-2286.

NESCAUM (1998) Northeastern states and eastern Canadian provinces mercury study: a framework for action. Northeastern States for Coordinated Air Use Management, Boston, MA.

Ng, A. and Patterson, C.C. (1979) Chronological variations in barium concentrations, lead concentrations, and lead isotopic compositions in sediments of four Southern California offshore basins. *Southern California Baseline Study: Benthic, Year 2, Vol. 11, Report 14.* Bureau of Land Management. Dept. of Interior Contract AA550-CT6-40.

Ng, A. and Patterson, C.C. (1982) Changes of Lead and Barium with Time in California Off-Shore Basin Sediments. *Geochimica Et Cosmochimica Acta* **46(11)**: 2307-2321.

Nriagu, J.O. (1994) Mercury pollution from past mining of gold and silver in the Americas. *Science of the Total Environment* **149/3**: 167-181.

Nriagu, J.O. and Pacyna, J.M. (1988) Quantitative assessment of worldwide contamination of air, water and soils by trace-metals. *Nature* **333**: 134-139.

Nriagu, J.O. and Wong, H.K.T. (1989) Dynamics of particulate trace metals in the lakes of Kejimkujik National Park, Nova Scotia, Canada. *The Science of the Total Environment* **87/88**: 315-328.

O'Driscoll (in review) Patterns of DGM and water chemistry. *In:* A Multi-disciplinary Study of Mercury Cycling in a wetland Dominated Ecosystem: Kejimkujik National Park, Nova Scotia. Rencz, A and O'Driscoll, N. (Eds.) Society of Environmental Toxicology and Chemistry, Submitted 2003.

O'Driscoll, N.J. and Evans, R.D. (2000) Analysis of methyl mercury binding to freshwater humic and fulvic acids by gel permeation chromatography/hydride generation ICP-MS. *Environmental Science and Technology* **34(18):** 4039-4043.

Oldfield, F., and Appleby, P.G. (1984) A combined radiometric and mineral magnetic approach to recent geochronology in lakes affected by catchment disturbance and sediment redistribution. *Chemical Geology* **44:** 67-84.

Patterson, C.C. (1971) Native copper, silver, and gold accessibility to early metallurgists. *Am. Antiq.* **36:** 286-321.

Petterson, C., Bishop, K., Lee, Y., and Allard, B. (1995) Relations between organic carbon and methyl mercury in humic rich surface waters from Svartberget catchment in Northern Sweden. *Water, Air and Soil Pollution* **80(1-4)**: 971-979.

Pirrone, N., Allegrini, I., Keeker, G.J., Nriagu, J.O., Rossman, R., and Robbins, J.A. (1998) Historical atmosphreic mercury emissions and depositions in North America compared to mercury accumulations in sedimentary records. *Atmospheric Environment* **32(5)**: 929-940.

Porcella, D.B. (1994) Mercury in the Environment: Biogeochemistry. *In* Mercury Pollution: Integration and Synthesis. C.J. Watras and J.W. Huckabee (eds.). Lewis P, M.ubl., Boca Raton, Fl. p 3-20.

Rada, R.G., Powell, D., and Wiener, J. (1993) Whole-lake burdens and spatial distribution of mercury in surficial sediments in Wisconsin Seepage lakes. *Candian Journal of Fisheries and Aquatic Sciences* **50**: 865-873.

Ramlal, P.S., Rudd, J.W.M., Furutani, A., and Xun, L. (1985) The effects of pH on methylmercury production and decomposition in lake sediments. *Canadian Journal of Fisheries and Aquatic Sciences* **42**: 685-692.

Rasmussen, P.E., Villard, D.J., Gardner, H.D., Fortescue, J.A.C., Schiff, S.L. and Shilts, W.W. (1998) Mercury in lake sediments of the Precambrian Shield near Hunstville, Ontario, Canada. *Environmental Geology* **33(2/3)**: 170-182.

Riget, F., Dietz, R., Asmund, G., and Johansen, P. (1997) Heavy metals in Greenland terrestrial and freshwater environments. Results from the AMAP programme. In Extended Abstracts from the AMAP International Symposium on Environmental Pollution in the Arctic, 1-5 June 1997, Tromsø, Norway. Vol. 1. Edited by L.-O. Reiersen. Arctic Monitoring and Assessment Programme, Oslo, Norway, pp. 375-377.

Ritson, P.I., Esser, B.K., Niemeyer, S., Flegal, A.R. (1994) Lead isotopic determination of historical sources of lead to Lake Erie, North America. *Geochimica et Cosmochimica Acta* **58:** 3297-3305.

Robbins, J.A., and Edginton, D.N. (1975) Determination of recent sedimentation rates in Lake Michigan using Pb-210 and Cs-137. *Geochimica et Cosmochimica Acta* **39:** 285-304.

Rognerud, S., Skotvold, T., Fjeld, E., Norton, S.A., and Hobæk, A. (1998) Concentrations of trace metals in recent and preindustrial sediments from Norwegian and Russian Arctic lakes. *Canadian Journal of Fisheries and Aquatic Sciences* **55:** 1512-1523.

Rosman, K.J.R., Chilsom, W., Boutron, C.F., Candelone, J.P., and Hong, S. (1994) Isotopic evidence to account for changes in the concentrations of lead in Greenland snow between 1960 and 1988. *Geochimica et Cosmochimica Acta* **58**: 3265-3269.

Rosman, K.J.R., Chrisholm, W., Hong, S., Candelone, J.P., Laffrezo, J.L., and Davidson, C.I. (1998) Lead from Carthaginian and Roman Spanish mines isotopically identified in Greeland ice dated from 600 B.C. to 300 A.D. *Environmental Science and Technology* **31**: 3413-3416.

Rossman, R. (1986) Trace metal concentrations in the offshore waters and sediments of Lake Superior. Great Lakes Research Division Special Report No. 121.

Rudd, J.W.M., Turner, M.A., Furutani, A., Swick, A., Townsend, B.E. (1983) The English Wabigoon River system .1. A synthesis of recent research with a view towards mercury amelioration. *Canadian Journal of Fisheries and Aquatic Sciences* **40**: 2206.

Rutherford, L.A. (1998) Mercury sources – Natural sources. *In* Mercury in Atlantic Canada. Environment Canada Technical Report. Burgess, N., Beauchamp, S., Brun, G., Clair, T., Roberts, C., Rutherford, L., Tordon, R., and Vaida, O., eds. Environment Canada - Atlantic Region, Sackville, N.B.

Scherbatskoy, T.D., Shanley, J.B., and Keeler, G. (1998) Factors controlling mercury transport in an upland forested catchment. *Water, Air and Soil Pollution* **105**: 427-438.

Schlesinger, W.H. (1991) Biogeochemistry: An Analysis of Global Change. Academic Press, Inc., San Diego.

Schuster, E. (1991) The behaviour of mercury in the soil with special emphasis on complexation and adsorption processes – A review of the literature. *Water, Air and Soil Pollution* **56**: 667-680.

Shaw, T. J., Gieskes, J. M., and Jahnke, R. A. (1990) Early diagenesis in differing depositional environments: The response of transition metals in porewater. *Geochimica et Cosmochimica Acta* **54:** 1233-1246.

Sheppard, Jonathan (2003) Personal communication. Park Interpreter/Supervisor. Kejimkujik National Park, Nova Scotia, Canada.

Shirahata, H., Elias, R.W., Patterson, C.C., and Koide, M. (1980) Chronological variations in concentrations and isotopic compositions of anthropogenic atmospheric lead in sediments of a remote subalpine pond. *Geochimica et Cosmochimica Acta* **44(2)**: 149-162.

Shotyk, W., Weiss, D., Appleby, P.G., Cheburkin, A.K., Frei, R., Gloor, M., Kramers, J.D., Reese, S., Van der Knaap, W.O. (1998) History of atmospheric lead deposition since 12,370 C-14 yr BP from a peat bog, Jura Mountains, Switzerland. *Science* **281**: 1635-1640.

Simonetti, A., Gariepy, C., and Carignan, J. (2000a) Pb and Sr isotopic compositions of snowpack from Quebec, Canada: Inferences on the sources and deposition budgets of atmospheric heavy metals. *Geochimica et Cosmochimica Acta* **61:** 5-20.

Simonetti, A., Gariepy, C., and Carignan, J. (2000b) Pb and Sr isotopic evidence for sources of atmospheric heavy metals and their deposition budgets in northeastern North America. *Geochimica et Cosmochimica Acta* **64:** 3439-3452.

Simonetti, A., Gariépy, C., Carignan, J., and Poissant, L. (2000c) Isotopic evidence of trace metal sources and transport in eastern Canada as recorded from wet deposition. *Journal of Geophysical Research* **105(D10)**: 12,263-12,278.

Slemr, F. and Langer, E. (1992) Increase in global atmospheric concentrations of mercury inferred from measurements over the Atlantic Ocean. *Nature* **335**: 434-437.

Stea, R.R. and O'Reilly, G.A. (1982) Till geochemistry of the Meguma Terrane in Nova Scotia and its metallogenic implications. *In*: Prospecting in Areas of Glaciated Terrain. P.H. Davenport (editor), Can. Inst. Min. Metall., pp. 92-104.

Strunk, J. L. (1991) The extraction of mercury from sediment and the geochemical partitioning of mercury in sediments from Lake Superior. M. Sc. Thesis, Michigan State University, E. Lansing, MI.

Stumm, W. and Morgan, J.J. (1996) Aquatic Chemistry: Chemical Equilibria and Rates in Natural Waters, 3rd Edition. J.Wiley and Sons, New York, NY.

Swain, E.B., Engstrom, D.R., Brigham, M.E., Henning, T.A., and Brezonik, P.L. (1992) Increasing rates of atmospheric mercury deposition in midcontinental North America. *Science* **257**: 784-787.

Sturges, W.T. and Barrie, L.A. (1987) Lead 206/207 isotope ratios in the atmosphere of North America as tracers of US and Canadian emissions. *Nature* **329**: 144-146.

Telmer, K., DesJardins, M. and Ferguson, P. (in review) Mercury in Lake Sediments and Porewaters. *In:* A Multi-disciplinary Study of Mercury Cycling in a wetland Dominated Ecosystem: Kejimkujik National Park, Nova Scotia. Rencz, A and O'Driscoll, N. (Eds.) Society of Environmental Toxicology and Chemistry. Submitted 2003.

Tessier, A., Fortin, D., Belzile, N., Devitre, R.R., and Leppard, G.G. (1996) Metal sorption to diagenetic iron and manganese oxyhydroxides and associated organic matter; narrowing the gap between field and laboratory measurements. *Geochimica et Cosmochimica Acta* **60**: 387-404.

Thirwall, (2000) Interlaboratory and other errors in Pb-isotope analyses investigated using a 207Pb-204Pb double spike. *Chemical Geology* **163:** 299-322.

Tremblay, A., Lucotte, M., and Rowan, D. (1995) Different factors related to mercury concentration in sediments and zooplankton of 73 Canadian lakes. *Water, Air, and Soil Pollution* **80:** 961-971.

Turner, L.J., and Delorme, L.D. (1996) Assessment of ^{210}Pb data from Canadian lakes using the CIC and CRS models. *Environmental Geology* **28:** 78-87.

U. S. Environmental Protection Agency (US EPA) (1994) Mercury Study Report to Congress, Volume II. Inventory of anthropogenic mercury emissions in the United States.

U.S. Environmental Protection Agency, (1999). Method 1631, Revision B: Mercury in Water by Oxidation, Purge and Trap, and Cold Vapour Atomic Flourescence Spectrometry, **http://www.epa.gov/ost/Methods/1631final.pdf**.

Van Cappellen, P.and Gaillard, J.-F. (1996) Biogeochemical dynamics in aquatic sediments. *In*: Reactive Transport in Porous Media, Clichtner, P.C., Steefel, C.I., and Oelker, E.H. (eds.), Mineralogical Society of America, **34:** 335-376.

Véron, A., Church, T.M., Patterson, C.C., Erel, Y., and Merrill, J.T. (1992) Continental origin and industrial sources of trace metals in the northwest Atlantic troposphere. *Journal of Atmospheric Chemistry* **14**: 339-351.

Verta, M., Tolonen, K., and Simola, H. (1989) History of heavy-metal pollution in Finland as recorded by lake-sediments. *Science of the Total Environment* **87/88**: 1-18.

Verta, M., Matilainen T., Porvari, P., Niemi, M., Uusi-Rauva, A., and Bloom, N.S. (1994) Methylmercury sources in boreal lake ecosystems. *In* Mercury Pollution: Integration and Synthesis. C.J. Watras and J.W. Huckabee (eds.). Lewis Publishers, Boca Raton, Fl. p 119-136.

Vile, M.A., Wieder, R.K., and Novak, M. (2000) 200 years of Pb deposition throughout the Czech Republic: patterns and sources. *Environmental Science and Technology* **34**: 12-21.

Watras, C.J., Bloom, N.S., Fitzgerald, W.F., Wiener, J.G., Rada, R., Hudson, R.J.M., Gherini, S.A., and Porcella, D.B. (1994) Sources and fates of mercury and methylmercury in remote temperate lakes. *In* Mercury Pollution: Integration and Synthesis. C.J. Watras and J.W. Huckabee (eds.). Lewis Publishers, Boca Raton, Fl. p 153-177.

White, W.M. (1997) Geochemistry. John Hopkins University Press.

Yang, H., Rose, N.L., Batterbee, R.W., and Boyle, J.F. (2002) Mercury and Lead budgets for Lochnagar, a Scottish mountain lake and its catchment. *Environmental Science and Technology* **36**: 1383-1388.

Zielinski, R.A., and Budahn, J.R. (1998) Radionuclides in fly ash and bottom ash: improved characterization based on radiography and low energy gamma-ray spectrometry. *Fuel* **77:** 259-267.

APPENDIX A: Coring and Porewater Sampling Equipment

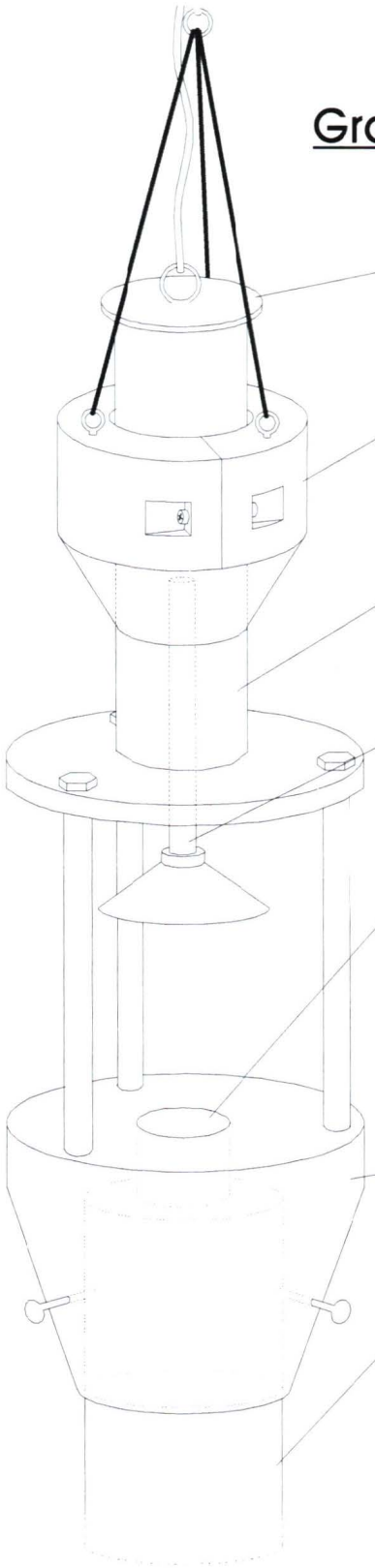

Gravity Corer

Top Plate: Prevents knocker from coming off and secures main cable.

Bullet shaped percussion knocker: a heavy cuff that can be raised and dropped, using a second cable to slowly force it further into sediments. The corer, therefore, does not need to be sent into the sediments with any velocity and so sediment perturbation is greatly reduced. The knocker can be removed.

Neck: Hollow tube housing 2 brackets to ensure true piston travel.

Piston and suction cup: density only slightly greater than water so that it rides up while corer is descending and then sinks to seal portal to core tube. This allows sediments to be pulled to the surface by suction alone without the aid of a core catcher.

Open barrel allows water to pass through the corer to limit bow wave and minimizing sediment perturbation.

Thumb Screw: secures core tube in corer. Nylon or nylon tipped to prevent damage to core tube.

Solid stainless steel corer body: secures the core tube and provides the weight to push the tube into the sediments. After the tube is mounted and fastened with the thumb screws, electrical tape is used to make an airtight seal between the corer body and the tube. This is required to maintain suction.

Core Tube: clear Lexan tube with the leading edge sharpened from outside surface only to maintain internal diameter. This minimizes smear while entering the sediment.

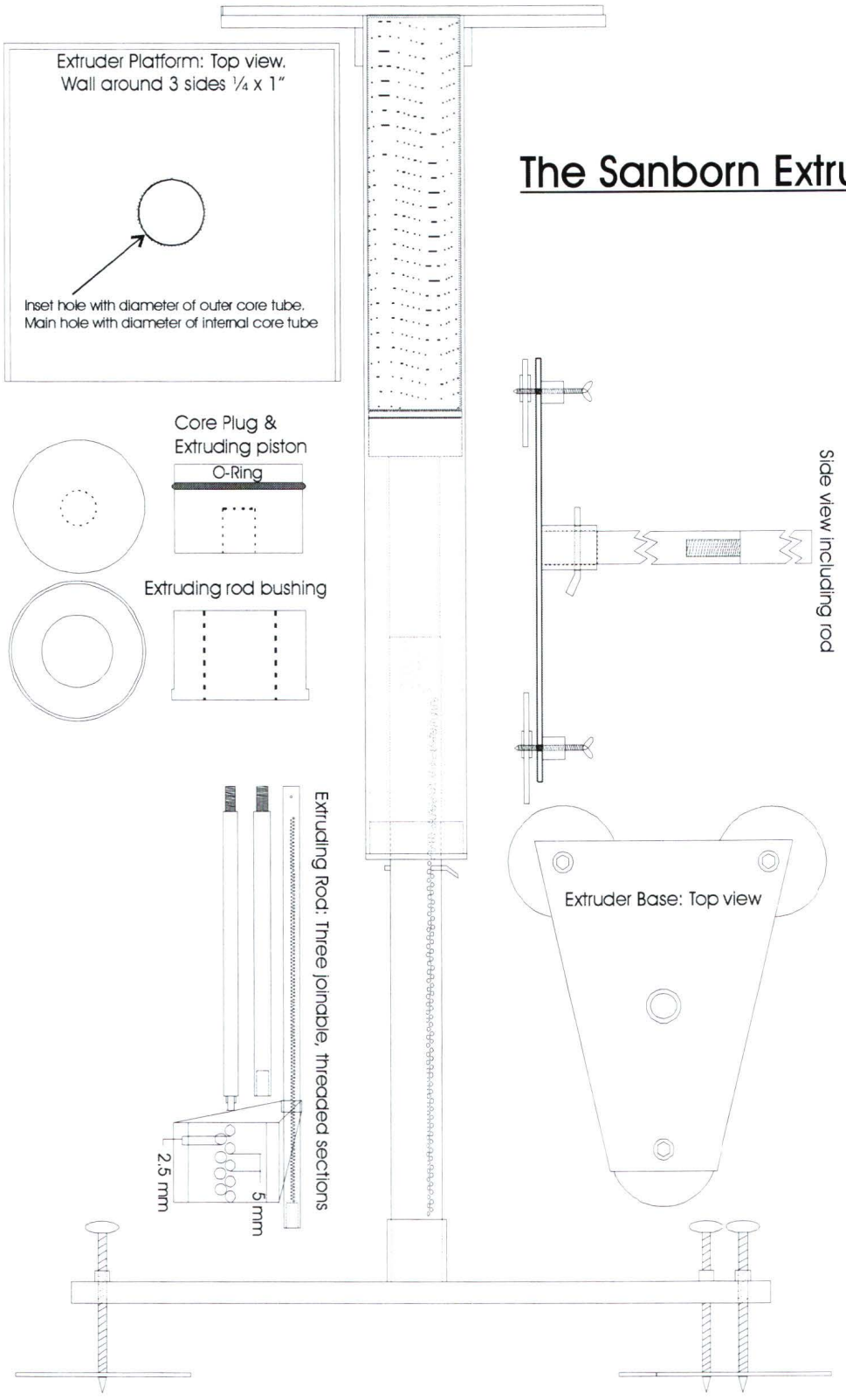
The Sanborn Extruder
Extruder Platform: Top view.
Wall around 3 sides ¼ x 1"
Inset hole with diameter of outer core tube.
Main hole with diameter of internal core tube
Core Plug &
Extruding piston
O-Ring
Extruding rod bushing
Side view including rod
Extruding Rod: Three joinable, threaded sections
2.5 mm
5 mm
Extruder Base: Top view

Porewater Peeper

Detail information on the dimensions of this porewater sampler is given in Chapter 6 - Methods and Analyses. Peeper shown here is a double peeper with two vertical rows of sampling chambers.

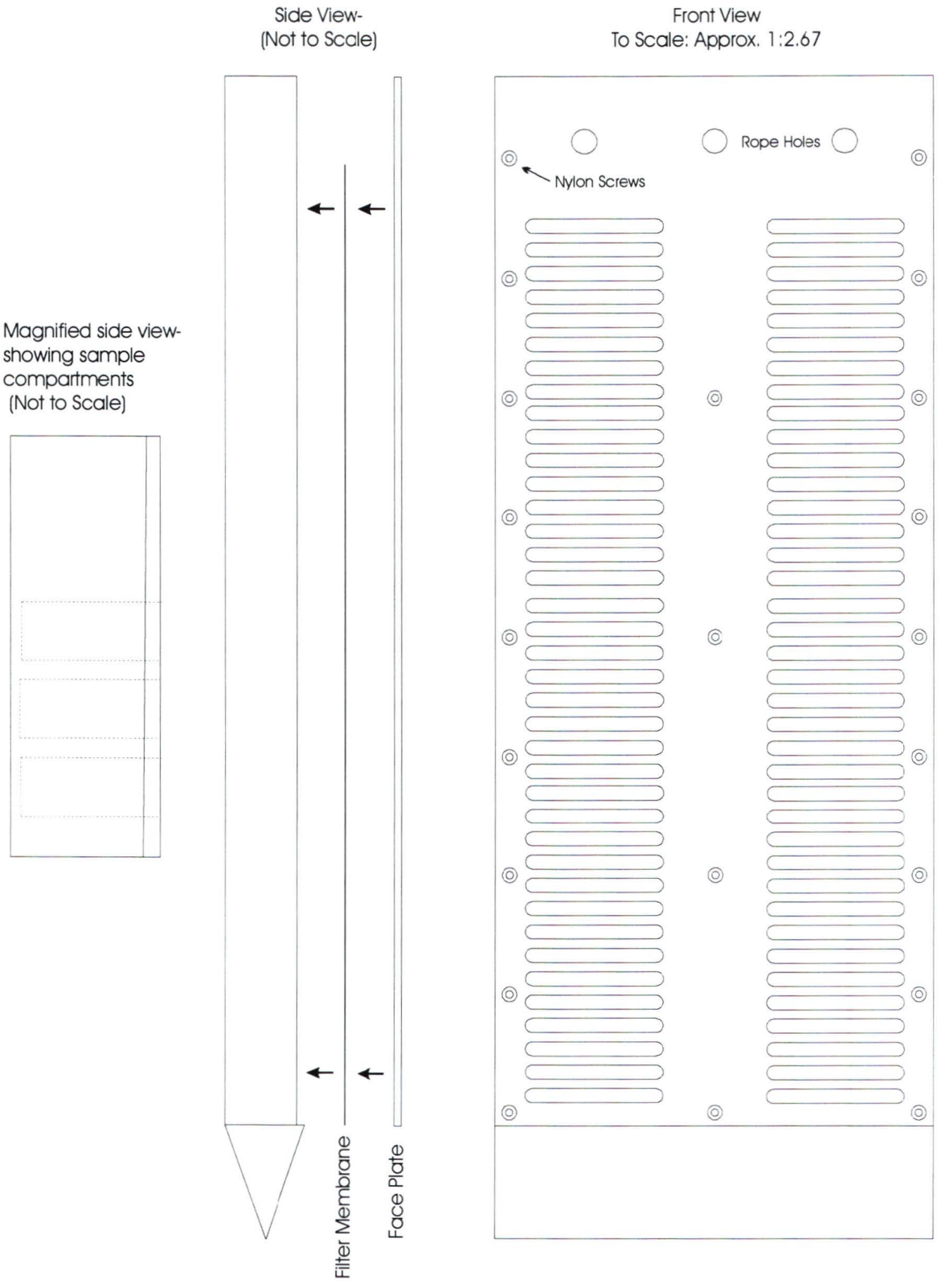

APPENDIX B: Bulk Density and Water Content Data

BIG DAM WEST LAKE

Depth	Particle Density (g/cm^3)				Water Content (%)			
(cm)	KJ99-BDW1	KJ99-BDW2	KJ00-BDW7	Average	KJ99-BDW1	KJ99-BDW2	KJ00-BDW7	Average
0.25	0.01			0.01	98.29			98.29
0.5	0.05		0.05	0.05	99.37		98.12	98.75
0.75	0.09			0.09	96.31			96.31
1.0	0.11		0.11	0.11	95.89		95.41	95.65
1.25	0.13			0.13	94.94			94.94
1.5	0.13	0.12	0.12	0.13	87.67	94.58	92.44	91.56
1.75	0.14			0.14	93.92			93.92
2.0	0.14	0.14	0.14	0.14	92.34	93.73	93.41	93.16
2.25	0.17			0.17	92.78			92.78
2.5	0.17	0.16	0.15	0.16	94.42	92.19	93.01	93.21
3.0	0.17		0.17	0.17	92.74		92.32	92.53
3.5	0.17		0.17	0.17	92.57		92.64	92.60
4.0	0.16		0.20	0.18	93.35		90.60	91.98
4.5	0.16	0.22	0.20	0.19	94.04	89.33	91.95	91.77
5.0	0.15	0.22	0.20	0.19	93.60	91.01	92.56	92.39
5.5	0.14	0.21	0.21	0.19	93.94	91.06	90.14	91.72
6.0	0.14		0.22	0.18	94.09		89.88	91.98
6.5	0.14		0.23	0.19	93.97		88.55	91.26
7.0	0.14		0.21	0.17	93.66		89.70	91.68
7.5	0.14		0.24	0.19	94.13		88.94	91.54
8.0			0.24	0.24			90.42	90.42
8.5	0.15		0.23	0.19	93.03		87.98	90.51
9.0			0.22	0.22			88.70	88.70
9.5	0.14		0.22	0.18	93.56		89.26	91.41
10.0		0.21	0.22	0.22		90.54	90.70	90.62
10.5	0.16			0.16	92.22			92.22
11.0		0.25		0.25		87.03		87.03
11.5	0.15			0.15	92.76			92.76
12.5	0.15			0.15	93.26			93.26
13.5	0.14			0.14	93.44			93.44
14.5	0.15			0.15	93.09			93.09
15.5	0.13			0.13	94.10			94.10
16.5	0.13			0.13	94.26			94.26
17.5	0.13			0.13	94.35			94.35
18.5	0.13			0.13	94.63			94.63
19.5	0.13			0.13	94.88			94.88
20.5	0.13			0.13	95.22			95.22
21.5	0.13			0.13	94.28			94.28
22.5	0.13			0.13	93.63			93.63
23.5	0.13			0.13	93.99			93.99
24.0		0.21		0.21		93.34		93.34
24.5	0.14			0.14	94.37			94.37

APPENDIX B *Continued*

BIG DAM WEST LAKE - *Cont'd*

Depth (cm)	Particle Density (g/cm^3)				Water Content (%)			
	KJ99-BDW1	KJ99-BDW2	KJ00-BDW7	Average	KJ99-BDW1	KJ99-BDW2	KJ00-BDW7	Average
25.5	0.14			0.14	94.20			94.20
26.5	0.14			0.14	94.02			94.02
27.5	0.15			0.15	94.48			94.48
28.5	0.15			0.15	93.21			93.21
29.5	0.15			0.15	93.02			93.02
30.5	0.16			0.16	93.27			93.27
31.5	0.16			0.16	93.38			93.38
32.5	0.17			0.17	92.94			92.94
33.5	0.17			0.17	92.81			92.81
34.5	0.18			0.18	92.54			92.54
35.5	0.19			0.19	92.28			92.28
36.5	0.19			0.19	92.21			92.21
37.5	0.19			0.19	92.45			92.45
39.5	0.20			0.20	91.64			91.64

BIG DAM EAST LAKE

Depth (cm)	Particle Density (g/cm^3)			Water Content (%)		
	KJ99-BDE2	KJ99-BDE3	Average	KJ99-BDE2	KJ99-BDE3	Average
0.5	0.03	0.07	0.05	97.74	96.47	97.11
1.0	0.10	0.13	0.11	95.25	94.31	94.78
1.5	0.12	0.14	0.13	95.38	94.31	94.85
2.0	0.13	0.15	0.14	94.80	93.35	94.08
2.5	0.14	0.15	0.15	92.96	93.43	93.19
3.0	0.15	0.17	0.16	93.39	93.70	93.55
3.5	0.16	0.18	0.17	92.91	92.33	92.62
4.0	0.17	0.18	0.18	92.84	92.71	92.78
4.5	0.19	0.19	0.19	90.95	92.71	91.83
5.0	0.19	0.19	0.19	91.48	91.31	91.40
5.5	0.20	0.20	0.20	90.74	91.96	91.35
6.0	0.18	0.21	0.19	91.12	91.87	91.49
6.5	0.19	0.22	0.20	91.57	90.54	91.06
7.0	0.19	0.21	0.20	91.65	91.83	91.74
7.5	0.18	0.22	0.20	91.84	91.51	91.67
8.0	0.18	0.21	0.20	92.23	90.38	91.31
8.5	0.19	0.23	0.21	91.67	90.20	90.94
9.0	0.18	0.24	0.21	92.33	90.29	91.31
9.5	0.18	0.22	0.20	91.59	90.57	91.08
10.0	0.19	0.22	0.20	91.31	90.07	90.69
11.0		0.22	0.22		87.96	87.96
12.0	0.17	0.22	0.19	92.31	90.20	91.25
13.0	0.18	0.22	0.20	91.95	90.64	91.29
14.0	0.19	0.22	0.20	91.82	90.89	91.35
15.0	0.18	0.23	0.20	91.76	90.46	91.11

APPENDIX B *Continued*

BIG DAM EAST LAKE - *Cont'd*

Depth (cm)	Particle Density (g/cm^3)			Water Content (%)		
	KJ99-BDE2	KJ99-BDE3	Average	KJ99-BDE2	KJ99-BDE3	Average
16.0	0.19	0.23	0.21	91.09	89.55	90.32
17.0	0.20	0.22	0.21	91.53	90.07	90.80
18.0	0.20	0.21	0.21	90.57	90.49	90.53
19.0	0.21	0.21	0.21	89.86	91.17	90.51
20.0	0.21	0.21	0.21	90.47	90.94	90.71
22.0		0.21	0.21		90.55	90.55
24.0		0.22	0.22		90.46	90.46
26.0		0.23	0.23		92.05	92.05
28.0		0.22	0.22		92.51	92.51
30.0		0.22	0.22		94.20	94.20
32.0		0.23	0.23		92.34	92.34
36.0		0.25	0.25		91.82	91.82
38.0		0.25	0.25		92.17	92.17
40.0	0.23	0.26	0.25	93.35	92.99	93.17

APPENDIX C: Activity Data for 210-Pb Dating

	Sample	In-situ depth (cm)	In-situ mid-depth (cm)	Uncompacted depth (cm)	Dry weight (g)	Cumulative dry weight (g/cm2)	Total Pb-210 (dpm/g)	Pb-214 (dpm/g)	Bi-214 (dpm/g)	Average supported Pb-210 (dpm/g)	St. Dev. supported Pb-210 (dpm/g)	Excess Pb-210 (dpm/g)	Excess Pb-210 (pCi/g)	Cs-137 (dpm/g)
BIG DAM WEST	BDW-1	1.0	0.5	1.0	6.52	0.04	11.55	2.27	2.43	2.35	0.12	9.20	4.14	2.63
	BDW-2	2.0	1.5	3.4	20.36	0.15	7.03	0.52	0.79	0.66	0.19	6.37	2.87	2.52
	BDW-3	3.0	2.5	6.0	27.21	0.30	6.19	0.91	1.05	0.98	0.10	5.21	2.35	2.08
	BDW-4	4.0	3.5	8.8	29.36	0.46	2.99	0.77	0.97	0.87	0.14	2.12	0.95	1.70
	BDW-5	5.0	4.5	11.7	32.36	0.63	1.25	0.74	0.85	0.80	0.08	0.46	0.21	0.81
	BDW-6	6.0	5.5	14.7	34.09	0.82	1.35	0.91	0.87	0.89	0.03	0.46	0.21	0.62
	BDW-7	7.0	6.5	17.8	36.71	1.02	1.00	0.79	0.72	0.76	0.05	0.24	0.11	0.60
	BDW-8	8.0	7.5	21.0	36.28	1.22	1.60	0.78	0.70	0.74	0.06	0.86	0.39	0.47
	BDW-9	9.0	8.5	24.8	36.56	1.42	2.33	1.08	1.18	1.13	0.07	1.20	0.54	0.59
	BDW-10	10.0	9.5	28.1	38.69	1.63	0.63	0.66	0.79	0.73	0.09	0.00	0.00	0.38
	BDW-12	12.0	11.5	34.9	39.64	2.07	0.78	0.73	0.81	0.77	0.06	0.02	0.01	0.17
	BDW-14	14.0	13.5	41.7	37.37	2.48	0.90	0.80	0.90	0.85	0.07	0.05	0.02	0.14
	BDW-16	16.0	15.5	48.5	36.87	2.88	1.60	0.89	0.90	0.89	0.01	0.11	0.05	0.12
	BDW-18	18.0	17.5	55.3	39.54	3.32	1.74	0.72	0.72	0.72	0.00	0.46	0.21	0.13
	BDW-20	20.0	19.5	62.0	38.56	3.74	0.76	0.68	0.77	0.73	0.06	0.03	0.01	0.06
BIG DAM EAST	BDE-1	1.0	0.5	1.0	9.75	0.05	17.16	1.00	1.13	1.07	0.09	16.10	7.25	6.57
	BDE-2	2.0	1.5	2.9	25.68	0.19	10.38	0.55	0.68	0.62	0.10	9.76	4.40	4.33
	BDE-3	3.0	2.5	5.2	28.94	0.35	7.99	0.50	0.60	0.55	0.07	7.44	3.35	4.40
	BDE-4	4.0	3.5	7.7	30.96	0.52	5.97	0.46	0.68	0.57	0.15	5.40	2.43	3.34
	BDE-5	5.0	4.5	10.6	32.26	0.70	2.12	0.57	0.66	0.61	0.06	1.50	0.68	2.65
	BDE-6	6.0	5.5	13.6	35.22	0.89	1.13	0.45	0.46	0.45	0.01	0.67	0.30	1.59
	BDE-7	7.0	6.5	16.5	34.57	1.08	2.05	0.57	0.58	0.57	0.01	1.48	0.66	1.27
	BDE-8	8.0	7.5	19.5	35.68	1.28	0.68	0.64	0.53	0.58	0.08	0.10	0.04	0.70
	BDE-9	9.0	8.5	22.5	33.57	1.46	1.12	0.90	0.70	0.80	0.14	0.32	0.14	0.66
	BDE-10	10.0	9.5	25.7	33.39	1.64	0.73	0.67	0.55	0.61	0.08	0.12	0.05	0.41
	BDE-12	12.0	11.5	31.7	33.67	2.01	0.92	0.67	0.48	0.57	0.13	0.34	0.15	0.24
	BDE-14	14.0	13.5	37.7	32.82	2.37	0.60	0.54	0.52	0.53	0.01	0.07	0.03	0.28
	BDE-16	16.0	15.5	44.3	33.57	2.74	0.79	0.68	0.52	0.60	0.11	0.18	0.08	0.20
	BDE-18	18.0	17.5	50.9	34.25	3.12	0.58	0.60	0.62	0.61	0.02	0.00	0.00	0.16
	BDE-20	20.0	19.5	57.3	32.25	3.47	0.68	0.59	0.66	0.63	0.05	0.06	0.03	0.14

APPENDIX D: Sediment Pb Isotope and Concentration data

Sequential Digestion Results

Core and Sample	Mid-depth (cm)	Age (yrs A.D.)	Partial Digest $^{206}Pb/^{207}Pb$	Partial Digest $^{208}Pb/^{206}Pb$	Partial Digest Pb (ug/g)	HF-HNO_3 Digest $^{206}Pb/^{207}Pb$	HF-HNO_3 Digest $^{208}Pb/^{206}Pb$	HF-HNO_3 Digest Pb (ug/g)	Summed Totals $^{206}Pb/^{207}Pb$	Summed Totals $^{208}Pb/^{206}Pb$	Summed Totals Pb (ug/g)
KJ00-BDW5-01	0.25	1998	1.202	2.056	18.98						
KJ00-BDW5-02	0.75	1997	1.205	2.053	19.23	1.211	2.052	4.24	1.208	2.052	23.47
KJ00-BDW5-03	1.25	1994	1.201	2.058	18.60	1.202	2.064	4.30	1.202	2.061	22.89
KJ00-BDW5-04	1.75	1989	1.204	2.035	17.84	1.190	2.065	5.02	1.197	2.050	22.86
KJ00-BDW5-05	2.25	1984	1.196	2.046	19.14	1.213	2.037	5.45	1.204	2.041	24.59
KJ00-BDW5-06	2.75	1979	1.194	2.043	20.82	1.198	2.093	5.42	1.196	2.068	26.25
KJ00-BDW5-07	3.25	1974	1.192	2.057	20.05	1.194	2.075	5.28	1.193	2.066	25.33
KJ00-BDW5-08	3.75	1968	1.193	2.053	16.03	1.214	2.040	5.23	1.203	2.046	21.25
KJ00-BDW5-10	4.75	1957	1.205	2.047	10.95	1.200	2.056	4.74	1.203	2.051	15.69
KJ00-BDW5-12	5.75	1945	1.209	2.043	8.09	1.217	2.034	4.92	1.213	2.038	13.02
KJ00-BDW5-14	6.75	1933	1.200	2.049	6.72	1.205	2.064	4.83	1.203	2.057	11.55
KJ00-BDW5-16	7.75	1921	1.211	2.030		1.202	2.064		1.207	2.047	
KJ00-BDW5-18	8.75	1906	1.212	2.036	4.65	1.196	2.075	4.87	1.204	2.056	9.52
KJ00-BDW5-20	9.75	1893	1.219	2.046	4.21	1.202	2.071	4.78	1.210	2.058	9.00
KJ00-BDW5-22	11.5	1863	1.212	2.032	4.49	1.194	2.099	4.59	1.203	2.065	9.09
KJ00-BDW5-24	13.5	***1834***	1.214	2.022	3.61	1.184	2.072	4.64	1.199	2.046	8.25
KJ00-BDW5-26	15.5	***1804***	1.222	2.020	3.45	1.208	2.037	4.16	1.215	2.029	7.60
KJ00-BDW5-28	17.5	***1773***	1.223	2.023	3.45	1.199	2.061	3.73	1.211	2.043	7.17
KJ00-BDW5-30	19.5	***1741***	1.236	2.008	3.30	1.217	2.032	3.90	1.227	2.020	7.20
KJ00-BDW5-32	21.5	***1730***	1.230	1.999	3.39	1.216	2.074	3.78	1.223	2.037	7.16
KJ00-BDW5-34	23.5	***1702***	1.213	2.025	3.35	1.219	2.018	3.85	1.216	2.022	7.20
KJ00-BDW5-36	25.5	***1675***	1.238	1.989	4.62	1.208	2.028	3.54	1.223	2.009	8.16
KJ00-BDW5-38	27.5	***1648***	1.232	2.007	3.29	1.213	2.046	3.22	1.222	2.027	6.52
KJ00-BDW5-40	29.5	***1621***	1.236	2.003	4.14	1.225	2.044	2.76	1.231	2.024	6.90
KJ00-BDW5-44	37	***1520***	1.239	2.008	3.74	1.198	2.075	2.51	1.218	2.042	6.26
KJ00-BDW5-48	45	***1412***	1.237	2.006	3.13	1.198	2.072	2.57	1.217	2.039	5.69

Note: Ages in bold italics were determined by extrapolation of sedimentation rate and are considered unreliable.

APPENDIX D *Continued*

Sequential Digestion Results - *Cont'd*

Core and Sample	Mid-depth (cm)	Age (yrs A.D.)	Partial Digest $^{206}Pb/^{207}Pb$	Partial Digest $^{208}Pb/^{206}Pb$	Partial Digest Pb (ug/g)	$HF\text{-}HNO_3$ Digest $^{206}Pb/^{207}Pb$	$HF\text{-}HNO_3$ Digest $^{208}Pb/^{206}Pb$	$HF\text{-}HNO_3$ Digest Pb (ug/g)	Summed Totals $^{206}Pb/^{207}Pb$	Summed Totals $^{208}Pb/^{206}Pb$	Summed Totals Pb (ug/g)
KJ99-BDW1-01	0.125	1999	1.194	2.052	17.83	1.176	2.093	2.70	1.192	2.057	20.54
KJ99-BDW1-02	0.375	1998	1.198	2.038	17.09	1.180	2.060	2.50	1.196	2.041	19.59
KJ99-BDW1-03	0.625	1996	1.196	2.042	17.11	1.196	2.049	4.72	1.196	2.043	21.84
KJ99-BDW1-04	0.875	1995	1.186	2.045	16.71	1.193	2.057	2.87	1.187	2.047	19.57
KJ99-BDW1-05	1.125	1993	1.202	2.032	16.79	1.190	2.054	3.11	1.200	2.035	19.90
KJ99-BDW1-06	1.375	1989	1.181	2.049	19.10	1.183	2.059	5.67	1.182	2.051	24.76
KJ99-BDW1-07	1.625	1986	1.186	2.041	19.01	1.188	2.048	5.68	1.186	2.042	24.69
KJ99-BDW1-08	1.875	1982	1.192	2.034	21.37	1.187	2.050	6.04	1.191	2.037	27.41
KJ99-BDW1-09	2.125	1979	1.188	2.042	18.91	1.191	2.040	5.70	1.189	2.042	24.61
KJ99-BDW1-10	2.375	1975	1.182	2.044	18.16	1.202	2.044	5.83	1.187	2.044	23.99
KJ99-BDW1-11	2.75	1969	1.195	2.056	15.69	1.208	2.049	2.34	1.197	2.055	18.03
KJ99-BDW1-12	3.25	1962	1.195	2.044	13.40	1.170	2.073	3.09	1.190	2.050	16.49
KJ99-BDW1-13	3.75	1954	1.207	2.041	10.80	1.218	2.046	2.53	1.209	2.042	13.34
KJ99-BDW1-14	4.25	1946	1.194	2.033	9.64	1.178	2.054	5.28	1.188	2.041	14.92
KJ99-BDW1-15	4.75	1937	1.184	2.044	8.96	1.193	2.054	4.94	1.187	2.048	13.90
KJ99-BDW1-16	5.25	1929	1.190	2.044	7.98	1.195	2.063	4.99	1.192	2.051	12.97
KJ99-BDW1-17	5.75	1921	1.206	2.035	6.69	1.194	2.042	5.70	1.201	2.038	12.39
KJ99-BDW1-18	6.25	1912	1.203	2.037	5.98	1.201	2.041	3.17	1.202	2.038	9.15
KJ99-BDW1-19	6.75	1903	1.201	2.025	5.54	1.212	2.046	3.83	1.206	2.034	9.37
KJ99-BDW1-20	7.25	1894	1.210	2.038	5.49	1.185	2.062	2.11	1.203	2.045	7.60
KJ99-BDW1-21	8.0	1880	1.209	2.035	5.49	1.201	2.050	2.70	1.206	2.040	8.18
KJ99-BDW1-22	9.0	1859	1.201	2.042	4.92	1.197	2.050	2.77	1.200	2.045	7.68
KJ99-BDW1-23	10.0	***1840***	1.200	2.029	4.75	1.185	2.063	4.09	1.193	2.045	8.84
KJ99-BDW1-24	11.0	***1821***	1.193	2.048	3.98	1.192	2.064	3.92	1.192	2.056	7.90
KJ99-BDW1-25	12.0	***1801***	1.208	2.046	3.43	1.197	2.061	7.87	1.200	2.056	11.29
KJ99-BDW1-26	13.0	***1781***	1.211	2.022	3.86	1.198	2.068	4.35	1.204	2.046	8.21
KJ99-BDW1-27	14.0	***1760***	1.217	2.020	3.58	1.196	2.055	4.55	1.206	2.040	8.13
KJ99-BDW1-28	15.0	***1739***	1.213	2.030	3.74	1.217	2.034	2.20	1.215	2.032	5.94
KJ99-BDW1-29	16.0	***1716***	1.221	2.030	3.65	1.210	2.031	2.43	1.217	2.030	6.08
KJ99-BDW1-30	17.0	***1695***	1.229	2.025	3.72	1.200	2.044	9.68	1.208	2.039	13.40

Note: Ages in bold italics were determined by extrapolation of sedimentation rate and are considered unreliable.

APPENDIX D *Continued*

Sequential Digestion Results - *Cont'd*

Core and Sample	Mid-depth (cm)	Age (yrs A.D.)	Partial Digest $^{206}Pb/^{207}Pb$	Partial Digest $^{208}Pb/^{206}Pb$	Partial Digest Pb (ug/g)	HF-HNO_3 Digest $^{206}Pb/^{207}Pb$	HF-HNO_3 Digest $^{208}Pb/^{206}Pb$	HF-HNO_3 Digest Pb (ug/g)	Summed Totals $^{206}Pb/^{207}Pb$	Summed Totals $^{208}Pb/^{206}Pb$	Summed Totals Pb (ug/g)
KJ99-BDW1-31	18.0	***1671***	1.230	2.015	3.80	1.199	2.065	5.76	1.211	2.045	9.56
KJ99-BDW1-32	19.0	***1649***	1.212	2.039	3.82	1.196	2.054	3.39	1.204	2.046	7.21
KJ99-BDW1-33	20.0	***1624***	1.215	2.037	3.86	1.192	2.065	6.48	1.201	2.054	10.34
KJ99-BDW1-34	21.0	***1618***	1.214	2.030	3.90	1.201	2.045	5.60	1.206	2.039	9.50
KJ99-BDW1-35	22.0	***1598***	1.216	2.026	3.96	1.204	2.051	3.23	1.210	2.037	7.19
KJ99-BDW1-36	23.0	***1578***	1.211	2.040	4.20	1.185	2.048	6.54	1.195	2.045	10.74
KJ99-BDW1-39	26.0	***1520***	1.208	2.035	4.36	1.197	2.066	5.37	1.202	2.052	9.73
KJ99-BDW1-40	27.0	***1500***	1.213	2.022	4.39	1.196	2.070	4.08	1.205	2.045	8.47
KJ00-BDE5-02	0.75	1995	1.194	2.060	49.29	1.211	2.035	2.85	1.194	2.059	52.14
KJ00-BDE5-03	1.25	1987	1.173	2.095	45.77	1.189	2.075	3.09	1.174	2.094	48.86
KJ00-BDE5-04	1.75	1978	1.180	2.069	46.86	1.194	2.047	3.56	1.181	2.068	50.42
KJ00-BDE5-05	2.25	1968	1.172	2.086	47.47	1.195	2.040	3.54	1.173	2.084	51.01
KJ00-BDE5-06	2.75	1958	1.199	2.037	48.76						
KJ00-BDE5-07	3.25	1947	1.191	2.051	48.85	1.191	2.076	4.11	1.191	2.052	52.96
KJ00-BDE5-08	3.75	1936	1.185	2.062	43.20	1.192	2.054	3.70	1.185	2.062	46.91
KJ00-BDE5-10	4.75	1910	1.208	2.035	29.72						
KJ00-BDE5-12	5.75	1883	1.219	2.058	17.90	1.195	2.063	2.62	1.217	2.058	20.52
KJ00-BDE5-14	6.75	1856	1.198	2.069	9.78	1.189	2.074	2.56	1.197	2.070	12.34
KJ00-BDE5-16	7.75	***1830***	1.202	2.072	7.20	1.196	2.094	2.24	1.201	2.076	9.44
KJ00-BDE5-18	8.75	***1802***	1.197	2.067	6.60	1.233	2.030	2.15	1.203	2.061	8.76
KJ00-BDE5-20	9.75	***1774***	1.204	2.042	6.06	1.185	2.121	2.93	1.200	2.057	8.99
KJ00-BDE5-22	11.5	***1726***	1.194	2.099	6.50	1.180	2.050	2.09	1.191	2.091	8.59
KJ00-BDE5-24	13.5	***1671***	1.209	2.068	5.58	1.204	2.056	2.20	1.208	2.065	7.79
KJ00-BDE5-26	15.5	***1612***	1.186	2.087	5.63	1.205	2.058	2.12	1.190	2.081	7.74
KJ00-BDE5-28	17.5	***1552***	1.211	2.048	5.37	1.213	2.066	2.61	1.211	2.052	7.98
KJ00-BDE5-30	19.5	***1494***	1.202	2.059	5.55	1.193	2.081	2.38	1.200	2.063	7.93
KJ00-BDE5-32	23	***1409***	1.204	2.066	5.34	1.200	2.069	2.12	1.203	2.066	7.46
KJ00-BDE5-34	27	***1300***	1.205	2.050	4.94	1.202	2.067	2.07	1.204	2.054	7.02
KJ00-BDE5-36	31	***1191***	1.184	2.082	5.09	1.183	2.076	2.27	1.184	2.081	7.36

Note: Ages in bold italics were determined by extrapolation of sedimentation rate and are considered unreliable.

APPENDIX D *Continued*

Sequential Digestion Results - *Cont'd*

Core and Sample	Mid-depth (cm)	Age (yrs A.D.)	Partial Digest $^{206}Pb/^{207}Pb$	Partial Digest $^{208}Pb/^{206}Pb$	Partial Digest Pb (ug/g)	HF-HNO_3 Digest $^{206}Pb/^{207}Pb$	HF-HNO_3 Digest $^{208}Pb/^{206}Pb$	HF-HNO_3 Digest Pb (ug/g)	Summed Totals $^{206}Pb/^{207}Pb$	Summed Totals $^{208}Pb/^{206}Pb$	Summed Totals Pb (ug/g)
KJ00-BDE5-38	35	***1082***	1.193	2.063	4.82	1.191	2.080	2.44	1.192	2.067	7.26
KJ00-BDE5-40	39	***973***	1.211	2.053	4.88	1.197	2.074	2.58	1.208	2.058	7.46
KJ00-BDE5-42	43	***864***	1.186	2.080	4.96	1.192	2.081	2.77	1.187	2.081	7.73
KJ99-BDE3-01	0.25	1998	1.196	2.094	43.77	1.170	2.082	4.17	1.195	2.093	47.94
KJ99-BDE3-02	0.75	1996	1.186	2.072	44.60	1.197	2.047	4.27	1.187	2.071	48.87
KJ99-BDE3-03	1.25	1989	1.189	2.063	43.19	1.204	2.036	3.78	1.190	2.062	46.98
KJ99-BDE3-04	1.75	1982	1.183	2.092	40.04	1.207	2.041	4.65	1.205	2.097	44.69
KJ99-BDE3-05	2.25	1974	1.181	2.093	32.44	1.202	2.023	4.26	1.203	2.096	36.69
KJ99-BDE3-06	2.75	1965	1.187	2.087	21.88	1.204	2.039	3.57	1.208	2.091	25.44
KJ99-BDE3-07	3.25	1956	1.188	2.086	16.94	1.200	2.059	3.12	1.208	2.092	20.06
KJ99-BDE3-08	3.75	1947	1.191	2.078	12.02	1.197	2.068	2.86	1.210	2.086	14.87
KJ99-BDE3-09	4.25	1937	1.192	2.068	10.94	1.209	2.040	2.68	1.213	2.072	13.62
KJ99-BDE3-10	4.75	1926	1.196	2.062	8.06	1.206	2.031	2.55	1.215	2.064	10.61
KJ99-BDE3-11	5.25	1915	1.197	2.060	7.67	1.189	2.065	2.42	1.212	2.070	10.09
KJ99-BDE3-12	5.75	1904	1.190	2.067	7.35	1.199	2.043	2.55	1.209	2.070	9.90
KJ99-BDE3-13	6.25	1893	1.197	2.053	6.38	1.179	2.087	2.22	1.209	2.070	8.59
KJ99-BDE3-14	6.75	1882	1.199	2.048	5.90	1.187	2.083	2.31	1.211	2.066	8.21
KJ99-BDE3-15	7.25	1871	1.195	2.052	5.69	1.157	2.095	2.25	1.200	2.072	7.93
KJ99-BDE3-16	7.75	1860	1.195	2.036	5.29	1.167	2.057	2.29	1.202	2.051	7.58
KJ99-BDE3-17	8.25	1849	1.192	2.055	5.19	1.202	2.048	2.12	1.210	2.061	7.31
KJ99-BDE3-18	8.75	***1838***	1.199	2.045	5.33	1.197	2.037	2.35	1.214	2.051	7.68
KJ99-BDE3-19	9.25	***1826***	1.193	2.061	4.90	1.183	2.061	2.23	1.205	2.069	7.13
KJ99-BDE3-20	9.75	***1814***	1.190	2.066	5.39	1.216	2.046	2.11	1.197	2.061	7.49
KJ99-BDE3-21	10.5	***1797***	1.193	2.064	5.57	1.196	2.052	2.11	1.194	2.061	7.68
KJ99-BDE3-22	11.5	***1775***	1.189	2.071	5.33	1.191	2.046	2.09	1.189	2.064	7.42
KJ99-BDE3-23	12.5	***1752***	1.194	2.066	5.71	1.193	2.037	2.35	1.193	2.058	8.06
KJ99-BDE3-24	13.5	***1730***	1.194	2.063	5.28	1.183	2.037	2.15	1.191	2.056	7.44
KJ99-BDE3-25	14.5	***1706***	1.192	2.052	5.23	1.188	2.067	2.16	1.191	2.056	7.39
KJ99-BDE3-26	15.5	***1681***	1.196	2.058	5.17	1.204	2.049	2.25	1.198	2.056	7.42

Note: Ages in bold italics were determined by extrapolation of sedimentation rate and are considered unreliable.

APPENDIX D *Continued*

Sequential Digestion Results - *Cont'd*

Core and Sample	Mid-depth (cm)	Age (yrs A.D.)	Partial Digest $^{206}Pb/^{207}Pb$	Partial Digest $^{208}Pb/^{206}Pb$	Partial Digest Pb (ug/g)	HF-HNO_3 Digest $^{206}Pb/^{207}Pb$	HF-HNO_3 Digest $^{208}Pb/^{206}Pb$	HF-HNO_3 Digest Pb (ug/g)	Summed Totals $^{206}Pb/^{207}Pb$	Summed Totals $^{208}Pb/^{206}Pb$	Summed Totals Pb (ug/g)
KJ99-BDE3-27	16.5	***1657***	1.195	2.053	5.35	1.196	2.050	2.26	1.195	2.052	7.61
KJ99-BDE3-28	17.5	***1632***	1.195	2.061	5.49	1.194	2.047	2.43	1.194	2.057	7.92
KJ99-BDE3-29	18.5	***1608***	1.196	2.059	5.55	1.218	2.043	2.75	1.203	2.054	8.29
KJ99-BDE3-30	19.5	***1584***	1.187	2.057	5.41	1.201	2.048	2.70	1.192	2.054	8.11
KJ99-BDE3-31	21	***1559***	1.189	2.053	5.72	1.177	2.081	2.66	1.185	2.062	8.38
KJ99-BDE3-33	25	***1470***	1.202	2.050	5.89	1.190	2.054	2.74	1.198	2.052	8.63
KJ99-BDE3-34	27	***1425***	1.204	2.055	6.13	1.184	2.080	3.10	1.197	2.063	9.22
KJ99-BDE3-35	29	***1380***	1.181	2.067	5.74	1.193	2.041	2.87	1.185	2.059	8.60
KJ99-BDE3-36	31	***1336***	1.196	2.042	5.65	1.188	2.040	2.80	1.193	2.041	8.45
LC-BDW-96-98	97		1.228	2.023	3.27	1.200	2.073	3.25	1.214	2.048	6.52
LC-BDW-108-110	109		1.221	2.037	4.97	1.187	2.080	6.80	1.201	2.062	11.76
LC-BDW-165-167	166		1.212	2.052	9.29	1.197	2.067	11.30	1.204	2.060	20.59
LC-BDW-233-234	233.5		1.220	2.044	11.14	1.192	2.081	10.82	1.206	2.062	21.95
LC-BDW-243-244	243.5		1.216	2.047	11.73	1.198	2.064	12.27	1.207	2.056	24.00
LC-BDW-350-351	350.5		1.214	2.051	11.87	1.200	2.064	12.96	1.207	2.058	24.83
LC-BDE-110-120	115		1.211	2.062	6.63	1.198	2.078	8.48	1.203	2.071	15.11
LC-BDE-135-150	142.5		1.196	2.084	7.75	1.192	2.074	9.45	1.194	2.078	17.20
LC-BDE-175-185	180		1.202	2.067	9.55	1.200	2.063	9.12	1.201	2.065	18.67
LC-BDE-196-199	197.5		1.200	2.068	11.97	1.197	2.070	11.86	1.198	2.069	23.83
LC-BDE-203-206	204.5		1.198	2.059	12.12	1.196	2.080	12.49	1.197	2.070	24.61
LC-BDE-266-271	268.5		1.204	2.057	9.94	1.203	2.048	11.99	1.203	2.052	21.93

Note: Ages in bold italics were determined by extrapolation of sedimentation rate and are considered unreliable.

APPENDIX D *Continued*

Total Digestion Results

Core and Sample	Mid-depth (cm)	Age (yrs A.D.)	$^{206}Pb/^{207}Pb$	$^{208}Pb/^{206}Pb$	Total Pb (ug/g)	Estimated Labile Pb (ug/g)
KJ00-BDW6-02	0.75	1997	1.198	2.156	21.55	18.29
KJ00-BDW6-03	1.25	1994	1.195	2.189	21.40	18.14
KJ00-BDW6-04	1.75	1989	1.201	2.202	22.63	19.37
KJ00-BDW6-05	2.25	1984	1.198	2.220	24.05	20.79
KJ00-BDW6-06	2.75	1979	1.199	2.223	23.74	20.48
KJ00-BDW6-07	3.25	1974	1.197	2.198	21.11	17.85
KJ00-BDW6-08	3.75	1968	1.197	2.170	15.48	12.22
KJ00-BDW6-10	4.75	1957	1.204	2.134	13.27	10.01
KJ00-BDW6-12	5.75	1945	1.203	2.057	10.36	7.10
KJ00-BDW6-14	6.75	1933	1.204	2.060	8.02	4.76
KJ00-BDW6-16	7.75	1921	1.204	2.061	7.88	4.62
KJ00-BDW6-18	8.75	1906	1.210	2.055	8.02	4.76
KJ00-BDW6-20	9.75	1893	1.212	2.046	7.98	4.72
KJ00-BDW6-24	13.5	***1834***	1.203	2.059	7.48	4.22
KJ00-BDW6-32	23	***1709***	1.212	2.053	6.87	3.61
KJ00-BDW6-40	39	***1493***	1.214	2.050	5.21	1.95
KJ00-BDE6-02	0.75	1997	1.187	2.075	42.02	39.64
KJ00-BDE6-03	1.25	1990	1.186	2.073	41.74	39.36
KJ00-BDE6-04	1.75	1984	1.187	2.073	42.13	39.75
KJ00-BDE6-05	2.25	1977	1.189	2.066	43.63	41.25
KJ00-BDE6-07	2.75	1970	1.190	2.074	42.68	40.30
KJ00-BDE6-08	3.25	1962	1.189	2.061	40.42	38.04
KJ00-BDE6-10	4.25	1945	1.186	2.070	29.36	26.98
KJ00-BDE6-12	5.25	1926	1.192	2.069	12.62	10.24
KJ00-BDE6-14	6.25	1907	1.196	2.073	7.72	5.34
KJ00-BDE6-16	7.25	1888	1.197	2.070	6.98	4.60
KJ00-BDE6-18	8.25	1869	1.192	2.084	7.13	4.75
KJ00-BDE6-20	9.25	1849	1.191	2.092	7.69	5.31
KJ00-BDE6-24	13	***1775***	1.190	2.086	7.36	4.98
KJ00-BDE6-32	22.5	***1588***	1.194	2.076	6.68	4.30
KJ00-BDE6-40	38.5	***1276***	1.192	2.081	7.20	4.82
KJ00-BDE6-50	58.5	***887***	1.197	2.073	7.44	5.06

Note: Ages in bold italics were determined by extrapolation of sedimentation rate and are considered unreliable.

APPENDIX E: Sediment Mercury Data

BIG DAM WEST LAKE				BIG DAM EAST LAKE			
Core and Sample	Mid-Depth (cm)	Age (yrs A.D.)	Hg (ng/g)	Core and Sample	Mid-Depth (cm)	Age (yrs A.D.)	Hg (ng/g)
KJ00-BDW6-01	0.25	1998	178.0	KJ00-BDE6-02	0.75	1997	111.6
KJ00-BDW6-02	0.75	1997	171.2	KJ00-BDE6-03	1.25	1990	120.5
KJ00-BDW6-03	1.25	1994	168.1	KJ00-BDE6-04	1.75	1984	113.2
KJ00-BDW6-05	2.25	1984	158.5	KJ00-BDE6-05	2.25	1977	109.2
KJ00-BDW6-06	2.75	1979	149.4	KJ00-BDE6-07	2.75	1970	110.7
KJ00-BDW6-07	3.25	1974	134.5	KJ00-BDE6-08	3.25	1962	104.0
KJ00-BDW6-08	3.75	1968	108.2	KJ00-BDE6-09	3.75	1954	95.3
KJ00-BDW6-09	4.25	1963	90.8	KJ00-BDE6-10	4.25	1945	85.6
KJ00-BDW6-10	4.75	1957	78.7	KJ00-BDE6-11	4.75	1936	67.2
KJ00-BDW6-11	5.25	1951	76.8	KJ00-BDE6-12	5.25	1926	65.1
KJ00-BDW6-12	5.75	1945	77.0	KJ00-BDE6-13	5.75	1917	49.0
KJ00-BDW6-13	6.25	1939	68.2	KJ00-BDE6-14	6.25	1907	56.0
KJ00-BDW6-14	6.75	1933	67.3	KJ00-BDE6-15	6.75	1897	46.0
KJ00-BDW6-15	7.25	1927	64.9	KJ00-BDE6-16	7.25	1888	51.8
KJ00-BDW6-16	7.75	1921	63.8	KJ00-BDE6-17	7.75	1878	47.9
KJ00-BDW6-17	8.25	1914	64.8	KJ00-BDE6-18	8.25	1869	55.0
KJ00-BDW6-18	8.75	1906	67.4	KJ00-BDE6-19	8.75	1859	53.8
KJ00-BDW6-19	9.25	1899	69.9	KJ00-BDE6-20	9.25	1849	59.6
KJ00-BDW6-20	9.75	1893	74.6	KJ00-BDE6-21	10	***1833***	48.8
KJ00-BDW6-22	11.5	1863	74.0	KJ00-BDE6-22	11	***1814***	48.7
KJ00-BDW6-24	13.5	***1834***	64.7	KJ00-BDE6-23	12	***1794***	45.3
KJ00-BDW6-26	15.5	***1804***	66.3	KJ00-BDE6-24	13	***1775***	46.9
KJ00-BDW6-28	17.5	***1773***	63.0	KJ00-BDE6-25	14	***1755***	44.9
KJ00-BDW6-30	19.5	***1741***	63.3	KJ00-BDE6-26	15	***1734***	47.0
KJ00-BDW6-32	23	***1709***	65.8	KJ00-BDE6-27	16	***1712***	42.2
KJ00-BDW6-34	27	***1655***	85.0	KJ00-BDE6-28	17	***1691***	44.6
KJ00-BDW6-36	31	***1601***	65.9	KJ00-BDE6-30	19	***1649***	41.0
KJ00-BDW6-38	35	***1547***	65.7	KJ00-BDE6-32	22.5	***1588***	38.9
KJ00-BDW6-40	39	***1493***	61.9	KJ00-BDE6-36	30.5	***1432***	35.9
KJ00-BDW6-42	43	***1439***	58.8	KJ00-BDE6-38	34.5	***1354***	38.6
				KJ00-BDE6-40	38.5	***1276***	35.9
				KJ00-BDE6-42	42.5	***1198***	36.5
				KJ00-BDE6-44	46.5	***1121***	30.2
				KJ00-BDE6-46	50.5	***1043***	31.2
				KJ00-BDE6-48	54.5	***965***	24.8
				KJ00-BDE6-50	58.5	***887***	26.9
				KJ00-BDE6-52	65.5	***751***	25.1
				KJ00-BDE6-54	73.5	***595***	28.6

Note: Ages in bold italics were determined by extrapolation of sedimentation rate and are considered unreliable.

APPENDIX F: Whole Lake Sediment Accumulation Calculation

BIG DAM WEST LAKE

Original Sediment Accumulation Data*						Sediment Accumulation Recalculation			
Original Class (m)	Class Thickness (m)	Class Area (m^2)	Class Volume (m^3)	Class DBD long cores (Mg/m^3)	Mass of dry sediment in class (Mg)	Class Depth Interval (cm)	Class DBD (Mg/m^3)	Class Volume (m^3)	Mass of seds in depth interval (Mg)
0.00 - 0.05	0.05	1189256	59462.8	0.0398	2369.5	0-0.5	0.029	5946.3	173
						0.5-1.0	0.102	5946.3	605
						1.0-1.5	0.126	5946.3	747
						1.5-2.0	0.142	5946.3	842
						2.0-2.5	0.165	5946.3	984
						2.5-3.0	0.168	5946.3	998
						3.0-3.5	0.169	5946.3	1006
						3.5-4.0	0.177	5946.3	1054
						4.0-4.5	0.193	5946.3	1146
						4.5-5.0	0.188	5946.3	1118
0.05 - 0.10	0.05	1174052	58702.6	0.0772	4534.0	5-6	0.184	11740.5	2163
						6-7	0.180	11740.5	2110
						7-8	0.212	11740.5	2486
						8-9	0.206	11740.5	2414
						9-10	0.200	11740.5	2346
0.10 - 0.15	0.05	1115603	55780.2	0.0813	4535.8	10-11	0.204	11156.0	2271
						11-12	0.207	11156.0	2312
						12-13	0.211	11156.0	2354
						13-14	0.215	11156.0	2395
						14-15	0.218	11156.0	2437
0.15 - 0.20	0.05	1072745	53637.3	0.1206	6471.0	15-16	0.222	10727.5	2383
						16-17	0.226	10727.5	2423
						17-18	0.230	10727.5	2463
						18-19	0.233	10727.5	2502
						19-20	0.237	10727.5	2542
0.20 - 0.25	0.05	1033701	51685.1	0.1794	9271.7	20-21	0.241	10337.0	2488
						21-22	0.244	10337.0	2527
						22-23	0.248	10337.0	2565
						23-24	0.252	10337.0	2603
						24-25	0.256	10337.0	2642
0.25 - 0.30	0.05	995748	49787.4	0.1873	9324.8	25-26	0.259	9957.5	2582
						26-27	0.263	9957.5	2619
						27-28	0.267	9957.5	2656
						28-29	0.270	9957.5	2693
						29-30	0.274	9957.5	2730
0.30 - 0.35	0.05	961175	48058.8	0.2741	13175.0	30-31	***0.2741***	9611.8	2635
						31-32	***0.2741***	9611.8	2635
						32-33	***0.2741***	9611.8	2635
						33-34	***0.2741***	9611.8	2635
						34-35	***0.2741***	9611.8	2635
0.35 - 0.40	0.05	928003	46400.2	0.3005	13944.6	35-40	***0.3005***	***46400.2***	***13945***
0.40 - 0.45	0.05	896489	44824.5	0.3601	16142.0	40-45	***0.3601***	***44824.5***	***16142***
0.45 - 0.50	0.05	865959	43298.0	0.3530	15283.6	45-50	***0.3530***	***43298.0***	***15284***
0.50 - 0.55	0.05	835452	41772.6	0.2270	9481.3	50-55	***0.2270***	***41772.6***	***9481***
0.55 - 0.60	0.05	803591	40179.6	0.2941	11816.2	55-60	***0.2941***	***40179.6***	***11816***
0.60 - 0.65	0.05	770425	38521.2	0.2061	7940.3	60-65	***0.2061***	***38521.2***	***7940***
0.65 - 0.70	0.05	737175	36858.8	0.2174	8012.0	65-70	***0.2174***	***36858.8***	***8012***
0.70 - 0.75	0.05	700242	35012.1	0.2353	8236.7	70-75	***0.2353***	***35012.1***	***8237***
0.75 - 0.80	0.05	660068	33003.4	0.1637	5402.0	75-80	***0.1637***	***33003.4***	***5402***
0.80 - 0.85	0.05	615465	30773.3	0.1602	4930.0	80-85	***0.1602***	***30773.3***	***4930***
0.85 - 0.90	0.05	582811	29140.6	0.2319	6757.4	85-90	***0.2319***	***29140.6***	***6757***
0.90 - 0.95	0.05	562404	28120.2	0.2191	6160.0	90-95	***0.2191***	***28120.2***	***6160***
0.95 - 1.00	0.05	541695	27084.8	0.2710	7340.6	95-100	***0.2710***	***27084.8***	***7341***
1.00 - 1.05	0.05	521348	26067.4	0.3109	8105.2	100-105	***0.3109***	***26067.4***	***8105***
1.05 - 1.10	0.05	502731	25136.6	0.3773	9483.3	105-110	***0.3773***	***25136.6***	***9483***
1.10 - 1.15	0.05	484689	24234.5	0.3637	8813.3	110-115	***0.3637***	***24234.5***	***8813***
1.15 - 1.20	0.05	466739	23337.0	0.5288	12341.1	115-120	***0.5288***	***23337.0***	***12341***

APPENDIX F *Continued*

BIG DAM WEST LAKE - *Cont'd*

Original Sediment Accumulation Data*						Sediment Accumulation Recalculation			
Original Class (m)	Class Thickness (m)	Class Area (m^2)	Class Volume (m^3)	Class DBD long cores (Mg/m^3)	Mass of dry sediment in class (Mg)	Class Depth Interval (cm)	Class DBD (Mg/m^3)	Class Volume (m^3)	Mass of seds in depth interval (Mg)
1.20 - 1.25	0.05	448819	22441.0	0.4944	11095.8	120-125	***0.4944***	***22441.0***	***11096***
1.25 - 1.30	0.05	430565	21528.3	0.6572	14148.9	125-130	***0.6572***	***21528.3***	***14149***
1.30 - 1.35	0.05	411946	20597.3	0.7156	14738.9	130-135	***0.7156***	***20597.3***	***14739***
1.35 - 1.40	0.05	391067	19553.4	0.3124	6108.6	135-140	***0.3124***	***19553.4***	***6109***
1.40 - 1.45	0.05	370820	18541.0	0.4487	8319.9	140-145	***0.4487***	***18541.0***	***8320***
1.45 - 1.50	0.05	350978	17548.9	0.4326	7591.5	145-150	***0.4326***	***17548.9***	***7592***
1.50 - 1.55	0.05	332635	16631.8	0.4165	6927.1	150-155	***0.4165***	***16631.8***	***6927***
1.55 - 1.60	0.05	316233	15811.7	0.4805	7597.6	155-160	***0.4805***	***15811.7***	***7598***
1.60 - 1.65	0.05	299673	14983.7	0.3315	4966.8	160-165	***0.3315***	***14983.7***	***4967***
1.65 - 1.70	0.05	283898	14194.9	0.4240	6018.6	165-170	***0.4240***	***14194.9***	***6019***
1.70 - 1.75	0.05	270066	13503.3	0.4116	5558.5	170-175	***0.4116***	***13503.3***	***5558***
1.75 - 1.80	0.05	257116	12855.8	0.3487	4483.4	175-180	***0.3487***	***12855.8***	***4483***
1.80 - 1.85	0.05	244954	12247.7	0.3645	4464.0	180-185	***0.3645***	***12247.7***	***4464***
1.85 - 1.90	0.05	233162	11658.1	0.3073	3583.0	185-190	***0.3073***	***11658.1***	***3583***
1.90 - 1.95	0.05	222091	11104.6	0.3349	3718.9	190-195	***0.3349***	***11104.6***	***3719***
1.95 - 2.00	0.05	211394	10569.7	0.5517	5831.3	195-200	***0.5517***	***10569.7***	***5831***
2.00 - 2.05	0.05	200892	10044.6	0.5741	5766.9	200-205	***0.5741***	***10044.6***	***5767***
2.05 - 2.10	0.05	190506	9525.3	0.6093	5803.9	205-210	***0.6093***	***9525.3***	***5804***
2.10 - 2.15	0.05	180129	9006.5	0.3372	3036.9	210-215	***0.3372***	***9006.5***	***3037***
2.15 - 2.20	0.05	169711	8485.6	0.3857	3272.6	215-220	***0.3857***	***8485.6***	***3273***
2.20 - 2.25	0.05	159144	7957.2	0.3347	2663.4	220-225	***0.3347***	***7957.2***	***2663***
2.25 - 2.30	0.05	148514	7425.7	0.3201	2377.2	225-230	***0.3201***	***7425.7***	***2377***
2.30 - 2.35	0.05	137583	6879.2	0.3251	2236.6	230-235	***0.3251***	***6879.2***	***2237***
2.35 - 2.40	0.05	127261	6363.1	0.33	2099.8	235-240	***0.33***	***6363.1***	***2100***
2.40 - 2.45	0.05	118716	5935.8	0.33	1958.8	240-245	***0.33***	***5935.8***	***1959***
2.45 - 2.50	0.05	112419	5621.0	0.33	1854.9	245-250	***0.33***	***5621.0***	***1855***
2.50 - 2.55	0.05	106628	5331.4	0.33	1759.4	250-255	***0.33***	***5331.4***	***1759***
2.55 - 2.60	0.05	101163	5058.2	0.33	1669.2	255-260	***0.33***	***5058.2***	***1669***
2.60 - 2.65	0.05	95985	4799.3	0.33	1583.8	260-265	***0.33***	***4799.3***	***1584***
2.65 - 2.70	0.05	91043	4552.2	0.33	1502.2	265-270	***0.33***	***4552.2***	***1502***
2.70 - 2.75	0.05	86262	4313.1	0.33	1423.3	270-275	***0.33***	***4313.1***	***1423***
2.75 - 2.80	0.05	81606	4080.3	0.33	1346.5	275-280	***0.33***	***4080.3***	***1346***
2.80 - 2.85	0.05	77112	3855.6	0.33	1272.3	280-285	***0.33***	***3855.6***	***1272***
2.85 - 2.90	0.05	72785	3639.3	0.33	1201.0	285-290	***0.33***	***3639.3***	***1201***
2.90 - 2.95	0.05	68594	3429.7	0.33	1131.8	290-295	***0.33***	***3429.7***	***1132***
2.95 - 3.00	0.05	64355	3217.8	0.33	1061.9	295-300	***0.33***	***3217.8***	***1062***
3.00 - 3.05	0.05	59820	2991.0	0.33	987.0	300-305	***0.33***	***2991.0***	***987***
3.05 - 3.10	0.05	55291	2764.6	0.33	912.3	305-310	***0.33***	***2764.6***	***912***
3.10 - 3.15	0.05	50719	2536.0	0.33	836.9	310-315	***0.33***	***2536.0***	***837***
3.15 - 3.20	0.05	45919	2296.0	0.33	757.7	315-320	***0.33***	***2296.0***	***758***
3.20 - 3.25	0.05	40819	2041.0	0.33	673.5	320-325	***0.33***	***2041.0***	***674***
3.25 - 3.30	0.05	36362	1818.1	0.33	600.0	325-330	***0.33***	***1818.1***	***600***
3.30 - 3.35	0.05	32339	1617.0	0.33	533.6	330-335	***0.33***	***1617.0***	***534***
3.35 - 3.40	0.05	28611	1430.6	0.33	472.1	335-340	***0.33***	***1430.6***	***472***
3.40 - 3.45	0.05	25994	1299.7	0.33	428.9	340-345	***0.33***	***1299.7***	***429***
3.45 - 3.50	0.05	23473	1173.7	0.33	387.3	345-350	***0.33***	***1173.7***	***387***
3.50 - 3.55	0.05	21037	1051.9	0.33	347.1	350-355	***0.33***	***1051.9***	***347***
3.55 - 3.60	0.05	18669	933.5	0.33	308.0	355-360	***0.33***	***933.5***	***308***
3.60 - 3.65	0.05	16709	835.5	0.33	275.7	360-365	***0.33***	***835.5***	***276***
3.65 - 3.70	0.05	14860	743.0	0.33	245.2	365-370	***0.33***	***743.0***	***245***
3.70 - 3.75	0.05	13080	654.0	0.33	215.8	370-375	***0.33***	***654.0***	***216***
3.75 - 3.80	0.05	11370	568.5	0.33	187.6	375-380	***0.33***	***568.5***	***188***
3.80 - 3.85	0.05	9732	486.6	0.33	160.6	380-385	***0.33***	***486.6***	***161***
3.85 - 3.90	0.05	8165	408.3	0.33	134.7	385-390	***0.33***	***408.3***	***135***
3.90 - 3.95	0.05	6685	334.3	0.33	110.3	390-395	***0.33***	***334.3***	***110***
3.95 +	0.05	5296	264.8	0.33	87.4	395+	***0.33***	***264.8***	***87***
			Total mass of sediments in BDW - only long core DBD (Mg)		**3.79E+05**		**Total mass of sediments in BDW - short and long core DBD (Mg)**		**4.13E+05**

Note: Values in bold italics in Sediment Accumulation Recalculation columns are as they appeared in Ferguson (2000)

* Original sediment accumulation data from Ferguson (2000)

APPENDIX F *Continued*

BIG DAM EAST LAKE

Original Sediment Accumulation Data*						Sediment Accumulation Recalculation			
Original Class (m)	Class Thickness (m)	Class Area (m^2)	Class Volume (m^3)	Class DBD long cores (Mg/m^3)	Mass of dry sediment in class (Mg)	Class Depth Interval (cm)	Class DBD (Mg/m^3)	Class Volume (m^3)	Mass of seds in depth interval (Mg)
0.00 - 0.05	0.05	529425	26471.3	0.05	1323.6	0-0.5	0.049	***2647.1***	130
						0.5-1.0	0.113	***2647.1***	299
						1.0-1.5	0.130	***2647.1***	344
						1.5-2.0	0.140	***2647.1***	370
						2.0-2.5	0.148	***2647.1***	392
						2.5-3.0	0.157	***2647.1***	415
						3.0-3.5	0.171	***2647.1***	452
						3.5-4.0	0.177	***2647.1***	469
						4.0-4.5	0.190	***2647.1***	503
						4.5-5.0	0.190	***2647.1***	503
0.05 - 0.10	0.05	468314	23415.7	0.06	1404.9	5.0-5.5	0.199	***2341.6***	466
						5.5-6.0	0.194	***2341.6***	454
						6.0-6.5	0.201	***2341.6***	472
						6.5-7.0	0.198	***2341.6***	464
						7.0-7.5	0.196	***2341.6***	460
						7.5-8.0	0.197	***2341.6***	461
						8.0-8.5	0.207	***2341.6***	484
						8.5-9.0	0.210	***2341.6***	492
						9.0-9.5	0.201	***2341.6***	471
						9.5-10	0.205	***2341.6***	479
0.10 - 0.15	0.05	438837	21941.9	0.06	1316.5	10-11	0.216	***4388.4***	950
						11-12	0.194	***4388.4***	852
						12-13	0.199	***4388.4***	873
						13-14	0.202	***4388.4***	885
						14-15	0.204	***4388.4***	895
0.15 - 0.20	0.05	415971	20798.6	0.07	1455.9	15-16	0.209	***4159.7***	869
						16-17	0.211	***4159.7***	876
						17-18	0.206	***4159.7***	858
						18-19	0.208	***4159.7***	865
						19-20	0.208	***4159.7***	865
0.20 - 0.25	0.05	396626	19831.3	0.08	1586.5	20-21	0.214	***3966.3***	850
						21-22	0.214	***3966.3***	850
						22-23	0.216	***3966.3***	855
						23-24	0.216	***3966.3***	855
						24-25	0.230	***3966.3***	913
0.25 - 0.30	0.05	378040	18902.0	0.0961	1816.5	25-26	0.230	***3780.4***	870
						26-27	0.225	***3780.4***	849
						27-28	0.225	***3780.4***	849
						28-29	0.224	***3780.4***	847
						29-30	0.224	***3780.4***	847
0.30 - 0.35	0.05	360681	18034.1	0.0946	1705.4	30-35	0.238	***18034.1***	4295
0.35 - 0.40	0.05	345413	17270.7	0.0940	1623.6	35-40	0.247	***17270.7***	4274
0.40 - 0.45	0.05	331067	16553.4	0.1429	2364.8	40-45	0.252	***16553.4***	4165
0.45 - 0.50	0.05	317804	15890.2	0.1217	1933.8	45-50	0.256	***15890.2***	4065
0.50 - 0.55	0.05	305147	15257.4	0.1280	1953.2	50-55	0.260	***15257.4***	3966
0.55 - 0.60	0.05	292807	14640.4	0.1154	1689.4	55-60	0.264	***14640.4***	3867
0.60 - 0.65	0.05	280222	14011.1	0.0501	702.6	60-65	0.268	***14011.1***	3759
0.65 - 0.70	0.05	267989	13399.5	0.0510	683.4	65-70	0.272	***13399.5***	3651
0.70 - 0.75	0.05	255636	12781.8	0.0529	676.0	70-75	0.277	***12781.8***	3535
0.75 - 0.80	0.05	242670	12133.5	0.0519	629.4	75-80	0.281	***12133.5***	3407
0.80 - 0.85	0.05	227667	11383.4	0.0883	1005.3	80-85	0.285	***11383.4***	3243
0.85 - 0.90	0.05	210564	10528.2	0.0889	936.1	85-90	0.289	***10528.2***	3044
0.90 - 0.95	0.05	195161	9758.1	0.1498	1461.5	90-95	0.293	***9758.1***	2862
0.95 - 1.00	0.05	181803	9090.2	0.2344	2130.8	95-100	0.297	***9090.2***	2704
1.00 - 1.05	0.05	168830	8441.5	0.2974	2510.7	100-105	***0.2974***	***8441.5***	***2511***
1.05 - 1.10	0.05	155624	7781.2	0.3499	2722.6	105-110	***0.3499***	***7781.2***	***2723***
1.10 - 1.15	0.05	143631	7181.6	0.4175	2998.6	110-115	***0.4175***	***7181.6***	***2999***
1.15 - 1.20	0.05	131731	6586.6	0.4652	3064.1	115-120	***0.4652***	***6586.6***	***3064***

APPENDIX F *Continued*

BIG DAM EAST LAKE - *Cont'd*

Original Sediment Accumulation Data*						Sediment Accumulation Recalculation			
Original Class (m)	Class Thickness (m)	Class Area (m^2)	Class Volume (m^3)	Class DBD long cores (Mg/m^3)	Mass of dry sediment in class (Mg)	Class Depth Interval (cm)	Class DBD (Mg/m^3)	Class Volume (m^3)	Mass of seds in depth interval (Mg)
1.20 - 1.25	0.05	120536	6026.8	0.4740	2856.9	120-125	***0.4740***	***6026.8***	***2857***
1.25 - 1.30	0.05	109861	5493.1	0.5169	2839.4	125-130	***0.5169***	***5493.1***	***2839***
1.30 - 1.35	0.05	100911	5045.6	0.4821	2432.3	130-135	***0.4821***	***5045.6***	***2432***
1.35 - 1.40	0.05	91932	4596.6	0.5009	2302.4	135-140	***0.5009***	***4596.6***	***2302***
1.40 - 1.45	0.05	81629	4081.5	0.4666	1904.4	140-145	***0.4666***	***4081.5***	***1904***
1.45 - 1.50	0.05	71807	3590.4	0.4486	1610.7	145-150	***0.4486***	***3590.4***	***1611***
1.50 - 1.55	0.05	64105	3205.3	0.4460	1429.5	150-155	***0.4460***	***3205.3***	***1429***
1.55 - 1.60	0.05	56880	2844.0	0.4910	1396.5	155-160	***0.4910***	***2844.0***	***1397***
1.60 - 1.65	0.05	50461	2523.1	0.4817	1215.3	160-165	***0.4817***	***2523.1***	***1215***
1.65 - 1.70	0.05	44357	2217.9	0.3609	800.4	165-170	***0.3609***	***2217.9***	***800***
1.70 - 1.75	0.05	38671	1933.6	0.3160	611.0	170-175	***0.3160***	***1933.6***	***611***
1.75 - 1.80	0.05	33015	1650.8	0.3467	572.4	175-180	***0.3467***	***1650.8***	***572***
1.80 - 1.85	0.05	27546	1377.3	0.4471	615.8	180-185	***0.4471***	***1377.3***	***616***
1.85 - 1.90	0.05	22381	1119.1	0.4242	474.7	185-190	***0.4242***	***1119.1***	***475***
1.90 - 1.95	0.05	18374	918.7	0.4242	116.7	190-195	***0.4242***	***918.7***	***390***
1.95 - 2.00	0.05	15044	752.2	0.4791	360.4	195-200	***0.4791***	***752.2***	***360***
2.00 - 2.05	0.05	12219	611.0	0.48	293.3	200-205	***0.48***	***611.0***	***293***
2.05 - 2.10	0.05	10400	520.0	0.48	249.6	205-210	***0.48***	***520.0***	***250***
2.10 - 2.15	0.05	9084	454.2	0.48	218.0	210-215	***0.48***	***454.2***	***218***
2.15 - 2.20	0.05	7881	394.1	0.48	189.1	215-220	***0.48***	***394.1***	***189***
2.20 - 2.25	0.05	6854	342.7	0.48	164.5	220-225	***0.48***	***342.7***	***164***
2.25 - 2.30	0.05	5779	289.0	0.48	138.7	225-230	***0.48***	***289.0***	***139***
2.30 - 2.35	0.05	4557	227.9	0.48	109.4	230-235	***0.48***	***227.9***	***109***
2.35 - 2.40	0.05	3498	174.9	0.48	84.0	235-240	***0.48***	***174.9***	***84***
2.40 - 2.45	0.05	2439	122.0	0.48	58.5	240-245	***0.48***	***122.0***	***59***
		Total mass of sediments in BDW - only long core DBD (Mg)			**6.27E+04**	**Total mass of sediments in BDW - short and long core DBD (Mg)**			**1.11E+05**

Note: Values in bold italics in Sediment Accumulation Recalculation columns are as they appeared in Ferguson (2000)

* Original sediment accumulation data from Ferguson (2000)

APPENDIX G: Big Dam West Lake Pb and Hg Accumulation Calculation

Sediment Accumulation Data			Pb Accumulation Calculations				Hg Accumulation Calculations			
Class Depth Interval (cm)	Class Area (m^2)	Mass of seds in depth interval (Mg)	Sample used for Pb data	Sample Depth Interval (cm)	[Pb] in sample (ug/g)	Pb in class (kg)	Sample used for Hg data	Sample Depth Interval (cm)	[Hg] in sample (ng/g)	Hg in class (g)
0-0.5	***1189256***	173.3	KJ00-BDW5-01	0-0.5	22.97	4.0	KJ00-BDW6-01	0-0.5	178.04	30.8
0.5-1.0	***1189256***	604.8	KJ00-BDW5-02	0.5-1.0	23.47	14.2	KJ00-BDW6-02	0.5-1.0	171.23	103.6
1.0-1.5	***1189256***	747.1	KJ00-BDW5-03	1.0-1.5	22.89	17.1	KJ00-BDW6-03	1.0-1.5	168.12	125.6
1.5-2.0	***1189256***	842.3	KJ00-BDW5-04	1.5-2.0	22.86	19.3	KJ00-BDW6-03 and -05	1.0-2.5	163.31	137.6
2.0-2.5	***1189256***	984.0	KJ00-BDW5-05	2.0-2.5	24.59	24.2	KJ00-BDW6-05	2.0-2.5	158.51	156.0
2.5-3.0	***1189256***	998.4	KJ00-BDW5-06	2.5-3.0	26.25	26.2	KJ00-BDW6-06	2.5-3.0	149.43	149.2
3.0-3.5	***1189256***	1005.7	KJ00-BDW5-07	3.0-3.5	25.33	25.5	KJ00-BDW6-07	3.0-3.5	134.51	135.3
3.5-4.0	***1189256***	1054.3	KJ00-BDW5-08	3.5-4.0	21.25	22.4	KJ00-BDW6-08	3.5-4.0	108.24	114.1
4.0-4.5	***1189256***	1145.5	KJ00-BDW5-08 and -10	3.5-5	18.47	21.2	KJ00-BDW6-09	4.0-4.5	90.79	104.0
4.5-5.0	***1189256***	1117.5	KJ00-BDW5-10	4.5-5	15.69	17.5	KJ00-BDW6-10	4.5-5.0	78.70	88.0
5-6	***1174052***	2163.2	KJ00-BDW5-12	5.5-6	13.02	28.2	KJ00-BDW6-11 and-12	5-6	76.94	166.4
6-7	***1174052***	2109.9	KJ00-BDW5-14	6.5-7	11.55	24.4	KJ00-BDW6-13 and-14	6-7	67.74	142.9
7-8	***1174052***	2485.9	KJ00-BDW5-14 and -18	6.5-9	10.53	26.2	KJ00-BDW6-15 and-16	7-8	64.37	160.0
8-9	***1174052***	2414.4	KJ00-BDW5-18	8.5-9	9.52	23.0	KJ00-BDW6-17 and-18	8-9	66.09	159.6
9-10	***1174052***	2346.1	KJ00-BDW5-20	9.5-10	9.00	21.1	KJ00-BDW6-19 and-20	9-10	72.27	169.5
10-11	***1115603***	2270.8	KJ00-BDW5-20 and -22	9.5-12	9.04	20.5	KJ00-BDW6-20 and -22	9.5-12	74.29	168.7
11-12	***1115603***	2312.2	KJ00-BDW5-22	11-12	9.09	21.0	KJ00-BDW6-22	11-12	73.99	171.1
12-13	***1115603***	2353.7	KJ00-BDW5-22 and -24	11-14	8.67	20.4	KJ00-BDW6-22 and -24	11-14	69.37	163.3
13-14	***1115603***	2395.1	KJ00-BDW5-24	13-14	8.25	19.8	KJ00-BDW6-24	13-14	64.75	155.1
14-15	***1115603***	2436.6	KJ00-BDW5-24 and -26	13-16	7.93	19.3	KJ00-BDW6-24 and -26	13-16	65.53	159.7
15-16	***1072745***	2382.8	KJ00-BDW5-26	15-16	7.60	18.1	KJ00-BDW6-26	15-16	66.32	158.0
16-17	***1072745***	2422.7	KJ00-BDW5-26 and -28	15-18	7.39	17.9	KJ00-BDW6-26 and -28	15-18	64.66	156.6
17-18	***1072745***	2462.5	KJ00-BDW5-28	17-18	7.17	17.7	KJ00-BDW6-28	17-18	63.00	155.1
18-19	***1072745***	2502.4	KJ00-BDW5-28 and -30	17-20	7.19	18.0	KJ00-BDW6-28 and -30	17-20	63.16	158.0
19-20	***1072745***	2542.3	KJ00-BDW5-30	19-20	7.20	18.3	KJ00-BDW6-30	19-20	63.32	161.0
20-21	***1033701***	2488.1	KJ00-BDW5-30 and -32	19-22	7.18	17.9	KJ00-BDW6-30 and -32	19-24	64.55	160.6
21-22	***1033701***	2526.5	KJ00-BDW5-32	21-22	7.16	18.1	KJ00-BDW6-30 and -32	19-24	64.55	163.1
22-23	***1033701***	2565.0	KJ00-BDW5-32 and -34	21-24	7.18	18.4	KJ00-BDW6-32	22-24	65.78	168.7
23-24	***1033701***	2603.4	KJ00-BDW5-34	23-24	7.20	18.8	KJ00-BDW6-32	22-24	65.78	171.2
24-25	***1033701***	2641.8	KJ00-BDW5-34 and -36	23-26	7.68	20.3	KJ00-BDW6-32 and -34	22-28	75.40	199.2
25-26	***995748***	2581.8	KJ00-BDW5-36	25-26	8.16	21.1	KJ00-BDW6-32 and -34	22-28	75.40	194.7
26-27	***995748***	2618.8	KJ00-BDW5-36 and -38	25-28	7.34	19.2	KJ00-BDW6-34	26-28	85.02	222.6
27-28	***995748***	2655.8	KJ00-BDW5-38	27-28	6.52	17.3	KJ00-BDW6-34	26-28	85.02	225.8
28-29	***995748***	2692.8	KJ00-BDW5-38 and -40	27-30	6.71	18.1	KJ00-BDW6-34 and-36	26-32	75.48	203.2
29-30	***995748***	2729.8	KJ00-BDW5-40	29-30	6.90	18.8	KJ00-BDW6-34 and-36	26-32	75.48	206.0
30-31	***961175***	2635.0	KJ00-BDW5-40 and -44	29-34	6.58	17.3	KJ00-BDW6-36	30-32	65.93	173.7

APPENDIX G *Continued*

Sediment Accumulation Data			Pb Accumulation Calculations				Hg Accumulation Calculations			
Class Depth Interval (cm)	Class Area (m^2)	Mass of seds in depth interval (Mg)	Sample used for Pb data	Sample Depth Interval (cm)	[Pb] in sample (ug/g)	Pb in class (kg)	Sample used for Hg data	Sample Depth Interval (cm)	[Hg] in sample (ng/g)	Hg in class (g)
31-32	***961175***	2635.0	KJ00-BDW5-40 and -44	29-34	6.58	17.3	KJ00-BDW6-36	30-32	65.93	173.7
32-33	***961175***	2635.0	KJ00-BDW5-44	32-34	6.26	16.5	KJ00-BDW6-36 and -38	30-36	65.81	173.4
33-34	***961175***	2635.0	KJ00-BDW5-44	32-34	6.26	16.5	KJ00-BDW6-36 and -38	30-36	65.81	173.4
34-35	***961175***	2635.0	KJ00-BDW5-44 and -48	32-38	5.98	15.7	KJ00-BDW6-38	34-36	65.68	173.1
35-40	***928003***	***13944.6***	KJ00-BDW5-48	36-38	5.69	79.4	KJ00-BDW6-38 and -40	35-40	63.77	889.3
40-45	***896489***	***16142.0***	KJ 00-BDW5-48 and LC-BDW-96-98	36-98	6.11	98.6	KJ00-BDW6-42	42-44	58.78	948.8
45-50	***865959***	***15283.6***	KJ 00-BDW5-48 and LC-BDW-96-98	36-98	6.11	93.4	KJ00-BDW6-42 and LC-BDW-50-53	42-53	53.12	811.9
50-55	***835452***	***9481.3***	KJ 00-BDW5-48 and LC-BDW-96-98	36-98	6.11	57.9	LC-BDW-50-53	50-53	47.46	450.0
55-60	***803591***	***11816.2***	KJ 00-BDW5-48 and LC-BDW-96-98	36-98	6.11	72.2	LC-BDW-58-60	58-60	37.22	439.8
60-65	***770425***	***7940.3***	KJ 00-BDW5-48 and LC-BDW-96-98	36-98	6.11	48.5	LC-BDW-58-60 and -65-67	58-67	36.22	287.6
65-70	***737175***	***8012.0***	KJ 00-BDW5-48 and LC-BDW-96-98	36-98	6.11	48.9	LC-BDW-65-67	65-67	35.22	282.2
70-75	***700242***	***8236.7***	KJ 00-BDW5-48 and LC-BDW-96-98	36-98	6.11	50.3	LC-BDW-72-74	72-74	36.19	298.1
75-80	***660068***	***5402.0***	KJ 00-BDW5-48 and LC-BDW-96-98	36-98	6.11	33.0	LC-BDW-78-80	78-80	30.41	164.3
80-85	***615465***	***4930.0***	KJ 00-BDW5-48 and LC-BDW-96-98	36-98	6.11	30.1	LC-BDW-84-86	84-86	33.92	167.2
85-90	***582811***	***6757.4***	KJ 00-BDW5-48 and LC-BDW-96-98	36-98	6.11	41.3	LC-BDW-84-86	84-86	33.92	229.2
90-95	***562404***	***6160.0***	KJ 00-BDW5-48 and LC-BDW-96-98	36-98	6.11	37.6	LC-BDW-96-98	96-98	56.85	350.2
95-100	***541695***	***7340.6***	LC-BDW-96-98	96-98	6.52	47.9	LC-BDW-96-98	96-98	56.85	417.3
100-105	***521348***	***8105.2***	LC-BDW-96-98 and -108-110	96-110	9.14	74.1	LC-BDW-101-103	101-103	46.49	376.9
105-110	***502731***	***9483.3***	LC-BDW-108-110	108-110	11.76	111.5	LC-BDW-108-110	108-110	34.53	327.4
110-115	***484689***	***8813.3***	LC-BDW-108-110 and -165-167	108-167	16.17	142.5	LC-BDW-108-110 and -116-118	108-118	34.21	301.5
115-120	***466739***	***12341.1***	LC-BDW-108-110 and -165-167	108-167	16.17	199.6	LC-BDW-116-118	116-118	33.90	418.3
120-125	***448819***	***11095.8***	LC-BDW-108-110 and -165-167	108-167	16.17	179.5	LC-BDW-124-126	124-126	29.76	330.2
125-130	***430565***	***14148.9***	LC-BDW-108-110 and -165-167	108-167	16.17	228.8	LC-BDW-124-126	124-126	29.76	421.0
130-135	***411946***	***14738.9***	LC-BDW-108-110 and -165-167	108-167	16.17	238.4	LC-BDW-132-134	132-134	6.62	97.5
135-140	***391067***	***6108.6***	LC-BDW-108-110 and -165-167	108-167	16.17	98.8	LC-BDW-132-133 and -151-153	132-153	5.25	32.0
140-145	***370820***	***8319.9***	LC-BDW-108-110 and -165-167	108-167	16.17	134.6	LC-BDW-132-133 and -151-153	132-153	5.25	43.6
145-150	***350978***	***7591.5***	LC-BDW-108-110 and -165-167	108-167	16.17	122.8	LC-BDW-132-133 and -151-153	132-153	5.25	39.8
150-155	***332635***	***6927.1***	LC-BDW-108-110 and -165-167	108-167	16.17	112.0	LC-BDW-151-153	151-153	3.87	26.8
155-160	***316233***	***7597.6***	LC-BDW-108-110 and -165-167	108-167	16.17	122.9	LC-BDW-158-160	158-160	5.19	39.4
160-165	***299673***	***4966.8***	LC-BDW-108-110 and -165-167	108-167	16.17	80.3	LC-BDW5-158-160 and -165-167	158-167	4.89	24.3
165-170	***283898***	***6018.6***	LC-BDW-165-167	165-167	20.59	123.9	LC-BDW-165-167	165-167	4.59	27.6
170-175	***270066***	***5558.5***	LC-BDW-165-167 and -233-234	165-234	21.27	118.2	LC-BDW5-165-167 and -183-185	165-185	5.32	29.5
175-180	***257116***	***4483.4***	LC-BDW-165-167 and -233-234	165-234	21.27	95.4	LC-BDW5-165-167 and -183-185	165-185	5.32	23.8
180-185	***244954***	***4464.0***	LC-BDW-165-167 and -233-234	165-234	21.27	94.9	LC-BDW-183-185	183-185	6.04	27.0
185-190	***233162***	***3583.0***	LC-BDW-165-167 and -233-234	165-234	21.27	76.2	LC-BDW5-183-185 and -193-195	183-195	5.30	19.0
190-195	***222091***	***3718.9***	LC-BDW-165-167 and -233-234	165-234	21.27	79.1	LC-BDW-193-195	193-195	4.57	17.0

APPENDIX G *Continued*

Sediment Accumulation Data			Pb Accumulation Calculations				Hg Accumulation Calculations			
Class Depth Interval (cm)	Class Area (m^2)	Mass of seds in depth interval (Mg)	Sample used for Pb data	Sample Depth Interval (cm)	[Pb] in sample (ug/g)	Pb in class (kg)	Sample used for Hg data	Sample Depth Interval (cm)	[Hg] in sample (ng/g)	Hg in class (g)
195-200	***211394***	***5831.3***	LC-BDW-165-167 and -233-234	165-234	21.27	124.0	LC-BDW-193-195 and -223-225	193-195	2.28	13.3
200-205	***200892***	***5766.9***	LC-BDW-165-167 and -233-234	165-234	21.27	122.7	LC-BDW-193-195 and -223-225	193-195	2.28	13.2
205-210	***190506***	***5803.9***	LC-BDW-165-167 and -233-234	165-234	21.27	123.4	LC-BDW-193-195 and -223-225	193-195	2.28	13.3
210-215	***180129***	***3036.9***	LC-BDW-165-167 and -233-234	165-234	21.27	64.6	LC-BDW-193-195 and -223-225	223-225	2.28	6.9
215-220	***169711***	***3272.6***	LC-BDW-165-167 and -233-234	165-234	21.27	69.6	LC-BDW-193-195 and -223-225	223-225	2.28	7.5
220-225	***159144***	***2663.4***	LC-BDW-165-167 and -233-234	165-234	21.27	56.6	LC-BDW-223-225	223-225	0.00	0.0
225-230	***148514***	***2377.2***	LC-BDW-165-167 and -233-234	165-234	21.27	50.6	LC-BDW-228-229	228-229	0.00	0.0
230-235	***137583***	***2236.6***	LC-BDW-233-234	233-234	21.95	49.1	LC-BDW-233-234 and -234-235	233-235	0.00	0.0
235-240	***127261***	***2099.8***	LC-BDW-233-234 and -243-244	233-244	23.02	48.3	LC-BDW-237-238	240-241	0.82	1.7
240-245	***118716***	***1958.8***	LC-BDW-243-244	243-244	24.08	47.2	LC-BDW-240-241 and -243-244	240-244	0.02	0.0
245-250	***112419***	***1854.9***	LC-BDW-243-244 and -350-351	243-351	24.46	45.4	LC-BDW-243-244 and -270-271	243-244	0.00	0.0
250-255	***106628***	***1759.4***	LC-BDW-243-244 and -350-351	243-351	24.46	43.0	LC-BDW-243-244 and -270-271	243-244	0.00	0.0
255-260	***101163***	***1669.2***	LC-BDW-243-244 and -350-351	243-351	24.46	40.8	LC-BDW-243-244 and -270-271	243-244	0.00	0.0
260-265	***95985***	***1583.8***	LC-BDW-243-244 and -350-351	243-351	24.46	38.7	LC-BDW-243-244 and -270-271	243-244	0.00	0.0
265-270	***91043***	***1502.2***	LC-BDW-243-244 and -350-351	243-351	24.46	36.7	LC-BDW-243-244 and -270-271	243-244	0.00	0.0
270-275	***86262***	***1423.3***	LC-BDW-243-244 and -350-351	243-351	24.46	34.8	LC-BDW-270-272	270-272	0.00	0.0
275-280	***81606***	***1346.5***	LC-BDW-243-244 and -350-351	243-351	24.46	32.9	LC-BDW-270-272 and -350-351	270-272	0.00	0.0
280-285	***77112***	***1272.3***	LC-BDW-243-244 and -350-351	243-351	24.46	31.1	LC-BDW-270-272 and -350-351	270-272	0.00	0.0
285-290	***72785***	***1201.0***	LC-BDW-243-244 and -350-351	243-351	24.46	29.4	LC-BDW-270-272 and -350-351	270-272	0.00	0.0
290-295	***68594***	***1131.8***	LC-BDW-243-244 and -350-351	243-351	24.46	27.7	LC-BDW-270-272 and -350-351	270-272	0.00	0.0
295-300	***64355***	***1061.9***	LC-BDW-243-244 and -350-351	243-351	24.46	26.0	LC-BDW-270-272 and -350-351	270-272	0.00	0.0
300-305	***59820***	***987.0***	LC-BDW-243-244 and -350-351	243-351	24.46	24.1	LC-BDW-270-272 and -350-351	270-272	0.00	0.0
305-310	***55291***	***912.3***	LC-BDW-243-244 and -350-351	243-351	24.46	22.3	LC-BDW-270-272 and -350-351	270-272	0.00	0.0
310-315	***50719***	***836.9***	LC-BDW-243-244 and -350-351	243-351	24.46	20.5	LC-BDW-270-272 and -350-351	270-272	0.00	0.0
315-320	***45919***	***757.7***	LC-BDW-243-244 and -350-351	243-351	24.46	18.5	LC-BDW-270-272 and -350-351	350-351	0.00	0.0
320-325	***40819***	***673.5***	LC-BDW-243-244 and -350-351	243-351	24.46	16.5	LC-BDW-270-272 and -350-351	350-351	0.00	0.0
325-330	***36362***	***600.0***	LC-BDW-243-244 and -350-351	243-351	24.46	14.7	LC-BDW-270-272 and -350-351	350-351	0.00	0.0
330-335	***32339***	***533.6***	LC-BDW-243-244 and -350-351	243-351	24.46	13.1	LC-BDW-270-272 and -350-351	350-351	0.00	0.0
335-340	***28611***	***472.1***	LC-BDW-243-244 and -350-351	243-351	24.46	11.5	LC-BDW-270-272 and -350-351	350-351	0.00	0.0
340-345	***25994***	***428.9***	LC-BDW-243-244 and -350-351	243-351	24.46	10.5	LC-BDW-270-272 and -350-351	350-351	0.00	0.0
345-350	***23473***	***387.3***	LC-BDW-243-244 and -350-351	243-351	24.46	9.5	LC-BDW-270-272 and -350-351	350-351	0.00	0.0
350-355	***21037***	***347.1***	LC-BDW-350-351	350-351	24.83	8.6	LC-BDW-350-351	350-351	0.00	0.0
355-360	***18669***	***308.0***	LC-BDW-350-351	350-351	24.83	7.6	LC-BDW-350-351 and -370-371	350-351	0.00	0.0
360-365	***16709***	***275.7***	LC-BDW-350-351	350-351	24.83	6.8	LC-BDW-350-351 and -370-371	350-351	0.00	0.0
365-370	***14860***	***245.2***	LC-BDW-350-351	350-351	24.83	6.1	LC-BDW-350-351 and -370-371	350-351	0.00	0.0
370-375	***13080***	***215.8***	LC-BDW-350-351	350-351	24.83	5.4	LC-BDW-370-371	370-371	0.00	0.0

APPENDIX G *Continued*

Sediment Accumulation Data			Pb Accumulation Calculations				Hg Accumulation Calculations			
Class Depth Interval (cm)	Class Area (m^2)	Mass of seds in depth interval (Mg)	Sample used for Pb data	Sample Depth Interval (cm)	[Pb] in sample (ug/g)	Pb in class (kg)	Sample used for Hg data	Sample Depth Interval (cm)	[Hg] in sample (ng/g)	Hg in class (g)
375-380	***11370***	***187.6***	LC-BDW-350-351	350-351	24.83	4.7	LC-BDW-370-371	370-371	0.00	0.0
380-385	***9732***	***160.6***	LC-BDW-350-351	350-351	24.83	4.0	LC-BDW-370-371	370-371	0.00	0.0
385-390	***8165***	***134.7***	LC-BDW-350-351	350-351	24.83	3.3	LC-BDW-370-371	370-371	0.00	0.0
390-395	***6685***	***110.3***	LC-BDW-350-351	350-351	24.83	2.7	LC-BDW-370-371	370-371	0.00	0.0
395+	***5296***	***87.4***	LC-BDW-350-351	350-351	24.83	2.2	LC-BDW-370-371	370-371	0.00	0.0
			Total accumulation of Pb (kg)			5304.7	**Total accumulation of Hg (kg)**			14.7
			Percentage of total mass of sediments			0.0013%	**Percentage of total mass of sediments**			0.0000036%

Note: - When more than one sample is listed in the "Sample Used" columns, the concentration values given are averages of those samples because there were either no samples at that depth or there were multiple samples at that depth range .

-Values in bold italics are from Ferguson (2000).

APPENDIX H: Big Dam East Lake Pb and Hg Accumulation Calculation

Sediment Accumulation Data			Pb Accumulation Calculations				Hg Accumulation Calculations			
Class Depth Interval (cm)	Class Area (m^2)	Mass of seds in depth interval (Mg)	Sample used for Pb data	Sample Depth Interval (cm)	[Pb] in sample (ug/g)	Pb in class (kg)	Sample used for Hg data	Sample Depth Interval (cm)	[Hg] in sample (ng/g)	Hg in class (g)
0-0.5	***529425***	129.9	KJ00-BDE5-02	0.5-1	52.14	6.8	KJ00-BDE6-02	0.5-1.0	111.64	14.5
0.5-1.0	***529425***	298.6	KJ00-BDE5-02	0.5-1	52.14	15.6	KJ00-BDE6-02	0.5-1.0	111.64	33.3
1.0-1.5	***529425***	344.4	KJ00-BDE5-03	1.0-1.5	48.86	16.8	KJ00-BDE6-03	1.0-1.5	120.45	41.5
1.5-2.0	***529425***	369.8	KJ00-BDE5-04	1.5-2.0	50.42	18.6	KJ00-BDE6-04	1.5-2.0	113.17	41.9
2.0-2.5	***529425***	392.1	KJ00-BDE5-05	2.0-2.5	51.01	20.0	KJ00-BDE6-05	2.0-2.5	109.15	42.8
2.5-3.0	***529425***	415.1	KJ00-BDE5-05 and -07	2.0-3.5	51.99	21.6	KJ00-BDE6-07	2.5-3.0	110.71	46.0
3.0-3.5	***529425***	452.2	KJ00-BDE5-07	3.0-3.5	52.96	23.9	KJ00-BDE6-08	3.0-3.5	104.01	47.0
3.5-4.0	***529425***	469.5	KJ00-BDE5-08	3.5-4.0	46.91	22.0	KJ00-BDE6-09	3.5-4.0	95.31	44.7
4.0-4.5	***529425***	502.6	KJ00-BDE5-08 and -12	3.5-6.0	33.71	16.9	KJ00-BDE6-10	4.0-4.5	85.61	43.0
4.5-5.0	***529425***	503.0	KJ00-BDE5-08 and -12	3.5-6.0	33.71	17.0	KJ00-BDE6-11	4.5-5.0	67.24	33.8
5.0-5.5	***468314***	466.4	KJ00-BDE5-08 and -12	3.5-6.0	33.71	15.7	KJ00-BDE6-12	5.0-5.5	65.13	30.4
5.5-6.0	***468314***	454.2	KJ00-BDE5-12	5.5-6.0	20.52	9.3	KJ00-BDE6-13	5.5-6.0	48.99	22.3
6.0-6.5	***468314***	471.8	KJ00-BDE5-12 and -14	5.5-7.0	16.43	7.8	KJ00-BDE6-14	6.0-6.5	56.01	26.4
6.5-7.0	***468314***	464.2	KJ00-BDE5-14	6.5-7.0	12.34	5.7	KJ00-BDE6-15	6.5-7.0	46.00	21.3
7.0-7.5	***468314***	459.8	KJ00-BDE5-14 and -16	6.5-8.0	10.89	5.0	KJ00-BDE6-16	7.0-7.5	51.78	23.8
7.5-8.0	***468314***	461.0	KJ00-BDE5-16	7.5-8.0	9.44	4.4	KJ00-BDE6-17	7.5-8.0	47.90	22.1
8.0-8.5	***468314***	484.3	KJ00-BDE5-16 and -18	7.5-9.0	9.10	4.4	KJ00-BDE6-18	8.0-8.5	54.97	26.6
8.5-9.0	***468314***	492.4	KJ00-BDE5-18	8.5-9.0	8.76	4.3	KJ00-BDE6-19	8.5-9.0	53.84	26.5
9.0-9.5	***468314***	471.4	KJ00-BDE5-18 and -20	8.5-10.0	8.87	4.2	KJ00-BDE6-20	9.0-9.5	59.59	28.1
9.5-10	***468314***	478.9	KJ00-BDE5-20	9.5-10.0	8.99	4.3	KJ00-BDE6-21	9.5-10.5	48.82	23.4
10-11	***438837***	949.8	KJ00-BDE5-20 and -22	9.5-12	8.79	8.3	KJ00-BDE6-22	10.5-11.5	48.74	46.4
11-12	***438837***	851.6	KJ00-BDE5-22	11-12	8.59	7.3	KJ00-BDE6-23	11.5-12.5	45.35	41.5
12-13	***438837***	873.3	KJ00-BDE5-22 and -24	11-14	8.19	7.2	KJ00-BDE6-24	12.5-13.5	46.93	39.6
13-14	***438837***	885.4	KJ00-BDE5-24	13-14	7.79	6.9	KJ00-BDE6-25	13.5-14.5	44.94	41.6
14-15	***438837***	895.1	KJ00-BDE5-24 and -26	13-16	7.76	6.9	KJ00-BDE6-26	14.5-15.5	46.97	40.2
15-16	***415971***	869.3	KJ00-BDE5-26	15-16	7.74	6.7	KJ00-BDE6-27	15.5-16.5	42.19	40.8
16-17	***415971***	875.6	KJ00-BDE5-26 and -28	15-18	7.86	6.9	KJ00-BDE6-28	16.5-17.5	44.56	36.9
17-18	***415971***	858.4	KJ00-BDE5-28	17-18	7.98	6.9	KJ00-BDE6-28 and -30	16.5-19.5	42.76	38.2
18-19	***415971***	865.3	KJ00-BDE5-28 and -30	17-20	7.96	6.9	KJ00-BDE6-30	18.5-19.5	40.97	37.0
19-20	***415971***	865.4	KJ00-BDE5-30	19-20	7.93	6.9	KJ00-BDE6-30	18.5-19.5	40.97	35.5
20-21	***396626***	849.8	KJ00-BDE5-30 and -32	19-24	7.69	6.5	KJ00-BDE6-30 and -32	18.5-23.5	39.91	33.9
21-22	***396626***	849.8	KJ00-BDE5-32	22-24	7.46	6.3	KJ00-BDE6-30 and -32	18.5-23.5	39.91	33.9

APPENDIX H *Continued*

Sediment Accumulation Data			Pb Accumulation Calculations				Hg Accumulation Calculations			
Class Depth Interval (cm)	Class Area (m^2)	Mass of seds in depth interval (Mg)	Sample used for Pb data	Sample Depth Interval (cm)	[Pb] in sample (ug/g)	Pb in class (kg)	Sample used for Hg data	Sample Depth Interval (cm)	[Hg] in sample (ng/g)	Hg in class (g)
22-23	***396626***	855.2	KJ00-BDE5-32 and -34	22-28	7.24	6.2	KJ00-BDE6-30 and -32	18.5-23.5	39.91	34.1
23-24	***396626***	855.2	KJ00-BDE5-34	26-28	7.02	6.0	KJ00-BDE6-32	21.5-23.5	38.86	33.2
24-25	***396626***	913.1	KJ00-BDE5-34 and -36	26-32	7.19	6.6	KJ00-BDE6-32 and -36	21.5-31.5	37.37	34.1
25-26	***378040***	870.3	KJ00-BDE5-36	30-32	7.36	6.4	KJ00-BDE6-32 and -36	21.5-31.5	37.37	32.5
26-27	***378040***	849.4	KJ00-BDE5-36 and -38	30-36	7.31	6.2	KJ00-BDE6-32 and -36	21.5-31.5	37.37	31.7
27-28	***378040***	849.4	KJ00-BDE5-38	34-36	7.26	6.2	KJ00-BDE6-32 and -36	21.5-31.5	37.37	31.7
28-29	***378040***	846.9	KJ00-BDE5-38 and -40	34-40	7.36	6.2	KJ00-BDE6-32 and -36	21.5-31.5	37.37	31.7
29-30	***378040***	846.9	KJ00-BDE5-40	38-40	7.46	6.3	KJ00-BDE6-32 and -36	21.5-31.5	37.37	31.7
30-35	***360681***	4295.0	KJ00-BDE5-40 and -42	38-44	7.60	32.6	KJ00-BDE6-36 and -38	29.5-35.5	37.22	159.9
35-40	***345413***	4274.0	KJ00-BDE5-42	42-44	7.73	33.0	KJ00-BDE6-40	37.5-39.5	35.88	153.4
40-45	***331067***	4165.3	KJ00-BDE5-42 and LC-BDE-110-120	42-120	11.42	47.6	KJ00-BDE6-42	41.5-43.5	36.55	152.2
45-50	***317804***	4064.5	KJ00-BDE5-42 and LC-BDE-110-120	42-120	11.42	46.4	KJ00-BDE6-44	45.5-47.5	30.19	122.7
50-55	***305147***	3966.2	KJ00-BDE5-42 and LC-BDE-110-120	42-120	11.42	45.3	KJ00-BDE6-46 and -48	49.5-55.5	28.01	111.1
55-60	***292807***	3866.7	KJ00-BDE5-42 and LC-BDE-110-120	42-120	11.42	44.2	BDE6-50	57.5-59.5		104.2
60-65	***280222***	3758.8	KJ00-BDE5-42 and LC-BDE-110-120	42-120	11.42	42.9	KJ00-BDE6-50 and -52	57.5-67.5		97.8
65-70	***267989***	3650.5	KJ00-BDE5-42 and LC-BDE-110-120	42-120	11.42	41.7	KJ00-BDE6-54	71.5-75.5	28.59	91.6
70-75	***255636***	3535.5	KJ00-BDE5-42 and LC-BDE-110-120	42-120	11.42	40.4	KJ00-BDE6-54 and LC-BDE-110-120	66-120	23.96	101.1
75-80	***242670***	3406.6	KJ00-BDE5-42 and LC-BDE-110-120	42-120	11.42	38.9	KJ00-BDE6-54 and LC-BDE-110-120	66-120	23.96	81.6
80-85	***227667***	3243.4	KJ00-BDE5-42 and LC-BDE-110-120	42-120	11.42	37.0	KJ00-BDE6-54 and LC-BDE-110-120	66-120	23.96	77.7
85-90	***210564***	3043.6	KJ00-BDE5-42 and LC-BDE-110-120	42-120	11.42	34.8	KJ00-BDE6-54 and LC-BDE-110-120	66-120	23.96	72.9
90-95	***195161***	2861.5	KJ00-BDE5-42 and LC-BDE-110-120	42-120	11.42	32.7	KJ00-BDE6-54 and LC-BDE-110-120	66-120	23.96	68.5
95-100	***181803***	2703.6	KJ00-BDE5-42 and LC-BDE-110-120	42-120	11.42	30.9	KJ00-BDE6-54 and LC-BDE-110-120	66-120	23.96	64.8
100-105	***168830***	***2510.7***	KJ00-BDE5-42 and LC-BDE-110-120	42-120	11.42	28.7	KJ00-BDE6-54 and LC-BDE-110-120	66-120	23.96	60.1
105-110	***155624***	***2722.6***	LC-BDE-110	110-120	15.11	41.1	KJ00-BDE6-54 and LC-BDE-110-120	66-120	23.96	65.2
110-115	***143631***	***2998.6***	LC-BDE-110	110-120	15.11	45.3	LC-BDE-110-120	110-120	19.32	57.9
115-120	***131731***	***3064.1***	LC-BDE-110	110-120	15.11	46.3	LC-BDE-110-120	110-120	19.32	59.2
120-125	***120536***	***2856.9***	LC-BDE-110-120 and -135-150	110-150	16.16	46.2	LC-BDE-110-120 and -135-150	110-150	17.71	50.6
125-130	***109861***	***2839.4***	LC-BDE-110-120 and -135-150	110-150	16.16	45.9	LC-BDE-110-120 and -135-150	110-150	17.71	50.3
130-135	***100911***	***2432.3***	LC-BDE-110-120 and -135-150	110-150	16.16	39.3	LC-BDE-110-120 and -135-150	110-150	17.71	43.1
135-140	***91932***	***2302.4***	LC-BDE-135	135-150	17.20	39.6	LC-BDE-135-150	135-150	16.10	37.1
140-145	***81629***	***1904.4***	LC-BDE-135	135-150	17.20	32.8	LC-BDE-135-150	135-150	16.10	30.7
145-150	***71807***	***1610.7***	LC-BDE-135	135-150	17.20	27.7	LC-BDE-135-150	135-150	16.10	25.9

APPENDIX H *Continued*

Sediment Accumulation Data			Pb Accumulation Calculations				Hg Accumulation Calculations			
Class Depth Interval (cm)	Class Area (m^2)	Mass of seds in depth interval (Mg)	Sample used for Pb data	Sample Depth Interval (cm)	[Pb] in sample (ug/g)	Pb in class (kg)	Sample used for Hg data	Sample Depth Interval (cm)	[Hg] in sample (ng/g)	Hg in class (g)
150-155	***64105***	***1429.5***	LC-BDE-135-150 and -175-185	135-185	17.93	25.6	LC-BDE-135-150 and -175-185	135-185	16.60	23.7
155-160	***56880***	***1396.5***	LC-BDE-135-150 and -175-185	135-185	17.93	25.0	LC-BDE-135-150 and -175-185	135-185	16.60	23.2
160-165	***50461***	***1215.3***	LC-BDE-135-150 and -175-185	135-185	17.93	21.8	LC-BDE-135-150 and -175-185	135-185	16.60	20.2
165-170	***44357***	***800.4***	LC-BDE-135-150 and -175-185	135-185	17.93	14.4	LC-BDE-135-150 and -175-185	135-185	16.60	13.3
170-175	***38671***	***611.0***	LC-BDE-135-150 and -175-185	135-185	17.93	11.0	LC-BDE-135-150 and -175-185	135-185	16.60	10.1
175-180	***33015***	***572.4***	LC-BDE-175-185	175-185	18.67	10.7	LC-BDE-175-185	175-185	17.11	9.8
180-185	***27546***	***615.8***	LC-BDE-175-185	175-185	18.67	11.5	LC-BDE-175-185	175-185	17.11	10.5
185-190	***22381***	***474.7***	LC-BDE-175-185 and -196-199	175-199	21.25	10.1	LC-BDE-175-185 and -203-206	175-206	8.61	4.1
190-195	***18374***	***389.7***	LC-BDE-175-185 and -196-199	175-199	21.25	8.3	LC-BDE-175-185 and -203-206	175-206	8.61	3.4
195-200	***15044***	***360.4***	LC-BDE-196-199	196-199	23.83	8.6	LC-BDE-175-185 and -203-206	175-206	8.61	3.1
200-205	***12219***	***293.3***	LC-BDE-203-206	203-206	24.61	7.2	LC-BDE-203-206	203-206	0.12	0.0
205-210	***10400***	***249.6***	LC-BDE-203-206	203-206	24.61	6.1	LC-BDE-203-206	203-206	0.12	0.0
210-215	***9084***	***218.0***	LC-BDE-203-206 and -266-271	203-271	23.27	5.1	LC-BDE-203-206 and -266-271	203-271	0.12	0.0
215-220	***7881***	***189.1***	LC-BDE-203-206 and -266-271	203-271	23.27	4.4	LC-BDE-203-206 and -266-271	203-271	0.12	0.0
220-225	***6854***	***164.5***	LC-BDE-203-206 and -266-271	203-271	23.27	3.8	LC-BDE-203-206 and -266-271	203-271	0.12	0.0
225-230	***5779***	***138.7***	LC-BDE-203-206 and -266-271	203-271	23.27	3.2	LC-BDE-203-206 and -266-271	203-271	0.12	0.0
230-235	***4557***	***109.4***	LC-BDE-203-206 and -266-271	203-271	23.27	2.5	LC-BDE-203-206 and -266-271	203-271	0.12	0.0
235-240	***3498***	***84.0***	LC-BDE-203-206 and -266-271	203-271	23.27	2.0	LC-BDE-203-206 and -266-271	203-271	0.12	0.0
240-245	***2439***	***58.5***	LC-BDE-203-206 and -266-271	203-271	23.27	1.4	LC-BDE-203-206 and -266-271	203-271	0.12	0.0
			Total accumulation of Pb (kg)			1502.0	**Total accumulation of Hg (kg)**			3.4
			Percentage of total mass of sediments			0.0013%	**Percentage of total mass of sediments**			0.0000031%

Note: - When more than one sample is listed in the "Sample Used" columns, the concentration values given are averages of those samples because there were either no samples at that depth or there were multiple samples at that depth range .

-Values in bold italics are from Ferguson (2000).

APPENDIX I: Porewater Data

Depth (cm)	Big Dam West Lake						Big Dam West Lake			
	pH	Redox (mV)	D.O. (mg/L)	Hg (pg/g)	Pb (ng/g)	Mn (ng/g)	pH	Redox (mV)	Pb (ng/g)	Mn (ng/g)
Peeper	KJ01-BDW-D4	KJ01-BDW-D4	Sed. Core	KJ01-BDW-D7	KJ01-BDW-P2	KJ01-BDW-P1	KJ01-BDW-D5	KJ01-BDW-D5	KJ01-BDW-F3	KJ01-BDW-F3
-5					0.30					
-4					0.30					
-3					0.45		5.7	555		
-2					0.30	23.66	5.6	529		
-1					0.67	19.65	5.7	521	0.442	3.918
0	***5.2***	***657***		***<2***	0.50	19.66	5.5	536	0.321	4.052
0.5			4.8							
1	5.3	637	1.1	3.04	0.65	22.23	5.2	539	0.47	47.81
1.5			0.6							
2	5.2	603	0.5		0.61	27.14	5.3	500	1.25	402.28
2.5			0.2							
3	5.2	545	0.4		0.59	31.05	***5.3***	***503***	***0.87***	***501.87***
3.5			0							
4	5.3	495		5.35	0.76	37.25	5.5	485	0.60	533.59
5	5.3	470		3.83	0.85	35.65	5.4	471	0.52	475.49
6	5.1	453		4.13	1.01	43.21	5	241	0.44	495.15
7	5.1	384	0		0.73	45.34	5.8	169	0.54	495.91
8	5.3	300		2.47	0.58	47.36	5.8	151	0.49	511.89
9	5.3	267		5.64	0.74	52.45	6	136	0.61	512.76
10	5.4	252	0		0.74	50.37	5.9	151	0.53	529.78
11	5.5	235		2.35	0.78	53.32	5.8	125		
12	5.5	236		3.93	0.97	52.15	5.9	122	0.87	474.43
13	5.6	228		5.21	0.95	52.59	5.9	126		
14	5.5	234		3.50	1.24	52.52	6	149	1.21	518.21
15	5.6	245		4.00	1.76	57.43	5.8	136		
16	5.7	235		3.13	1.63	57.38	5.9	146	1.33	493.46
17	5.6	235		3.62		58.90	6	158		
18	5.7	226		6.88	1.20	62.67	6	144	1.26	480.40
19	5.6	254		5.75	1.33	68.72	5.9	149		
20	5.7	255			1.42	80.59	6	178	1.17	454.84

APPENDIX I *Continued*

Depth (cm)	Big Dam West Lake						Big Dam West Lake			
	pH	Redox (mV)	D.O. (mg/L)	Hg (pg/g)	Pb (ng/g)	Mn (ng/g)	pH	Redox (mV)	Pb (ng/g)	Mn (ng/g)
Peeper	KJ01-BDW-D4	KJ01-BDW-D4	Sed. Core	KJ01-BDW-D7	KJ01-BDW-P2	KJ01-BDW-P1	KJ01-BDE-D5	KJ01-BDE-D5	KJ01-BDE-F3	KJ01-BDE-F3
21	5.8	259		3.09	1.64	75.05	5.9	186		
22	5.7	260		4.76	1.52	85.45	5.9	185	0.81	447.20
23	5.6	281		5.02	1.92	85.06	5.9	236		
24	5.6	266		4.35	2.56	90.94	5.8	185		
25	5.6	279		4.89	2.53	89.44	6	183	1.40	434.93
26	5.7			3.20	2.61	85.09	6	195		
27	5.8	250			2.82	88.27	6	190		
28	5.8			5.95	3.31	86.53	5.8	202	1.53	416.40
29	5.7	240		5.43	2.95	86.70	5.8	209		
30	5.8	251	0	6.58	3.21	93.66	5.9	193		
31	5.8	268		4.54	3.19	92.17	5.9	205	1.50	413.02
32	5.9	266		5.00	2.87	93.28	5.8	206		
33	5.8	250				95.33	5.6			
34	5.9	278				104.94	5.9	234		
35	5.6	305				100.67				
36	5.8	263								
37	5.9	262	0							

Values in bold italics indicate location of observed rust stains on sampling equipment. Location of rust stains for KJ00-BDW-P1 and -P2 are unknown due to absence in field notes.

APPENDIX J: Precipitation Pb Isotope Data

Sample Number	Date (week of...)	206Pb/ 204Pb	abs err	207Pb/ 204Pb	abs err	208Pb/ 204Pb	abs err	208Pb/ 206Pb	abs err	206Pb/ 207Pb	abs err
4	03-Jul-01	18.194	0.008	15.619	0.010	37.998	0.033	2.089	0.001	1.165	0.0003
9	07-Aug-01	18.652	0.018	15.675	0.022	38.358	0.073	2.057	0.002	1.190	0.0006
15	15-Sep-01	18.352	0.009	15.693	0.011	38.320	0.034	2.088	0.001	1.169	0.0003
19	16-Oct-01	18.335	0.008	15.636	0.010	38.117	0.033	2.079	0.001	1.173	0.0003
21	30-Oct-01	18.614	0.009	15.642	0.010	38.269	0.034	2.056	0.001	1.190	0.0003
22	06-Nov-01	18.331	0.010	15.660	0.011	38.197	0.035	2.084	0.001	1.171	0.0003
25	27-Nov-01	18.266	0.028	15.658	0.023	38.072	0.069	2.084	0.001	1.167	0.0008
25 rerun	27-Nov-01	18.302	0.021	15.664	0.023	38.114	0.076	2.083	0.002	1.168	0.0007
28	18-Dec-01	18.489	0.025	15.728	0.018	38.455	0.073	2.080	0.002	1.176	0.0011
28 rerun	18-Dec-01	18.289	0.029	15.560	0.025	37.975	0.067	2.076	0.001	1.175	0.0003
32	15-Jan-02	18.365	0.011	15.600	0.012	38.076	0.036	2.073	0.001	1.177	0.0003
34	29-Jan-02	18.711	0.009	15.677	0.010	38.500	0.034	2.058	0.001	1.194	0.0003
38	26-Feb-02	18.713	0.012	15.691	0.012	38.522	0.038	2.059	0.001	1.193	0.0003
40	12-Mar-02	18.566	0.008	15.623	0.010	38.281	0.033	2.062	0.001	1.188	0.0003
42	26-Mar-02	18.432	0.015	15.648	0.015	38.231	0.043	2.074	0.001	1.178	0.0003
44	09-Apr-02	18.350	0.009	15.629	0.011	38.178	0.034	2.081	0.001	1.174	0.0003
46	23-Apr-02	18.466	0.008	15.649	0.010	38.252	0.033	2.071	0.001	1.180	0.0003
48	07-May-02	18.793	0.008	15.646	0.010	38.572	0.033	2.052	0.001	1.201	0.0003
53	11-Jun-02	18.591	0.010	15.670	0.011	38.398	0.035	2.065	0.001	1.186	0.0003

Analyses by Janet Gabites, Geochronology Laboratory, Department of Earth and Ocean Sciences, UBC. Results have been normalized using a fractionation factor of 0.15% based on multiple analyses of NBS981 standard lead, and the values in Thirlwall., 2000.

VITA

Surname: DesJardins Given Names: Michelle J'aime

Previous Surname: Watson

Place of Birth: Matsqui, British Columbia, Canada

Educational Institutions Attended:

University of Victoria, British Columbia	1995-2003
Camosun College, Victoria, British Columbia	1993-1995

Degrees Awarded:

B.Sc. (Honours and Distinction)	University of Victoria	2000

Publications:

Telmer, K., DesJardins, M., and Ferguson, P. (in review) Mercury in Lake Sediments and Porewaters. In: *A Multidisciplinary Study of Mercury Cycling in a Wetland Dominated Ecosystem: Kejimkujik Park, Nova Scotia*. Rencz, A. and O'Driscoll, N. (Eds). Society of Environmental Toxicology and Chemistry. Submitted 2003.

Telmer, K. and Watson, M. (2001) Lake Sediments – Mercury and Lead Isotope Analysis, p.18-23. *In* O'Driscoll, N., Clair, T., and Rencz, A. (Editors) Cycling of Mercury in Kejimkujik National Park: Toxic Substance Research Initiative Project #124 Summary, December 2001, Occasional Report no.18, Environment Canada, Sackville, NB, 93 pp.

UNIVERSITY OF VICTORIA PARTIAL COPYRIGHT LICENCE

Title of Thesis:

Lead and Mercury Inputs to Lakes in Kejimkujik National Park, Nova Scotia: Sources, Accumulation, and Remobilization.

Author 

Michelle J'aime DesJardins

August 29, 2003